



**Politecnico  
di Torino**

Master's Degree programme in  
**Territorial, Urban, Environmental and Landscape Planning**

Curriculum: Planning for the Global Urban Agenda

**Multi-scalar energy modelling and solar analysis  
for the urban built environment:  
The case study of Toronto, Canada.**

Supervisor:  
Prof. Guglielmina Mutani

Candidate:  
Francesca Vecchi

Co-supervisor:  
Prof. Umberto Berardi

Academic Year 2021/2022



# Table of contents

1. INTRODUCTION	
1.1. Introduction to the work	1
1.2 Energy mapping towards sustainable energy management	2
2. LITERATURE REVIEW	
2.1 Energy modelling for the urban environment	5
2.2 Top down vs. bottom-up models	6
2.3 Data driven vs. process driven models	8
2.4 Engineering models: data, steps, and implementation	10
2.5 Variables influencing energy consumption	12
2.5.1 Climatic and geographic features	12
2.5.2 Building variables	13
2.5.3 Urban variables	15
2.6 Examples of energy models	16
2.6.1 Classification of top-down and bottom-up studies	16
2.6.2 An example of hybrid model for Canada: CHREM	18
2.7 Solar photovoltaic analysis	20
2.7.1 Potential of renewable photovoltaic technology	20
2.7.2 Solar photovoltaic assessment methods	22
3. METHODOLOGY	26
3.1 Available input data	27
3.2 Housing stock classification	28
3.3 Realising a statistical model: from block to building consumption	29
3.3.1 Method by subtraction	29
3.3.2 Method by equation	29
3.4 Top-down statistical models	32
3.4.1 Energy uses by dwelling types	32
3.4.2 Statistical models to assess residential consumption	33
3.5 GIS-based solar PV assessment	35
3.6 Engineering optimisation model	38
3.6.1 URBANopt as a simulation tool	38
3.6.2 Baseline scenario	40
3.6.3 Solar optimisation	41
3.6.4 Cost-optimal analysis	49
4. FRAMING THE CANADIAN CONTEXT	
4.1 Geographical and climate context	51
4.2 Introducing Toronto	54
4.2.1 Changes in housing and population	54

4.2.2	Temperature trends	55
4.3	Energy sector	
4.3.1	National energy profile	58
4.3.2	National energy goals	59
4.3.3	Toronto: energy policies towards decarbonisation	61
4.4.	Elaboration of energy dataset: from national to city scale	
4.4.1	Available sources for assessing energy consumption	64
4.4.2	Characterisation of energy consumption in the Ontario province	68
4.4.3	HDDs and CDDs	75
4.4.4	The Toronto 2030 Platform	77
4.4.5	Assessment of energy consumption: neighbourhood scale	84
5. APPLICATION OF THE STATISTICAL MODEL		
5.1	Preliminary steps	90
5.2	Assessment of energy consumption: from block to building scale	93
5.2.1	Model I: method by subtraction	97
5.2.2	Model II: method by equation	101
5.3	Result assessment and comparison	104
5.4	Regression analyses	108
5.4.1	Electricity: SC and App consumption	109
5.4.2	Natural gas: SH and DHW consumption	111
5.5	GIS-based extension	114
5.6	Solar analysis	116
5.7	Results and considerations	122
6. BLOCK-SCALE OPTIMISATION		
6.1	Modelling with URBANopt	125
6.2	Residential input data	126
6.3	Selection of residential blocks	130
6.4	Evaluation of the baseline scenario	132
6.4.1	Detached block	133
6.4.2	Semidetached block	134
6.4.3	Low rise apartment block	135
6.4.4	High rise apartment block	136
6.4.5	Comparison	137
6.5	Solar optimisation: single building vs. aggregated evaluation	138
6.5.1	Detached block	139
6.5.2	Semidetached block	141
6.5.3	Low rise apartment block	143
6.5.4	High rise apartment block	146
6.5.5	Comparison	149
6.6	Cost-optimal analysis towards resilience	151
6.6.1	Considered aspects and options	151

6.6.2	Hourly profiles: single dwellings and aggregated blocks	152
6.6.3	Scenarios for weather-related grid outages	156
6.7	Cost-optimal results and comparison	158
6.7.1	Low-density residential blocks	158
6.7.2	Apartment building blocks	163
6.8	Result and considerations	167
7. CONCLUSIONS		170
REFERENCES		172
APPENDIX		
I.	Building code evolution	182
II.	Housing evolution in Canada	184
III.	Energy consumption by the Comprehensive Energy Use Database	187

# 1. INTRODUCTION

## 1.1. Introduction to the work

Climate changes, global warming, and the limited availability of traditional energy resources represent central matters for cities and governments. Anthropogenic activities are greenhouse gas (GHG) emitting, and a rapid reduction of emissions is necessary to face climate issues and pursue a more sustainable development. The global oil crisis of the 1970s preceded a period of research into energy conservation and switching to alternative resources. In the last decades, targets of GHG reduction and energy transition have been at the centre of several international frameworks, as the Kyoto Protocol in 1997, the IPCC reports, and the more recent Paris Agreement in 2015.

The energy sector is responsible for about 60% of GHG emissions affecting all the productive sectors [1]. Buildings cover about 30% of the global final energy consumption, among which urban ones are responsible for 60% of the final energy use [2]. Urban buildings still rely mainly on the use of fossil fuels for energy consumption whose availability is shrinking. To face these challenges, higher building efficiency and installation of renewable resources should be supported and integrated also in urban denser environment. A green urban transition would contribute to build more resilient cities, energy mix and power systems to face future climate challenges. Indeed, reducing building consumption and increasing local alternative production have been progressively at the centre of energy policies globally, as for the Sustainable Development Goals (SDGs). Local distributed generation can improve self-sufficiency of customers towards a prosumers profile (consumers and producers) and possible community-based projects. The aim is to achieve more resilient urban configuration to improve energy security and reliability towards future challenges.

The characterisation of building stock is an essential initial step to assess most demanding areas, pressures on the energy grid and then identify the best type of actions to introduce. As a preliminary analysis, building energy models allow to estimate consumption, related to energy and technical features, urban and socio-economic variables [3]. Models can rely on multi-sectoral and multi-scalar datasets, based on their availability and ranging from district to single building level. Energy modelling can also estimate the potential production of renewables. The main renewable source in dense city environment is solar, considering the low availability of physical space for other technologies, as wind or hydroelectric [4]. Solar technology can exploit roof areas and walls to deliver locally produced energy. However, the complexity of urban areas and the daily variation of solar output require accurate modelling approaches and tools [5].

Based on the ongoing energy challenges, this work provides an energy characterisation of an urban environment to support energy planning. The research assesses fundamental energy aspects of urban systems, including energy consumption of the residential sector, and rooftop photovoltaic production. Local solar resources represent an opportunity to increase self-sufficiency of dwellings and reduce dependence from the main power grid. The assessment of respective potentials is the starting point to understand the city energy configuration, implement accessible tools to visualise it and guide new policies and actions towards energy transition and community-based implementations.

The case study of the research is the central district of the City of Toronto, the so-called TOcore,

which is the analysed area by the Toronto 2030 Platform [6]. The focus is on the residential sector, which covers 43.1% of gross floor area in the TOcore district and which includes different dwelling types. The 2030 Platform represents the starting point for the elaborations on residential blocks and the tool in which results could be integrated. While several studies consider analyses only on one scale, the work proposes a multi-scalar methodology to assess building consumption and rooftop solar production:

- a top-down statistical model and GIS-based solar assessment at the urban level;
- an engineering model and PV solar optimisation at the block level.

The static regression model is based on disaggregated energy data of the building block values for electricity and natural gas consumption, retrieved from the Toronto 2030 Platform. The solar potential on GIS environment is then balanced to the dwelling electricity consumption to estimate the monthly coverable share. The evaluation is then shifted at the block scale, using the modelling software URBANopt [7]. Simulations for residential energy consumption guide the optimisation of solar installation on rooftops, according to the introduced assumptions. URBANopt allows also to simulate the resilience of local distributed generation with off-grid temporal ranges, on which the local system could be sized. Multiple configurations of distributed generation are assessed to understand variations and benefits of community-based scenarios rather than stand-alone. Finally, the cost-optimal analysis identifies the economic feasibility of each intervention related to the reached level of self-sufficiency. The work provides an integration of the Toronto Platform itself, which currently stops at the block level and lacks building-scale evaluations. At the same time, increasing electrification is one of the pathways proposed by the Toronto 2030 District and for which solar installation must be considered. Overall, the links between similar energy issues and urbanisation are progressively central for urban spatial planning choices.

## 1.2 Energy mapping towards sustainable energy management

In a unprecedented period of urban growth, urbanisation represents a key driver of sustainable development if carefully planned and managed [8]. This is the core statement of the New Urban Agenda (NUA), which consists of a shared vision by 167 countries for a sustainable urbanisation process discussed in 2016. Until 2026, the NUA will guide programmes and urban policies for sustainable development in cities because it discusses the relations between responsible urbanisation, policymaking, and development, also involving energy-related matters. The configuration of settlements, buildings and infrastructures determine cost and resource efficiencies for energy, renewable generation, and resilience. The agenda fosters the wide access to affordable and innovative energy services by increasing energy efficiency in buildings, renewable diffusion, and their synergies in district systems and community-level projects. The NUA approach to energy-related matters reflects the 2015 Paris Agreement and the statements of the Sustainable development Goals [8]. During the negotiation of the 2030 Agenda from which SDGs are featured, the role of energy was increasingly recognized for economic and social development and necessary to eliminate poverty [9]. Indeed, the SDG 7 aims at the “access to affordable, reliable, sustainable and modern energy for all” [10]. The goal 7 supports the increase of renewable share, improvement of energy efficiency and promotion of investments in upgrading infrastructures and cleaner technologies [10]. The supported shift from fossil-based

to renewable and zero-emitting energy sources of production and consumption is defined as energy transition [11], for which cities cover a key role [12]. Investments in low-carbon energy systems will greatly contribute not to overcome the 2°-1.5° target for climate change, introduced by the 2015 Paris Agreement [9]. Related themes of security, resilience, and access to resources (among which, energy) for urban environment is recalled in the SDG 11 – Make cities and human settlements inclusive, safe, resilient, and sustainable.

Energy strategies, policies and plans should be integrated to the urban planning process to physically contribute to urban sustainability [12]. However, energy management and energy transition are even more challenging in urban environments due to the complexity and interrelation of different factors. The irregular spatial distribution of built infrastructures, energy consumption and production in cities can be studied with energy mapping tools for decision-making and planning process. They represent a support to understand the relations between different urban factors and energy distribution [12]. Energy maps show the characterisation of energy patterns by spatialising and visualising results, which have risen importance in the last decades. The localisation of energy data support interventions, underline priorities for policies and guide strategies [12]. Energy mapping encompasses a set of variables to display, which include spatial distribution of energy consumption, socio-economic factors, features of the building stock, climate characterisation, land uses and renewable assessment. Analysis at the urban scale requires data to be collected, processed, and displayed mainly in a georeferenced city map, using Geographic Information System (GIS). GIS is commonly used in energy sector to spatialise and visualise energy consumption and production to specific units or building levels [13]. However, GIS assessments require large dataset and good resolutions to shape useful results.

The energy consumption of buildings uses data directly from real acquisitions or, more commonly, derived from modelling techniques. The availability and usability of measured energy data are often limited by technical, privacy and financial issues. Spatial resolution of energy-related aspects may not be sufficiently accurate or do not have a standardised scale of analysis [12]. Aggregated data are generally more accessible, but the recording scale and misalignment with building units may not fit the purpose of the study [13]. Considering temporal resolutions, annual data are often feasible for mapping and planning purposes because the focus is on localisation of energy features rather than time variability. On the other hand, high-resolution temporal data estimates the fluctuating nature of demand and renewable resources [12].

Moreover, energy assessments are often based on top-down aggregated estimations on annual basis rather than real acquisition data [12]. Models referred to a city portion tend to cluster buildings for a manageable scale: the more the structures are aggregated and simplified, the less the building heterogeneity will be displayed, and the quality of the final output is likely to worsen [14]. On the other hand, more detailed inputs are increasingly available for the quantification of renewable energy potentials (mainly solar) from open-source datasets, as DSM and DEM, from which small to large case studies can be developed. Therefore, a balance should be considered between resolution, quality of outputs and approximation, completeness of energy inputs in mapping.

Tools for visualising urban and energy phenomena represent communication strategies, which must be included in effective planning practices; they can also simulate future trends in coming years affected by climate changes [12] [15]. Maps showing energy demand are enabling tools for new policies and for addressing incentives which can lead to structural changes in energy efficiency, renovations, and

consumption reduction. Maps showing renewable potentials provide geospatial information to guide energy transition perspectives and investment towards clean energies [12]. Similar tools can support the actual building process in decision-making and action implementation.

To be effective, new methodologies must integrate consumption data and production from more decentralised renewables, especially for solar in cities [16]. Energy maps are informative tools for citizens to increase awareness on consumption and renewable possibilities for the considered buildings. For administrations, energy mapping can be a starting point to implement cross-sectoral actions for urbanisation and planning strategies. This integrated vision promoted by the NUA, and the Agenda 2030 requires interdisciplinarity rather than silos-approach and rely on the coordination among different levels of governance.

## 2. LITERATURE REVIEW

### 2.1 Energy modelling for the urban environment

Among Sustainable Development Goals by UN, the SDG 11 “Sustainable cities and communities” focuses on the improvement of living standards and decrease of energy consumption in cities and settlements. Cities occupies only around 2% of total global land [8], but buildings cover a significant global share of energy and materials use in urban areas. In this scenario, management of energy demand and optimisation of urban design is fundamental. Several and different urban building energy models (UBEMs) and tools have been developed [17]. Models are a representation, simplification, and a simulation of the reality, which aim at describing meaningful characteristics of real objects. In the case of UBEMs, they are designed according to the research purposes and data available, from which assumptions and conditions can vary. The use and elaboration of measured energy values can help local governments in identifying new energy policies. One step forward in data acquisition for UBEMs is the approval of energy use disclosures [18], even if privacy limits still affects collection and data distribution for households [3].

Energy models estimate the energy consumption of buildings and possible savings, thanks to the elaboration and visualisation of different data. Purposes of models can range from the determination of supply requirements at a macro-scale (for a city, region, or national level) to the impacts of technologies upgrades at micro-scale [3]. UBEMs can consider a range of characteristics related to and influencing the building stock.

Energy models were introduced from the early Sixties, even if they were developed more deeply after the first oil crisis in 1973. Energy shortage and cost increase implied a more careful evaluation of consumer behaviours, generally with a hierarchical approach [3]. Since then, different methods were realised based on the energy study purpose(s), requirements, and data available [19]. The growing heterogeneity of models led to the introduction of several classifications with different criteria, as purpose and structure of the model [20], or more comprehensive frameworks based on a set of criteria [21] [22]. Grubb et al. [23] structured a first classification of energy system models distinguishing top-down and bottom-up approaches, short-term and long-term and the sectoral coverage. Hourcade et al. [20] stated that top-down and bottom-up models consider differently the introduction of new technologies, the economic decision-making and the long-term impacts of markets and institutions. Van Beck [21] integrated the main analytical distinction with other seven aspects regarding goals, methodology, frame, and type of data.

The distinction in top-down and bottom-up models was applied by several following studies [3] [24] [20] [25], with often a further internal subdivision and different applicability of the adopted simulation. One of the most acknowledged classifications was formulated by Swan and Ugursal [3]: they distinguished top-down and bottom-up modelling techniques, applied for the residential sector. The focus and aims on the bottom-up approaches have been then enhanced by the review of Kavgic et al. [26]. The consumption of housing stock has been the most widely analysed by studies: indeed, it covers approximately 30% of global consumption and shows complex and interrelated features which determines a high variability. Residential sector includes a wide range of building geometries and si-

zes, materials, system losses and maintenance, occupant behaviours, which can highly impact on the overall consumption [3].

UBEMs can have variable spatial and temporal scales. Models can be dynamic and estimate consumption differences updated in time as well as multi-scalar, simulating energy demand according to different scales of analysis. Considering time, UBEMs can be classified as non-steady (dynamic simulation), quasi-steady (monthly or daily) and steady models that avoid temporal matters: the more accurate the resolution is, the longer is generally the time of analysis [27] [28]. Eventual critical areas for energy consumption can be spatialised with a GIS support, having geo-referenced data. The use of GIS has progressively interested UBEMs in different phases, from data preparation to the application of the model [24]. One of the opportunities and challenges with GIS is to assess the demand at an urban scale, considering not only building variables but also the surrounding urban area and local climate conditions [27]. In this way, the developed models can interest from few buildings in a city block to a district until an entire city. Choice of the appropriate spatial-temporal scales and approaches depends on the purpose of the study, availability and quality of input data and usable computing resources [28].

## 2.2 Top down vs. bottom-up models

Different approaches are applied to assess the energy consumption or performance of buildings, according to the research goals and considered scale, type of expected results, availability, and accuracy of input data. Three main approaches can be identified: top-down, bottom-up and hybrid. The distinction between top-down and bottom-up is based on the relation between input data and the whole housing sector [3].

- Top-down models

They adopt historic aggregate energy and energy-related data at municipal, regional, national scale (given by energy providers) and attributes average consumption for the entire building stock to provide long-term projections [29]. Results for existing buildings can be compared to different macro-economic variables (as unemployment, ageing index, income), energy price, general climate, investigating the link between energy and economic sectors [26] [29] [30]. Specific data are not required because they estimate building energy consumption from long-term link between energy and some drivers. These drivers are mainly socio-econometric, technical, and physical [17].

The initial models for policy making consisted of highly aggregated top-down and economic-oriented [21]. The use of the top-down approach has started from the energy crisis of the late Seventies: the purpose was to assess consumer behaviours by broad national energy planning in case of changing supply and pricing. Main advantage is the need of little detail of the actual consumption processes: an example is the annual housing energy model of the U.S. by Hirst et al. (1977) [3]. Considering the residential sectors, top-down models determine the effect on energy demand by long-term changes or transitions, primarily for the purpose of determining supply requirements [3]. On the other hand, the distribution of consumptions and emissions in the urban space cannot be distinguished in detail nor the impact of new interventions (i.e., retrofit measures) because values are equal for the whole considered area and based on past economic trends [26] [30].

Top-down models generally focus on links and past trend in a macro-economic vision rather than on the physical aspects pertaining to single buildings [26]. The related strength is the need for only aggregate data, the simplicity to be developed, and reliance on historic sector values [3]. However, the dependence on past relations between energy and other aspects might also be not appropriate when dealing with future trends as climate change issues. Environmental, social, and economic conditions may be remarkably different to previous ones [17] [26]. According to Torabi et al. [24] and Swan and Ugursal [3], top-down techniques can be considered suitable for large-scale analysis but not for the identification of the potential improvements by new technologies or of future trends as climate change.

- Bottom-up models

They simulate the energy demand for a single or groups of buildings from which describe the distribution of consumption at wider level and integrated framework [17] [29]. Bottom-up models start from the full simulations (disaggregated level) by single building to then transpose results generally at a wider scale. In contrast to top-down approaches, the process begins from disaggregated data to then provide some levels of agglomeration [21].

They can identify the energy consumption of individual end-uses or building, which can be then extrapolated to represent the regional or national situation, based on weighting of the modelled sample [3]. Bottom-up models are often applied to identify the most cost-effective options to achieve carbon reduction targets, according to the best available technologies and processes. Technological potentials and performance savings on building stock is useful to guide policy perspectives [26]. However, the description of each component needs to be sufficiently accurate [26] [31]. Valid levels of accuracy require extensive and detailed data and longer time of elaboration [30]. The main consequence caused by high level of details is that the input requirements are greater than top-down models, which imply more complexity of calculation or simulation techniques. Bottom-up approaches may also neglect relations between technological systems and occupants as well as the impacts of external factors, as interactions between energy consumption and market (i.e., prices) [26]. To obtain more similar results to the actual demand, bottom-up models can be calibrated with a correction factor, derived from the comparison with real measured data (as from energy providers) [30] [32].

Among bottom-up typologies, the most widely used are building physics-based models, which apply thermos-physics simulations on a sample of buildings to estimate energy consumption by calculations [33]. The required input are physically measurable variables, as efficiency of heating systems, technical and thermal (U-values) information on walls, roof, floor, windows, doors, internal temperatures, ventilation rates, number of users, external temperatures, etc. The combination of building physics and empirical data allows to estimate energy demand and carbon reduction, also for future evolving perspectives and with different scenarios. They can represent evidence-based simulations for medium to long-term energy supply strategy and policy implementation. One of the main weaknesses is the assumptions about behaviours on energy consumption, for instance the impact of changing demography, daily hours of occupancy and heating system use [17].

Another distinction can be based on the applied time horizon: static or short-term bottom-up models use a short temporal range and perform the energy system in a target year, whereas long-term ones assess its longer evolution until a target year [31].

Recent efforts to develop decision support tools have integrated top-down or bottom-up urban models

with geographical information systems (GIS) to obtain input data for several buildings, estimate their performance and visualize results in a format accessible for urban planners and designers [28]. A summary of main advantages and disadvantages of the two approaches is reported in Table 1.

Table 1. Summary of main pros and cons of top-down and bottom-up models.

	Pros	Cons
Top-down	<ul style="list-style-type: none"> <li>Identify relationships between energy consumption and socio-economic variables</li> <li>Use of energy and economic aggregated data, based on observed market behaviour</li> <li>Focus on interactions at larger scale</li> <li>Easier to develop and adapt</li> </ul>	<ul style="list-style-type: none"> <li>Reliance on past energy and economic data to assess future trends</li> <li>Lack of building-related details</li> <li>Less suitable to assess technology and retrofit-related policies</li> <li>Determination of end-use consumptions based on simulations</li> </ul>
Bottom-up	<ul style="list-style-type: none"> <li>Simulate current and future technologies to meet demand</li> <li>Base for policies to be more effectively targeted at consumption</li> <li>Quantify impacts and benefits of implementation of different technologies</li> </ul>	<ul style="list-style-type: none"> <li>Negligible consideration of market economic interactions</li> <li>Require several technical data and detailed input information</li> <li>External assumptions to describe human behaviour</li> <li>Computationally intensive</li> </ul>

- Hybrid models

The separation between top-down and bottom-up is leaving space for more integrated and merged approaches [21]. Hybrid models use the energy demand of some reference buildings and adapt them to evaluate the consumption of a city. They combine top-down macro-economic models with at least one bottom-up simulation [31]. Through a detailed spatial representation of the stock, including socio-economic data, it is possible to associate to each building its consumption to assess energy needs at the building, neighbourhood, or city scale [34].

## 2.3 Data driven vs. process driven models

Each modelling technique show specific strengths, weaknesses, potentials, and applicability [3]. The objectives of the research will guide the approach of the energy model to assess building consumptions. The accuracy of the models is related to the reliability and completeness of the dataset. The level of detail of the available input data can vary significantly, leading to the use of different techniques which attempt to take advantage of the information. Data availability can lead to two main simulations [29]:

- Statistical data-driven (especially for top-down models)

They are based on the data elaboration through statistical regression, machine learning and algorithms. Statistical methods rely on historical disaggregated energy values and regression analyses which are applied to attribute energy demand to end-uses. Once their relationships have been established, the model can estimate the energy consumption of dwellings of the residential stock [3]. Data-driven methods are applied for energy

prediction, which uses real measured data and predefined databases for building type, vintage, and location. In this case, normal distribution, average, variance of energy consumption allows to discard anomalous data. They use energy consumption values from a sample of buildings and different techniques to regress the relationships between end-uses and energy demand [29]. Statistical techniques can include macroeconomic, energy price and income, and other regional or national indicators, acquiring strengths from top-down approaches [3].

According to Torabi et al. [24], statistical techniques can be distinguished in:

### 1. Regression analysis

It identifies the relation between energy demand and relevant drivers. Regression analyses are based on parameters or combinations of parameters, which affect building energy consumption [3]. Several statistical models use techniques of regression, which are easy to develop. Regression methods are implemented to derive inverse statistical models, which assume building inputs from known outputs, such as energy consumption data, locational datasets, and public records [28]. They do not require detailed data, relying on census information or consumption bills, although they need a wide sample to set up accurate models. Even if they allow to estimate the energy consumptions also at the building level, regression analyses do not result to be as detailed as the engineering ones. The flexibility is limited to simulate different scenarios of intervention for energy efficiency [26].

### 2. Conditional Demand Analysis method (CDA)

The CDA regression relies on the presence of end-use appliances: by regressing total dwelling energy consumption onto the set of appliances (binary or count variable), the identified coefficients represent the use level and rating. It is a regression-based method suitable for working with large datasets, generally using appliance surveys and energy billing data from occupants [3]. However, it requires a dataset with variety of appliances to produce reliable results. Its lack of flexibility and details limit the analysis of impacts on demand by efficiency and retrofit measures. CDA capabilities are constrained by the variables in the equation rather than allowing tests for new interventions [33].

### 3. Neural network model (NN)

It adopts a simplified mathematical model with a dense interconnected structure, by which all end-uses affect one another through a series of parallel “neurons” [3]. The technique assesses causal relationships between several variables and parameters, according to a large training dataset. It has been used for prediction problems at both single building and larger scale due to the ability to evaluate non-linear energy consumption (as energy loads) and impacts of socio-economic factors [33].

- Engineering methods

Engineering methods (EM) are based on modelling of geometrical and thermos-physical features to evaluate building performance [17]. They rely on dwelling characteristics and end-uses to calculate the energy demand, based on power ratings, usages, heat flows and thermodynamic principles [35] and without using historical energy consumption values. Historical energy data can be then adopted to calibrate outputs [3]. EMs are generally based on physical features and calculations in and around buildings, which are used to analyse costs and dynamic performances for structure clusters, with high spatial and temporal resolutions [28]. In the energy balance equations, they can introduce both building level as well as urban context characteristics, referred to the urban environment as sky view factor, urban canyon effect, solar exposition [36] [37]. EMs rely on simulation software which require sufficient user experience, computational efforts and input data preparation, even if the higher degree

of flexibility allows to calculate a wider range of impacts [17] [33].

In contrast to statistical models, bottom-up EMs can evaluate the impacts of new technological solutions (i.e., on-site energy generation and storage) and associated GHG emissions [3]. Despite requirements for a larger dataset, the versatility of EMs helps to identify mix of policies and renovation measures for large building stocks as well as optimise urban energy systems for existing and new developments [17]. One of the main weaknesses is the difficult link between behavioural aspects of occupants and energy consumption, which are only defined by a priori assumptions [3] [25] [26].

According to Swan and Ugursal [3], EMs can be distinguished into:

#### 1. Archetype method

It is based on the definition of representative classes (with key features, as vintage, size, house type) on which buildings are aggregated. Archetypes have thermos-physic characteristics that are inserted in building simulation software to assess energy consumption. The estimations of archetypes are scaled up to represent the regional-national housing stock by multiplying the single result by the number of total buildings which fit the archetype description [3]. Indeed, this has been often applied for bottom-up building models at the national or regional levels to understand the aggregated impact of energy efficiency policies and new technologies [35]. However, characterisation and representativeness for a wide set of structures is the main challenge [24]. Depending on the level of detail, archetypes can represent the link of appliances and end-uses within the house, especially with progresses in software capabilities [3].

#### 2. Sample method

It uses data collected from surveys and monitoring campaign to model the building stock behaviour. Limited applications of sample method have been adopted at local level [38]. Input sample data for the model characterises a variety of houses within the stock. If the sample represents regional or national stock, the building consumption can be estimated with appropriate weightings. Considering variability of housing, this technique needs a sufficiently large database of representative dwellings [3].

#### 3. Population energy consumption

This technique utilises distributions of appliance and use to assess energy consumption of each end-use, following appliance ratings. It reflects the energy consumption of household appliances based on their ownership saturation rate. This approach does not give back interactions amongst end-uses because it generally calculates them separately [3]. Population energy consumption can be feasible to understand the electric distribution load of an area or to estimate energy demand of appliances [39].

## 2.4 Engineering models: data, steps, and implementation

Several methodologies and software have been developed in recent years to model in detail building stock in an engineering-based approach for UBEMs [17]. Modelling software are evolving rapidly, each one with proper characteristics and more specific applications.

A wider access to building data helps to develop more detailed simulations and perform a wider range of analyses. However, administrations often collect data in different formats, with heterogenous terminologies, temporal and spatial resolutions. Besides location and related weather dataset (also with projection for future years), two main steps establish the input setting phase: the building stock geometry and the thermophysical properties [17].

The geometry input includes building shapes, window opening ratios and terrain data, which can be derived from existing dataset or created by scratch [35]. Individual building models can have high resolution, also considering internal subdivisions and rooms. However, a simplification of the geometry can be required to decrease the computational efforts of several buildings together. Several tools are integrated with GIS files (e.g., CityGML, GeoJSON, Shapefile, OpenStreetMap) because its formats are the most common to store information by municipalities [17].

The association of the thermophysical and schedule properties to the building geometry can involve construction assemblies, HVAC systems, equipment loads and occupant behaviour. These parameters can be measured for a small group of buildings, whereas it is impractical for wider urban areas [35]. Simplifications are generally applied using archetypes: they represent prototype and representative of the modelled stock, which quickly describe the building geometry and use [3]. A large amount of data is often required to derive prototypes. Therefore, most tools include already default archetypes which are assigned via basic data, such as construction year, building use (e.g., residential, office, commercial), and typology (tower, detached house, etc.). Realising archetypes requires two subsequent steps: the segmentation divides the investigated building stock into groups based on building shape, age, use, climate, and systems. The characterisation identifies for each one a set of thermal properties and usage patterns and can be based on a sample (i.e., an actual, real building within the group) or a virtual building (i.e., statistical building data) [35]. The characterisation also includes occupants' behaviours and interactions with the building (i.e., opening windows, switching lights, use of appliances), which impact on energy consumption [3]. The occupants' presence is mainly assumed in a deterministic approach (i.e., via predefined fixed schedules). Probabilistic models are under study to consider the stochastic attitude of occupants and their movements between the different and numerous thermal zones of an urban model [17]. The set of research on occupants' behaviours is facing another complex aspect of UBEMs, or rather movement of people between buildings and in the city. For analysing spatial-temporal patterns, the financial unfeasibility of sensors favours the use of data from mobile devices and Wi-Fi [17].

Further aspects should be considered in the choice of the optimal modelling software: the scale (i.e., number of buildings or area) and the type of project (i.e., retrofit on existing structures or new construction), easily managed by a tool.

Archetypes may not represent differences characterising the real city. Dynamic archetypes evolving in time, diversity of occupant behaviours and socio-economic conditions among buildings of the same occupancy type should be considered to have a more realistic energy demand patterns [26].

The possibility of UBEMs to support policy pathways depends on how reliable and representative simulation results are. Engineering models do not rely on historic consumption data, which may be used for calibration and validation phases [3]. UBEM predictions may be remarkably different from measured energy-use results because of variabilities and uncertainties (i.e., infiltration, occupant behaviours), especially in case of a large stock of buildings. According to the analysis made by Reinhart and Cerezo [35], the discrepancy between aggregated annual measured and energy use models for multiple buildings can range between 7% and 21% for heating loads and 1 and 19% for total energy use intensity (EUI). Accuracy decreases at the single- building scale, as for regional and urban simulations. When dealing with new settlements or developing cities, the geometry could change rapidly, so that the use of 3D software could return the evolving landscape [17]. UBEM tools are progressively developing, introducing new features and possibilities for innovative modelling [17]

[28]. As more information becomes publicly available and computational resources evolve, detailed simulations at the district and city scales will be integrated with transportation, air quality, urban heat island effect, electrical power distribution for the urban context [18].

Together with building-related interventions, EMs can assess on-site energy generation and collection towards more decentralised energy systems [3]. Recently, energy grids become more interconnected and flexible due to the diffusion of decentralised generation and the integration of renewable energy sources. Local energy systems should serve multiple consumers and optimise the use of locally produced energy based on different load profiles. Energy networks, eventual storages, community, and single-user renewable energy systems are progressively included in the simulations and shaped to meet the energy building profiles [17]. The analysis of building clusters allows greater integration than considering them as stand-alone structures or individual prosumers. Larger-scale simulations are effective in case of on-site renewable energy production (mainly PV) and integration with the main energy grid: district energy systems can take advantage of thermal load diversities of the served group of buildings [28]. The perspective is towards modelling of urban energy communities, mostly based on solar resources.

## 2.5 Variables influencing energy consumption

Previous studies [17] [25] [40] underlined the way building energy consumption is influenced by a set of variables related to different aspects, as climate, building-related characteristics, and relation with the urban context. Structuring a dataset is the starting and fundamental component to work on energy models. Most analyses are focused on housing characterisation, even if consumption values may be more difficult to be obtained [3]. Building functions have a substantial influence on the energy demand, both in relation to their use (such as ventilation or internal loads), and to the construction characteristics. Their definition is therefore fundamental to assess values of the thermal and electrical energy requirements [34].

Main energy-related variables are quickly described in the paragraph and a classification of main case studies with related key data is then analysed, distinguishing the three main modelling approaches.

### 2.5.1 Climatic and geographic features

The climate and micro-climate conditions (as air temperature, relative humidity, solar irradiance, HDD) vary across regions and impact on the energy consumption of structures.

Meteorological datasets are commonly adopted in building simulations with different timeframes. Data can be both measured, especially from national services, or synthetic build on modelling mainly from commercial database (i.e., Meteonorm). Although it is acknowledged the sensitivity of building heating and cooling loads to climate change, standard-year weather files rarely consider future climate trends [41] [42]. Past weather data might not well represent recent or future events because updates of typical year weather files are infrequent [42]. To overcome limitations, additional steps are required, i.e., climate change weather file generator tools (i.e., CCWorldWeatherGen and WeatherShift™) or multi-year simulations. Simulation tools are based on general circulation models and assessment reports by the Intergovernmental Panel on Climate Change (IPCC) on emission scenarios that provide

possible future climate projections [41]. These types of datasets can be used to estimate future trends of climate-related data of energy consumption, as heating and cooling degree days.

### *Heating degree days*

The heating consumption of buildings depends on the outdoor air temperature and on the required energy for heating or cooling the environment to maintain an indoor thermal comfort. According to the variation of temperature, the building demand changes based on the altitude at which it is located and to the year, which may have colder or milder seasons. Therefore, the heating degree days (HDD) are needed to assess the necessary energy to heat an environment compared to a reference temperature, generally taken as 18°C, during a year. Annual HDDs is the summation for all days in the heating season of the positive differences between the reference comfort temperature (fixed at 18°C) and the mean outdoor temperature:

$$\text{HDD} = \sum T (T_{\text{reference}} - T_{\text{outdoor}})$$

With  $T_{\text{reference}} = 18^{\circ}\text{C}$ .

### *Cooling degree days*

Cooling degree days (CDD) are equal to the number of degrees Celsius above a given comfort temperature, which is generally set at 18°C, 21°C or 24°C. The challenge could be to identify the most realistic temperature threshold for turning on space cooling. Generally, surveys [43] and datasets [44] use 18°C as fixed value (or 65°F in the North America [45]), while comfort setpoints are higher.

$$\text{CDD} = \sum T (T_{\text{reference}} - T_{\text{outdoor}})$$

With  $T_{\text{reference}} = 18, 21, 24^{\circ}\text{C}$ .

CDDs are fundamental to calculate the necessary energy to cool an environment compared to a reference temperature. As underlined by recent studies on North America [45], Canadian cities [46] and Brazilian households [47], space cooling loads are likely to increase due to rising temperature and CDDs will become more important to consider in energy analyses.

## **2.5.2 Building variables**

Building characteristics influence the structure behaviour and the consumption along the year. Input data can have different levels of detail, according to the type of analysis and aims. Three main groups of input data can be distinguished [29], which are often influenced by the period of construction:

- building geometry, as shape, height, number of floors, heated volume and heat loss surfaces, from which derive the compactness factor (S/V ratio);
- thermos-physical features, fundamental to build engineering models, which include thermal transmittance, absorption coefficient for solar radiation, emissivity of opaque and transparent envelope and thermal capacities of heated zones;
- system efficiencies and operation conditions, which include space heating, space cooling, ventilation and DHW.

Ferrando et al. [17] and Sola et al. [41] distinguished two steps in the building stock characterisation: typology for building archetypes and geometry definition. The former requires more specific information referred to the single class and have a higher level of detail for engineering models. The latter

works on existing datasets to extract footprint information, as cadastres, GIS, remote sensing, and satellite images. According to Mutani et al. [48], for the case study of Turin, Italy residential demand for space heating is mainly affected by five key variables: climate (related to HDDs), construction period, S/V ratio, percentage of heated volume and peculiar features of the stock linked to the construction tradition. The link between period of construction, geometrical and material characteristics is analysed also by the engineering model in [36], which classifies the housing dataset in four archetypical clusters and show different correlations. Building data can derive from different sources and can be integrated by Geographical Information Systems (GIS) to be related to the surrounding context [41] and visualise in accessible formats [28].

### ***Basic information: footprint, height, number of floors***

Initial information for building geometry is the set of footprints, from which the gross ground area of structures can be assessed. The building height allows to identify the number of storeys, generally setting each floor as 3 m high for dwellings. Floor height can vary with functions (i.e., commercial, industrial, office), age of construction and type of floor (i.e., habitable, attic, basement).

### ***Gross heated surface***

It is obtained from the base area per the number of floors.

$$\text{Gross heated surface (m}^2\text{)} = \text{Area} * \text{n}^\circ \text{ of floors}$$

### ***Gross heated volume***

It is the multiplication between the base area and the average height of one floor (3 m), according to the number of floors.

$$\text{Heated gross volume (m}^3\text{)} = \text{Area} * \text{n}^\circ \text{ of floors} * \text{Height per floor}$$

### ***Loss surface***

The loss surface (m<sup>2</sup>) is the wall area being directly in contact with the external environment or with non-heated rooms. In case of a stand-alone structure, it is equal to:

$$\text{Loss S (m}^2\text{)} = 2 * \text{Area} + (\text{Perimeter} * \text{Height})$$

While in case of attached buildings, the common portions must be not considered from the loss surface:

$$\text{True Loss S (m}^2\text{)} = \text{Loss S} - \text{Common S}$$

The calculation of loss surfaces requires GIS to identify common walls and their areas, based on the building shapefile. The procedure will identify shared lines between two or more polygons and the related area is then deleted from the overall loss surfaces.

### ***Compactness factor***

The surface-to-volume ratio (S/V, m<sup>2</sup>/m<sup>3</sup>) is the relation between the loss surface and gross heated volume, which represent the compactness of the structure. Low values for compact structures reduce heat exchanges between buildings and outdoor context: therefore, they are generally preferable even if they also reduce the solar heat gains. On the other hand, higher S/V ratio are for low and stand-alone buildings, which show a large heated loss surface compared to high-rise.

### *Users behaviour*

Related to the functions, energy consumption is affected by the behaviour of building occupants, according to the fixed air temperature, daily schedules and used electrical appliances. The profile load of building usages will have different peaks and maximum values for each function (i.e., housing, offices, industrial structures) [37] and impact on overall consumption. The integration on consumer behaviours and consequences on economic outcomes is especially a challenge for bottom-up physics model, in which often assumptions are made [3].

### **2.5.3 Urban variables**

Energy models should not consider buildings as stand-alone structures but as located and related to the surrounding context and microclimatic variations [49]. In the urban environment, energy building consumption is influenced by variables at distinct scales, as the overall city design, the relationship between built and open spaces, the materials adopted in external surfaces, presence of obstructions and vegetation. Therefore, the morphological aspects influence the demand, the human comfort of spaces and the air quality. For these reasons, starting from the Seventies with Martin and March [50], urban aspects have been increasingly included in energy models.

In a dense building stock as in city environment, the urban heat island (UHI) effect increases by anthropogenic sources, built-up surface and limited natural areas. By UHI, absorption of shortwave radiation grows, while longwave radiation and mean wind speed decreases, so that the urban mean air temperature is higher compared to rural one [41]. Different tools can be used to identify the urban microclimate environment, as ENVI-met which considers heat fluxes from vegetation, water and soil [51], or the non-commercial software Radiance for solar and daylight assessments [52]. Considering the influence of urban form on building performance, the compactness of built configuration can be described using:

- building Coverage Ratio (BCR), defined as the percentage of built area compared to a sample area; it can go from 0 (empty lot) to 1 (full lot);
- building Density (BD,  $\text{m}^3/\text{m}^2$ ), defined as the ratio between built volume and a sample lot, by which high values suggest high densities and vice versa;
- canyon height-to-width ratio (H/W, m/m), defined as the ration between building heigh and distance between two buildings. For urban microclimates around buildings, urban canyons cause an increase in solar radiation absorption and consequently higher air temperatures, lower wind speeds, and worse air quality;
- solar exposure ( $H/H_{\text{avg}}$ , m/m), which is the ratio between the building height (H) and the surrounding buildings average height ( $H_{\text{avg}}$ );
- main orientation of streets (MOS), with limited shade for East-West orientation and more shade for a North-South axes [49] [37].

However, the urban form and its impact on building consumption will not be the focus of this research and it will not be deeply analysed.

## 2.6 Examples of energy models

Different energy modelling approaches and variables have been used in several studies to assess building consumption and other energy-related aspects. The two following paragraphs provide a classification of representative studies for top-down and bottom-up models and a presentation of a hybrid model applied to the Canadian residential sector. The hybrid model for Canada is selected because it applied both an engineering and a statistical model to the country of interest for this study.

The aim is to understand how theoretical aspects of energy models have been applied to real case studies in different ways.

### 2.6.1 Classification of top-down and bottom-up studies

Table 2 and Table 3 report a classification of representative top-down and bottom-up studies on the building sector. The studies are presented in chronological order from the end of the XX century to more recent applications. Main points reported are the investigated energy aspects, the type of approach, significant variables for the results, geographical scale, and assumed case study.

Table 2. Classification of top-down building energy models.

Authors	Year	Energy Aspect	Type of Elaboration	Main Variables	Scale	Case study
Hirst, Lin, Cope	1977	Housing consumption model	Statistical	Demographic (household formation and housing choices) and economic changes (fuel prices and income); technology component	National	US housing
Bentzen, Engsted	2001	Long-term annual energy demand	Regression models	Household income, energy price and HDD.	National	Denmark
Tornberg, Thuvander	2005	Consumption rates of different sources	Statistical	Measured energy data; building features	Groups of buildings	Goteborg, Sweden (68,200 buildings)
Labandeira, Labeaga, Rodriguez	2006	Energy consumption for electricity, natural gas, propane, automotive fuel, public transport, and food	Regression models	Demographic, economic (income), and climate variables	National	Spain (27,000 houses)
Siller, Kost, Imboden	2007	Impacts of renovations and new construction to achieve energy consumption and GHG emissions	Regression models	Building type, energy standards, efficiency, heat demand per area and DHW systems.	National	Switzerland
Summerfield, Lowe, Oreszczyn	2010	Average delivered energy to households	2 multiple regression models	Annual delivered energy, price, and temperature	National	UK household since 1970

Wiesmann, Lima Azevedo, Ferrao, Fernandez	2011	Electricity consumption	Regression models	Income, appliances ownership, floor area, household size, climate effects.	Municipal	Portugal
Mutani, Vicentini	2013	Electricity demand and PV potential supply	Statistical	Radiation components	Municipality	Turin (IT)
Mutani, Fontanive, Arboit	2018	Space heating demand, energy performance classes	Statistical	Type of buildings, quality of materials, SV ratio, residential density	Building, district	Gran Mendoza (AR)
Mutani, Todeschi	2020	Monthly thermal energy balance	Engineering	Period of construction, sky view factor, main orientation of streets, relative district height	Building, district	Turin (IT)
Mutani, Todeschi	2021	Energy performance; retrofit potential	Engineering	Period of construction, energy savings by EPCs	Building to city	Turin (IT)

Table 3. Classification of bottom-up building energy models

Authors	Year	Energy Aspect	Type of Elaboration	Main Variables	Scale	Case study	Tool(s) adopted
Tonn, White	1988	Electricity use	Regression	Housing characteristics, ethical motivations	Building	100 homes with wood heat	-
Douthitt	1989	Space heating fuel use	Regression	Fuel price trend, building structure, climate, occupant features, income.	Building	370 homes	-
Kohler, Schwaiger, Barth, Koch	1997	Mass, energy, and monetary flow	Engineering by archetypes	Age, use, materials, and operations.	Building	German building sector	-
Jones, Lannon, Williams	2001	Energy consumption	Engineering by archetypes (5 by age +20 built form)	Age, built morphology, building features.	Urban	Neath Port Talbot, UK	GIS, integrated with a drive-pass survey
Shimoda, Fujii, Morikawa, Mizuno	2004	End-use energy	Engineering by archetypes (20 dwelling types + 23 household)	Number of family members, appliance ownership and ratings	Urban	Osaka, Japan.	-
Yao, Steemers	2005	Appliance energy consumption	Engineering by archetypes (4 housing types and 100 households)	Appliance ownership, average appliance use, average appliance rating.	National	UK	Thermal resistance method
Clarke, Ghauri, Johnstone, Kim, Tuohy	2008	Total energy consumption	Engineering by archetypes (3240 classes)	Thermodynamic determinants	National	Scotland	Software ESP-r

Delmastro, Mutani, Corgnati	2016	Space heating demand; retrofit options based on 4 scenarios	Statistical	Energy requirements matched with socio-economic variables	Building to census	District 3 in Turin (IT)	GIS
Delmastro, Mutani, Corgnati	2017	Space heating demand; energy density	Statistical	Period of construction; SV ratio; heated volume	Building to census, until city	Turin (IT)	GIS, Excel
Torabi Moghadam, Toniolo, Mutani, Lombardi	2018	Space heating demand	Statistical	Period of construction; SV ratio, building use	Building, census	Settimo Torinese, TO (IT)	GIS, Excel

## 2.6.2 An example of hybrid model for Canada: CHREM

An example of hybrid model is the Canadian Hybrid Residential End-use Energy and Emission Model (CHREM), based on a record of 17,000 detailed houses. The CHREM was developed to study the residential end-use energy consumption in Canada, and to evaluate the impacts of different energy efficiency technologies [53]. This model involved two modelling components, one statistical and one physics-based that aim at estimating the energy consumption of appliances and lighting, domestic hot water, space heating and cooling. The CHREM employed a calibrated neural network model to assess the annual consumption of energy-end uses which were mainly influenced by occupant behaviour. Estimation of space heating and cooling were made by the high-resolution building performance simulation package ESP-r because of the lack of historic data for statistical analysis of new technologies. The CHREM relied on the representative dataset of houses, which allowed to assess energy consumption and GHG emissions on the available sample. CHREM was applied for comparative technical and economic analysis on a wide range of building retrofit and fuel switching scenarios for assessing energetic and emissions impact by the building code. Its first aim was to investigate the impacts of different carbon reduction strategies of the upgrading standards R-2000 (1994) and NECH (National Energy Code for Housing, 1996).

The Canadian residential stock was divided into five main types of dwellings:

1. single-detached,
2. single-attached, with at least one shared wall in a neighbour, which include semi-detached houses, duplex and row or terrace houses,
3. apartments (less than five storeys),
4. high-rise apartments (with five storeys and more),
5. mobile homes.

The first two categories cover around 60% of the households in Canada and were responsible for the higher share of residential energy consumption: therefore, they were the only one considered in this model, selected in a range of climate, vintage and construction types, dimensions, and energy sources [54]. Moreover, the stock was divided in four vintage groups (pre-1941, 1941-1966, 1967-1978, 1978 or later), but energy efficiency measures (upgrading from 10 to 90%) were assessed only on houses built in 1966 or later. Improvements on older structures were unfeasible for their limited useful life and energy savings could not balance the intervention costs. Therefore, main limitations of the model

were the omission of mid and high-rise multi-family buildings (30% of Canadian residential stock), and that scenarios avoided older housing (pre-1967) to evaluate energy efficiency policies.

The study employed two energy modelling parts, statistical and engineering (physics-based techniques), which were used to estimate the consumption of domestic appliances and lighting (AL, 20% of overall consumption), domestic hot water (DHW, 22%) and space heating-cooling. Space heating covered the greatest share due to the cold climate. The AL and DHW loads were mainly influenced by occupant behaviour, while heating by building construction fabric, system components, and climatic conditions. Space cooling demand varied with occupant behaviour and housing thermal features.

- Engineering model: it creates 16 archetypes based on types of houses, further integrated with the 1993 Survey of Household Energy Use to create 8,767 house descriptions.

For each of them, the energy consumption was estimated and calibrated through energy billing data available for 2,524 of these houses. The EM predicts the SC and SH energy consumption of dwellings. The results were used to assess the demand of the Canadian housing sector, with following evaluation of efficiency upgrades and GHG emissions by occupant behaviours. The CHREM model managed a significant building stock and used an engineering approach to identify the impacts of energy retrofits. However, variations of the thermal envelope were limited to the number of archetypes, imposed appliances ratings, and did not cope with the variety of occupant behaviours [25].

- Statistical model: considering the limits for users' behaviours by the EM, further research was conducted with two statistical models.

The neural network regression identified the link between residential consumption and several input variables, while the conditional demand analysis determined the impact of each appliance in the housing energy demand. The regression of energy consumption onto input data allowed to consider demographic factors and user behaviours [25]. Overall, the three methods showed a similar accuracy, slightly better for NN. Therefore, a hybrid model was proposed by Aydinalp-Koksal and Ugursal [33] which integrated bottom-up engineering and statistical NN techniques. The NN method assessed the AL and DHW consumption and allowed high interaction between inputs and outputs. The dwelling database was integrated with socioeconomic and demographic values from the 2007 census statistic data. The calculated AL and DHW loads were then integrated into the engineering model, after being normalised by the corresponding annual house consumption.

Although loads and characteristics were incomplete, space heating simulations shown average annual per house consumption from 72 to 144 GJ for the five Canadian regions, with an average value of 108 GJ. Preliminary results by the NN techniques present: annual AL consumption for individual houses ranges from 18 to 72 GJ with an average value of 43 GJ; annual DHW consumption per house were between 100 to 400 litres per day, with a daily average value of 200 l/d.

Main strength of the model is to assess performance of new technologies on the housing stock, only if detailed descriptions on dwelling characteristics and components are provided [54]. However, important data as obstructions, roof slope and orientation still lack to assess introduction of solar technologies.

## 2.7 Solar photovoltaic analysis

### 2.7.1 Potential of renewable photovoltaic technology

Renewable energy resources (RES) are low environmental impact and approximately inexhaustible over time, differently from traditional non-renewable sources, as oil, coal, natural gas. Main RES for electricity production is photovoltaic, wind, hydroelectric, geothermal. Due to environmental benefits and progressive accessibility, the transition process to these energy forms is central for a sustainable low-carbon transition and to reduce the dependence on traditional fuels, which are destined to run out. According to IRENA [55], benefits from renewable capacity will be even more pronounced in 2022, when high fossil fuel prices are likely to continue to rise. Renewable capacity is expected to continue to increase in the years ahead to reduce the impacts of fossil fuels and reach the net-zero emissions targets by national and global policy frameworks. RES can contribute to satisfy the demand of urban environments, among which photovoltaic (PV) demonstrated the highest potential for local micro-generation in the energy mix [56].

Two main solar technologies have been developed in the last 40 years: photovoltaic and thermal. Solar photovoltaic (PV) transforms sunlight into electricity, exploiting the properties of semiconductors of their modules. Solar thermal collectors convert sun energy into domestic hot water, but they are less competitive and less popular. The progressive mass production of PV allowed costs reduction of materials and PV cells (around -90% from 2008 to 2018 [57]) and improvement of their efficiencies [58]. The competitiveness and equal cost with other energy sources led to the rapid development of PV technologies and increasing awareness of solar potentials by customers and governments [4]. Photovoltaic installations have increased in different countries in the last decade: by the end of 2021, over 843 GW of PV systems have been installed globally [55].

Solar cells can be realised with only one (less efficient) or multiple layers of light-absorbing materials [59]. Different materials for PV cells were developed in the last decades, generally distinguished in three main generations. The first generation involves traditional crystalline-silicon modules, as monocrystalline and polycrystalline. Monocrystalline cells are made from a single crystal of silicon while polycrystalline have solar cells composed from a conglomerate of silicon fragments melted together [60]. Silicon modules are the most common considering that costs are lower than for other materials due to large-scale and standardised production [61]. The second generation is composed by thin-film cells. The second generation offers lower production costs and minimise the quantity of used material, but with worse performance [59]. Thin film technology modules are lagging crystalline silicon modules in efficiency, costs, and lifetime. In 2020, only 5% of solar production was covered by thin-film modules [61]. The advantage of thin film consists of the smaller efficiency drop with warmer temperature, which is advantageous for areas with high solar radiation. The third generation includes innovative non-silicon panels and have great potential to increase efficiency while reducing costs. From the more recent family, perovskite solar cells have a great potential to become popular due to increasing efficiency (about 20% tested in laboratory) and low manufacturing costs, despite low stability [61].

PV modules and arrays cover only a part of the system to produce direct current (DC). Indeed, the costs of a whole PV installation depend on both module prices and other balance of the system (BOS) components, which cover the largest economic amount for a solar plant [61]. Although the modu-

le price is shown as price per unit of installed nominal power, the required surface to achieve that electric power depends on the technology efficiency [61]. The efficiency ( $\eta$ ) of the selected PV panels is the share of sunlight converted into power, calculated as the ratio between collected and produced energy. Values of monocrystalline panels varies between 16 and 24% while polycrystalline ranges between 14 and 20% [60]. Most advanced technologies can reach physical limits around 30% for monocrystalline silicon. Together with efficiency, the degradation rate of panels over time also influences the total energy produced from a technological perspective. The degradation rate quantifies the power decline over time. A median value of 0.5%/year has been assessed by [62] on nearly 2,000 measured values on modules from the literature. Higher degradation translates into less power produced and limit future cash flows, which simultaneously depends on PV efficiency [62].

As the efficiency improves, costs of modules increase and, on the contrary, cost of BOSs generally decreases. BOS involve all the components of the PV system expect for PV panels, as inverters, batteries, eventual sensors, mounting structure [59]. However, if BOS components are comparable on the market, the so-called soft costs represent expenses connected with project, land, administration, margins, taxes, etc. Soft costs may vary country to country and with the type of installation, and their share in the total price becomes significant especially for residential-scale PV system [61].

The site selection is a critical point in the installation of solar projects. Changes in irradiation directly determine the amount of produced electricity during the life cycle of the technology [59]. Obviously, locations with higher solar radiation are the most suitable for PV usage. However, solar resources have a low geographic density, an uneven distribution in the globe and a scarce programmability [4]. The amount of solar energy hitting the panels varies with the latitude, the geographical location, and the amount of incident radiation. Outputs depend also on the exposure, inclination, orientation of the panels, but also on the period of the year, local climate, and natural phenomena. Variability or intermittency of solar output determines electricity production only when the weather allows it, or rather when sunlight and atmospheric conditions are favourable [63]. Energy storage contributes to address solar fluctuations and satisfy the demand when production is insufficient. However, the variability and constraints of solar generation related to the surrounding context implies careful assessment to define the most performative areas and estimate the coverable share of electricity.

Solar photovoltaic is generally installed as distributed power generation at the local level. Distributed generation (DG) consists of any energy source of limited power directly (generally, less than 10 MW), connected to the distribution network or stand-alone [64]. Solar DGs can have several advantages compared to traditional utility scale systems. They operate at the back of the meter selling the overproduction to the main grid. Different schemes have been introduced for solar overproduction, as net-metering, with generally size limits of 10-100 kW, and feed-in-tariffs, even if charges are generally lower than the market prices [64]. Distributed local systems contribute to decrease peak load and pressures on the power network, improve reliability of electricity and minimise transmission-distribution energy losses [65]. Distributed energy production maximises the use of existing local resources, based on environmental characteristics and space availability [66], local self-consumption and self-sufficiency [67]. The complementarity of central systems and DGs allow to improve security and reduce the load. DG systems represent a rapid and automatic backup solution, especially with storage, providing energy support for infrastructure in case of emergency conditions (outages, blackouts) and peak demand. On the other hand, the power fluctuation cause by intermittency of solar output remains a great challenge for the integration to the centralised network [68].

Restrictions for solar installations are diffused in urban context, for which PV systems must be integrated to structures. Buildings turned into the largest source of urban space for increasing PV generation, despite unexploited capacity [4] [69]. On residential and commercial scales, the saturation of PV installations depends on the available roof space [66]. The complexity of urban landscapes makes rooftops attractive for on-site PV production [4]. Being the best situated part for solar harvesting, the evaluation of feasible areas is crucial in the implementation of roof-integrated PV technologies, even more in city dense environments [4] [69]. Several factors linked to roof design affect PV performance, such as surface orientation, inclination, shading, and building obstructions. Shading and obstacles mainly derive from adjacent buildings, trees, chimneys, skylights, etc [58]. Existing barriers to a further diffusion of PV technologies can be considered as insufficient awareness about solar potentials and lack of publicly available information about suitable available rooftop surfaces [69].

### 2.7.2 Solar photovoltaic assessment methods

Accurate and easily accessible tools to evaluate distributed PV potential are central to guide appropriate policy and support investments by stakeholders [69]. Planning PV installations requires a consistent analysis of spatial and temporal resource variations [5]. Therefore, it is fundamental to identify technical and geographical limits, from which the assessment of solar potential supports utility planning and grid capacity accommodation [70]. Several methods have been developed to estimate suitable rooftop area and potential PV generation, with different levels of complexity and detail. Most of methodologies consider solar irradiation maps on roof surfaces and geographical information for the respective site [58]. Rather than relying on literature only, project-specific validation methods and criteria are required. However, most of the solar-assessment studies have limited information on the accuracy of results. The validation could be with other computer models, with solar resource data from installed buildings or by physically inspecting buildings [71].

Three main estimations of rooftop available surface in urban settings are identified by the National Renewable Energy Laboratory (NREL), which are influenced by data availability and scale of studied area [4] [71] [72]:

- constant-value methods, which consider typical rooftop configurations and estimate a multiplier applicable to an entire region.

The existing building-based data are used with the rule-of-thumb assumptions to evaluate the proportion of sloped versus flat roofs, the number of buildings with suitable rooftop orientations, and the share of space obstructed by other components. Constant-value methods are simple and not computationally intensive, because the complexity of rooftops and surrounding objects are not considered. Constant-value methods can also exploit correlations between roof areas and population density for estimating the total roof availability in the region [66];

- manual selection methods from sources such as aerial photography, DEM, DSM.

This is a more refine, precise but time-spending approach of identifying suitable rooftop space than constant-value methods [72]. It cannot be applied to large sites or scales [4];

- GIS-based methods, which are the majority and the most effective.

Assumed values for rooftop features are input into a computer model, and the GIS software identifies areas of high suitability. Therefore, they are not made using predetermined constant values or by manually selecting buildings. GIS-based methods adopt primarily 3D models to determine solar values

or shadow effects. 3D models derive from orthophotography or light detection and ranging (LiDAR) data, and they are combined with slope, orientation, and building structure to evaluate the local solar energy generation potential. GIS-based analyses consider the urban environment using DSMs, as the presence of disturbing elements: the more accurate the input data are (e.g., the DSM precision), the better the outputs can return real values [67]. The emergence of LiDAR sources improved mapping for dense urban areas, providing more refined details [4] and interaction of natural and anthropic elements [5]. GIS methodology works for evaluations for cities or zones because high resource requirements do not support national-level analyses [66].

Table 4 sums up the main advantages and disadvantages of the three techniques to identify the feasible rooftop surface for solar PV technologies.

Table 4. Main advantages and disadvantages of methods to assess roof available surface for PV installations.

	Advantages	Disadvantages
Constant-value	<ul style="list-style-type: none"> <li>• Easy to compute and apply</li> <li>• No time or resource-intensive</li> <li>• Applicable to large scales</li> </ul>	<ul style="list-style-type: none"> <li>• Lack of consideration of rooftop features</li> <li>• Extended application of assumptions</li> <li>• Complex results validation</li> </ul>
Manual selection	<ul style="list-style-type: none"> <li>• Detailed</li> <li>• Based on local specificities</li> </ul>	<ul style="list-style-type: none"> <li>• Time-intensive</li> <li>• Not easily replicable and scalable</li> </ul>
GIS-based	<ul style="list-style-type: none"> <li>• Detailed</li> <li>• Replicable in different context</li> <li>• Easily changeable parameters of analysis</li> </ul>	<ul style="list-style-type: none"> <li>• Time and computer-resource intensive</li> <li>• Required expertise</li> <li>• Feasible for limited areas</li> </ul>

Solar radiation estimations can use different solar models, ground-based meteorological stations, or satellite measurements [4]. The most common GIS methodology can work on ArcGIS or QGIS, based on building footprints and/or surface models of the area.

In QGIS, the r.sun module is based on the methodology for distributed computation of solar irradiation and irradiance. The module is raster-based with spatially variable input and output data or as spatially uniform constants. It estimates beam, diffuse, and reflected components of the clear-sky and real-sky global irradiance and irradiation for horizontal or inclined surfaces. Sky obstruction by local terrain features is assessed using DSM or DEM by a shadowing algorithm, which is scalable to different region sizes [5]. The r.sun model has been applied in the web-based tool Photovoltaic Geographical Information System (PVGIS) [73].

The Solar analyst tool in ArcGIS assess the global, direct, and diffuse insolation maps based on the DSM of the studied area. Solar analyst considers the atmospheric effects, latitude, and elevation, daily and seasonal sun position, shadows, and topography related to the DSM while ignoring local weather and temperature. This tool requires the diffuse proportion of global radiation and the transmittivity values adjusted to the local conditions of the region. However, it ignores the ground reflected component, which can increase the assessed solar radiation around 7% for south-facing panels [4].

Table 5 reports a summary of key solar assessment studies which used GIS tools. Studies are reported in chronological order. The solar analysis tool, the considered constraint for solar installation, the usable rooftop and electricity produced (if available) are the aspect considered. Each case study has a different scale of application, which can range to more extended to few buildings.

Table 5. Summary table of representative territorial solar assessment studies.

Authors	Year	Tool	Constraints for suitable roof area	Usable rooftop area	Electricity produced	Scale	Case study
Compagnon	2004	Radiance/Day-sim (simulate lighting scenarios)	min. 1,000 kWh/m <sup>2</sup>	from 6.5% to 21%	-	61 buildings	Fribourg, Switzerland
Pelland and Poissant	2006	Retrieved from Environment Canada CERES	-	40% rooftop, 15% facades	53 TWh, which is roughly 46% of residential electricity	national	Canada
Jofierka and Kanuk	2009	GRASS r.sun (solar radiation tool)	available roof area based on roof types	around 35% of residential and 59% of total rooftop space	more than 25 GWh/y, which is 45% of electricity consumption	urban, with 1440 buildings	Bardejov, Slovakia
Santos et al.	2011	ArcGIS Area Solar Radiation tool	10 m <sup>2</sup> contiguous, more than 1.68 MWh/m <sup>2</sup> of solar radiation, slope less than 45°	49% of total buildings	-	urban neighbourhood of 6 km <sup>2</sup>	Lisbon, Portugal
Nguyen and Pearce	2012	GRASS r.sun (solar radiation tool)	SE to SW facing (90° to 270°), slope within 15° of local latitude	43,440 m <sup>2</sup> , which is 33% of projected areas of all roofs	for mono-Si, 5 MWp from flat and 4.8 MWp from tilted roofs	sample of 100 buildings	Kingston, Ontario
Latif et al.	2012	LIDAR-based, Google Earth	max slope 15°/30°, SE to SW facing, min. 1,000 W/m <sup>2</sup> , min. 2.6 m <sup>2</sup>	-	-	city	Georgetown, Malaysia
Gagnon, Margolis, Melius, Philips, Elmore	2016	ArcGIS Area Solar Radiation tool	at least 80% of energy produced by an unshaded system of same orientation, W to E facing, max. 60° tilt, min. 10 m <sup>2</sup> contiguous	32% of total rooftop area (26% for small, 49% for medium and 66% for large buildings)	overall, 1,118 GW and 1,432 TWh/y, which is 39% of national electricity sale	national, aggregated by ZIP code	47 cities in the US
Kouhestani et al.	2018	GIS and light detection	max 60° slope, no NE to NW facing, min. 10 m <sup>2</sup> contiguous	2,372,000 m <sup>2</sup> , which is around 30% of total roof areas	218 MWp and 301 (+/- 29) GWh/y, which is 38% of electricity	city	Lethbridge, Alberta
Odeh and Nguyen	2021	SunSPoT online tool and PVSYST software	> 4 m <sup>2</sup> suitable area, max 60° slope	from 28.9% to 65.7% by suburb	from 41.03 GWh/y to 75.9 GWh/y and from 68% to 187% (surplus) of covered energy consumption, based on the suburb	400 houses from 4 suburbs	Sydney, Australia

Muhammed et al.	2021	ArcGIS Area Solar Radiation tool, PVGIS	30° tilt angle	26,224.95 m <sup>2</sup> (50%)	9.3 - 8.7 MWh/y	urban	part of Madinaty city in Egypt
Mutani and Todeschi	2021	ArcGIS Area Solar Radiation tool	SE with -60°, SW with +30°, NW with +120° and NE with -150°	different tested scenarios	different tested scenarios (from 41.5 to 35.7% SSI)	7 typical residential buildings	Turin, Italy

Generally, GIS-based approaches have different scales of application. For instance, the method developed by Gagnon et al. [72] includes exclusively the physical configuration of rooftops, which is replicable on a national scale and customisable based on varying PV technologies [71]. Other studies [4] [5] employ techniques that focus more on sunlight and shade obstructions. The level of detail strongly predicts sunlight availability on rooftops but makes it difficult to estimate rooftop availability at larger scales due to the higher amounts of data and intensive computer processing requirements. Despite the level of detail, GIS-based results do not often consider the cost-optimal sizing and the integration of PV installations with the network to offset energy demand. The diffused PV installation requires a flexible grid to support a different generation capacity and the eventual installation of storage [72]. Local distribution requirements could be affected and change under rising levels of distributed PV installations which can work at aggregated scales [72]. The readiness of local energy network can support the exchange of energy surpluses eventually produced, especially for community-scale projects [58].

### 3. METHODOLOGY

This work assesses the energy consumption of residential buildings with a top-down statistical followed by an engineering approach. The consumption calculation is integrated to the assessment of solar potential on rooftops. The case study is the central district of Toronto, Ontario, which is an area corresponding to the Toronto 2030 Platform [6]. The elaboration attempts to balance sufficiently detailed results with the limited availability of data on which models are built.

The steps consist of a multi-scalar strategic methodology to assess the energy consumption and potential solar contribution to electricity for the residential sector:

- multi-scalar means that is developed on two levels of assessment, which are the urban scale (for a whole city or city district) followed by the block scale (by group of buildings);
- strategic because the analyses can be used by policymakers and planners to build line of actions for energy transition of an urban area.

The two scales have different approaches for identifying the energy consumption (electricity and natural gas) and solar rooftop potential (Figure 1):

- a top-down statistical approach and GIS-based solar assessment are performed at the city scale. Aggregated energy data to develop the static regression model are retrieved from the 2030 Toronto Platform, while the GIS solar evaluation is built on a LiDAR Digital Surface Model (DSM);
- an engineering simulation by archetypes is then developed with URBANopt to both assess energy consumption and optimise solar PV. The software package allows a multi-scale calculation for both single buildings and building district.

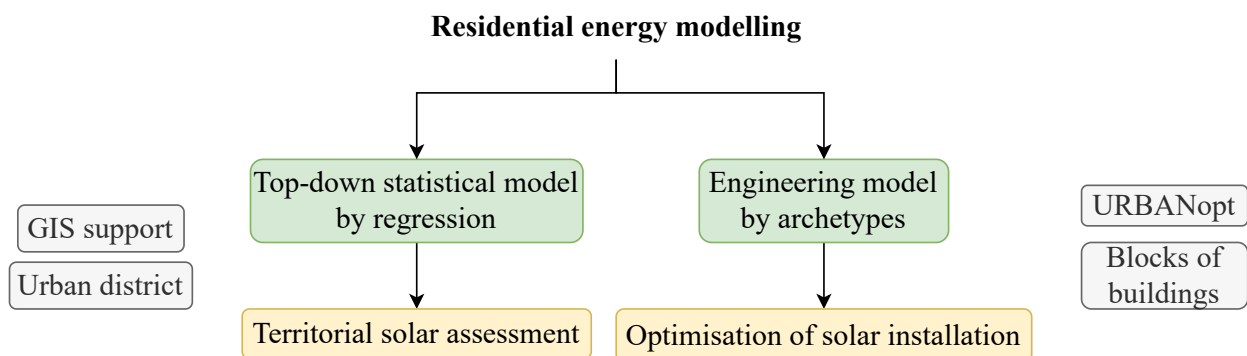


Figure 1. Simplified schema of the multi-scale methodology applied for building energy consumption and solar analysis.

The multi-level elaboration and the integration of different data sources for the urban context make the methodology applicable to other cities. Disaggregation of clustered energy data could be a recurrent challenge in high-density populated areas due to limited spatial resolution, unwillingness to share by providers and privacy constraints [12]. At the same time, the need for more refined evaluation is often required to shape new policies and energy targets for future years. The multi-scalar methodology attempts to address these issues for a complex urban environment.

### 3.1 Available input data

The methodology is based on a GIS environment, where layers with different spatial resolution can be geo-localised and overlapped (Figure 3, Section 3.1). The top-down statistical model will work on three main spatial scales, which are also integrated in the engineering one:

- building
- block of buildings
- neighbourhood.

The model is based on the urban downtown core of Toronto, studied by the Toronto 2030 Platform. The main challenge will be the availability of sufficiently detailed dataset for both functions and energy consumption. Energy consumption data (by energy sources) are disaggregated from block to single building level due to lack of more granular values. As mentioned before, the residential sector has been the most investigated by energy models, even if structures show a significant variability. This study will consider only housing function, distinguishing main archetypes based on the local residential characterisation.

Data sources at different levels provide the following information:

1. from the 2017 building shapefile [74], height and ground floor area, while number of floors, S/V ratio, heat loss surfaces, useful heated surface and air gross volume can be derived;
2. at the block level retrieved from the 2030 Toronto Platform [6], energy consumption for electricity and natural gas based on 2017 (kWh/y), function category and vintage mix (% gross floor area (GFA)), energy use intensity (kWh/m<sup>2</sup>/y), GHG emissions (tCO<sub>2</sub>/y). The block energy modelling applied the ASHRAE 90.1 (2004) templates for residential buildings. Evaluations by single structure were then aggregated by block: indeed, consumption by single building is not available nor displayed by the Platform due to restrictions;
3. from the 2016 neighbourhood profiles for the City of Toronto [75], socio-economic variables, among which population.

The data analysis starts in GIS environment, where the shapefile with building footprints [74] is cleaned from non-habitable and non-heated structures (garages, canopies, patios, etc.): they are not relevant in the consumption assessment and do not have the same features of housing stock. The aggregated block data of energy consumption are then overlapped with single building shapes to obtain an overview of demand distribution and neighbourhood profiles [75].

Building functions are not available for single structure: the building shapefile did not contain single uses, while Open Street Map (OSM) dataset is only partially filled. For this reason, consumption data are considered only for highly residential block (at least, 95% residential of the total ground floor area (GFA) displayed by the Platform [6]). The zoning by-law 569-2013 [76] provides a further validation of residential areas on which the models are based. In case of 95% residential GFA by blocks, the remaining 5% is derived from homogeneous blocks of that remaining function (100% GFA) and then subtracted from the total consumption.

## 3.2 Housing stock classification

Buildings included in the selected residential blocks are classified in main dwelling archetypes. Recurrent residential typologies are identified based on previous studies and surveys (Table 6), in this case for the Canadian context, and then applied to the local housing stock.

Table 6. Classification by dwelling types in Canada from selected studies and surveys.

Source / Type	Year	Housing classification
Survey of Household Energy Use [77]	Data measured in 2015, published in 2017.	Detached, semi-detached, low-rise apartments, high-rise apartments, mobile homes.
Comprehensive Energy Use Database 2020 [43]	Data from 2010 to 2018, published in 2020.	Single-detached, single-attached, apartments, mobile homes.
A residential end-use energy consumption model for Canada [53]	1998	Single-detached, single-attached, apartments less than 5 storeys, high-rise.
Neighbourhood Profiles for the City of Toronto [75]	2016	Single detached, semi-detached, row houses, duplex, apartments less than 5 storeys, apartments more than 5 storeys, movable homes.
Energy consumption trends of Multi-Unit Residential Buildings in the city of Toronto [78]	2012	Low-rise (less than 5 storeys) and high-rise MURBs.

The implemented classification attempts to be comprehensive and distinguish main dwelling differences, avoiding eventual overlapping and having homogeneous conditions in each class.

Four residential classes have been identified with the support of GIS (Table 7), where both the number of floors and the S/V ratio are available for each dwelling. For each residential block, the dwelling type is identified according to the S/V ratio. The S/V value is calculated from the building shapefile as the ratio between heat loss surfaces and heated volume of the structure.

Table 7. Main dwelling types and classification features.

Dwelling type	Main features	S/V ratio range	Mean S/V ratio	Median S/V ratio
Detached houses	No shared wall; between 2 and 3 floors	$\geq 0.6$	0.71	0.67
Semi-detached houses	At least one shared wall with another property	$0.4 \leq x \leq 0.6$	0.53	0.55
Low-rise apartments	Less than 5 storeys; multiple units	$0.3 \leq x \leq 0.4$	0.34	0.35
High-rise apartments	Equal or more than 5 storeys; multiple units	$x \leq 0.3$	0.26	0.25

The classification is based on the urban area considered by the 2030 Toronto Platform. Only urban zones are modelled, without distinguishing urban, rural zones, and outskirts, as in the case of Grand Mendoza [79]. Semi-detached dwellings compose the broader type because it includes other sub-classes considered in the studies. However, a further subdivision would have increased risks of overlapping, especially due to the limited information available at the building scale. Energy consumption will be distinguished by these housing classes, identified for the residential blocks of the central Toronto area. The simplification of housing variety helps to extend the model to the whole Toronto.

### 3.3 Realising a statistical model: from block to building consumption

Aggregated energy consumption data are available only at the block scale (group of buildings), distinguished by energy sources in the 2030 Toronto Platform. Values need to be disaggregated at the single building scale to build then the statistical models. Therefore, two methods are applied to derive dwelling annual demand for natural gas and electricity (Figure 3, Section 3.2): the method by subtraction (paragraph 3.3.1) and the method by equation (paragraph 3.3.2).

In case of 95% residential GFA for the block, the remaining 5% consumption is derived from homogeneous blocks of that function by the Platform and then subtracted from the total energy-use. The comparison of results with provincial data will guide the selection of the most appropriate for assessing building consumption from block values for Toronto.

A methodology flowchart of both methods is reported in Figure 2, distinguishing assessment of preliminary data, aim and steps for the two cases.

#### 3.3.1 Method by subtraction

The method by subtraction is directly based on block consumption data and their relationships. The distinction of building consumption is simple and easy to replicate in other cases.

It consists of finding homogeneous blocks (by function and age) and utilise the block value divided by the useful heated surface (or volume). The energy intensity for specific uses and ages can be extended to other blocks, where the unknown consumption share is then subtracted from the overall demand. According to the category mix at the block level and the distribution of housing types within it, block can be: residentially homogeneous, with at least 95% of GFA covered by that category and 100% block vintage mix; housing mix, with an heterogeneous composition.

The electricity and natural gas intensities ( $\text{kWh}/\text{m}^2/\text{y}$ ) of homogeneous residential blocks derives from the division of the total block consumption for electricity and natural gas by the useful heated surface (UHS, from the building shp. on GIS). The averages of the energy intensities by dwelling type and age are then used for blocks with housing mix. The known consumption ( $\text{kWh}/\text{m}^2/\text{y} \cdot \text{UHS}$ ) is subtracted from the whole block energy value. The remaining consumption is divided by the remaining UHS to obtain the energy intensity of the other dwellings in the block. In this way, an energy characterisation can be easily obtained for the highly residential areas, divided by housing category.

#### 3.3.2 Method by equation

The method by equation follows dwelling relations for energy consumption showed in the national Survey of Household Energy Use (SHEU) [77] for Canada. The survey distinguishes values by the four dwelling types and construction age and reports an extended classification of the household and structure types. This method can be applied to other case studies if an energy survey is available for the consider territory with distinction by representative residential types.

Before describing the equation, it is important to underline that most of detached and semi-detached houses (98%) were built before 1980: the main year of construction is confirmed by the national survey [77]. Homogeneous detached blocks show similar values, especially for energy intensity.

According to the block and building data, the realised equation to calculate single dwelling consumption on an Excel spreadsheet is:

$$\text{Block consumption} = UHS_{DTC} * x + UHS_{SMDTC} * (x * a) + UHS_{LR} * (x * b) + UHS_{HR} * (x * c) \quad (1)$$

where:

- $UHS_{DTC}$ ,  $UHS_{SMDTC}$ ,  $UHS_{LR}$ ,  $UHS_{HR}$  are the useful heated surfaces respectively of detached houses/semi-detached houses/low-rise apartments/high-rise apartments for the selected block, distinguished by S/V ratio on GIS respectively;
- $x$  is the consumption of detached houses before 1980 given by the survey [77] and calibrated to the modelled block consumption;
- $a$  is the multiplicative coefficient given by the share between the calibrated consumption of detached houses before 1980 and of semi-detached houses for the considered age [77]
- $b$  is the multiplicative coefficient given by the share between the calibrated consumption of detached houses before 1980 and of low-rise apartments for the considered age [77]
- $c$  is the multiplicative coefficient given by the share between the calibrated consumption of detached houses before 1980 and of high-rise apartments for the considered age [77].

The multiplicative coefficients are calculated as  $a = 1 - ((C_{DTC} - C')/C_{DTC})$ , where:

- $C_{DTC}$  is the consumption of detached houses before 1980 by the survey [77];
- $C'$  is the consumption to assess.

The Equation 1 firstly needs to identify the  $x$  value, which represents the detached houses consumption of the selected block for electricity and natural gas. In case blocks do not have any detached dwelling, semi-detached houses (or following residential type) represent the  $x$  in the equation. The multiplication between the  $x$  value and the considered coefficient (Equation 1) will identify the energy intensity for the selected dwelling type by energy source. The reference year for each block has been selected according to the higher share of GFA in the vintage mix of the Platform [6] because the age at the single building scale was not available.

The method by equation may be more complex than the subtraction method. However, once the equation is step up with UHS (m<sup>2</sup>) for each dwelling type, results are faster to obtain on an Excel spreadsheet. The suitability of the equation for Toronto relies on the availability of provincial survey which distinguishes data by single dwelling types and by age. In case a detailed residential survey is unavailable for the case study, the method by equation is not suggested because relations of energy consumption among dwelling types cannot be performed.

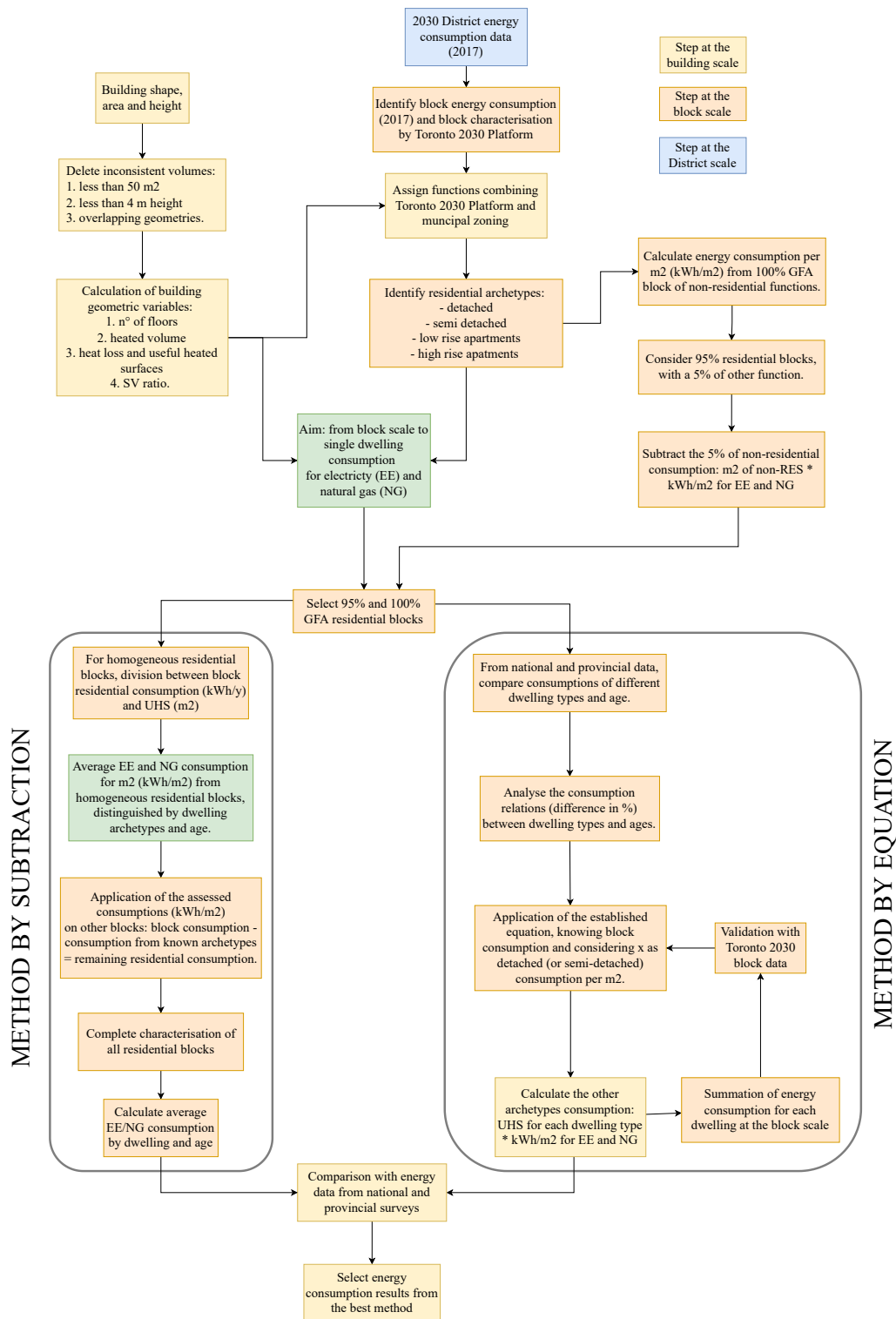


Figure 2. Methodology flowchart from block to building scale energy consumption, with both applied methods.

### 3.4 Top-down statistical models

The comparison of results between the two methods and provincial data allows to select the most appropriate for the residential stock of Toronto. Building values of energy consumption are then used to identify energy end-uses. Energy-end uses by dwelling types and independent building-related variables allow to build statistical regression models (linear or multiple).

#### 3.4.1 Energy uses by dwelling types

The identified electricity and natural gas consumptions by single dwelling determine different energy components in the residential load. The considered uses are domestic hot water, space heating, cooling, appliances-lighting, which are the main end-use outputs. Each energy end-use is assumed to be satisfied by electricity or natural gas according to the database of the provincial survey for 2017 [43]. Domestic hot water (DHW) and space heating (SH) result mainly covered by natural gas, while space cooling (SC) and appliances (App) by electricity (Figure 3, Section 3.3).

Considering the Canadian climate, SC is not a major component even if it is likely to increase with the rising temperature trends based on projections. According to Ontario data for 2017 [43], SC is assessed as 14% of electricity demand for detached houses, 9.4% for semi-detached and 5.1% for apartments. Appliances-lighting cover the remaining part of electrical consumption for the residential sector.

According to NRCan [80], the mean daily DHW per person is 75l for washing, cleaning, showering, bathing. Downscaling the number of inhabitants per buildings from neighbourhood data, the DHW consumption per building and per m<sup>2</sup> have been calculated. Then, the share of annual natural gas used is identified from the block values, through the following equation:

$$Q_{u,d} = V \cdot p \cdot c_p \cdot \Delta T / \eta_{DHW} \quad (2)$$

where:

- $Q_{u,d}$  is the daily natural gas consumption for DHW;
- $V$  is the daily volume of water used per person, assumed as 75l;
- $p$  is the water density (1kg/l);
- $c_p$  is the water specific heat (1.163 Wh/KgK);
- $\Delta t$  is the temperature difference between the outlet (assumed as 49°C) and the inlet (water supplied to the heater, assumed as 11°C) temperature, according to [80];
- $\eta_{DHW}$  is the efficiency of heat exchanger system, considering 0.9 for DHW systems with natural gas boiler.

The result (kWh) from (2) is multiplied by number of days in one year, then number of inhabitants in a building and divided by the UHS (m<sup>2</sup>) to obtain the DHW consumption by m<sup>2</sup>. The remaining share of natural gas demand is assumed to cover space heating for each building.

### 3.4.2 Statistical models to assess residential consumption

The assessed energy use data allows to realise a statistical analysis for estimating residential energy consumption (Figure 3, Section 3.4). The model is based on the central area of the Toronto 2030 Platform and then applicable to the whole City of Toronto. The key point is the identification of independent variables which can influence energy consumption for dwellings. In case of satisfying correlations, linear or multiple linear regressions can be performed and extended to obtain energy profiles. Variables influencing the four energy uses are identified by:

- the Pearson's correlation that is used to measure how a variable is linearly correlated to the considered energy-use;
- the coefficient of determination, which shows that dependent variable can vary with changes of independent variables;
- the significance F, which confirms that the regression is statistically significant, and the p-value <5%, which reports how each variable is statistically significant.

To develop and test the statistical model, the fundamental requirement is the availability of data, which is one of the greatest challenges for the model. Indeed, the lack of functions and age for single buildings limits the development of specific evaluations. Data are based on three levels mentioned before:

- buildings shapefile [74], the most specific but limited to the typological aspects;
- blocks data, from the Toronto 2030 Platform [6];
- neighbourhood profile [75], which are more general but includes socio-economic variables for the residential sector.

Correlations are performed for the disaggregated energy data, distinguishing the four housing types. To be consistent, the  $R^2$  must be higher or equal to 0.6, even if it could be higher in other cases. Indeed, the lack of functions and age by single buildings limited more specific evaluations and higher correlations.

The statistical regressions realised for the area of the Toronto 2030 Platform by energy uses can be then extended to other city areas to simulate the residential building consumption. The building shapefile is necessary to identify typological data, while the 147 Neighbourhood Profiles [75] distinguish the share of housing by age of construction (before 1960, 1961-1980, 1981-2000, 2001-2005, after 2005). The statistical model can be applied only on residential areas identified by the zoning by-law [76] (Table 8).

Table 8. Classification of residential zones based on the zoning scheme. Source: [76].

Zoning code	Zone Type	Permitted dwelling types
10.10	Residential	Detached, semi-detached, townhouse, duplex, triplex, fourplex, apartment building.
10.20	Residential detached	Detached.
10.40	Residential semi-detached	Detached, semi-detached.
10.60	Residential townhouse	Detached, semi-detached, townhouse.
10.80	Residential multiple	Detached, semi-detached, duplex, triplex, fourplex, apartment building.
15.10	Residential apartment	Apartment building.
15.20	Residential apartment commercial	Apartment building.

The steps of the statical model have been summed up in the following schema (Figure 3), divided by:

- collection of data at three different scales;
- disaggregation of energy consumption (electricity and natural gas) from block to building level;
- assessment of residential energy end-uses;
- realisation of regression analyses and identification of the statistical models.

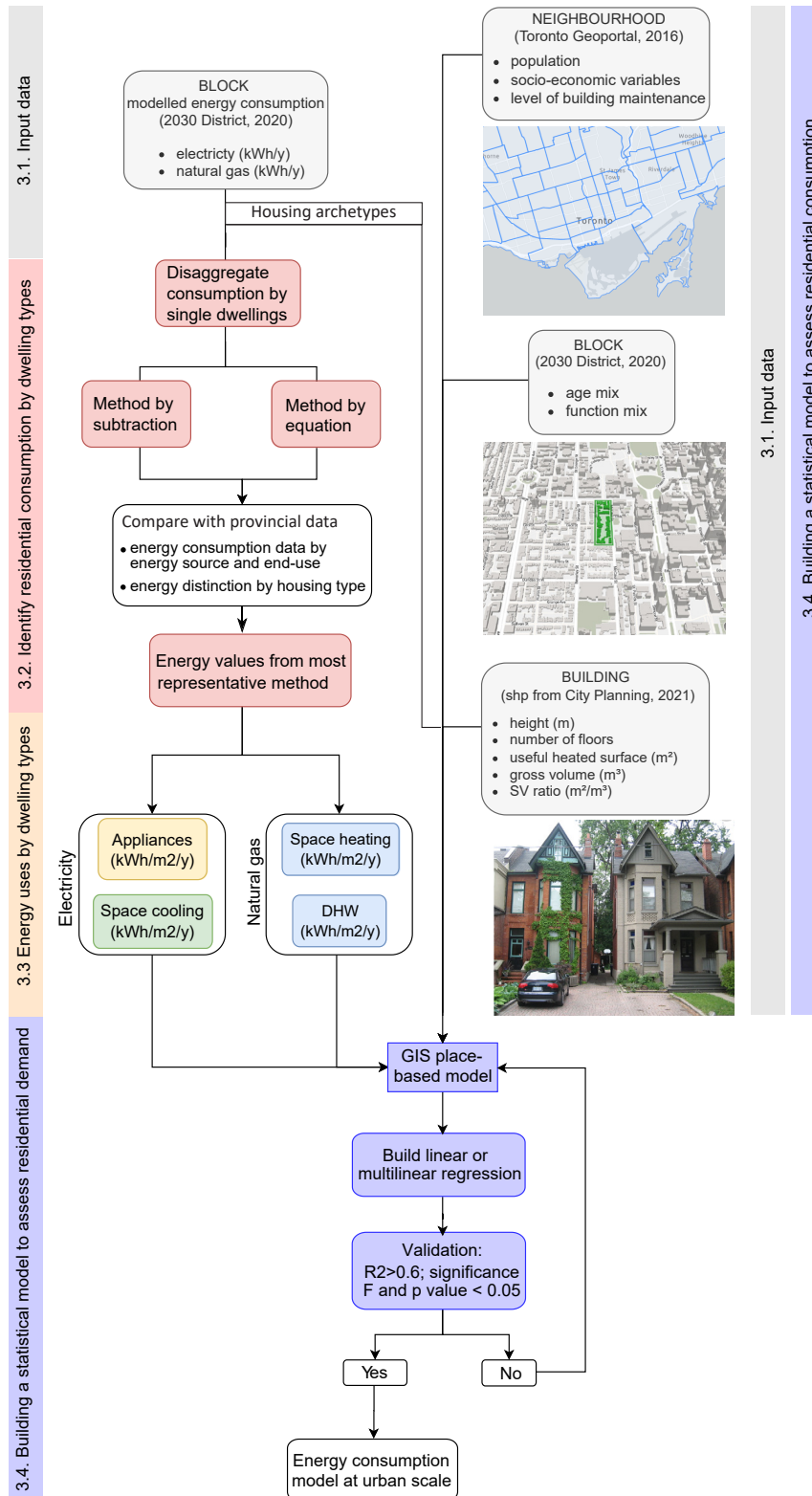


Figure 3. Methodology flowchart with the main steps, from disaggregating energy data, energy-end uses calculation to top-down statistical model.

### 3.5 GIS-based solar PV assessment

The installation of solar technologies can support the transition towards more decentralised energy systems for cities, in which rooftops represent the most suitable areas for residential buildings [81]. Evaluation of solar photovoltaic (PV) output needs to estimate the resource availability, the physically suitable area, and the overall technology's performance.

The rooftop PV potential is calculated for the previous residential buildings to understand the possible coverable electricity share. Roof-mounted equipment is the most feasible and cost-effective option for solar systems in residential applications [82]. In ArcGIS environment, the Area Solar Radiation tool was run on the LiDAR-Derived Digital Surface Model (DSM, year 2015, 0.5 x 0.5m) [83]. The DSM described the elevation for buildings, tree canopies, and bridges, while ground or digital elevation model (DEM) represents only the topography [4].

The area considered by the Toronto 2030 Platform is selected, with the following parameters:

- time configuration: year with monthly interval;
- year: 2017, according to the Toronto 2030 Platform;
- hour interval: 1h, with outputs for each interval;
- calculation directions: 16;
- diffuse model types: standard overcast sky;
- diffuse proportion and transmissivity are calculated respectively from PVGIS portal [73] and Meteororm software [84], with coordinates for the Toronto city hall.

Diffuse radiation and transmissivity are grouped according to the average daily hours of light per month. The grouping criterion follows the standard deviation from the average value of hours of light for all months. For the four intervals ( $\mu + SD$ ,  $\mu + 2 SD$ ,  $\mu - SD$  and  $\mu + 2 SD$ ), the mean diffuse radiation and transmissivity are inserted to launch the GIS elaborations. For each folder created by the Solar Radiation tool, only the considered months from the respective interval are selected for a total of 12 shapefiles (1 per month). Results of the Area Solar Radiation tool are then converted with "Raster to point" tool, aggregated in only one shapefile and joined by location with the building polygons. The grid-code for each month represents the monthly solar radiation (Wh/m<sup>2</sup>), from which the annual cumulative radiation (kWh/m<sup>2</sup>/year) and average daily radiation by month (kWh/m<sup>2</sup>/month) can be calculated.

In this work, three recent PV technologies has been selected considering their efficiencies  $\eta$  (Table 9): monocrystalline silicon (InP crystalline cell,  $\eta=0.24$ ), polycrystalline silicon (GaAs multicrystalline,  $\eta=0.18$ ), and thin film (CzTS thin film,  $\eta=0.11$ ) according to updated efficiency values in 2021 [85]. However, PV module efficiency is expected to keep improving in the next future [72].

Table 9. Technical characterisation of selected PV technologies. Suorce [85].

Classification	Efficiency (%)	Fill factor (%)	Voc (V)	Test centre
InP crystalline cell	24.2 ± 0.5	82.6	0.939	NREL
GaAs multicrystalline	18.4 ± 0.5	79.7	0.994	NREL
CzTS thin film	11.0 ± 0.5	69.3	0.7306	NREL

The results of incident solar radiation are calculated to obtain the PV electrical potential production as:

$$E = PR H_s \eta_{pv} S \quad (3)$$

where:

- E is the electrical energy produced by year from PV (kWh/y);
- PR is the performance index of an implemented system ( $\approx 0,75$ ) [4] [86];

PR compares the actual annual AC energy and the expected DC output of an ideal PV system, including losses at the same location. PR is strictly influenced by actual insolation, various losses (shading, module efficiency, and system losses). McKenney et al. [87] realised spatial models of global insolation and PV potential for Canada assuming a PR equal to 0.75. Pelland and Poissant [88] evaluated the potential of building integrated photovoltaics (BIPV) in Canada with PR equal to 0.75 for PV systems. Therefore, 0.75 is the considered value for the territorial solar assessment.

- $H_s$  is the cumulative annual solar radiation (kWh/m<sup>2</sup>/year);
- $\eta_{pv}$  is the conversion efficiency of PV modules [86];
- S is the net surface of the PV module (m<sup>2</sup>), assumed as 40% of the roof area;

This is roughly the portion with better solar exposure, based on results of previous studies [4] [89] [90]. Pelland and Poissant [88] considered a 40% rooftop area for residential buildings in the PV analysis for Canada, which is in line with results for other assessments analysed in Table 5. At the same time, solar panels generally require an installation area 2.5 times greater than their own surface, which entails that around 40% of the suitable projected area is devoted to PV modules [91]. This first step consists of a constant-value method for identifying suitable areas, keeping a GIS support.

However, the suitable roof surface by equation (3) represents only an estimated and provisional value. Different locations must have specific attributes, which can be retrieved from two previous studies. The SolarTO map [92] is an online tool already available to assess the solar output for the City of Toronto, based on a GIS methodology. The solar assessment on the city of Lethbridge, Alberta [4] introduces a multi-criteria GIS-based approach to estimate solar PV potential of buildings. This second approach allows to have a more accurate identification of suitable area to install solar panels, based on features and local constraints of residential rooftops (see Table 5).

Starting from these two characterisations, constraints are added to obtain more precise results:

- the minimum available roof area should be 30 m<sup>2</sup> [92];
- single areas on the same roof should be greater than 10 m<sup>2</sup>, which is equal to a 1.5 kW system with a 15%-efficient panel feasible for a residential production [4] [72];
- area should receive at least 800 kWh/m<sup>2</sup>/y of annual solar radiation [92];
- roof slope should be equal or less than 45° [92].

The slope is assessed with the Slope (3D Analyst) tool in GIS and then the required slope interval is selected by Raster Calculator. The optimal angle for PV panel is 35° by PVGIS [73]. The optimal PV tilt angle varies with latitude. Tilt angles equal to latitude generally produce more annual electricity than others, while those with slopes greater than latitude generate more constant production but have lower annual output [4]. Lower slopes have higher production in summer, whereas steeper tilt angles favour generation in winter. Higher slopes reduce the difference between summer and winter energy production, and the annual energy flow is more consistent. Lower slopes determine fluctuation of generated electricity, with a remarkable seasonal change;

- rooftops should face South or South-East, which are the optimal orientation, while the SolarTO [92] platform excludes only the north-facing area.

For the Toronto municipal town hall, PVGIS [73] assesses -2° as optimal azimuth angle for PV instal-

lation. Solar panels towards a specific direction maximise performance. Azimuth (Aspect) identifies the direction that the surface slope faces at the installed location [4]. The roof exposure is calculated with the Aspect (Spatial Analyst) tool in GIS which categorised surfaces into nine classes. Then, the Raster Calculator selects only the South (157.5-202.5°) and South-East (112.5-157.5°) surfaces, as shown in Figure 4.

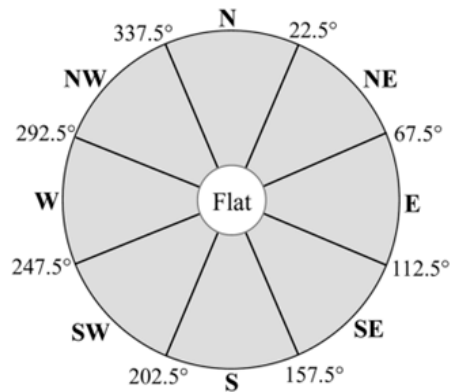


Figure 4. Rooftop azimuth classes identified by the Aspect tool on ArcGIS. Source: [4].

Selected area of Raster files from the Aspect and Slope tools are then converted into polygons, which are the feasible rooftop surfaces to install PV panels. Some areas can be shared between two roofs, and they require to be properly split. Therefore, the building polygon are exploded (Merge to Single part) and then converted into lines. Lines separate the polygons of feasible portion for solar installation into distinct features. In this way, miscalculations among rooftops are avoided in case of adjacent buildings.

12 Joins by location (respectively one for each month) allow then to match the usable areas with the average solar radiation, given by the grid-code in Wh/m<sup>2</sup>. The “contain” match option is selected and the grid-code field is calculated as mean value of all points within that polygon.

The same building can contain more than one feasible area, especially in case of row houses or low-rise dwelling which are described by only one polygon. Therefore, areas in the same roof are aggregated by the Summarise tool, with the rule “sum” for all the feasible surfaces and “mean” for grid-code solar radiation of each month.

From the grid-code solar radiation, the annual, mean monthly and mean daily values can be assessed. Only residential blocks selected for the statistical models are analysed. The previous equation (3) is applied to identify the electrical output by month for each building, having three different PV technologies.

The equations by the statical model for electricity determine the consumption for appliances and space cooling for each dwelling. The balance between PV output and electrical residential consumption is firstly performed annually and then monthly, due to the non-linearity and solar discontinuity, especially during winter months [86]. At the same time, summer months can show an additional load for space cooling. Projections include an increase of cooling loads also in Canadian cities due to rising temperature trends for climate change [93].

### 3.6 Engineering optimisation model

The second part of the methodology consists of shifting the analysis at the block level, with an engineering model by residential archetypes. The variability of building energy consumption and the integration of local renewable energies is implemented in several energy modelling tools. Each software is more suitable for a specific scale of analysis, as single building or district, and related data elaboration. URBANopt is chosen because the aim is to work not only on the single building scale, but also on the block energy relations. The main steps of the methodology are reported in Figure 5, including the adopted tools, the input data for the simulations of building consumptions and PV optimisations until the cost-optimal analysis for different solar installations.

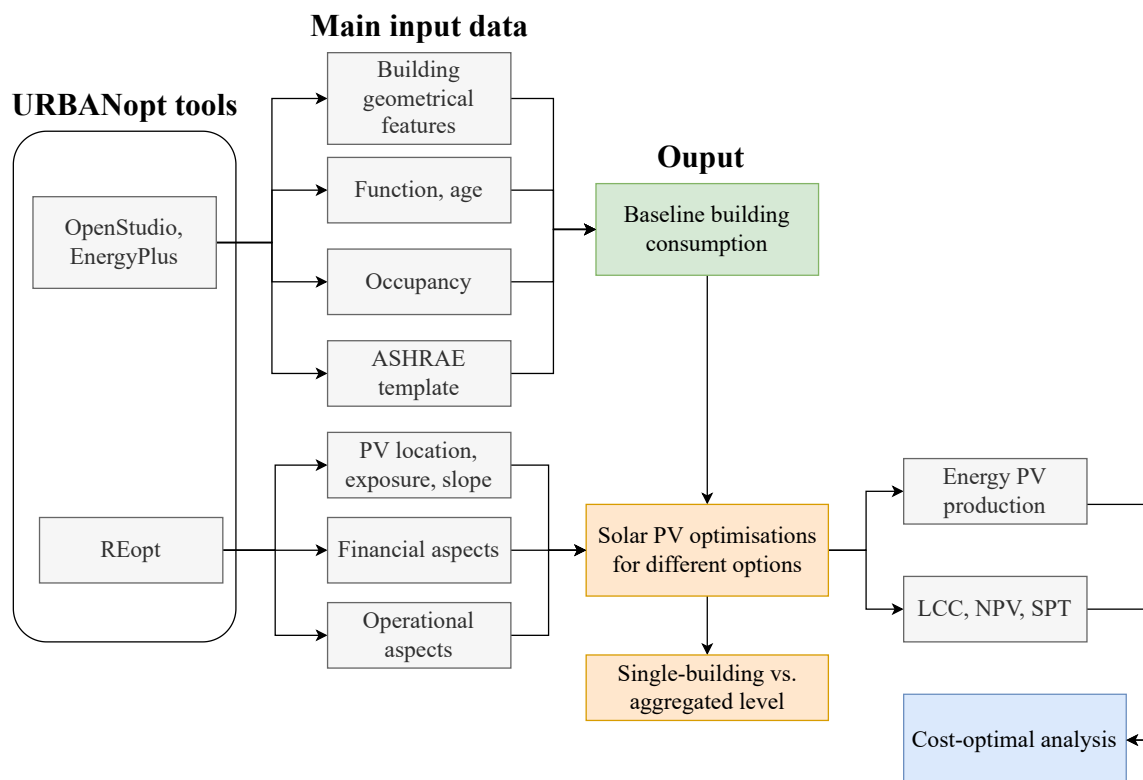


Figure 5. Methodology steps for the block-scale evaluation with URBANopt.

#### 3.6.1 URBANopt as a simulation tool

The aim of the evaluation is not a detailed and punctual analysis of single components of dwellings, but rather start from the single to understand how to integrate solar PV of a group of dwellings in an urban context. The adopted simulation tool is the URBANopt package (Urban Renewable Building and Neighbourhood optimization) which addresses the evaluation of building consumption and optimisation of solar installations. URBANopt works at the block-district scale, without focusing on the single structure only. Evaluations often consider PV as standalone interventions on rooftops which satisfy only the demand of the considered building. URBANopt attempts to estimate the integration of technologies in a wider scale, considering their fluctuations, relation with the main network and eventual impacts on the load. Block-scale evaluations can be applied to consumption and implementation of new technologies, mainly solar PV.

URBANopt is a simulation open-source platform based on EnergyPlus and OpenStudio, developed by the US National Renewable Energy Laboratory (NREL). It is a software kit of open-source modules and not a user interface or end-user tool. The modules can be customised to perform new workflows for urban design, as the interactions between buildings, distributed energy resources (DERs) and electrical distribution network [94]. These tools can be applied in real-life assessments to support decisions from stakeholders and policymakers [94]. In 2016, URBANopt was introduced to simulate the energy performance of low energy districts, including district heating and cooling systems. Primary use cases for URBANopt are represented in Figure 6, from modules on single buildings up to district energy systems. The interest of this study are the first two sections to estimate the dwelling consumption and optimise solar PV on rooftops for a group of structures.

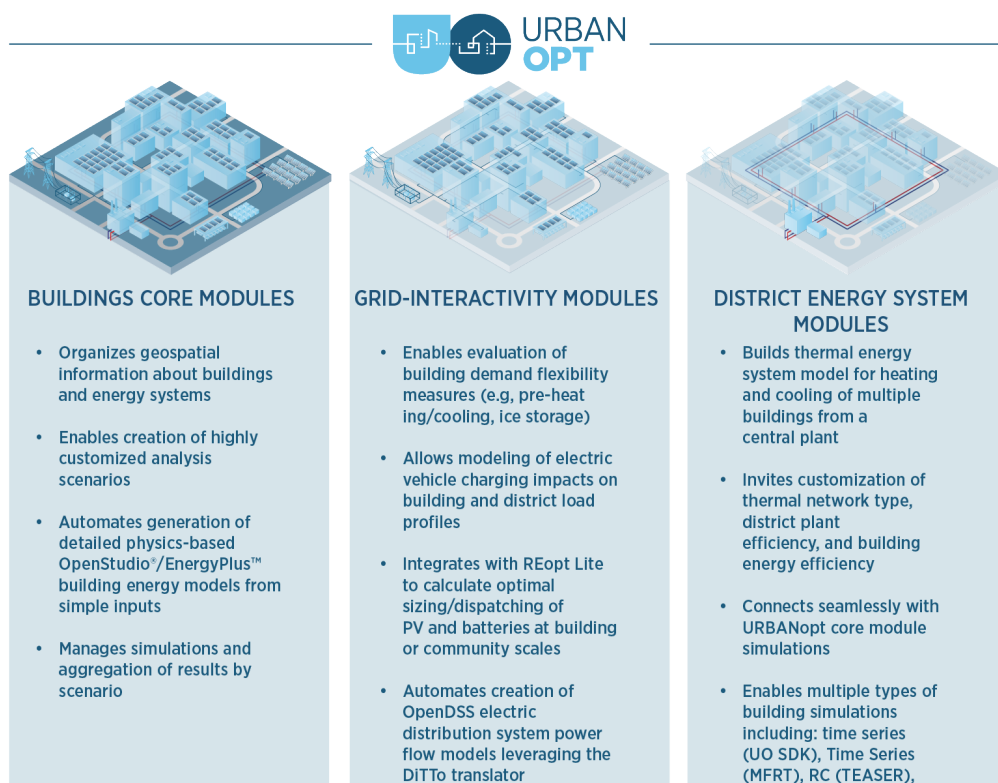


Figure 6. Diagram of different URBANopt modules and technologies to enable each capability. Source: [7].

URBANopt runs simulations with REopt Lite API to optimise RES installations. REopt Lite is a technical and financial decision-making tool for cost-optimal design of DERs, such as PV, battery storage, wind, and generator technologies. The REopt model was realised to assess assets, decision variables and identify a cost-optimal solution and sizing. Customer's energy requirements, local specific goals and constraints should optimise behind-the-meter energy assets [95]. Inputs for REopt model can be classified in site-specific (as consumption and costs for all loads), technology features and other drivers of optimisation. Outputs include sized technologies, dispatch strategies, and financial parameters in the project lifecycle [95]. REopt uses Radiance to assess the production of PV systems in a 3d model, based on the hourly solar radiation. Radiance is widely used and includes reflections from natural and anthropic obstructions in its evaluations [52]. REopt results can be optimised at the single building scale, which optimises each structure's load individually, or scenario level, which assumes the district as an aggregated load. Both cases are performed for the selected residential blocks to identify which could be the most advantageous option for solar PV technology.

### 3.6.2 Baseline scenario

Simulations on URBANopt are performed for the residential blocks of the 2030 Toronto Platform (residential GFA  $\geq$  95% of block GFA), previously used for building the statistical model.

Building footprints [74] in GIS are used as starting point for the identification of main properties, which must be inserted in the workflow to assess energy use intensity (EUI, kWh/m<sup>2</sup>/y) and consumption. The residential modelling archetypes that the version 8.0.2 of URBANopt support are:

1. single-family detached
2. single-family attached
3. multifamily, which will include low and high-rise dwellings.

Each archetype works on OpenStudio models, which can be customised by the user. The default characterisation can be changed according to the housing stock, to the available set from URBANopt. and optional-compulsory fields for each residential feature. Some information has been directly assessed on GIS while others from previous studies on downtown Toronto housing stock.

The shapefile of building geospatial information is directly available on GIS, with division in blocks as provided by the 2030 Toronto Platform. The used coordinate system is EPSG:4326 (WGS 84) and the format is further checked in geojson.io website [96] to avoid any error during the data elaboration.

Geometry and occupancy calculated in GIS are:

- year built (retrieved from the Platform) and building status (existing);
- floor area (ft<sup>2</sup>), as footprint area multiplied by number of stories;
- number of stories (above and below ground), retrieved from building height. Both detached and semi-detached have been considered with a basement (floor below ground), while mid and high-rise without it;
- number of stories above ground, retrieved from building height in the building shapefile [74];
- footprint area (ft<sup>2</sup>), retrieved from building area in the building shapefile [74];
- number of occupants, which must be divisible by the number of residential units and defaults is the total number of bedrooms in the building. It is calculated from the neighbourhood data as average residential density (inhabitants/m<sup>2</sup>) (see Paragraph 3.4.1);
- number of residential units, which is required for single-family attached and multifamily residential buildings. The number of inhabitants per residential unit has been retrieved from the neighbourhood profiles [75] and then applied according to the number of occupants;
- number of bedrooms, required for residential buildings and must be divisible by the number of residential units. Neighbourhood profile reports the average number of occupants per bedroom: from the number of occupants, the number of bedrooms for each dwelling has been retrieved.

The information of building components and thermo-physic properties are checked from recent studies of housing stock for the central area of Toronto, which analysed the characterisation of different dwelling archetypes:

- for detached and semi-detached, Jermyn (2008) [97], Blaszak (2010) [98], Niger (2016) [99];
- for low and high rise, Binkley, Touchie, Pressnail (2012) [100], Huang (2012) [101], Alsaadani et al. (2016) [102].

The previous studies are integrated to two different ASHRAE frameworks:

- • detached and semi-detached are only considered by the Residential IECC 2006, while previous ASHRAE templates did not distinguish low-density housing;

- low-rise and high-rise are joined in midrise apartments in the DOE reference standard for dwellings realised before 1980 and after 1980, while multifamily is the category in the Residential IECC for more recent buildings. However, the current version of URBANopt does not support anymore the DOE Midrise framework. For this reason, the descriptive input files are modified based on the pre 1980 and 1980-2004 values and verified with the previous 3 studies.

ASHRAE elaborations are recognised, widely used in energy modelling and were applied for the realisation of the 2030 Toronto Platform.

The ASHRAE framework varies with different climatic zones. The calculated hourly energy consumption profile is based on the typical meteorological year (TMY), diversified by climate zones too. The insertion of Canadian weather file caused crashes in the elaboration because a URBANopt function of climate zone for the residential workflow does not have a mapping of locations outside of the US. Therefore, the weather file is selected for the city of Buffalo, New York in the US, which is included in the same climate zone of Toronto (5A).

The obtained shapefiles are then converted in GeoJSON format. The GeoJSON files with the full residential characterisation are launched in a Git Bash terminal for the baseline scenario (business as usual). The software distinguishes the energy consumption components for heating (space and water), cooling, appliances and lighting.

### 3.6.3 Solar optimisation

The simulation of the baseline scenario is the starting point for the solar optimisation in URBANopt. The dwelling rooftops can be used to install PV panels to cover an annual share of electricity. The assessed consumption and the economic feasibility guide the possible PV sizing with REopt.

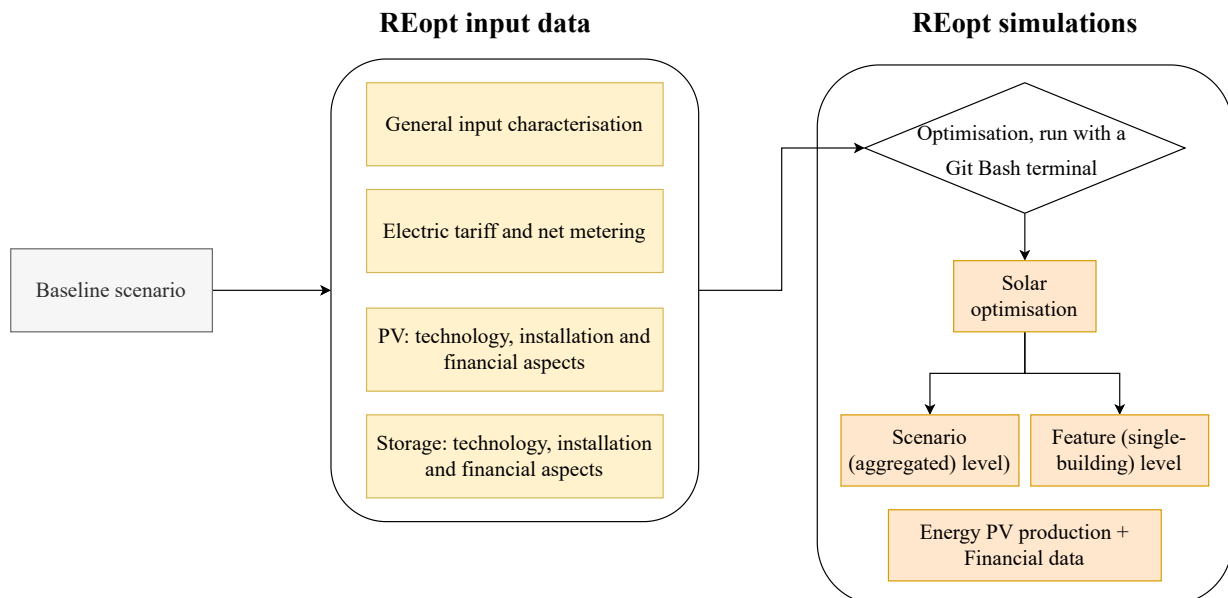


Figure 7. Summary schema of input data and steps for simulations in REopt, included in URBANopt.

Solar analyses are performed for rooftop installations for on-grid scenarios, with time steps of 1 hour [95]. Ground and community configuration are not feasible in an urban dense area as Toronto downtown, even if they might be interesting in less dense and outer zones. Input data about the installable

technologies are required for both technical and financial sides. Latitude and longitude coordinates of the site are used to identify renewable energy resource availability and climate impacts on load profiles [95]. REopt requires NREL geographical information datasets to calculate the renewable production profiles. The hourly solar irradiance values are from TMY3 data from the 1991-2005 National Solar Radiation Database [95]. The evaluation engine Radiance determines the solar radiation including the building dimensions, orientations, and reflections of surrounding objects.

The required set of parameters are summarised in Figure 7 and explained in detail below.

### ***General input characterisation***

- On grid – off grid simulation
- Annual nominal operation and maintenance (O&M) cost escalation rate: 0.02 [62]
- Annual nominal utility electricity cost escalation rate: 0.05 [92]
- Analysis years: 25 [4].

A solar PV array is expected to last 25 years with periodic maintenance, while the inverter will need to be replaced once during. The replacement cost is included in the annual maintenance costs.

### ***Electric Tariff***

- Net metering limit: 500 kW for systems by the Ontario Reg. 541/05 Net Metering [103], based on the maximum output capacity of the equipment.

In Ontario, net metering consists of a billing arrangement between an electricity customer and their local distribution company. The customer can generate electricity only from renewable sources while remaining connected to the main electricity grid. When overproduction occurs, the electricity surplus is sent to the grid for a credit on the electricity bill. The credits can be carried over for up to 12 months and the agreement can be renewed. Billing is calculated by subtracting the value of the electricity amount return by the local generator from the value of the electricity consumed from the generator. Bills are calculated by the distributor for the eligible renewable generator in two ways [103]:

1. If  $D + E \leq C$ , then  $A = B + C - (D + E)$
2. If  $(D + E) > C$ , then  $A = B$

where:

- A is the bill price in the billing period, generally monthly;
- B are the total charges that are not calculated based on the customer's electricity consumption by the distributor;
- C are the total charges for consumed electricity by the generator from the distribution system during the billing period. C is the value of electricity consumption;
- D is the total values of electricity returned during the billing period to the distributor by the generator. It is calculated on the same basis of the customer's consumption of electricity but without adjustments for total losses;
- E are collected electricity credits that have not been used in the previous billing period.

In any billing period where  $E + D - C$  has a positive value, E is assigned for the calculations of the next billing period. In all other cases, the value of E is equal to \$0 for the following period. In case the value of E has been positive for 10 months for all billing periods, the distributor reduces the value of any remaining electricity credits to \$0 and E is set to \$0 for the next billing period.

Before 2021, net metering in Ontario was limited to only a single electricity user with renewable

generation connected behind the meter. As a result, the model was unfeasible for community-scale renewable generation. In September 2021, the community net-metering model was introduced for demonstration projects with Ontario Re. 679/21 [104]. Electricity surplus on site can be sent to the grid for a credit, which are shared among multiple residents and businesses. In case of solar, buildings or other spaces with more roof surface could host larger generation and other less suitable could still share the credits to lower energy bills. Currently, demonstration projects are limited to a 10 MW for a 10-year term (until 2028), selected on a case-by-case basis [105]. In scenario-level optimisations, 10 MW is applied as limit to access to community net metering.

For net-metering, the electricity sold back to the grid is purchased at the existing Time-of-Use (TOU) rates. In this case, the considered TOU rates for 2017 are explained below.

- Interconnection limit: 10 kW for micro-generation, considered as a residential user by the company Hydro One [106].
- Utility label: Label attribute of utility rate structure from <https://apps.openei.org/IURDB/> REopt accepts complex tariff structures with both peak demand charges and time of use (TOU) consumption rates. Rates are queried from the OpenEI Utility Rate Database and the utility websites themselves [95]. The serving company in the central area of Toronto is the Toronto Hydro Electric System Ltd and the Residential Time of Use Rate (TOU) is considered.

The TOU rates vary according to the demand. Rates are cheapest when demand is lower, as during evenings, on weekends and on holidays, and higher prices in peak hours. People use electricity differently depending on the season: a summer (May 1-October 31) and a winter (November 1-April 30) set are established, keeping cheapest rates all day in weekends and on holidays. In summer months, electricity peaks are registered in the hottest part of the afternoon, when air conditioners are generally on. Winter limited daylight means two electricity-use peaks, or rather in the morning and in late afternoon. In Ontario, most of the baseload power derives from sources like nuclear and large hydro-electric plants, which run all the time. During high demand times, if all the baseload power is used, the province adopts other sources like natural gas-fired generation, which typically costs more than baseload [107]. Therefore, the TOU rate distinguishes are three periods (Figure 8; Figure 9):

- off-peak, when electricity demand is lowest and when Ontario households and small businesses use most of their electricity, nearly two thirds of it;
- mid-peak when demand for electricity is moderate. They are during daytime, but not the busiest;
- on-peak when demand is highest and are the busiest times of day.

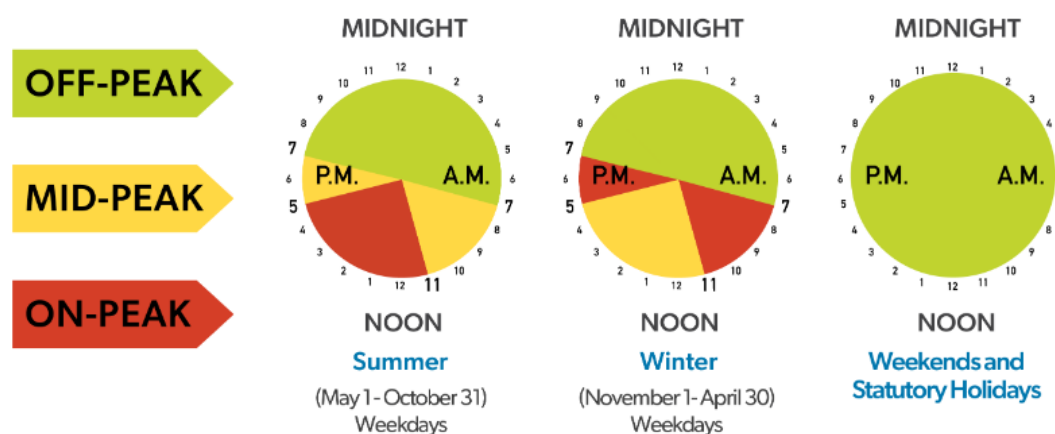
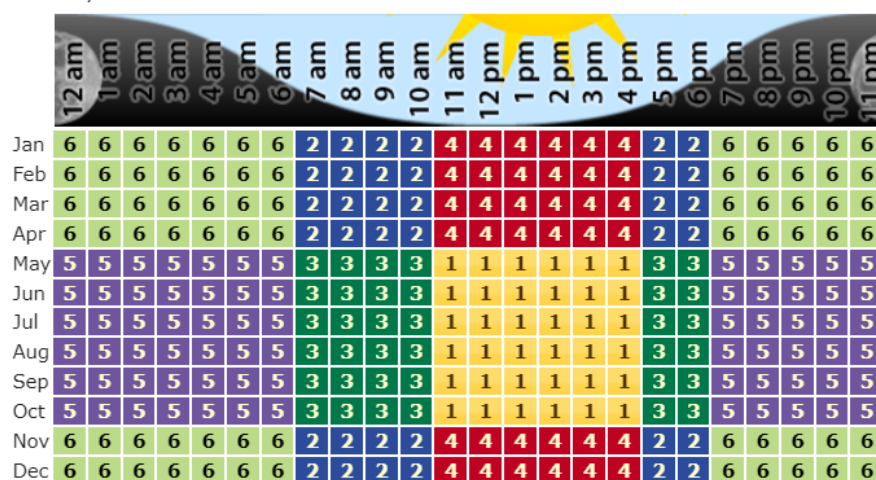


Figure 8. Electricity time-of-use rate periods in summer; weekends/holidays, and winter by the Toronto Hydro Electric System Ltd, Residential Time of Use Rate. Source: [107]

Weekday Schedule



Weekend Schedule

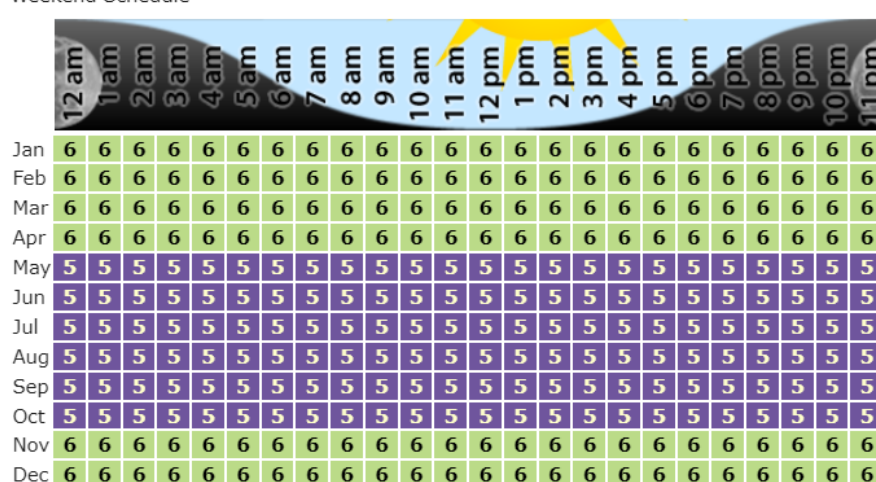


Figure 9. Weekday and weekend schedules, based on utility period and costs for the Toronto Hydro Electric System Ltd, Residential Time of Use Rate. Source: [108].

All consumers pay a share of global adjustment, which is already included in the TOU tariffs. For most electricity companies, the global adjustment is the difference between the guaranteed price and the amount the generators earn in the wholesale marketplace [107].

Table 10 reports the rate for 2017 which are used in the simulations and the rates for November 2022 to April 2023. The more recent prices are slightly higher than in 2017: this could be due to multiple factors, as the war in Ukraine, the long-term impacts of Covid19 and the evolution in demand.

Table 10. Tiered energy usage charge structure by the Toronto Hydro Electric System Ltd, Residential Time of Use Rate. Source: [108].

Period	Rate 2017 (\$/kWh)	Adjustments (\$/kWh)	Rate November 1, 2022-April 30, 2023 (\$/kWh)
1	0.132	0.074082	0.151
2	0.132	0.074082	0.151
3	0.095	0.028022	0.102
4	0.095	0.028022	0.102
5	0.065	0.026894	0.074
6	0.065	0.026894	0.074

***PV technology and financial side***

REopt can integrate multiple technological features and constraints in the simulation. It can also consider any available federal, state, and local incentives for renewable technology, including cost-based incentives, production-based incentives, and tax incentives [95].

Fixed information applied for the three PV technologies are:

- location: roof.
- Roof-mounted PV characterises residential installations, where panels are attached to the roof plane with standoffs that allow limited air flow between the module and roof surface [109].
- annual PV O&M cost per kW (US\$/kW/y): 20 US\$/kW/y [62].
- O&M includes asset cleaning, administration costs, replacement of broken parts and inverter [109].
- MACRS years - Duration over which accelerated depreciation will occur (set to zero to disable): 5
- MACR bonus - Percent of upfront project costs to depreciate in year one in addition to scheduled depreciation: 1
- MACR reduction - Percent of the ITC value by which depreciable basis is reduced: 0.5
- percentage of capital costs that are credited towards federal taxes: 0
- percentage of capital costs offset by state incentives: 0
- state rebates based on installed capacity: 1,000 (\$/kW) from the Canada Greener Homes Grant [110].
- maximum state rebate: 5,000 \$ for detached and semi-detached and 20,000 \$ for MURBs<sup>1</sup>, based on the Canada Greener Homes Grant [110].

The Canada Greener Homes Grant offers a grant to install solar PV system (panels and an inverter) that converts sunlight into electricity. To be eligible, all the equipment must be purchased in Canada and the total system peak power capacity must be at least equal to 1.0 kW DC. High-rise buildings are not included in the grant, but owners can access to the High-rise Retrofit Improvement Support Program (Hi-RIS) [111]. Owners can make an agreement to undertake improvements to reduce energy and water consumption, financed by the municipality. Once works are completed, a special charge is added to tax bills for a range from 5 to 20 years, with a fixed rate on the property. The special charge is equal to the sum of cost of improvements, cost of borrowing and administrative costs incurred by the City. However, the Hi-RIS is not considered in the simulations because it is not an incentive but a form of credit.

- annual rate of degradation in PV energy production: 0.005 [62] [92].

The production of PV technologies tends to decline in time and the REopt model only optimizes over one year. Therefore, the economic production profile considers a yearly degradation [95].

- azimuth angle: 178, based on PVGIS [73].

For a fixed array, the azimuth is the angle clockwise from North describing the faced direction. For the northern hemisphere, increasing the azimuth favours afternoon production, while decreasing it favours morning energy output [109].

- PV system performance losses: 0.14 [67] [72].

The considered losses are the following:

<sup>1</sup> A low-rise Multi-Unit Residential Building is defined by the Part 9 of the National Building Code of Canada (1971) as a dwelling three or fewer storeys above ground and with area not exceeding 600 m<sup>2</sup>. MURBs must either be stacked (up/down) or have a common area. Retirement homes, townhouses and side-by-side attached units/houses are not MURBs [101]. MURBs over three storeys above ground or over 600 m<sup>2</sup> in area are not eligible for the Canada Greener Homes Grant.

Table 11. Values of PV system losses considered in the URBANopt simulations. Source: [109].

Category	Value (%)
Soiling	2
Shading	3
Snow	0
Mismatch	2
Wiring	2
Connections	0.5
Light-induced degradation	1.5
Nameplate rating	1
Age	0
Availability	3

- PV array type: 1 - Rooftop, Fixed. (Other options are 0: Ground Mount Fixed (Open Rack); 2: Ground Mount 1-Axis Tracking; 3: 1-Axis Backtracking; 4: Ground Mount, 2-Axis Tracking)
- PV DC-AC ratio: 1.2 [4] [72].

A direct current to alternating current (DC-to-AC) relation of a system is the ratio of the nameplate capacity of PV modules to the AC-rated capacity of inverters. It should minimise the cost of solar produced electricity. For example, a system with a DC-AC ratio equal to 1.2 would have 8.33 kW of inverters installed for every 10 kW of PV capacity [72]. For a system with a high DC to AC ratio, when the array's DC power output overcomes the inverter's DC input size, the inverter limits the array's power output by increasing the DC operating voltage. A common and feasible range is 1.10 to 1.25, although large-scale systems can achieve 1.50 [109].

- PV inverter efficiency: 0.96 [72]
- PV system tilt: 35°, which is the optimal slope for Toronto based on [73].

For a fixed installation, the tilt angle is the angle from the array horizontal, where 0° = horizontal, and 90° = vertical. Angles between 23° and 56° above horizontal (0°) are recommended [82].

A tilt equal to the latitude does not necessarily maximize the annual output: lower tilt angles support peak production in the summer, whereas higher angles have lower irradiance in winter months. A lower tilt angle can minimize costs of racking and mounting hardware, or risks of wind damage. Generally, tilts greater than the location's latitude support energy production in the winter, while angles less than the site latitude in the summer [109]. PV systems are typically intended to maximise summer production [82]: therefore, the 35° mounting angle is chosen.

- PV ground cover ratio: 0.4 for gable roofs [4], 0.7 for flat roofs [72] of the total available roof area. Indeed, suitable surface for PV is limited by technological and structural constraints [95].

The financial values of the three technologies are selected based on NREL studies and the evolution of PV prices. BOS and soft costs cover a significant part of the overall amount, as mentioned in paragraph 2.7.1. Rather than panel prices, installation costs are related mainly for its manufacturing, labour costs, and market-related variables as illustrated in Figure 10. The power optimiser option is the considered one as weighted average between installer and integrator. Power optimisers allow designs with different roof configurations (orientations and tilts) to track the maximum power, providing optimised solution at the module level. Power optimiser solutions also reach the highest market share in residential sector (37%), based on 2018 levels [112]. The weighted average for PV power optimiser

option is 2.59 US\$/W DC, in which 0.47 \$ is estimated by NREL to be covered by an average module costs. The share of PV panel price in Figure 10 for power optimiser-weighted average is changed with more updated costs for the three technologies (Table 12).

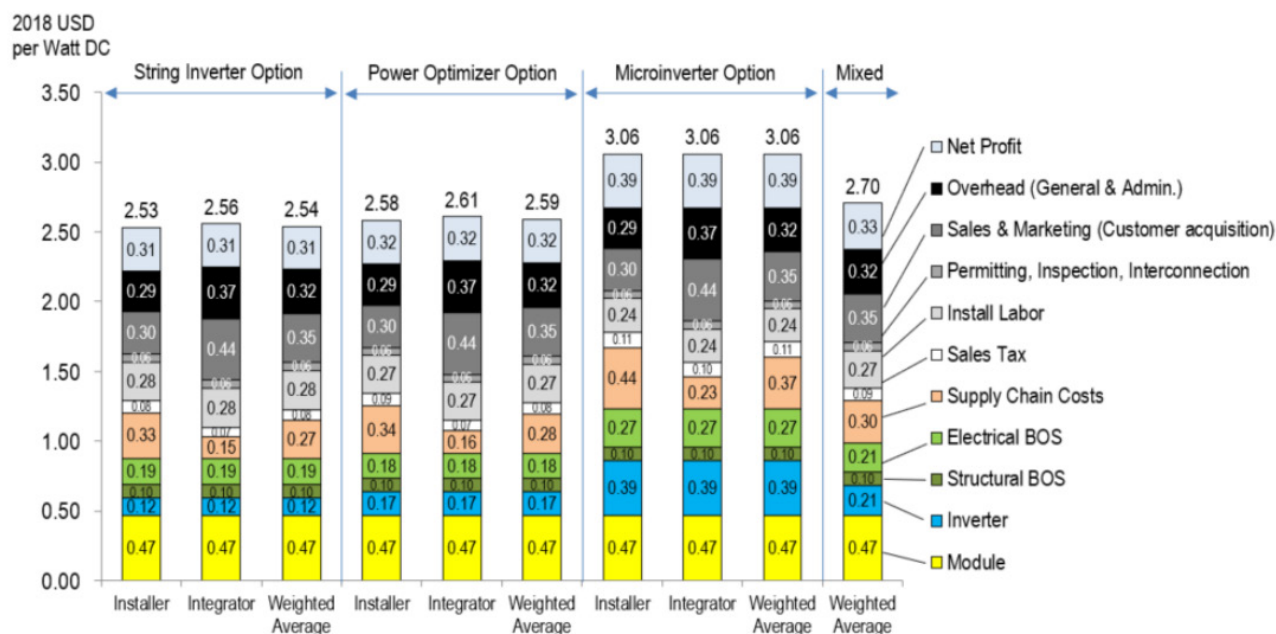


Figure 10. First 2018 quarter U.S. benchmark, considering a 6.2-kW residential system cost (2018 US\$/Wdc). Source: [112].

IRENA [55] showed that yearly average prices for crystalline modules increased between 4% and 7% in 2021 compared to 2020 due to supply chain disruptions and higher material costs. Rising prices were also influenced by other issues as pandemic-related logistics, lower pace of production and shipping difficulties. Therefore, PV module prices are considered for 2020, which are registered slightly before disturbances from the COVID-19 pandemic. Prices in US\$/W<sub>p</sub> are selected from the PVInsight dataset (<http://pvinsights.com/>) for 2020, cited by [61]. Table 12 distinguishes minimum, maximum, and average prices for monocrystalline, polycrystalline silicon and thin-film modules.

Table 11. Minimum, maximum, and average prices in US\$/W<sub>p</sub> for each PV technology. Source: [61].

Technology	Min US\$/W <sub>p</sub>	Max US\$/W <sub>p</sub>	Average US\$/W <sub>p</sub>
Monocrystalline-Si	0.185	0.380	0.2
Polycrystalline-Si	0.160	0.290	0.177
Thin film	0.2	0.320	0.221

Performance and financial information applied for the three PV technologies are [61] [112]:

- monocrystalline silicon (InP crystalline cell,  $\eta=0.24$ ), with PV module type: 1 – Premium and installed PV cost (US\$/kW): 2,500;
- polycrystalline silicon (GaAs multicrystalline,  $\eta=0.18$ ), with PV module type: 0 – Standard and installed PV cost (US\$/kW): 2,410;
- thin film (CzTS thin film,  $\eta=0.11$ ), with PV module type: 2 - Thin Film and installed PV cost (US\$/kW): 2,440.

## Storage

Energy storage is modelled as a “reservoir” in REopt: energy produced during one time step can be consumed later. REopt does not specifically model battery chemistries, but rather introduces constraints to ensure operations within the manufacturer’s specifications [95]. The default values are representative of lithium-ion batteries, which are the most popular [109]. A round-trip efficiency limits a minimum state of charge, charging and discharging rates, and number of cycles per day. The model can select and size both the capacity and power delivery.

- Battery maximum kW: 10 kW, which is the residential range based on NREL evaluations [113].
- Battery inherent efficiency independent of inverter and rectifier: 0.95 [114].
- Battery inverter efficiency: 0.96 (default).

The inverter’s nominal DC-to-AC conversion efficiency is defined as the inverter’s rated AC power output divided by its rated DC output [109].

- Battery rectifier efficiency: 0.96 (default).

The rectifier’s nominal AC-to-DC conversion efficiency is defined as the rectifier’s rated DC power output divided by its rated AC output [109].

- Minimum allowable battery state of charge, as a percentage of the device capacity: 0.2 (default).
- Total upfront battery power capacity costs (e.g., inverter, BOS) (\$/kW): 840 [114].
- Total upfront battery costs (\$/kWh): 420 [114].
- Battery power capacity replacement cost at time of replacement year (\$/kW): 410 [114].
- Battery energy capacity replacement cost at time of replacement year (\$/kWh): 250 [114].
- Number of years from start of analysis period to replace inverter: 10 [109].
- Number of years from start of analysis period to replace battery: 10 [109].
- Duration over which accelerated depreciation will occur: 7 [109].
- Percent of the ITC value by which depreciable basis is reduced: 0.5 [109].
- Total investment tax credit in percent applied toward capital costs: 0.

#### **Generator** (only for power outage hypotheses)

- Installed diesel generator costs (\$/kW): 500 [109].
- Diesel costs (\$/gal): 3 [109].
- Annual diesel generator fixed operations and maintenance costs (\$/kW): 10 [109].
- Generator only runs during grid outages and does not sell back energy to the grid. The critical load that must be met during a blackout is set as 50% of the usual load profile.
- Incentives are not available.

Based on the selected input data, REopt solar optimisations can be run by single buildings or by aggregated scenario. In both cases, the simulations return:

1. technical outputs, which include the average yearly PV production and total energy consumption (kWh/y), covered share of electricity consumption (with hourly load), size of the PV (kW and m<sup>2</sup>) and storage (kW);
2. financial outputs, which involve reduction in energy expenses, lifecycle costs (LCC) and net present value (NPV).

The net present value (NPV) is the sum of all discounted net benefits of the project over its lifetime, back to its present value. The NPV represents the subtraction between LCC in a business-as-usual scenario and an investment scenario, in this case the profitability of solar rooftop projects. A PV in-

stallation is financially feasible if the NPV is greater than zero because it is the present value of the savings [4]. Small systems with limited areas are the most likely to fail. However, decreasing PV costs and improved efficiencies contribute small areas to be compensated, produce more energy, and become financially attractive. Lifecycle cost (LCC) is the present value of all costs, after taxes and incentives for each project option. The aim of the REopt optimisations is to minimise LCC at the end of the evaluation period. The calculation of LCC includes [95]:

- capital costs: investments to buy PV panels, storage units, and other auxiliary equipment;
- operating expenses: fixed and variable operation and maintenance (O&M) costs, equipment replacement costs, fuel costs, utility purchases, financial losses incurred due to grid outages;
- operating revenues: net metering revenues, expenses of energy purchased from the main grid, production-based incentives, and WTE tipping fees;
- incentives, tax benefits: federal, state, and utility incentives, accelerated depreciation schedules.

Cash flows during the considered period are calculated by escalating the present costs at project inflation and utility cost escalation rates, then discounting to the present. The results of baseline scenario and solar optimisation show the optimal configuration for a financial-oriented approach, based on the technical inputs and economic parameters.

### 3.6.4 Cost-optimal analysis

The cost-optimal analysis returns a suitable range of energy performance that is reasonable to support from an economic and energy point of view. Cost-optimal can compare the economic feasibility of different interventions, considering costs, incentives, and eventual revenues [115]. In this study, REopt simulations are performed with different input data for distinct scenarios for each residential block. Multiple REopt optimisations are run to identify which is the most convenient combination to maximise self-sufficiency among:

- only PV panels, with and without net metering;
- PV panels and battery, with and without net metering;
- optimisation for hypothetical winter and summer blackouts, with and without net metering.

PV panels (monocrystalline, polycrystalline, and thin film) and batteries adopt values explained in paragraph 3.6.3. For the third type of scenario, the outage is defined as an off-grid period with start date, time, from which the software automatically calculates the blackout duration (number of hours). Durations, locations, and eventual damage from past power outages are not reported in any datasets for Canada or for Toronto. Therefore, periods on which perform the resilience analyses with an off-grid window are selected in the historical meteorological dataset for Toronto [116]. The selected year is 2017, in line with previous steps, using hourly data. Two recurrent types of weather events are considered, based on studies on contributions of climate change on blackouts [117] [118]: extremely low temperatures and heatwaves. The duration is assumed to be of 24 hours. The DG system will be sized to minimize the life cycle cost of energy to sustain the critical load during a power outage. In general, an outage start date when the electrical load is higher (often summer) will identify larger system sizes that can support the critical load during more outages. On the contrary, an outage period when the load is lower range will shape smaller system sizes which can satisfy fewer outages [109].

Performing these hypotheses, the cost-optimal analysis allows to identify the optimal size and confi-

guration of PV and eventual battery, based on global costs and energy-related parameters. The PV installation and backup technologies are assessed on a 25-year lifetime. Two energy-related parameters are considered: self-consumption and self-sufficiency. Self-consumption (SC/P) is the ratio between the energy locally produced and the overall PV production. Self-sufficiency (SC/C) is the ratio between the energy locally produced and the total electricity consumption [119], which represents the main one. Evaluations are considered for scenario-level optimisations for the four residential blocks.

Global costs (US\$/block) of installed technologies are based on the LCCs, which are minimised by the REopt optimisation. Global costs are related to the level of self-consumption (SC/P) and self-sufficiency (SC/C) reached by each combination for the considered residential blocks. The cost-optimal identifies the self-sufficiency level that corresponds to the lowest lifecycle costs. The cost-optimal mix contributes to increase the electricity self-sufficiency of the residential buildings by PV while decreasing the reliance on traditional fuels.

Further financial aspects considered are the net present value (explained above) and the simple payback time. The simple payback time (SPT) is the necessary number of years to recover the initial investment costs. The payback time identifies if savings from the implementation of one or multiple measures are sufficient to repay the initial investments.

Results can help policy makers to understand which is the most suitable energy policy, installation of renewable or retrofit interventions that can be funded for the building stock [2]. Each dwelling typology and aggregation will show different trends and reachable levels of self-sufficiency for electricity.

## 4. FRAMING THE CANADIAN CONTEXT

### 4.1 Geographical and climate context

Canada is the second largest country in the world, with 37,593,384 inhabitants in 2020 unevenly distributed in 9.98 million km<sup>2</sup> [120]. Population is mostly concentrated in the largest cities, as Toronto, Montreal, and Vancouver, while a relevant portion of the nation is sparsely inhabited in the interior plains. The territory extends towards Greenland, Arctic Ocean until the North Pole (from 42° to 83° approximately), with rigid and unfavourable climate conditions for human settlements, and from East to West for almost 7.560 km, across six time zones. Canada counts 10 provinces, as shown in Figure 11.



Figure 11: Division in the 10 provinces of Canada. Source: [121].

Canada counts a wide variety of climates due to its great latitude extent. The regions farthest from water basins are the coldest during winter and the warmest in summer months, with higher seasonal excursions. The Great Lakes mitigate the weather in both southern Ontario and Quebec, while in the North temperatures are lower. Except for the West coast, Canadian winter season has average temperatures below freezing and with continuous snow cover, which can be extended to April.

The solar radiation greatly varies in the country. Norther and North-West portions have the lowest solar production potential, with less than 1,000 kWh/kW/y (Figure 12). Southern Canada can reach values above 1,400 kWh/kW/y in the centre and around 1,300 in the lake area.

Canada involves by six HDD ranges: its Southern part is influenced by lakes, while the Norther one by the Arctic Pole with more rigid temperatures during the whole year. The magnitude of energy consumption differs throughout Canada's regions, based on climate variations, energy supply and building features. Technologies applied to the housing stock can be more effective for specific regions

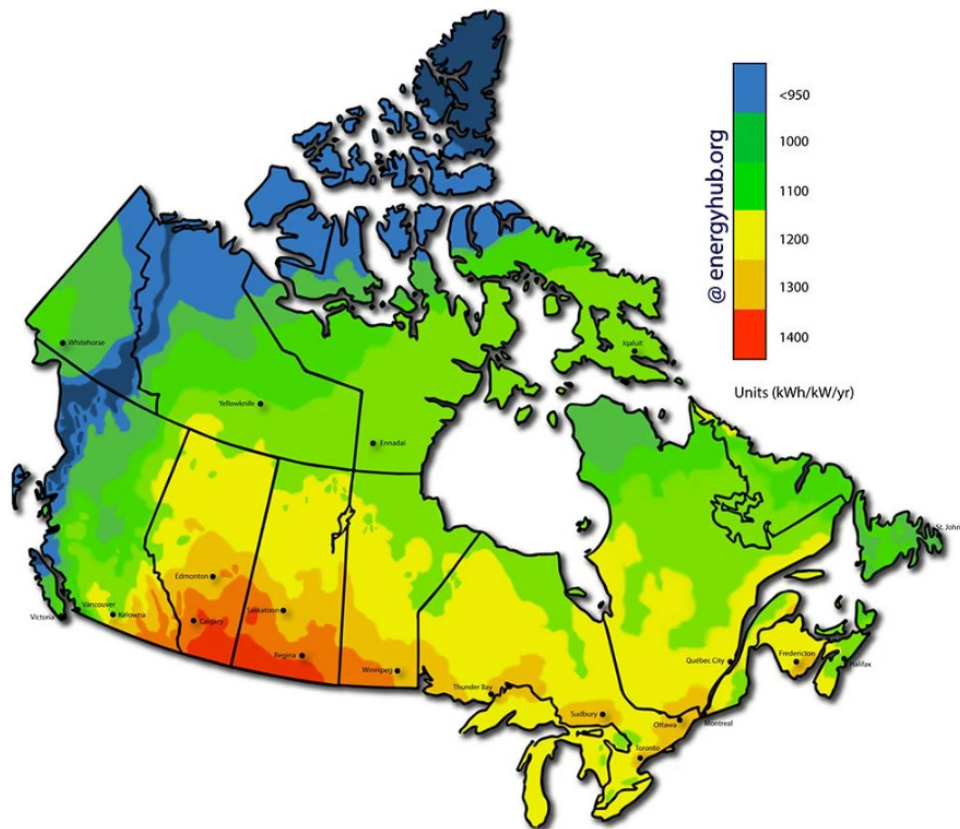


Figure 12. Solar energy map for Canada, distinguished in Provinces. Source: [122].

rather than others [25]. In this term, regions of Atlantic Canada and British Columbia are characterised by warmer heating seasons than other interior areas, with lower values of HDDs.

All these climatic conditions impact on the energy demand of buildings. Building energy consumption has been progressively influenced by global warming and climate change. The mean annual temperature in Canada increased around  $1.7^{\circ}\text{C}$  from 1948 to 2016, with even greater warming in the northern region (North of  $60^{\circ}$  latitude) around  $2.3^{\circ}\text{C}$  [123]. In a future perspective, effects will include limited extreme cold and more frequent extreme hot days, heatwaves, shorter snowfalls, and rising sea levels. The North already registers severe impacts of higher temperatures and intensification is expected in coming years, as less predictable sea ice conditions, infrastructure damage and shortened winter road seasons [124]. Stronger warming in the North and the East has been connected to changes in large-scale ocean circulation patterns [125]. Six of the 10 warmest years have been registered during the last 15 years, with 2010 being the record warmest ( $3.0^{\circ}\text{C}$  above the 1961–1990 reference value), while the coldest year since 1948 occurred in 1972 at  $2.0^{\circ}\text{C}$  below the reference value. Summer warming is registered across the country, with the warmest summer reported in 2012 [123].

Since 2008, cold events continue to decrease. The frequency of cold nights during winter (when the daily minimum temperature is below the daily 10th percentile) has decreased between 1950 and 2010 for most weather stations across Canada. On the other hand, the frequency of warm days during summer (when the daily maximum temperature is above the daily 90th percentile) has increased nationally, with exception only in the Canadian Prairies [125].

Future temperature rising have anthropogenic GHG emissions as primary long-term contributor [125]. Emissions and temperature trends have been assessed for different scenarios (known as Representative Concentration Pathways) by the Government of Canada [126]:

- RCP8.5: high global emission scenario, which indicates global average warming levels of 3.2 to

5.4°C by 2090.

- RCP4.5: medium global emission scenario, which involves measures to mitigate climate change and indicates global average warming levels of 1.7 to 3.2°C by 2090.
- RCP2.6: low emission global scenario, based on significant mitigation actions and with global average warming levels of 0.9 to 2.3°C by 2090.

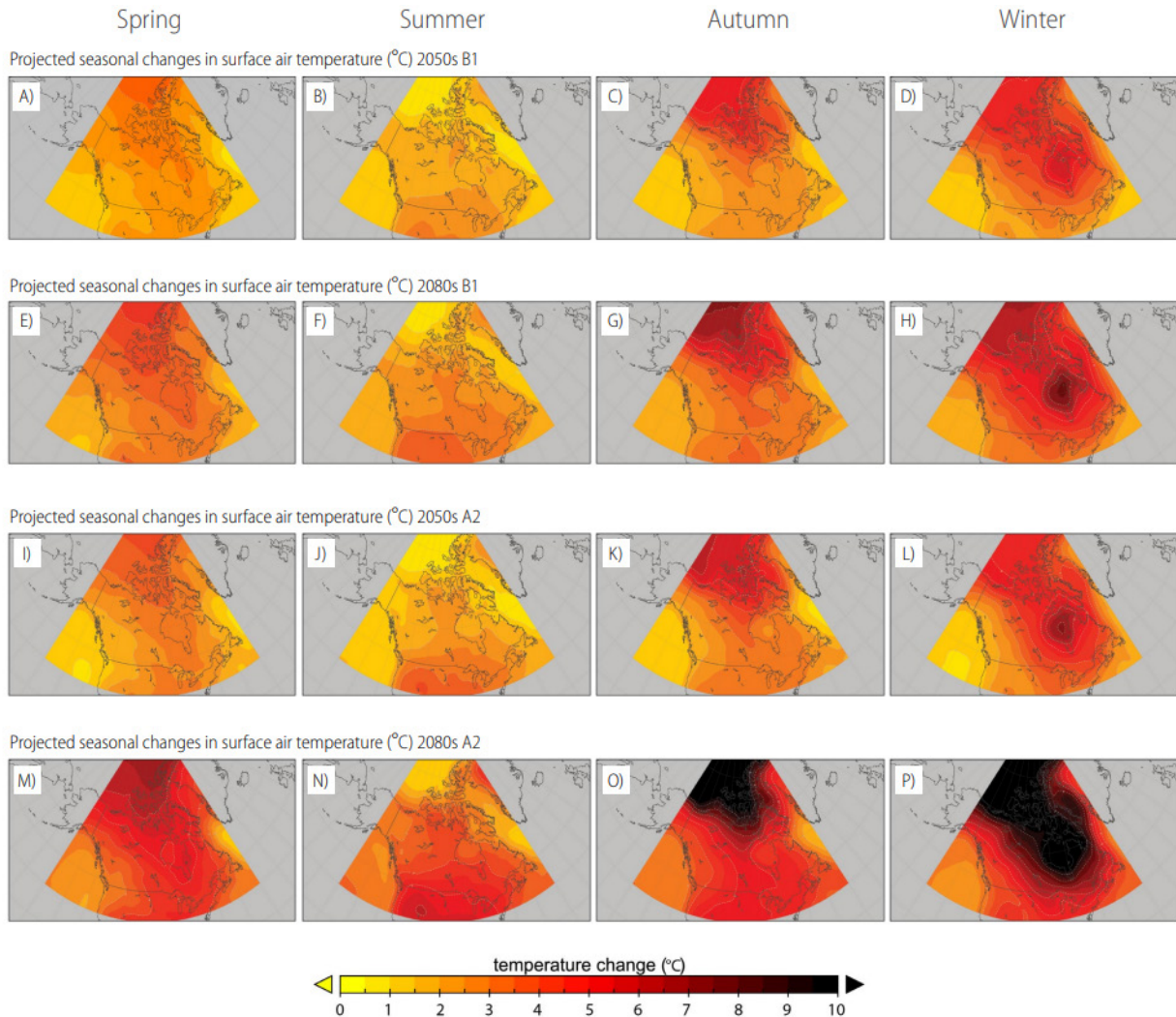


Figure 13. Projected seasonal changes in temperature across Canada for the middle and end of the 21st century under various SRES scenarios. Changes are expressed relative to average values between 1961-1990. Source: [125].

Future projections by scenario elaborations underlined that North America have 90-100% probability to warm along XXI century. The annual mean warming in Canada is likely to overcome global mean warming in most areas, with higher values in northern regions [125]. Seasonal projected variation for warming includes major increases in winter at high latitudes (northern Canada) and in summer in southern Canada. Summertime warming is generally expected to be more uniform, with largest modifications assessed for the continental interior [125] (Figure 13).

Higher temperature impact on cities, where natural areas are more limited and sealed surfaces contribute even stronger to temperature rising, as in the case of Toronto. According to climate projections by Climate Atlas of Canada [127], temperature will increase both during winter and summer compared to historical data. Especially in the hottest months, more frequent heatwaves have been registered in the Greater Toronto Area, with peaks in 2021: indeed, the administration introduced a Heat Relief Strategy to reduce the risks of heat-related illness.

## 4.2 Introducing Toronto

### 4.2.1 Changes in housing and population

Toronto is the capital of the Ontario province and the largest city in Canada. It represents the financial and commercial centre of the country, and its location on Lake Ontario and proximity to United States has favoured it along time [128]. It is developed along the northwest shore of Lake Ontario, part of the six Great Lakes, which influence the local climate. The City of Toronto covers around 630 km<sup>2</sup> with 2,794,356 inhabitants in 2021 (7.6% of Canada's total population) while Greater Toronto and Hamilton Area (GTHA) counts 7,281,694 (19.7% of Canada's total population) [129]. The population has grown mainly by international migration (more than 65% components of population growth).

The City of Toronto has identified 140 social planning neighbourhoods to help local planning (Figure 14). The highest population growths are registered in Downtown (especially Church-Yonge Corridor and Waterfront Communities-The Island), Midtown, south Etobicoke, and several north-west neighbourhoods [129]. Downtown Toronto (17 km<sup>2</sup>) is composed by 16 neighbourhoods in 2016 and counted around 250,000 inhabitants in 2015. The 2017 annual employment survey counted 1.5 million jobs at 75,620 business in the city [130]. Almost half a million worked in the area and around 300,000 commuted to it from other wards across the city [131]. Professional, scientific, and technical services companies cover the largest employee pool, overcoming manufacturing and retail from 2006 [130]. The financial services sector continues to grow in Toronto, employing more than 250,000 people.

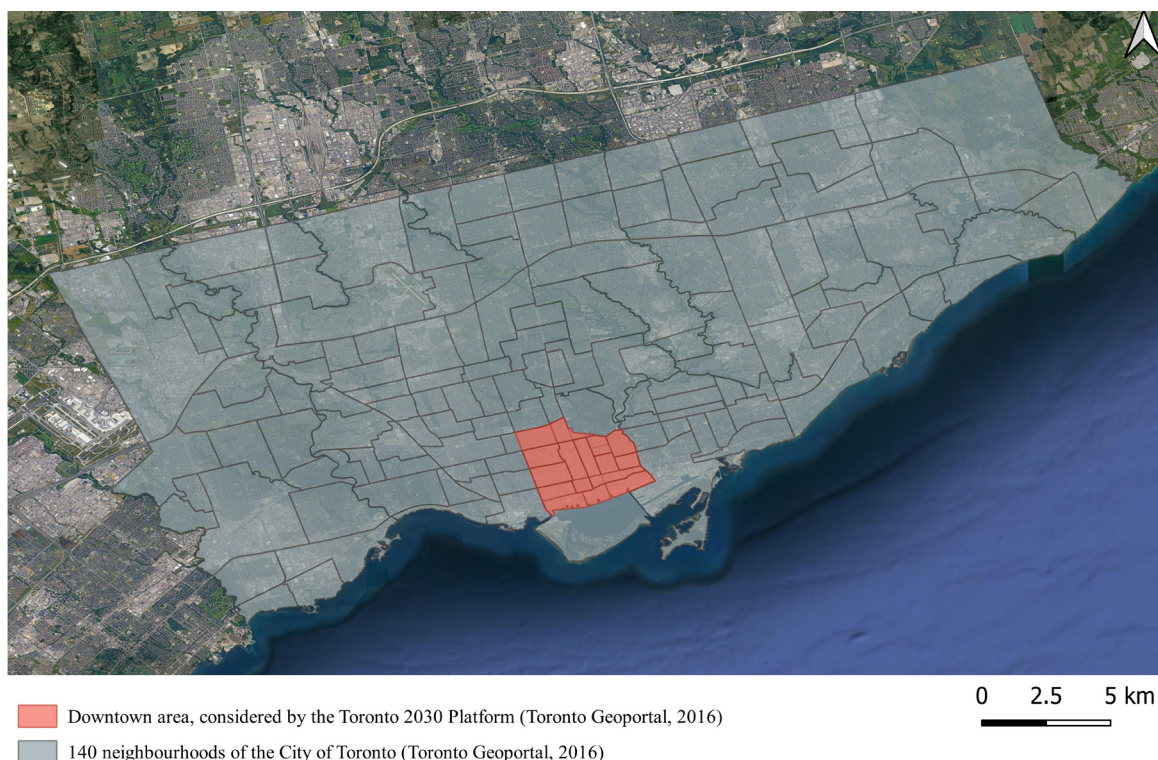


Figure 14. Boundaries of the City of Toronto divided by the 140 neighbourhoods and the Downtown TOcore area.

People continuously move within the city and generate further demand in the housing stock [132]. The number of occupied private dwellings increased from 1,112,929 in 2016 to 1,160,892 in 2021 but with shrinking household size. The number of people per household has been declining between 2001 and 2021 for the City of Toronto, respectively from 2.63 to 2.41 average inhabitants [129]. The

traditional post-war household by family is no longer the driving force and the housing occupancy has changed: non-family households are indeed growing more than family ones. In 1996, the larger population group was composed of people aged 15-34. Since 2011, Toronto has registered a 'double peaked' in young adults aged 15-34 and in elderly aged 50-69. The connections between people, households and the changing housing stock became more diversified and complex [132]. Household and housing sizes reflect the growth of non-family nuclei, mainly for younger and elderly people. Affordability issues may drive to more rental solutions rather than ownership, diverting the demand elsewhere [132]. Different and evolving typologies of housing have also an impact on energy uses and energy consumption of dwellings.

Population in Toronto is living in an increasingly denser urban environment. In 2016, houses and low-rise units were more than mid and high-rise ones. However, from 1996 to 2016, 77% increase in household has been registered for mid/high-rise apartments. Almost all types of households are progressively preferring higher-density and taller buildings and households aged 35-49 progressively prefer apartments rather than ground-related housing. The construction of apartments greater than 5 storeys has increased progressively from 36.7% in 1996 to 44.3% in 2016, while the growing rate of houses and low-rise have declined [132]. Toronto counts more than 2.5 times the number of households living in mid/high-rises (493,135 units) compared to the Rest of the GTHA (188,550 units). Indeed, houses and low-rise are the dominant dwelling types in the GTHA.

Population growth is concentrated in Toronto where more recent condominiums have smaller units and a shrinking unit size, from a high of 1,144 ft<sup>2</sup> in 1997 to 665 ft<sup>2</sup> in 2017 and mainly one-bedroom units (56.4% of all units built between 2006 and 2016). The City counts a prevalence of rent units, especially for 15-34 aged households, while a larger segment of elder people own low-rise houses. Between 2011 and 2016, owner households (49,730) have increased around three times compared to the number of renter ones (15,285), mainly in condominiums. The issue of affordability will continue to characterise Toronto housing market: new rents might be around 40% higher than existing paid rent [132].

Projections for Toronto forecast 3.40 million people by 2041 and the 86.3% of future built units is proposed in high-rise buildings. According to the population growth share [133], half of neighbourhoods shows double or more inhabitants. The average size of household and type of housing are key aspects in projecting the number of required dwellings for the future. The declining household size implies more dwelling units for the same population compared to 20 years ago.

## 4.2.2 Temperature trends

Toronto is located in the climate zone 5A – cool humid, according to the Koppen climate classification. The continental climate is influenced by the proximity of Lake Ontario: winter temperatures are milder than other Canadian areas, even if they can be decreased by wind, while summer are hot and humid. Western winds and the Great Lakes also influence precipitation, which is relatively homogeneous during the year (annually, 834 mm) and in winter, it mainly turns to snow with a 131 cm average [128].

The climograph for normal values between 1981 and 2010 (Figure 15) shows higher average temperatures in July (26°C), with a decreasing trend in winter and mean values below zero for January and February. Precipitation trends appear more discontinuous along the year and characterise by peaks in

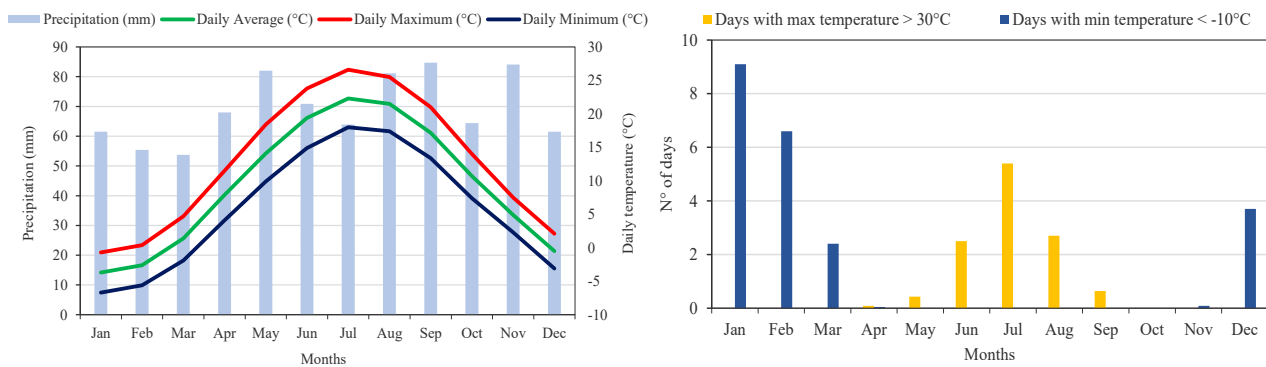


Figure 15. Climograph with temperature and precipitation normal values, for 1981–2010 time range (left) and number of days with temperature above 30°C and below -10°C, for 1981-2010 time range (right). Source: [134].

May, September, and November. Colder days have been registered in January, which represents the coldest month and the one with more snowfalls. Temperatures above 30°C have a peak in July even if lower than colder days (Figure 15). The normal values on a 30-year scale are progressively evolving due to the impacts of climate change. The rising trend of temperatures from the mid of the century is registered for Toronto central weather station (latitude 43°37'39" N, longitude 79°23'46" W, elevation 76.80 m), in line with the Canadian trends.

A rising trend in the average monthly temperature is currently registered and also for future projections (Figure 16). Toronto shows the highest increase in August and February, even if lower than Quebec City, between 2056 and 2075. Toronto registers the maximum estimated temperatures along all the year, with an average above 26° for July and August. The increase in winter mean monthly temperatures is likely to reduce heating demand and relate emissions. On the other hand, the rising summer trends will significantly impact on the cooling load, with additional demand for electricity. Projections point out an increase in solar radiation and a decrease in humidity: this will imply more agreeable conditions for the winter but not during summers [135]. Projections also assess more limited snowfall due to higher temperatures.

GHG concentration is one of the greatest inputs from human activities which will influence climate trends [127] and which is central for energy-related policies in Toronto (see Paragraph 4.3.3). Global climate models help to describe climate variations in the future and a series of possible conditions. The average values of rising temperatures are results of ensemble over the 1976-2005, 2021-2050 and 2051-2080 periods for Toronto and are reported by the high (90th percentile) and low (10th percentile) probability (Figure 17). In the case of high-carbon scenario (continue to emit GHG emissions as usual from burning fossil fuels), the hottest summer days are likely to have 4.8 °C (mean) more compared to 1976-2005 temperatures in Toronto. Longer-term projections register significant changes compared to average values for 1976-2005. Mean temperatures will increase in all seasons and annually and tropical nights are likely to be more than double. Precipitation occurrences would be smoother among seasons. Overall, years will be warmer and with low temperature. Recent short and intense rainstorms have impacted on Toronto in the last decade. Researchers have projected an increase in the intensity of short-duration storms as effect of climate change in the area [136].

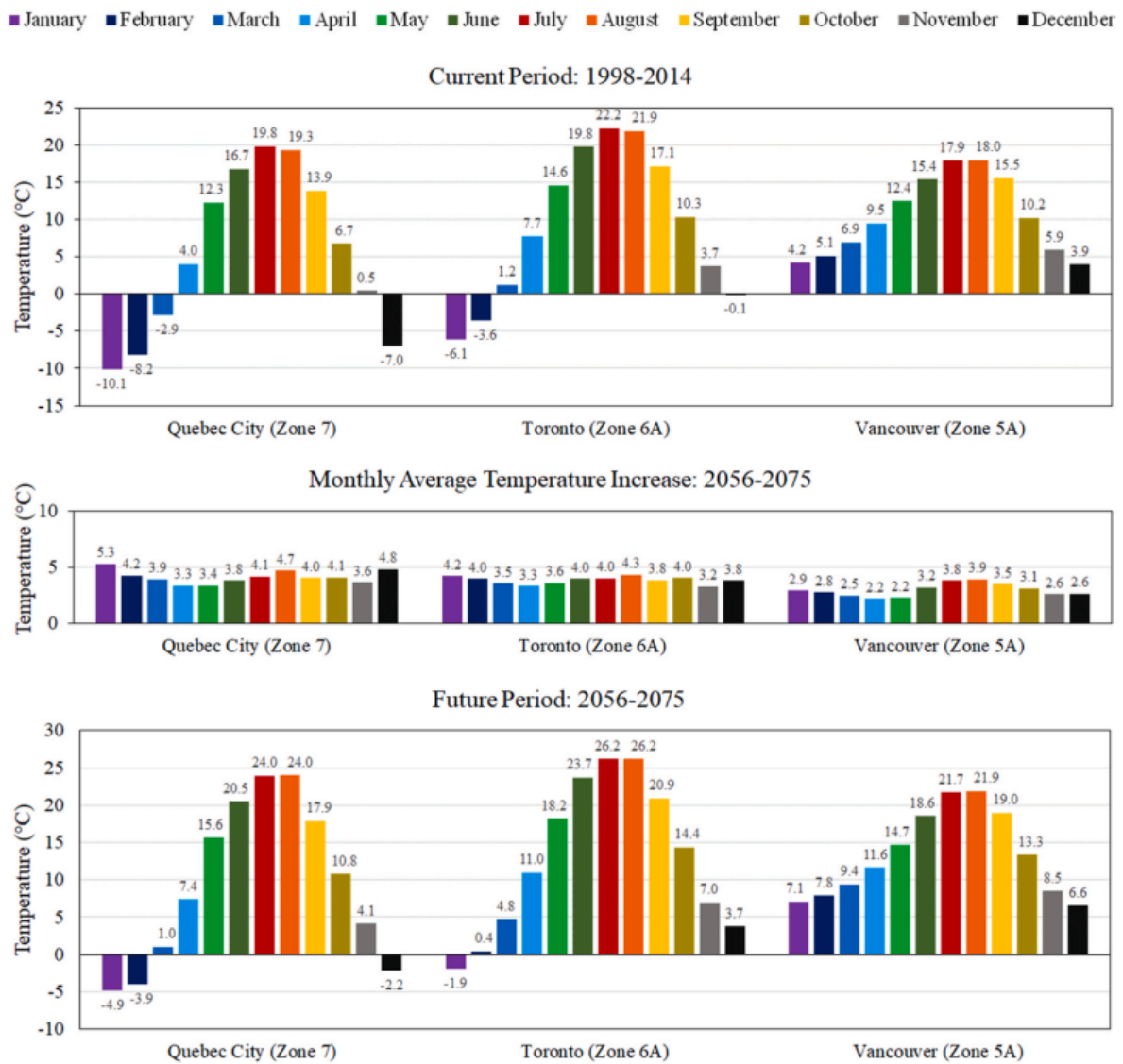


Figure 16. Mean monthly air temperatures for Quebec City, Toronto, and Vancouver under current and future climate conditions. Source: [135].

Change	1976-2005		2051-2080	
	Mean	Low	Mean	High
Typical hottest summer day	33.6 °C	35.3 °C	38.4 °C	42.0 °C
Typical coldest winter day	-21.4 °C	-18.1 °C	-13.4 °C	-8.5 °C
Number of +30 °C days per year	12	31	55	80
Number of +20 °C nights per year	8	28	47	69
Number of below-zero days per year	122	45	72	96
Annual precipitation	793 mm	699 mm	870 mm	1058 mm
Frost-free season (days)	188	203	232	263

Figure 17. Climate change projections in high-carbon scenario for Toronto. Source [127].

## 4.3 Energy sector

### 4.3.1 National energy profile

Energy makes up 10% of the nation's gross domestic product and is a main source of investments and generator of jobs [137]. Based on the Energy Trilemma index (Figure 18), Canada gets a balanced grade of AAA and ranks 4th place globally [138]. Vast resources, diverse electricity generation and high stability and resilience of the overall system strengthen Canada position, with a strong import independence. The overall Equity performance remains strong, but affordability of electricity prices experiences a further decline continuing a decade long downward trend. Electrification is one of the central applied pathways with energy efficiency and fuel substitution to meet net-zero targets. However, the Environmental Sustainability is the lowest since 2006 due to high-emitting industrial activities and its per capita emissions level. In 2020, because of the COVID-19 pandemic, Canada's energy sector dealt simultaneously with a global crisis in crude oil supply and a decline in demand. Demand has returned to almost pre-COVID levels and increases in production contributed to higher GHG emissions from energy, mainly from oil and gas.

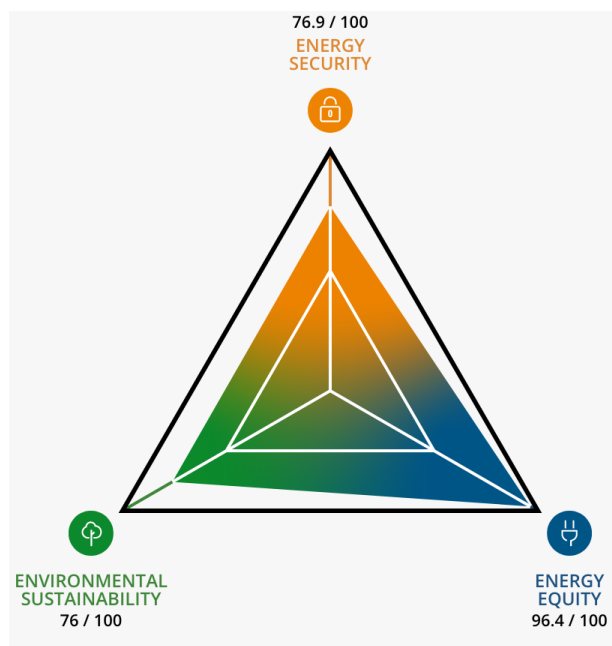


Figure 18. Energy Trilemma profile for Canada in 2022. Source: [138].

Most demanding energy end-use sectors are industrial (52%), transportation (23%), residential (13%) and commercial (12%); except for commerce, projections show increasing consumption trends by 2050 [139]. Fuels combustion in energy industries represents the 26% and buildings the 13% of overall GHG emissions in 2020 (88 Mt out of 672 Mt CO<sub>2</sub> eq.) [140]. Around 85% emissions from residential buildings derive from fossil fuel combustion to satisfy space and water heating. Despite the efficiency improvements and the greener electricity production in the past 10 years, population and economic growth will still rise emissions in the future [141]. Moreover, Canada is also the only G7 country whose emissions have risen since the Paris Agreement, highlighting the challenges in

<sup>2</sup> The World Energy Council has defined the three dimensions of energy sustainability towards a transition to a more decentralised system: energy security, environmental sustainability, and energy equity, which are intertwined in the Energy Trilemma [138]. These aspects are also taken up and pursued by the UN 2030 Agenda.

meeting its climate change engagements and decarbonisation path [138].

Among resources, Canada has a significant hydroelectric production, which covers more than 60% of electricity [142] (Figure 19). The remaining electricity share is satisfied by a set of resources, as natural gas, nuclear generation, wind, coal, biomass, petroleum. Heavy dominance of hydropower and nuclear allows Canada electricity system to be 83% non-emitting, among the cleanest in the world and aiming at 90% by 2030 [137]. Canada is devoting investments to coordinate different territorial entities. A better interconnectivity for electricity across regions and jurisdictions will be fundamental to ensure progress across Canada to meet national targets [137]. The generation from renewable resources (mainly wind and solar) increased from 2005, but still covers 5% and 0.3% respectively in 2020. Most of wind and solar installations are concentrated in Ontario.

The continued cost reduction favoured the diffusion of solar electricity throughout Canada. The province of Ontario leads the country with a cumulative installed PV capacity of 2,833 MWp as of 31st December 2017, covering more than 97% of the national total [144]. Considering the minor share in Northern parts, from 2017, research on the performance, cost, and durability of PV systems in the arctic was prior to support the clean electricity program in Canadian northern territories [144]. In the last decade, increasing investments have supported distributed storage: CanmetENERGY registered more than \$70M in storage pilot projects [145].

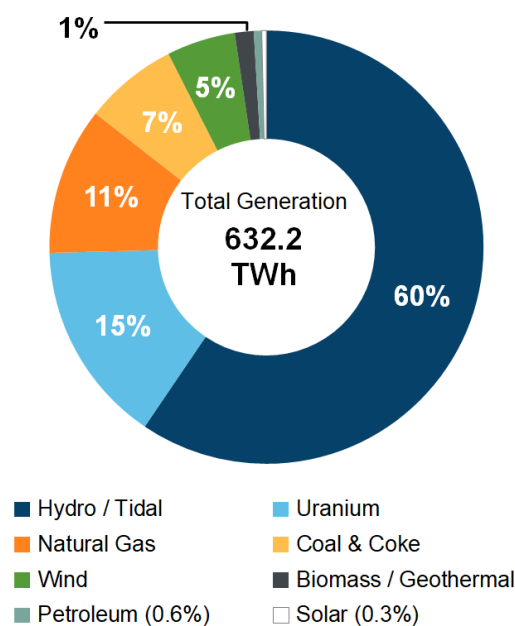


Figure 19. Electricity generation by source in Canada for 2019. Source: [143].

### 4.3.2 National energy goals

Canada shows a relatively high energy intensity due to the more rigid climate. In 2017, the Office of Energy Efficiency of Resources estimated that residential energy use was 61.6% by space heating and 19.3% by water heating [146]. Therefore, target new and existing buildings is fundamental to reduce consumption (mainly heating) and GHG emissions. Energy transition for Canada is based on [147]:

- decarbonisation of electricity by decreasing carbon-emitting sources and increasing non-emitting alternatives;
- electrification, fuel-switching and improving transportation sector;

- energy efficiency and behavioural changes which include improvements in energy uses.

In 2016, following the Paris Agreement, the Pan-Canadian Framework on Clean Growth and Climate Change (PCFCGCC) represented the collective plan for economic growth with reduction of emissions and improvement of building resilience to adapt to climate change. The ambitious aim is a 30% reduction below 2005 levels of greenhouse gas (GHG) emissions and to reach the Net-Zero by 2050 [137]. A collaborative approach between provincial, territorial, and federal governments contributes to reduce GHG emissions and enable sustainable development [148].

The PCFCGCC framework is based on four main pillars:

1. pricing carbon pollution (reinforced in the recent COP26), which will push new businesses and increase efficiencies, even if it is not sufficient as a stand-alone measure.

The identified price on carbon pollution started at \$20 per tonne in 2019 and will rise to \$170 in 2030. Since 2019, every jurisdiction has identified a price on carbon pollution or choose the federal framework. The federal government set minimum ‘benchmark’, that all provinces must meet [149].

2. adapt and build resilience, by which infrastructures and communities need to be sufficiently prepared to face climate hazards and extreme weather events.

The government introduced multiple investments in infrastructure to face major natural disasters and weather events (including a 10-year Disaster Mitigation and Adaptation Fund from 2018) [150]. Strengthening resilience, security, and ability to recover from hazards of the power electric grid is also the focus of the Joint US-Canada Electric Grid Security and Resilience Strategy [151]: the collaboration should sustain improvements and planning investments for a cross-border grid integration.

3. investments in clean technology, innovation, and jobs to ensure and strengthen an international and competitive position of the country.

The increase of clean fuels (hydrogen, advanced biofuels, renewable natural gas, sustainable aviation fuel and synthetic fuel) represents a main component for low-carbon future in Canada. Currently, they overall cover less than 6% of total energy supply, but between 10% and 51% of national energy demand is expected to be satisfied in 2050 [137].

4. complementary climate actions, which can reduce emissions. Tools have been introduced as new energy efficiency standards and codes for transports and buildings. A more detailed analysis of building code evolution is reported in Annex I.

The programs by 2030 are expected to create new jobs, reduce energy costs, and promote a long-term decarbonisation. Measures involve also GHG reporting requirements for large emitters and plans to phase out from coal-fired electricity generation by 2030. Electricity and fuel switching are included in the 2030 Emissions Reduction Plan (Table 13), which outlines sector-by-sector path for Canada to achieve -40% emission by 2030 and net-zero by 2050 [152].

Table 13. Main sectors addressed by the 2030 Emission Reduction Plan. Source: [152].

Economic sector	Estimated change 2005-2030	Implemented actions	New actions
Buildings	- 37% GHG emissions	<ol style="list-style-type: none"> <li>1. \$2.6 billion Greener Homes Grant;</li> <li>2. \$ 1.5 billion Green and Inclusive Community Buildings program;</li> <li>3. public Buildings Retrofits Initiative and the Commercial Building Retrofit Initiative.</li> </ol>	<ol style="list-style-type: none"> <li>1. \$150 million investment to develop a net zero buildings strategy by 2050 (Canada Green Buildings Strategy);</li> <li>2. support to communities to retrofit and upgrade homes and buildings, including affordable housing with loans and pilots.</li> </ol>

Electricity	- 88% GHG emissions	<ol style="list-style-type: none"> <li>1. phase-out of coal, natural gas regulation and price on carbon pollution;</li> <li>2. funding programs for clean electricity (RES and Smart Grid);</li> <li>3. funding for transition off diesel in rural and remote Indigenous communities.</li> </ol>	<ol style="list-style-type: none"> <li>1. additional investments on grid decarbonisation and commercially ready RES technologies;</li> <li>2. improve connectivity (i.e., transmission lines) and exchange of clean energy among regions.</li> </ol>
Oil and gas	- 31% GHG emissions	<ol style="list-style-type: none"> <li>1. federal regulations to reduce methane emissions by 40-45% by 2025 below 2012 levels;</li> <li>2. emissions Reduction Fund (ERF) - Onshore Program to push oil/gas companies to invest in green solutions;</li> <li>3. investment tax credit for capital used in carbon capture, utilization, and storage.</li> </ol>	<ol style="list-style-type: none"> <li>1. capping emissions</li> <li>2. improvements in carbon capture, storage and utilization;</li> <li>3. further reduction of methane emissions (75% below 2012 levels by 2030);</li> <li>4. delete subsidies for fossil fuels by public financing;</li> <li>5. support of workers along the transition.</li> </ol>

As a part of the PCFCGCC [148], the Government also supports the development of the first Canada National Adaptation Strategy. It aims at increasing collaboration among multi-level bodies and establish a national measuring framework to assess progress. At the end of 2020, the Healthy Environment and a Healthy Economy plan sustained the path towards net-zero emissions by 2050, with policies to target energy efficiency and demand side [153]. The plan included new fundings for upgrading municipal and community buildings (as the Low carbon Economy Fund), with also residential loan for low-income, and the aim to achieve net-zero carbon of 75% of government office floor space from 2030. A 30% carbon reduction in construction projects by 2025 is linked in the plan with manufacturing of green products, involving both building materials, equipment, and technologies. The recent COP26 in Glasgow, Scotland further reinforced the previous objectives, with the reduction from 40% to 45% from 2005 levels by 2030. Among the announcements, the Canadian commitment aims at fastening the energy transition toward a grid with net-zero emissions by 2035, which is already greatly supported by the hydropower production and coal limitation [154].

### 4.3.3 Toronto: energy policies towards decarbonisation

Toronto emissions have decreased by 38% since 1990, despite population growth and continuous rise of gross domestic product. The City issues its emissions inventory every two years and has introduced different programs to address GHG reduction, in line with national framework [155].

In 2021, the City of Toronto adopted the Net Zero Strategy to cut GHG emissions at community scale by 2040, anticipating 10 years compared to the initial and to national goals. The city targets compared to 1990 levels are: -30% by 2020, -45% by 2025, -65% by 2030 and net zero by 2040 [156]. Primary sectors of GHG emissions in Toronto are buildings by 57%, mainly caused by space and water heating from natural gas, followed by transportation especially with personal vehicles (36%) and waste (7%). Indeed, main energy sources of GHG emissions are natural gas and electricity used in buildings, transportation fuels (primarily gasoline), and waste sector [155]. Mid-term goals for 2030 have been established and are summarised in Table 14 for residential and energy sectors.

Net reduction implies significant actions on energy use in buildings because of their primary role in the city's GHG emissions. New projects need to follow the Toronto Green standard for low-and hi-

Table 14. Mid-term goals for 2030 by the TransformTO Net Zero Strategy for buildings and energy. Source: [155].

Sector	2030 goals	Contributing strategies
Homes and buildings	<ul style="list-style-type: none"> <li>design of new homes and buildings to be near-zero GHG emissions;</li> <li>50% reduction of GHG emissions from existing buildings compared to 2008.</li> </ul>	<ul style="list-style-type: none"> <li>Toronto Green Standard (new development, private and city-owned)</li> <li>Net Zero Existing Buildings Strategy (existing homes and buildings in Toronto)</li> <li>Net Zero Carbon Plan (city-owned facilities)</li> </ul>
Energy	<ul style="list-style-type: none"> <li>50% of energy coming from RES or low carbon;</li> <li>25% of commercial and industrial floor area with low carbon thermal energy sources.</li> </ul>	<ul style="list-style-type: none"> <li>Integrated in the other strategies for buildings, transports, electricity, and productive sector</li> </ul>

gh-rise residential, commercial office, large retail structures.

On the other hand, existing building often have dated components and systems which increase carbon emissions and consumption. Therefore, the City of Toronto developed a Net Zero Existing Building Strategy to implement the decarbonisation of the existing building stock. The building sector is distinguished in four main types: institutional and large commercial, small commercial and industrial, MURBs and single-family house. According to modelling, the main emission contribution is from single family housing (31%), followed by MURBs (Figure 20).

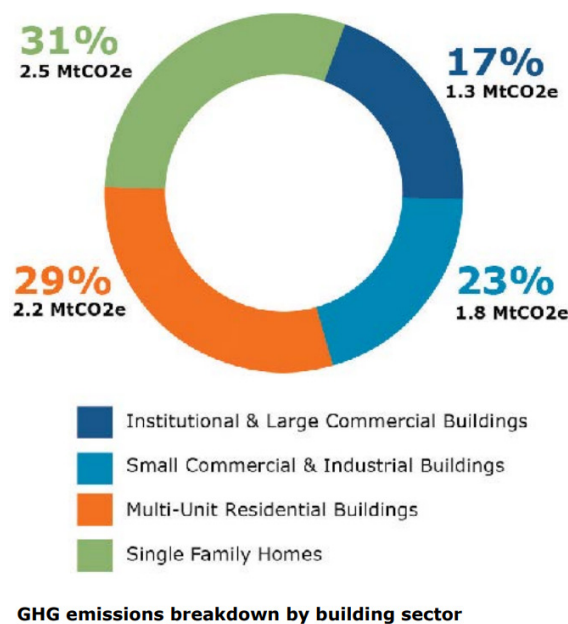


Figure 20. Main building sources of GHG emissions by TransformTO Net Zero Strategy. Source: [157].

Each building group has different energy features and construction components as well as ownership models. The shares of electricity and natural gas consumption tend to be different, according to these variations. For instance, the role of natural gas is generally more relevant for single family structures, and it is remarkably the main component in GHG emissions (Figure 21).

In the Net Zero Existing Building Strategy, different possible actions for the building stock were combined to assess effects to reach zero emissions by 2050. The exploration of measures let emerge a reduction over 80% by 2050 on existing buildings (baseline year as 2016), while business as plan will reduce emissions only by 34%.

No mix of packages is feasible for a zero-emission target, for which further measures need to be introduced, as renewable generation, carbon offsets, grid decarbonisation.

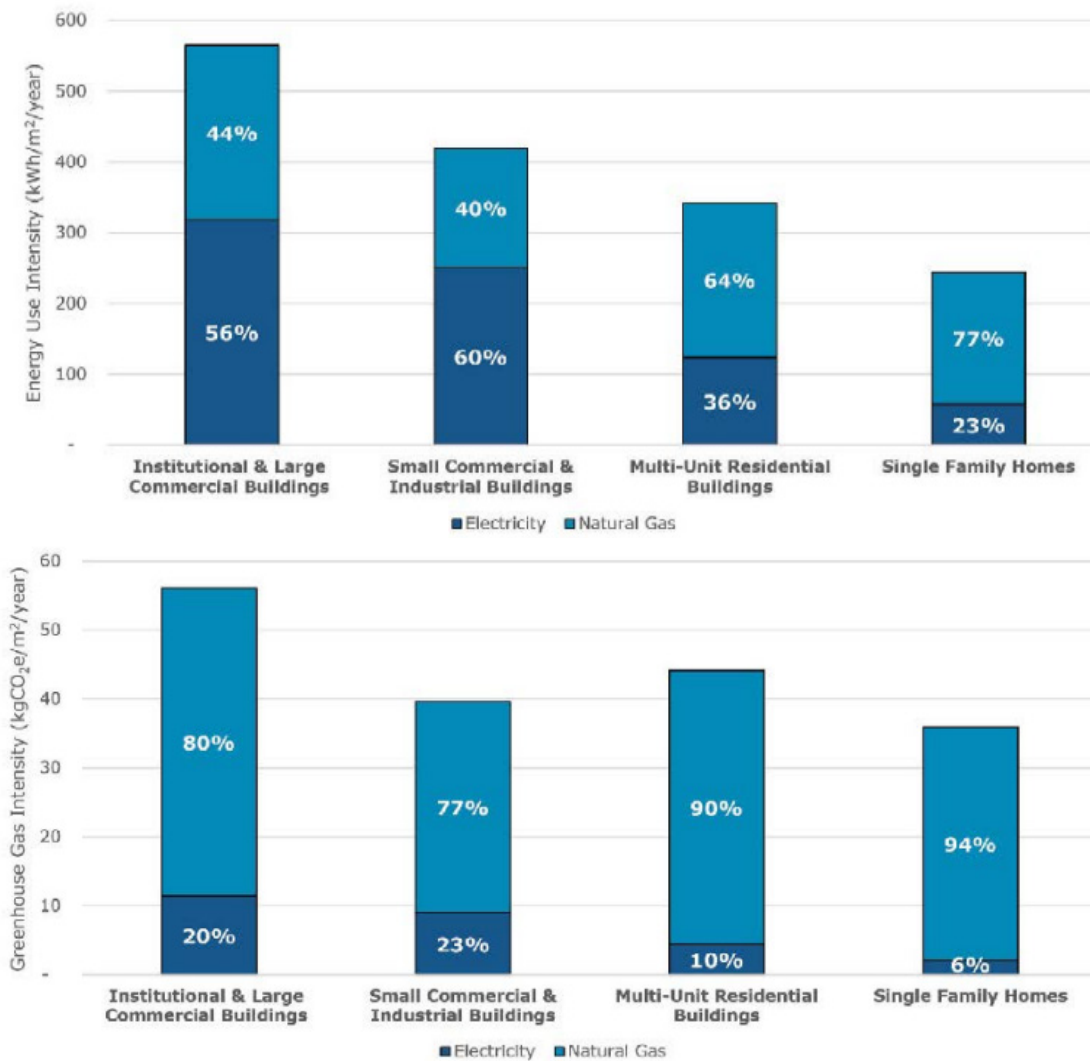


Figure 21. Share of annual energy use intensity for electricity and natural gas (above) and share of GHG emissions for electricity and natural gas (below) by building sector. Source: [157].

Rather than package performance, decarbonisation implies implementation of multiple actions over time, with prioritisation in the near-term and investments across different systems. Building deep retrofits will require significant financial commitment by owners (and longer return of investments), while short-term interventions cannot achieve the same emissions savings. The switching to lower carbon resources can represent the lowest cost to greatly cut emissions. Solar PV improves all retrofit packages and can address grid overload issues: therefore, should be promoted for all suitable locations. The Strategy [157] highlights three main city-scale conclusions:

1. speed of change in the building sector must be balanced with feasibility of measures. A 3% average change in floor area per year was considered, in relation to other studies. Incentives and programs need to face housing and population growth and have a coordinated offer;
2. deep emissions retrofits are not cost effective for building owners. Strong regulation and financial support are required to support efficiency improvements;
3. switching to lower-carbon sources is necessary and, if implemented carefully, is the most economical way to achieve deep emissions reductions. The alignment of fuel-switching and renewable generation contributes to cost savings in the city and support a decarbonization of the grid.

Possibilities to realise renewable energy systems within the city are already available and help to con-

trol the costs of electricity over time. Renewable generation can include both community-scale (i.e., district energy, community-scale renewables) and site level (i.e., heat pumps, PV, and battery storage) implementations.

The Strategy has recommended a first near-term introduction of voluntary policies (2022-2024) followed by a transition to mandatory requirements for medium (2025-2029) and long (after 2030) term [157]. None of the actions will achieve reduction targets without performance improvements in the existing buildings. Over \$300 billion in building retrofits are necessary between 2020 and 2050 by all levels of government and the private sector (and not only homeowners) for an 80% emissions-reduction in existing stock. Fuel switching from natural gas to electric systems and a clean electricity grid are the two most impactful technical requirements [157].

The municipality also introduced programs to deliver funding, expertise, and support to building owners through the Better Buildings Partnership (BBP) [158] to improve energy efficiency and reduce GHG emissions in residential, commercial, institutional, and industrial buildings.

## 4.4. Elaboration of energy dataset: from national to city scale

### 4.4.1 Available sources for assessing energy consumption

The impact of building sector on GHG emissions and energy consumption led to the realisation of surveys at different scales to assess building demand. For Canada, documents and data collection are available for reporting energy consumption by sectors, years, and geographical area.

Different groups within Natural Resources Canada (NRCan) developed residential and non-residential surveys. In 1993, the first Survey of Household Energy Use (SHEU) was released, followed by updated versions in 1997, 2003, 2007 and 2015 (more recent one), which assessed the housing stock considering typological, consumption and technological features [77]. The main strength of these studies is the provision of an unbiased characterisation of the present housing stock from billing energy data: it can be useful for assessing the appliance penetration levels, for building energy models and for calibrating results. On the other hand, surveys often provide only a limited set of data required for energy modelling, which may not completely describe the differentiation of housing stock.

Considering the variety of available resources, main data sources for residential and non-residential sector will be described briefly below.

- Survey of Household Energy Use (SHEU) [77], lastly released in 2017.

The 2015 SHEU was conducted as a joint national project between Statistics Canada and Natural Resources Canada to collect housing energy consumption data and household characteristics, including factors affecting energy residential demand. The survey distinguished single detached and double/row houses, mobile homes, low-rise and high-rise apartments. Data were collected through an initial computer-assisted telephone interviews with dwelling owners and renters, followed by a paper mail-back questionnaire or energy household suppliers. Survey sections divide dwelling characteristics, appliances, electrical devices, heating and cooling equipment and energy consumed by households. The respondent sample was approximately of 6,000 for estimating 13 million households: therefore, the quality of data has a coefficient of variation (acceptable, use with caution, too unreliable to be pu-

blished). While the national survey covers the whole Canada, the 2015 SHEU has been referred also the Census Metropolitan areas (43 censuses in 2015), with same data quality assessment but different data division.

Source	Author (s)	Year of energy data	Territorial level	Sample	Types of buildings
Survey of Household Energy Use (2017)	NRCan	2015	National and provinces	Approximately 6.000 households	All residential dwellings
Survey of Household Energy Use for Census Metropolitan Areas (2017)	NRCan	2015	43 Metropolitan areas	From SHEU	All residential dwellings

- Survey of Energy Consumption of Multi Unit Residential Buildings (SECMURBs) [159], released in 2018.

The survey estimates energy consumption of a sample of 11,715 MURBs from the municipalities of Halifax, Ottawa-Gatineau, Toronto, Hamilton, Winnipeg, Calgary, and Vancouver for 2018. A MURB consists of a building or set of buildings with multiple apartments. They have a primary exterior access, and all apartments are connected by an interior door and central corridor. Its minimum footprint must be no less than 600 m<sup>2</sup> or have at least four floors. Properties defined as hotels, residence hall/dormitories, and senior care community facilities were not considered. Responses were weighted for each municipality and the aggregated results were derived to achieve the total count of MURB properties. Due to some data limitations (i.e., property type, FAR, following retrofits), only the aggregated data for the whole eight municipalities are available, while not for single municipalities.

Source	Author (s)	Year of energy data	Territorial level	Sample	Types of buildings
Survey of Energy Consumption of MURBs (2018)	NRCan	2018	Eight main municipalities	11,715	Multi-Unit Residential Buildings

- Industrial Consumption of Energy Survey – Energy Use in the Canadian Manufacturing Sector 2000-2019.

The survey provides estimates of energy consumption by manufacturing and the results are used by NRCan to track energy efficiency improvements, according to evaluations on energy use and sources, energy intensity divided by productive subsectors.

Source	Author (s)	Year of energy data	Territorial level	Sample	Types of buildings
Industrial Consumption of Energy Survey (2019)	Statistics Canada; NRCan	2000-2019	National	-	Manufacturing industrial activities

- Survey of Commercial and Institutional Energy Use (SCIEU) [160], released in 2014.

The survey provides energy and typological information of commercial and institutional buildings (office, medical office, school, care facilities, warehouses, hospitality, hospitals, food and beverage and non-food retail stores), by estimates. Therefore, coefficient of variation are provided to indicate the reliability of values, even if valuable improvements have been made compared to the 2009 survey.

Source	Author (s)	Year of energy data	Territorial level	Sample	Types of buildings
Survey of Commercial and Institutional Energy Use (2014)	NRCan	2014	National	-	Commercial and institutional buildings

- Comprehensive Energy Use Database [43], released in 2020.

This database provides an overview of sectoral energy markets and GHG emissions in the overall Canada and in each region, divided by residential, commercial/institutional sector, industrial, transportation and agricultural functions. It consists of a re-structurisation of previous databases, with further improvements.

The main disadvantage is that the analysis on housing types only distinguishes detached and attached houses, apartments, and mobile houses.

Source	Author (s)	Year of energy data	Territorial level	Sample	Types of buildings
Comprehensive Energy Use Database (2020)	NRCan	2000-2018	National and provinces	-	Residential, commercial/ institutional sector, industrial.

- Report for energy use and GHG emissions for the Broader Public Sector [161], released annually from 2011 to 2019.

In Ontario, following the Regulation 507/18, the Broader Public Sector (BPS) organisations need to report annually and publish energy use and GHG emissions and develop a five-year conservation plan, which needs to be updated every five years. BPS organizations include municipalities, municipal service boards, school boards, universities, colleges, and hospitals, even if other can voluntarily report. Results must describe raw energy consumption and GHG emission data, data normalised according to weather conditions and GHG emissions, those BPS organizations that did not report their 2013-2017 energy consumption data.

Source	Author (s)	Year of energy data	Territorial level	Sample	Types of buildings
Energy use and GHG emissions for the BPS	Ministry of Energy	From 2011 to 2019	Ontario	More than 5.000 BPS organisations	Broader public sector

- Ontario Energy Quarterly [162]: electricity, oil, and gas reports

The Ontario Energy Quarterly provides an updated report of the province's energy sector, released by the Ontario government every three months. Data are divided in electricity, oil and gas and include their prices, mix, energy consumption and conservation, demand, and supply for the area, which is the most inhabited of Canada.

Source	Author (s)	Year of energy data	Territorial level	Sample	Types of buildings
Ontario Energy Quarterly	Ontario Ministry of Energy; Ontario Power Generation; Ontario Energy Board; Independent Electricity System Operator	From 2014 to 2021	Ontario	All buildings	All buildings

- Annual energy consumption and GHG emissions report (2018) (and dataset) [163].

The report provides information on the 2017 energy consumption and GHG emissions for 1,482 City of Toronto buildings and sites, according to the Ontario Green Energy Act (GEA) 397/11. The City of Toronto is responsible for acquiring energy and water consumption bills from various utility providers for several service agencies and divisions, from which analysis has been structured on demand and energy intensity trends.

Source	Author (s)	Year of energy data	Territorial level	Sample	Types of buildings
Annual energy consumption and GHG emissions report (2018)	Environment & Energy Program Administration; Environment & Energy Division; City of Toronto	2017, but dataset available from 2011 to 2018	City of Toronto	1,482 buildings	Public buildings and facilities of City of Toronto

- 2019 – 2024 Energy Conservation and Demand Management Plan [164].

As required by the regulation 507/18, the plan includes for the selected buildings in the City of Toronto energy cost and consumption patterns in 2018, efficiency measures implemented between 2014-2018 and measures planned for implementation between 2019-2024, annual renewable energy generation. The analysed structures include administrative offices and facilities, ambulance stations, animal centres, childcare facilities, community centres, cultural and recreational facilities, police stations, public libraries. The residential sector is not included.

Source	Author (s)	Year of energy data	Territorial level	Sample	Types of buildings
2019-2024 Energy Conservation and Demand Management Plan (2019)	Environment & Energy Program Administration; Environment & Energy Division; City of Toronto	2018	City of Toronto	604 buildings	Public buildings and facilities of City of Toronto

- Energy consumption trends of multi-unit residential buildings (MURBs) in the city of Toronto [100].

This study is applied to a sample of 40 MURBs to assess their energy intensities and consumption: indeed, apartment buildings cover the 56% of dwellings in the City of Toronto. The 40 considered MURBs account for 1.9% of the mid and high-rise population in Toronto and had construction dates from 1960 to 2003, heights from 5 to 28 storeys and between 24 and 250 suites in each structure. Correlations have been performed between energy demand and building characteristics to find which variables had the greatest influence on consumption trends. Prior to analysis, monthly natural gas and electricity data were normalized using a standard weather year following the Canadian Weather for Energy Calculations (CWEC) and anomalous data deleted.

Source	Author (s)	Year of energy data	Territorial level	Sample	Types of buildings
Energy consumption trends of multi-unit residential buildings in the city of Toronto (2020)	Binkley C., Touchie M., Pressnail K.	2020	City of Toronto	40 buildings	MURBs

The Survey of Household Energy Use (SHEU) [77] and the Comprehensive Energy Use Database [43] are used in the following methodology to provide a characterisation of Ontario energy consu-

mption (Paragraph 4.4.2) and to compare results from the statistical model (Paragraph 5.6). These two sources are selected because they subdivide the residential consumption in main archetypes for low-density and multifamily dwellings and by period of construction. Moreover, they provide average data for single residential buildings rather than only aggregated estimations. The subdivision by typologies and age allows comparisons with disaggregated energy consumption from the block scale, on which regression analyses will be based.

#### 4.4.2 Characterisation of energy consumption in the Ontario province

The Comprehensive Energy Use Database [43] makes available a full range of energy data for the Canadian provinces from 2000 to 2018, distinguishing detached, attached and apartments. A characterisation of energy consumption in Ontario, distinguished also by type of housing and of output, can help to describe the full set of variables. The availability of the number of households, the total floor area (given directly by the database) and the number of inhabitants (by the Census Profile, 2016) allow to assess the consumption intensity for main energy aspects. Except for trend analyses, data have been selected for 2017, to be comparable with the Toronto 2030 Platform.

The main used energy source is natural gas (59.4% in 2018) rather than electricity (29.2% in 2018), with an increasing trend in the most recent period: on the other hand, marginal resources are heating oil and wood, which count for less than the 15% (Figure 22).

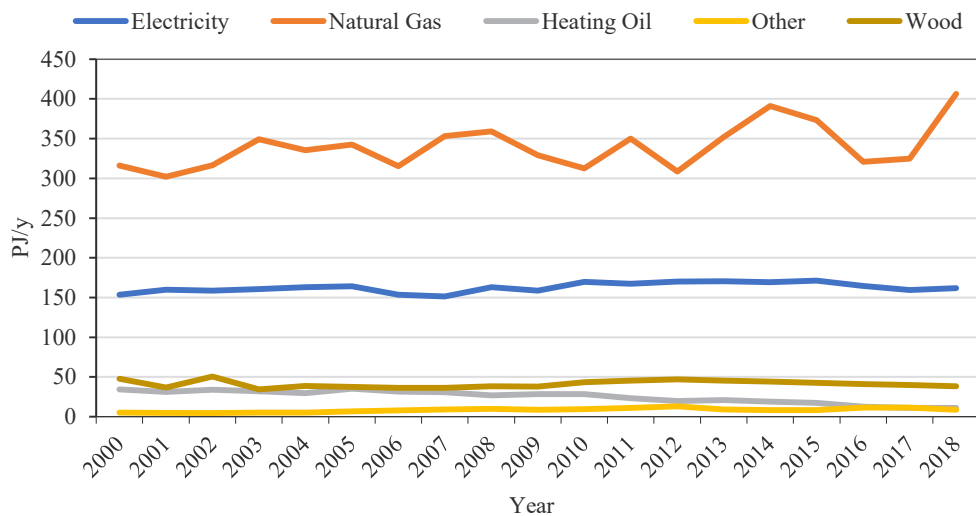


Figure 22. Energy use by energy sources between 2000 and 2018. Source: [43].

At the same time, among energy final uses, main role is clearly covered by space heating (63.5% in 2018), considering the variable but generally harsh Canadian climate (Figure 23). The cooling share is progressively growing due to the rising trend of temperatures and diffusion of AC systems in dwellings, as confirmed for data from 1990 to 2017 [146].

Both heating and cooling are generally used only for a fraction of the day (morning and evening) when households are at home, while for the rest of the day they are generally turned off. Cooling systems are assumed to interest only a portion of the dwelling (and overall volume) (Table 15). Values have been already normalised for heating and cooling consumption, which can vary according to annual climate and temperature trends.

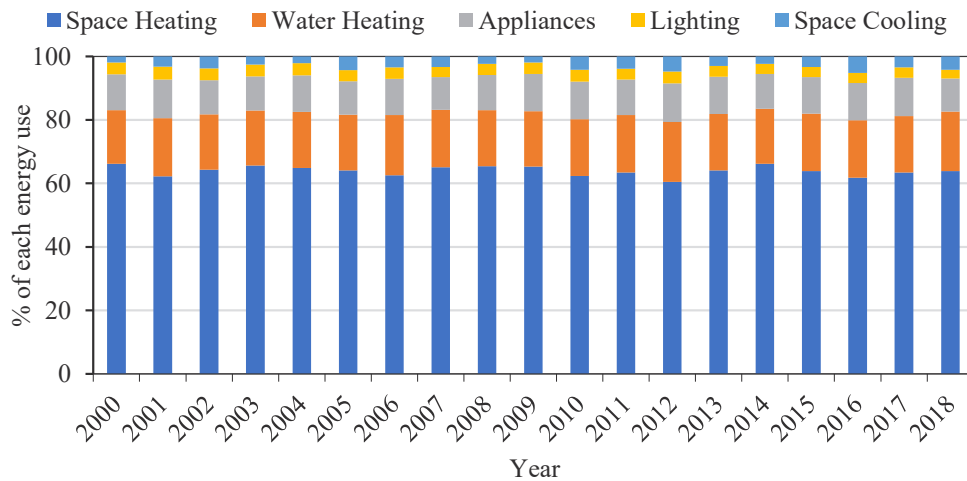


Figure 23: Secondary energy use by end use between 2000 and 2018. Source: [43].

Table 15. National sample on which housing data are analysed in the Comprehensive Energy Use Database.

Overall data	Values in 2017
Total floor space (million m <sup>2</sup> )	821.9
Cooled floor space (million m <sup>2</sup> )	631.6 (76.85% of the total floor space)
Households	5,403,000
Inhabitants (NRCan, 2016)	13,448,494

A detailed characterisation of overall energy consumption is provided in Annex III. The subdivision of residential consumption by sources and end-uses can be summarised by the following tree scheme (Figure 24), by which:

- water heating is assumed to be 100% satisfied by natural gas (30% of the whole natural gas consumption)
- appliances (41% of electricity), lighting (11%) and space cooling (12%) are fully covered by electricity; the sum of the three components counts for the 64.4% of electricity
- space heating is satisfied by natural gas (which is the remaining 70%), electricity for a more limited share (which is the remaining 54% of electricity), heating oil, wood and other.

Therefore, contributions in space heating are 66% natural gas, 16% electricity, 11% wood, 3% heating oil and 3% other sources (which include coal and propane).

A further distinction of consumption can be made by housing types. In the Database (2020) [43], the division is simplified compared to other sources: the considered archetypes are only single detached, single attached and apartments, without distinguishing low-rise and high-rise. The energy characterisation for each residential type is provided by the database, while the average consumptions per household and intensities (kWh/m<sup>2</sup>) have been calculated. The mean values for each inhabitant cannot be calculated because the population by type of dwelling is not provided. Higher values for floor space and number of households are reported for single detached, followed by apartments (Table 16).

Considering the period of construction, most of the stock has been realised before 2000, especially for single detached houses [165]. Most relevant concentration is registered between 1984 and 1995 (Figure 25), while lower values for the more recent years due to limited demand in the housing market.

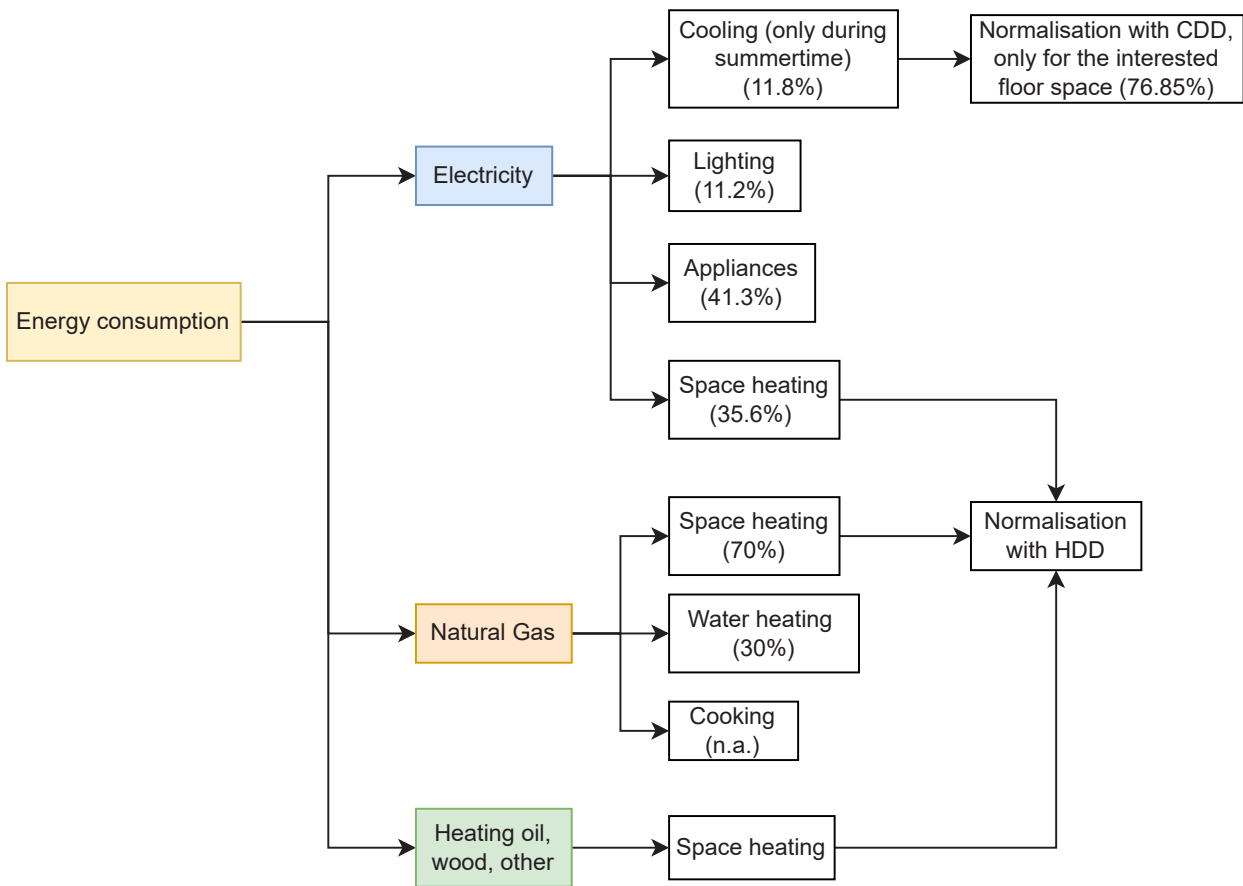


Figure 24: Summary scheme for consumptions by energy sources, according to Comprehensive Energy Use Database.

Table 15. National sample of which housing data are analysed in the Comprehensive Energy Use Database.

Data	Single detached	Single attached	Apartments
Floor space (million m <sup>2</sup> )	539.7	123.9	155.8
Households (thousands)	3,023.0	820.3	1,544.8

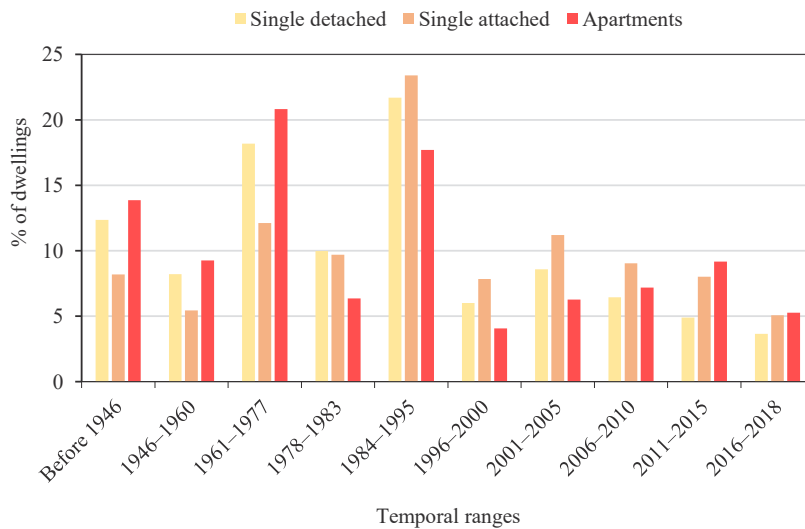


Figure 25: Housing stock by vintage mix in 2017 in Ontario. Source [43].

Natural gas prevails in the heating system, balanced by higher values of electricity for attached and apartments (which can have more recent installations) and dual older systems for single detached. Water heating shows equal values for all categories (higher for natural gas), so that probably a simplification was applied for the calculations.

Table 15. National sample of which housing data are analysed in the Comprehensive Energy Use Database.

Energy source or system	Single detached	Single attached	Apartments
Heating system			
Heating Oil – Normal Efficiency	0.0	0.0	0.0
Heating Oil – Medium Efficiency	5.9	6.4	6.5
Heating Oil – High Efficiency	0.0	0.0	0.0
Natural Gas – Normal Efficiency	0.0	0.0	0.3
Natural Gas – Medium Efficiency	16.7	17.2	17.1
Natural Gas – High Efficiency	47.8	52.8	53.9
Electric	10.0	15.4	16.8
Heat Pump	9.9	4.1	1.4
Other	1.0	1.1	1.1
Wood	0.0	2.2	2.3
Dual Systems			
Wood/Electric	3.8	0.2	0.1
Wood/Heating Oil	3.5	0.2	0.1
Natural Gas/Electric	0.8	0.3	0.3
Heating Oil/Electric	0.5	0.1	0.2
Water heater by energy source			
Electricity	20.9	20.9	20.9
Natural Gas	74.7	74.7	74.7
Heating Oil	2.8	2.8	2.8
Steam	0.0	0.0	0.0
Other	0.7	0.7	0.7
Wood	1.0	1.0	1.0

Energy intensity (kWh/m<sup>2</sup>/y) is always higher for single detached, followed by single attached and apartments (Figure 26): this could be due to the higher loss surfaces, which contribute to higher dispersions and significant consumptions, as well as aged systems and structures. One more time, it is confirmed the greater demand for natural gas, compared to electricity, and more significant wood-related use for single detached which can have older heating systems.

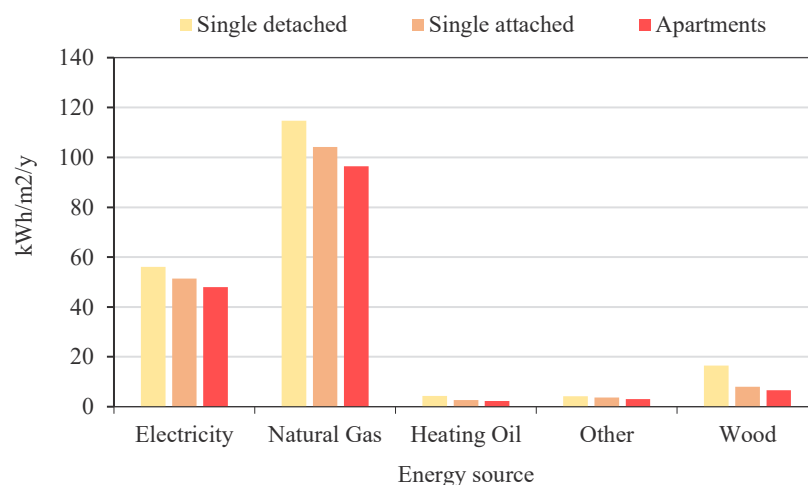


Figure 26: Energy consumption per m<sup>2</sup> by energy source and distinguished by dwelling types. Source: [43].

Even greater differences emerge from space heating consumption, while water heating and appliances show higher shares on the overall for apartments (Figure 27). The contribute of heating is still remarkable compared to other usages: therefore, in case of retrofits or specific policies, it should be the main aspect to act upon, especially for isolated dwellings.

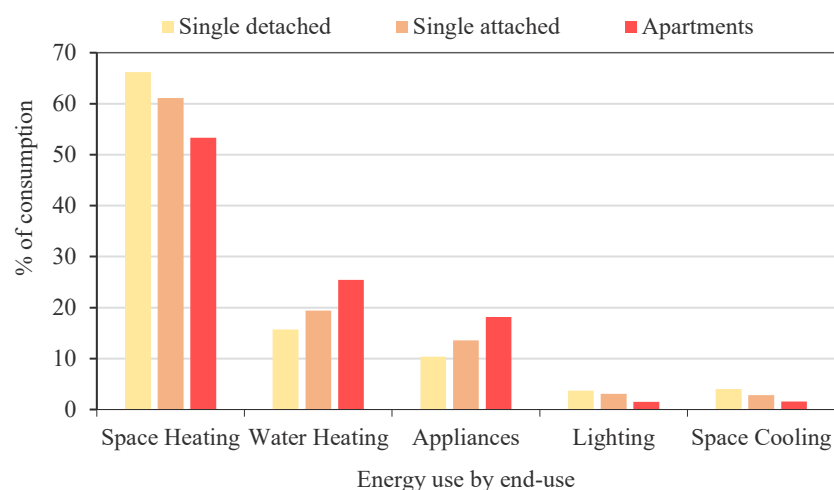


Figure 27. Share of consumption for energy end-uses per household by dwelling types. Source: [43].

The following tables provide the full energy characterisation for the three housing types, which show different share of energy end uses.

Table 18. Energy use by energy source and end-use for detached dwellings in Ontario. Source: [43].

Single detached	Share (%)	PJ	kWh/m <sup>2</sup>	kWh/Household
Energy Use by Energy Source				
Electricity	28.6	108.9	56.06	10,009.17
Natural Gas	58.6	222.8	114.65	20,469.19
Heating Oil	2.2	8.4	4.35	776.28
Other	2.1	8.1	4.18	745.63
Wood	8.4	32.1	16.52	2948.51

Energy Use by End-Use				
Space Heating	66.2	251.8	129.58	23,133.75
Water Heating	15.7	59.7	30.75	5,490.24
Appliances	10.4	39.5	20.33	3,628.99
Lighting	3.7	14.1	7.28	1,299.32
Space Cooling	4.0	15.2	7.82	1,396.49

Table 19. Composition of energy sources by energy end-uses for detached dwellings in Ontario. Source: [43].

Single detached	Composition
Electricity	Space heating (36.8%), appliances (36.3%), lighting (13%), space cooling (14%)
Natural gas	Space heating (73%), water heating (26.8%)
Heating oil, wood, and others	Space heating (100%)

Table 20. Energy use by energy source and end-use for single attached dwellings in Ontario. Source: [43].

Single attached	Share (%)	PJ	kWh/m <sup>2</sup>	kWh/Household
Energy Use by Energy Source				
Electricity	30.2	22.9	51.43	7,765.24
Natural Gas	61.3	46.5	104.23	15,737.49
Heating Oil	1.6	1.2	2.71	409.30
Other	2.2	1.6	3.66	553.09
Wood	4.7	3.6	8.04	1,213.43
Energy Use by End-Use				
Space Heating	61.1	46.3	103.89	15,686.46
Water Heating	19.4	14.7	33.04	4,988.21
Appliances	13.6	10.3	23.06	3,481.48
Lighting	3.1	2.3	5.23	789.13
Space Cooling	2.9	2.2	4.86	733.28

Table 21. Composition of energy sources by energy end-uses for single attached dwellings in Ontario. Source: [43].

Single attached	Composition
Electricity	Space heating (35.6%), appliances (44.8%), lighting (10.2%), space cooling (9.4%)
Natural gas	Space heating (68.3%), water heating (31.7%)

Heating oil, wood, and others	Space heating (100%)
-------------------------------	----------------------

Table 22. Energy use by energy source and end-use for apartments in Ontario. Source: [43].

Apartments	Share (%)	PJ	kWh/m <sup>2</sup>	kWh/Household
Energy Use by Energy Source				
Electricity	30.7	26.9	47.96	4,836.83
Natural Gas	61.7	54.1	96.41	9,723.14
Heating Oil	1.5	1.3	2.31	232.83
Other	2.0	1.7	3.09	311.43
Wood	4.2	3.7	6.61	667.06
Energy Use by End-Use				
Space Heating	53.3	46.8	83.43	8,413.47
Water Heating	25.4	22.3	39.79	4,012.50
Appliances	18.1	15.9	28.34	2,858.36
Lighting	1.5	1.3	2.39	241.10
Space Cooling	1.6	1.4	2.44	245.84

Table 23. Composition of energy sources by energy end-uses for apartments in Ontario. Source: [43].

Apartments	Composition
Electricity	Space heating (30.8%), appliances (59.1%), lighting (5%), space cooling (5.1%)
Natural gas	Space heating (58.7%), water heating (41.3%)
Heating oil, wood, and others	Space heating (100%)

According to the previous information, main indicators considered for the following steps are:

- electricity and natural gas consumption per m<sup>2</sup>, from which the shares of main energy end-uses can be assessed, distinguishing housing types;
- energy-end uses, which will characterise the dwelling profiles;
- both energy use by energy source and end use can be identified by household when sufficient data are available. For developing the following models, the number of households was available only at neighbourhood scale, while at block level useful heated surface and volumes can be calculated.

### 4.4.3 HDDs and CDDs

The consumption of buildings depends on the outside air temperature, especially for energy that is used to heat (or cool) the indoor environment to maintain thermal comfort. The consumption of a building differs with respect to its altitude and to the year, which may show colder or milder seasons. Energy consumptions need to be comparable from different locations: in this case, values are from Toronto and from national surveys. Toronto is in the Southern portion of the nation and along the shore of Lake Ontario, which contributes to mitigate the local climate. The city is in the 3000 HDD belt, included in the climatic zone 5A. Landlords are responsible for providing heat to a minimum air temperature of 21 degrees Celsius from September 15 to June 1. For Toronto, the HDDs and CDDs can be provided by different websites (Table 24), referring to both the national and local values. The most complete and constantly updated dataset is [166], which will be considered in the following steps. The  $T_{\text{reference}}$  can be identified with different values, according to the aims of the study. Most of the available sources set the temperature at 18°C, which works for HDDs. However, it is not a suitable value for indoor cooling, generally identified at 26°C. The problem for Canada is that mean outdoor temperatures above 26°C are quite difficult to be detected, even if they are likely to increase due to global warming.

Table 24. Summary table of HDD and CDD datasets for Toronto.

Website	$T_{\text{Reference}}$ HDD/CDD	Time range	Type of measure	Lacking data	Name of station(s)
Natural Resource Canada NRCan [127]	18°C	1950 - 2095	Derived from 24 global climate models, statistically downscaled and compared with historical data	Not complete	Toronto
Natural Resource Canada NRCan [127]	18°C	1950 - 2013	Historical measured data (annual)	Yes only until 2013	Toronto
ClimateData.ca [44]	18°C	1840 - 2022	Measured data (monthly), for different stations	Not complete	Toronto
ClimateData.ca [44]	18°C	1950 - 2100	Calculated by CMIP5 climate model, downscaled and bias-adjusted (annual)	Complete	Toronto
Toronto weather stats [166]	18°C	1997 - 2021	Measured (annual)	Complete	TORONTO INTL A (Toronto Pearson Int'l Airport)
Historical climate data from NRCan [134]	18°C for CDD; 18°C and 24°C for HDD	1840 - 2022	Measured (hourly and monthly); standard values for 30-year period	Not complete	Toronto stations and suburbs
BizEE software [167]	To be selected, from 18°C to 26°C	Maximum 36 months before	Measured (daily, weekly, monthly or average for 5 years)	Complete, but referred to maximum 36 months before or average for 5 years.	Toronto stations and suburbs

The historical (1950-2013) and the forecasted trends show a decrease in annual HDDs and, therefore, an increase in temperature related to global warming (Figure 28). This perspective appears even more clear by 2095, with consequences on energy consumption in the long period. While annual modelled HDDs do not follow exactly the measured values, they are coherent with the overall descending trend.

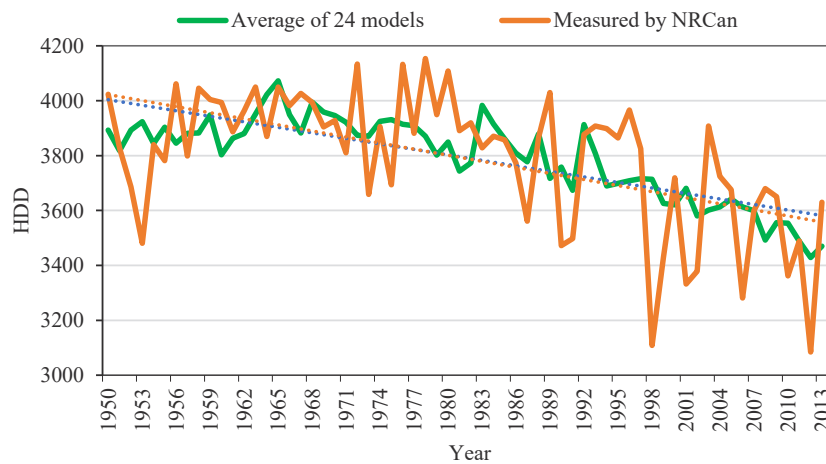


Figure 28. HDD trends with  $T_{reference} = 18^{\circ}\text{C}$  between 1950 and 2013, by the average of 24 models and measured by NRCan. Source: [127].

The decreasing values of HDDs related to changing temperature trends are confirmed by the long-term 30-year average values, assessed by NRCan (Table 25).

Table 25. Monthly normal values of HDDs in 30-year ranges for Toronto City Centre station for 1961-1990, 1971-2000 and 1981-2010, with  $T_{reference} = 18^{\circ}\text{C}$ . Source: [134].

Time range	Jan	Feb	Mar	Apr	May	Jun	Jul	Aug	Sep	Oct	Nov	Dec	Year
1981 - 2010	673.9	580.6	514.6	306.3	135	26.2	2.4	5.1	62.5	227.3	391.7	572.6	3498.2
1971 - 2000	688.8	600.1	518.2	313.8	134.7	28.2	2.3	5.9	65.5	230.2	395.3	586.6	3569.7
1961 - 1990	701	618.5	528.1	316.7	145.8	31.3	3.2	7.5	67.2	227.2	392.4	605.3	3644

While winter period is characterised by heating, cooling systems are used in warmer months for keeping an indoor thermal comfort. The CDD is the summation for all days in the cooling season of the positive differences between the mean outdoor temperature and the reference comfort temperature. The decreasing values in the heating season are balanced by the rising temperatures in the warmer months (from May to September), which imply higher CDDs with an increasing trend already from the last century. For most datasets, the reference temperature is assumed at  $18^{\circ}\text{C}$ , even if the cooling systems are generally turned on with higher temperatures. Trends in Figure 29 are analysed with the  $18^{\circ}\text{C}$  threshold, but higher values will be considered for Toronto. Projections for CDDs confirm the perspective of higher temperatures, especially during summers, with more frequent and longer heatwaves which will impact too on energy consumption (Figure 29).

The only website (degreedays.net) providing CDD above  $26^{\circ}\text{C}$  threshold shows a peak for 2020, even if previous years are not available. The lack of sufficiently completed data for  $26^{\circ}\text{C}$  leads to the consideration of  $24^{\circ}\text{C}$  as threshold for calculating CDDs, from the data of Natural Resource of Canada [127]. The website reports the normal values for the Toronto station (113m a.s.l.) for the 1981-2010 reference period (necessary to set normalisation of consumption). Values underline an increasing in CDDs in the two 30-year periods (Table 26), due to rising temperature and cooling needs for Toronto.

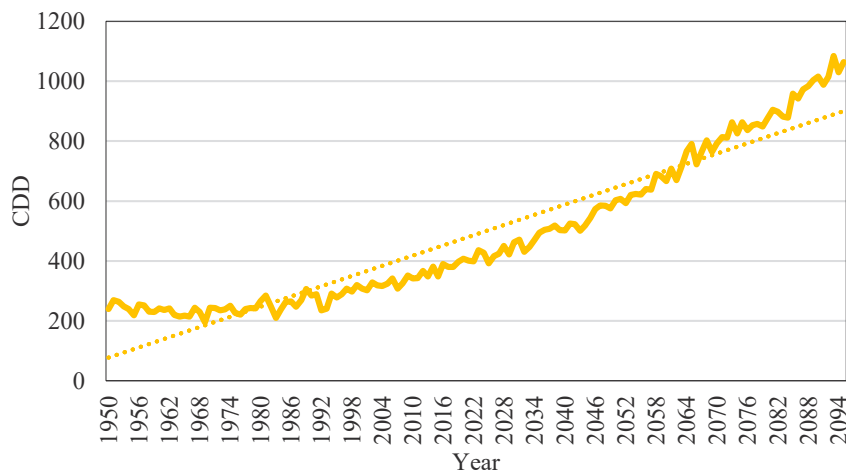


Figure 29. Forecasted CDDs trend until 2095, with  $T_{reference} = 18^{\circ}\text{C}$ . Source: [127].

Table 26. Monthly normal values for CDDs for Toronto City Centre station for 1971-2000 and 1981-2010, with  $T_{reference} = 24^{\circ}\text{C}$ . Source: [134].

Time ranges	Jan	Feb	Mar	Apr	May	Jun	Jul	Aug	Sep	Oct	Nov	Dec	Year
1981 - 2010	0	0	0	0.1	0.4	4.9	17.7	10.7	2	0	0	0	35.8
1971 - 2000	0	0	0	0.1	0.4	3.9	15.5	8.6	1.7	0	0	0	30.2

HDDs and CDDs will be fundamental in the following steps for the normalisation of heating and cooling consumption. Data from different locations can be influenced by the annual weather and not directly comparable. Therefore, the relation with HDDs and CDDs of a specific year (which reflect the temperature trend) lead to a normalised result.

#### 4.4.4 The Toronto 2030 Platform

The introduction of policies to reduce emissions and the modelling of energy data reflects new mapping instruments. The Toronto 2030 Platform is an online tool (Figure 30) developed by the Canadian Urban Institute to report building performance and improvements towards GHG reduction targets in the central Toronto 2030 District. The Toronto 2030 District is a private-public initiative aimed at achieving a low-carbon future, exploiting stakeholders' collaboration. It is part of a network of 23 districts across North America cities to achieve targets of the Architecture 2030 Challenge and Paris Agreement [168]. For existing buildings, the aim is to reduce GHG emissions in line with Canadian national perspectives and Toronto policies, while for new constructions net-zero structures by 2030 [168].

The Toronto 2030 District is developing research and engagement activities to define pathways for a zero-carbon district by 2030, following different steps [168]:

- Phase 0 - Pathways to Net Zero Background Working Paper, completed in September 2020, which included the full range of parameters, drivers for change and potential barriers to overcome;
- Phase 1 - Completed Heating Energy Supply Decarbonization Report (Fuel Switching), for which three options have been assessed (technically and financially): renewable natural gas, hydrogen and electrification;

- Phase 2 - Energy Efficiency options (Coming Soon);
- Phase 3 - Developing Integrated Decarbonization Pathways (In Progress);
- Phase 4/5 - Community-directed, district-supported pilot projects, and reporting lessons learned (In Progress).

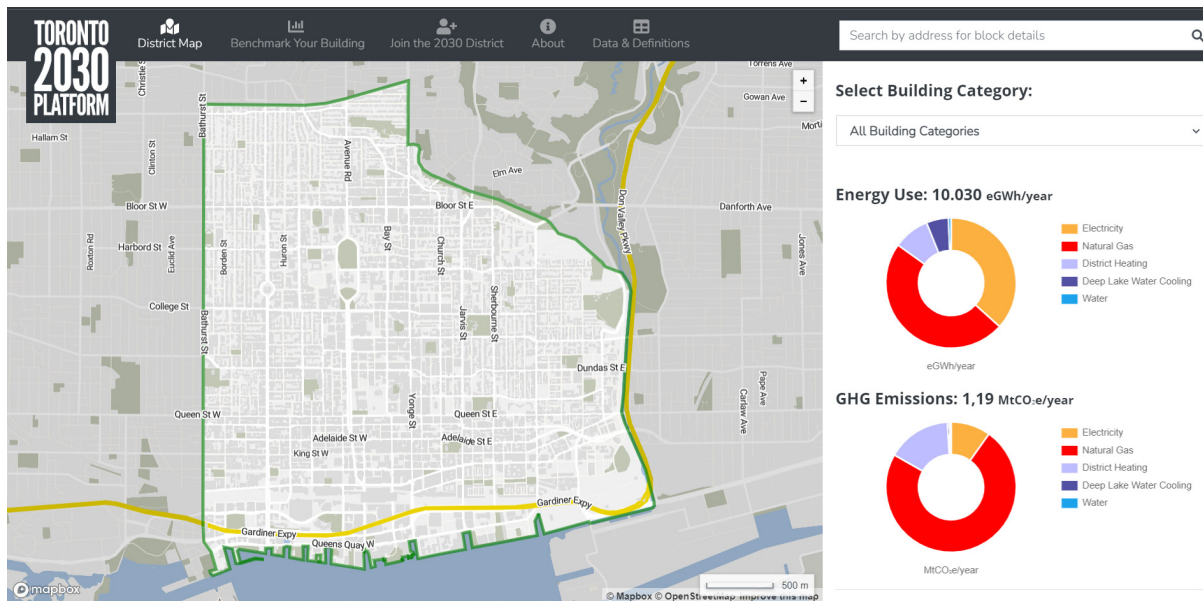


Figure 30. Online tool and downtown area considered by the 2030 Toronto Platform. Source: [6]

The online platform displays information at the block scale:

- Block profile: building category and vintage mix (by GFA percentage).

The building functions are distinguished in office (small, street-level office units up to large multi-storey office towers), retail & hospitality (all retail, restaurants, hotel, and entertainment establishments), multi-unit residential (all buildings with 7 or more residential units), residential (all buildings with 6 or fewer residential units), institutional (schools, post-secondary campuses, long-term care facilities, and hospitals) and industrial (warehouses and manufacturing).

The period of construction by block is divided in pre-1980, 1980-2004 and post-2004, to follow the subdivision provided by the ASHRAE framework.

- Energy performance, with minimum and maximum values: GHG from buildings and from transportation (tCO<sub>2</sub>e/year, energy use intensity (kWh/m<sup>2</sup>/year), electricity (MWh/year), natural gas and water (eMWh/year) and, if used, steam and deep lake cooling (eMWh/year).

Due to licensing restrictions, energy consumption from bills is available only for the whole TOcore district: therefore, block-level values were modelled based on information about building size, age, occupancy and, consequently, they are not directly measured at this scale. In case of incomplete structures' characterisation, additional data was integrated by Internet and Google Street View.

Table 27: Energy types, sources and emission factors applied in the Toronto 2030 Platform. Source: [6].

Energy source Annual energy use	Source	GHG emissions Factor
Electricity	Toronto Hydro	32 grams CO <sub>2</sub> e / kWh
Natural Gas	Enbridge Inc.	1874.6 grams CO <sub>2</sub> e / m <sup>3</sup>
Steam (District Heat)	Enwave Energy Corporation	73.8 grams CO <sub>2</sub> e / lb

Deep Lake Water Cooling	Enwave Energy Corporation	41.3 grams CO <sub>2e</sub> / ton-h
Water	City of Toronto	114.4 grams CO <sub>2e</sub> / m <sup>3</sup>

Table 28. Data sources used for modelling (buildings and transports) the Toronto 2030 Platform. Source: [6].

Modelled aspect	Year	Source
Building Energy Models based on ASHRAE 90.1	-	Ryerson University; ASHRAE
Commercial Buildings Energy Consumption Survey	2003	US Energy Information Administration, with conversion to Toronto climate zone
Transportation Models based on Transportation for Tomorrow Survey	2011	University of Toronto; Ontario Ministry of Transportation
Energy Use and Total Floor Area for Institutional Buildings	2016	Ontario Ministry of Energy, Broader Public Sector GHG Emissions
Building Age, Occupancy Type, and Total Floor Area	2017	Municipal Property Assessment Corporation
Building Outlines and 3D Massing	2017	City of Toronto, Planning Division

The platform adopts a top-down engineering approach. Block data are modelled results based on ASHRAE guidelines and on 2017 district energy consumption available from local energy providers (Table 27; Table 28; Table 29). From measured values at the district level by energy providers, building energy simulations were modelled for single blocks based on ASHRAE 90.1 (2004) Standard for climate zone 5A and using information on building size, age, occupancy. Consequently, displayed values on the platform are not directly measured at the block or building scales.

The ASHRAE 90.1 (2004) Standard for climate zone 5A was used for low-rise and high-rise apartments (Table 29). The prototypes are pre-1980, 1980-2004, and post 2004. ASHRAE has only a more recent version of the template (IECC 2015) for single family dwellings (detached and attached) for new residential constructions (Table 29): therefore, distinctions by construction period were not available and are not performed in the Platform for these two categories. A set of four heating systems and four foundation types were matched to create the single-family prototypes.

Table 29. Dwelling characterisations by ASHRAE framework.

Modelled aspect	Single-family	Mid-rise and High-rise apartment
ASHRAE version	2015 IECC	DOE pre-1980; DOE 1980-2004; 90.1 2004
Wall type	Wood frame	Steel frame
Wall R-value	2.75 m <sup>2</sup> K/W (U <sub>max</sub> = 0.36 W/m <sup>2</sup> /K)	Pre 1980: 1.13 m <sup>2</sup> K/W 1980-2004: 2.15 m <sup>2</sup> K/W Post 2004: 3.23 m <sup>2</sup> K/W

Roof type	Gable roof	Built-up flat roof, insulation entirely above deck
Roof R-value	2.4 m <sup>2</sup> K/W (U <sub>max</sub> =0.365 W/m <sup>2</sup> /K)	Pre 1980: 2.50 m <sup>2</sup> K/W 1980-2004: 3.38 m <sup>2</sup> K/W Post 2004: 5.56 m <sup>2</sup> K/W
Floor-to-ceiling height (m)	2.5	3.05
Window U-value	0.32 W/m <sup>2</sup> /K	Pre-1980: 3.53 W/m <sup>2</sup> /K 1980-2004: 3.35 W/m <sup>2</sup> /K Post 2004: 2.33 W/m <sup>2</sup> /K
Window SHGC	0.34	Pre-1980: 0.41 1980-2004: 0.39 Post-2004: 0.39
Window-to-wall ratio	0.13	Pre-1980: 0.15 1980-2004: 0.15 Post-2004: 0.30
Foundation U-value	Slab: U = 0.15 W/m <sup>2</sup> /K crawl space: U = 0.31, heated space: U= 0.37, unheated space: U=0.53	Pre-1980 and 1980-2004: 0.54 Post 2004: R-2.6 ci (U <sub>max</sub> = 0.321 W/m <sup>2</sup> /K)
HVAC system	Electric resistance, gas furnace, oil boiler or heat pump	Gas boiler, split AC system DX, gas water heater
Electricity plugs and process (W/m <sup>2</sup> )	14.05	Pre-1980: 5.38 1980-2004: 5.38 Post-2004: 6.67
Infiltration (ACH)	0.11	Pre-1980: 0.7 1980-2004: 0.7 Post-2004: 0.14

For this reason, the aim will be to disaggregate the energy consumption calculated for the whole blocks to the buildings within the area. Starting points will be the measured energy demand for the 2030 District in 2017 and the modelled block profile in the Toronto 2030 Platform.

The whole view distinguishes both the consumption by energy sources and by building functions, letting emerge the main energy characteristics for the area.

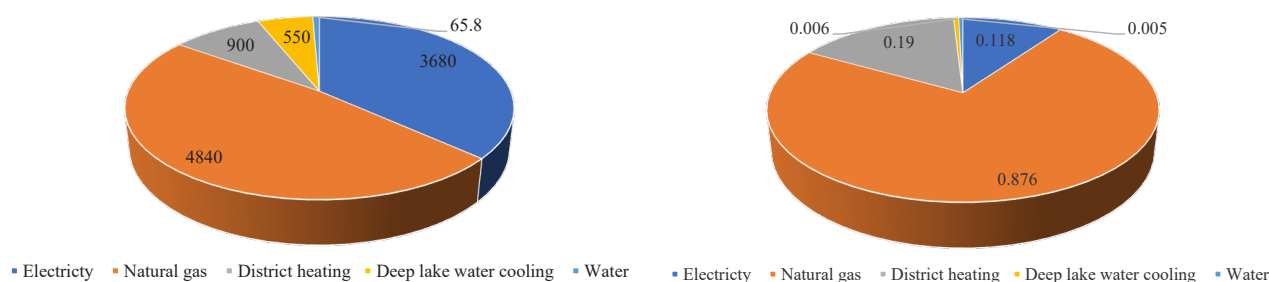


Figure 31. Energy shares by different sources (left) and GHG emissions shares (right) of the 2030 District, according to 2017 energy data. Source: [6].

Table 30. Main characteristics of the 2030 District, based on 2017 values. Source: [6].

Data	Value for the 2030 District
GHG emissions from transportation to the district (MtCO <sub>2</sub> /year)	1.48
Energy use intensity - EUI (ekWh/m <sup>2</sup> /year)	320

Number of structures	7,216
Gross Floor Area (m <sup>2</sup> )	31,329,000

According to Figure 31, the most used energy source is natural gas, which mainly contribute in GHG emissions, while a lower share is from electricity. District heating and deep lake cooling interest only some areas of the district (generally, the closest to the waterfront) and, therefore, count for a minimum share in the overall energy panel.

The distinction of consumption and emissions (Figure 32) by function provides a further overview of the situation, where the relevant demand for natural gas is confirmed. The most energy demanding and emitting sector is commercial, which a remarkable share of GFA and number of structures mostly distributed along the main infrastructural axes (designated as commercial areas also by the zoning plan). Multi-unit residential prevails on the residential one due to the remarkable presence of high-rise apartments in the central area, while dwelling with less than 7 units are more limited and spread around the outer suburbs. MURBs have also higher energy intensity, impacting more on the energy balance of the district. Industrial sector represents a minor share in energy use due to its limited presence in the downtown area, leaving room for more-tertiary oriented function as offices (Table 31).

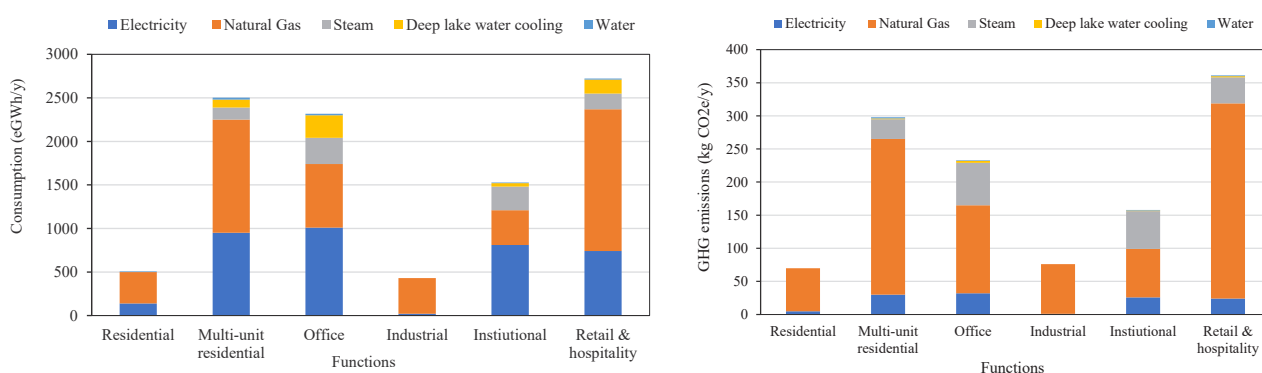


Figure 32. Energy consumption (left) and GHG emission (right) by function in the 2030 District for 2017. Source: [6].

Table 31. Main features of the 2030 District by function, based on 2017 energy data. Source: [6].

	Residential	MURB	Office	Industrial	Institutional	Retail & Hospitality
Mean energy use intensity (kWh/m <sup>2</sup> /y)	179	234	268		440	491
N° of structures		3034	2603	26	561	4690
Gross floor area (m <sup>2</sup> )	2,848,000	10,711,000	8,671,000	61,000	3,495,000	5,544,000
% Gross floor area	9	34.1	27.6	0.1	11.1	17.6
Electricity (eGWh/y)	140	950	1010	20	810	740
Calculated electricity intensity (kWh/m <sup>2</sup> /y)	49.16	88.69	116.48	327.87	231.76	133.48
Natural Gas (eGWh/y)	360	1300	730	410	400	1630
Calculated natural gas intensity (kWh/m <sup>2</sup> /y)	126.40	121.37	84.19	6,721.31	114.45	294.01

Steam (eGWh/y)	0	140	300	0	270	180
Deep lake water cooling (eGWh/y)	0	90	260	0	40	160
Water (eGWh/y)	6	22.5	18.2	0	7.3	11.6

Based on the Platform, a comparison with results from other surveys for Ontario is applied, considering data from the SHEU (2017) measured for 2015 [77] and the Comprehensive Energy Database (NRCan, 2020) referred to 2018 [43]. The application of values for Toronto requires a preliminary normalisation due to different locations on which they are applied and, consequently, different weather conditions for heating consumption (see Paragraph 4.4.3). The following equation has been applied to the considered values (and will be used also in the next steps too):

$$C_{\text{norm}} = C_{\text{real}} * (\text{HDD})/(\text{HDD}_{\text{real}})$$

where:

- $C_{\text{norm}}$  is the normalised consumption (kWh/m<sup>2</sup>/y)
- $C_{\text{real}}$  is the real consumption for a precise year (kWh/m<sup>2</sup>/y)
- HDD is the conventional value of heating degree days for the location given by law or calculated on a reference year (based on a 30-year range)
- $\text{HDD}_{\text{real}}$  is the value of heating degree days for the location for a precise year (in this case, 2015 and 2017).

The same calculation can be applied for cooling, which is fundamental for consumption during summer. The following values (Table 32; Table 33) are applied for normalising data from 2015 and 2017 for different locations. However, HDDs and CDDs for Ontario appear extremely high, probably due to the inclusion of areas near the North Pole, which greatly increase the final value. Despite the extension of the province (more than 1 million km<sup>2</sup>), 92% population lives in the highly urbanised corridor from Windsor to Ottawa, including Toronto, which covers only the 12% of the whole province. Therefore, rather than the data from Climate Atlas of Canada, the HDD and CDD indexes provided by the Energy Database have been considered for the normalisation of Ontario (Table 32; Table 33).

Table 32. Summary table for consumption normalisation based on HDDs for 2015 and 2017.

Location	Conventional HDD	Conventional HDD	HDD <sub>real</sub> for 2015	Multiplicative coefficient	HDD <sub>real</sub> for 2017	Multiplicative coefficient	Source of HDD <sub>real</sub>
Toronto	3,520	Given by 2012 Ontario Building Code (OBC), SB-12, effective by March 15, 2013.	3769	0.93	3518	1.00	weatherstats.ca [166]
Ontario	6,270.48	Calculated on a 30-year range.	5860	1.07	6156.8	1.02	climateatlas.ca [127]

The normalisation should not be applied to the whole consumption but only to the share of uses influenced by weather conditions and for different dwelling types (reference to Figure 24), which are space heating and space cooling with the respective multiplicative factors.

Table 33. Summary table for consumption normalisation based on CDDs for 2015 and 2017.

Location	Conventional CDD	Conventional CDD	CDD <sub>real</sub> for 2015	Multiplicative coefficient	CDD <sub>real</sub> for 2017	Multiplicative coefficient	Source of CDD <sub>real</sub>
Toronto	35.8	Calculated on a 30-year range (1981-2020), at 24°C.	25.3	1.41	11.6	3.09	NRCan [134]

Table 34. Normalisation indexes for HDDs and CDDs for 2015 and 2017.

Variable	Index for Ontario, 2015	Index for Ontario, 2017	Source
HDD	0.92	0.92	NRCan (2020)
CDD	1.36	1.36	NRCan (2020)

Table 35. Distinction of dwelling types by SHEU, NRCan and the Toronto 2030 Platform.

Division provided by data sources		
SHEU	NRCan	Toronto 2030 Platform
Single detached	Single detached	Residential
Double/row houses	Single attached	
Low-rise apartments	Apartments	Multi-unit residential
High-rise apartments		

Table 36. Comparison of electricity consumption normalised in 2017 for the central station of Toronto-City Centre.

Source	Electricity consumption (kWh/m <sup>2</sup> /y)			
	SHEU	NRCan	Toronto 2030 Platform	
Data info	Measured in 2015 for Ontario and normalised	Measured in 2017 for Ontario and already normalised	Measured in 2017 for Toronto and not normalised	Normalised values for 2017
Single detached	39.74	56.06	49.16	61.23
Semi-detached houses	41.89	51.43		
Low-rise apartments	88.33	47.96	88.69	87.26
High-rise apartments	49.69			

Table 37. Comparison of natural gas consumption normalised in 2017 for the central station of Toronto-City Centre.

Source	Natural gas consumption (kWh/m <sup>2</sup> /y)			
	SHEU	NRCan	Toronto 2030 Platform	
Data info	Measured in 2015 for Ontario and normalised	Measured in 2017 for Ontario and already normalised	Measured in 2017 for Toronto and not normalised	Normalised values for 2017
Single detached	101.79	114.05	126.40	128.17
Semi-detached houses	105.04	104.23		
Low-rise apartments	166.78	96.41	121.37	122.79
High-rise apartments	185.31			

The comparison of data lets emerge some differences:

1. electricity demand has lower values by the SHEU (2017) and higher by NRCan (2020), while the Platform seems to have higher results especially for residential dwellings;
2. NRCan (2020) registers a contained value for apartments, which is more similar to the high-rise one distinguished by the SHEU (2017), while the Toronto Platform closer to low-rise by SHEU (2017);
3. natural gas is characterised by progressively increasing values by SHEU (2017), while decreasing for NRCan (2020) with decreasing S/V ratio;
4. the alignment of data is not accurate due to the different classes used by the surveys and the generalisation in residential/multi-unit adopted by the Platform for privacy issues. Apartments are the most difficult ones to be assessed due to the variegated distinctions.

As mentioned before, the main weakness of the Toronto 2030 Platform is the analysis limited to the block scale, by estimating energy consumption from measured district data. A deeper estimation of structure demand can provide a more precise diversification as well as contribute to guide future energy-related policies for the building-stock. Therefore, the aim of the following steps is to disaggregate consumptions for single buildings from block values, according to their specific characteristics, and then apply a statistical top-down approach.

#### 4.4.5 Assessment of energy consumption: neighbourhood scale

Before the energy model at the building scale, an overall analysis is applied to the 11 neighbourhoods of the 2030 District, according to the Neighbourhood Profile for 2016 [75] released by the City of Toronto (latest available). The City of Toronto currently counts 140 social planning neighbourhoods, introduced in the late Nineties. The division showed in Figure 33 was developed to help government and community organizations by spatially providing socio-economic data. Their limits do not change over time and are defined by main streets, former boundaries, or natural boundaries such as rivers. Their population goes from 7,000 to 10,000 inhabitants.

The neighbourhood scale is the most detailed to provide socio-economic information due to privacy issues, while a more specific overview (as blocks) is not available. Therefore, an initial analysis has been performed for neighbourhoods, based on the overall District energy information.

Neighbourhood characterisation distinguishes the share of housing types and the period of construction. An overview of neighbourhoods by dwelling types shows the clear prevalence of buildings that have more than 5 floors, especially in the central areas of downtown (Figure 33; Figure 34). Less dense housing solutions (with less than 3 storeys) are more common in areas closer to downtown borders. The residential development of Toronto was concentrated before 1980, especially for the outer neighbourhoods, while the waterfront area is characterised by a more recent growth, mainly by high-rise solutions (Figure 35). Indeed, new urban planning policies, space constraints and financial benefits favoured the construction in height in the downtown and sprawl in the nearby suburbs.

Similar types of buildings will have different characteristic as well as different consumption values, with generally higher population densities. Residential skyscrapers are generally matched or close to other businesses (as retail or offices), while low-density housing blocks are mostly “mono-functional”, having other functions along major commercial streets and/or areas.

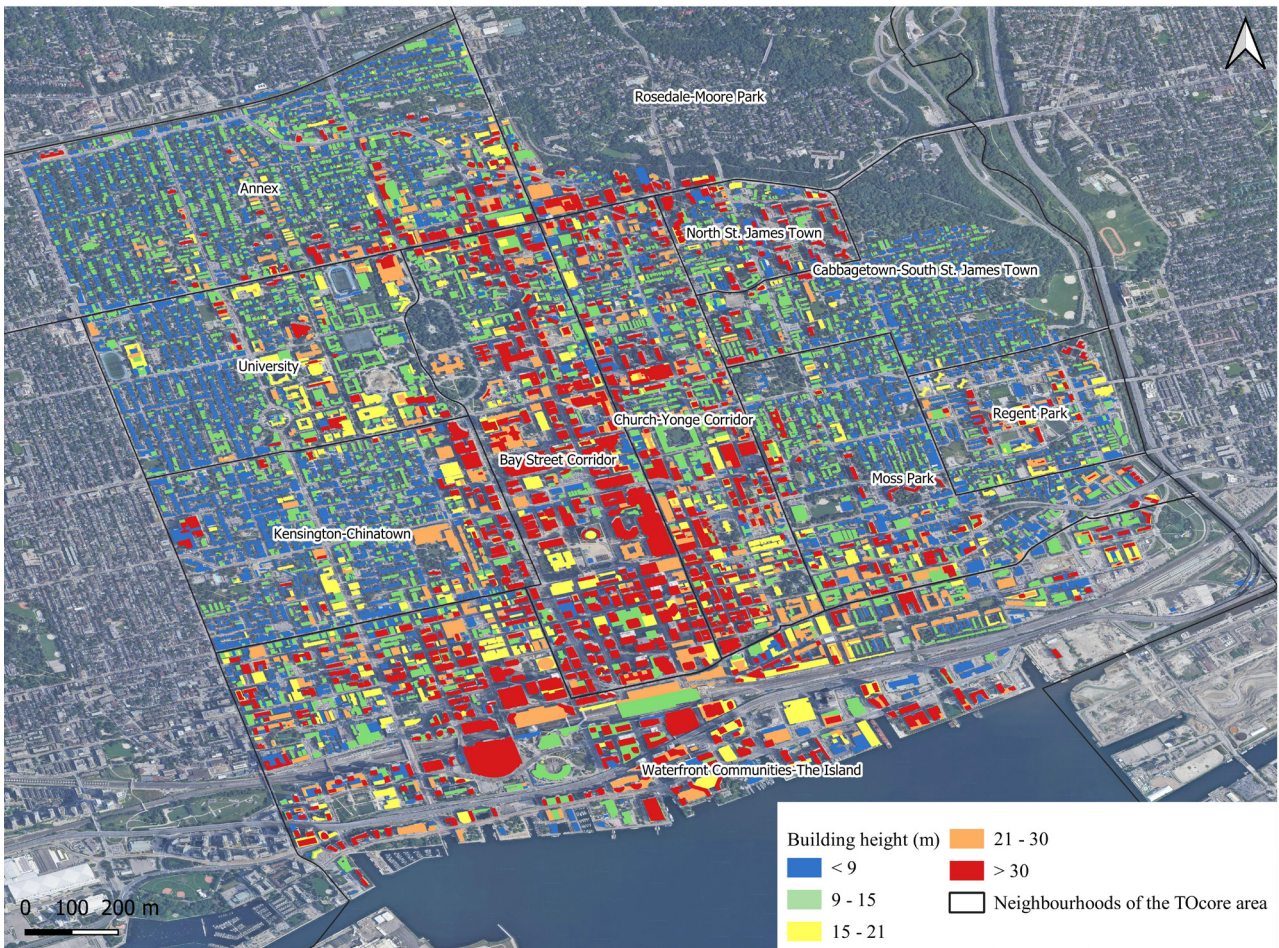


Figure 33. Classification of building height (m) for the TOcore area and localisation of the 11 neighbourhoods. Source: own elaboration of [74] [75].

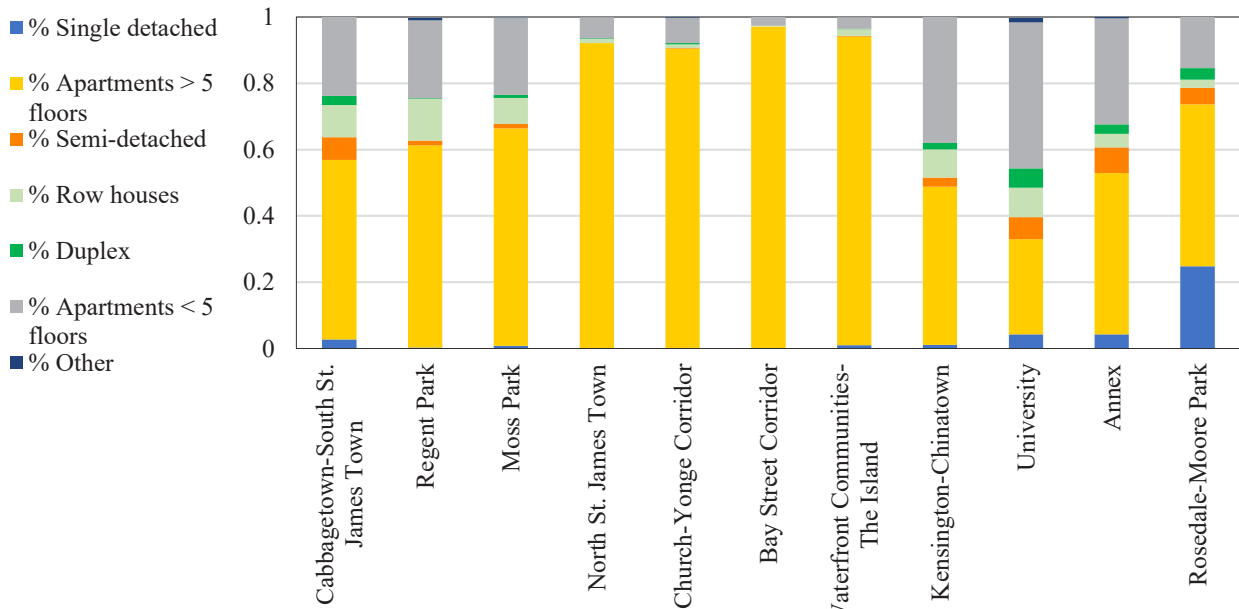


Figure 34: Overview of dwelling types by neighbourhood. Source: own elaboration of [75].

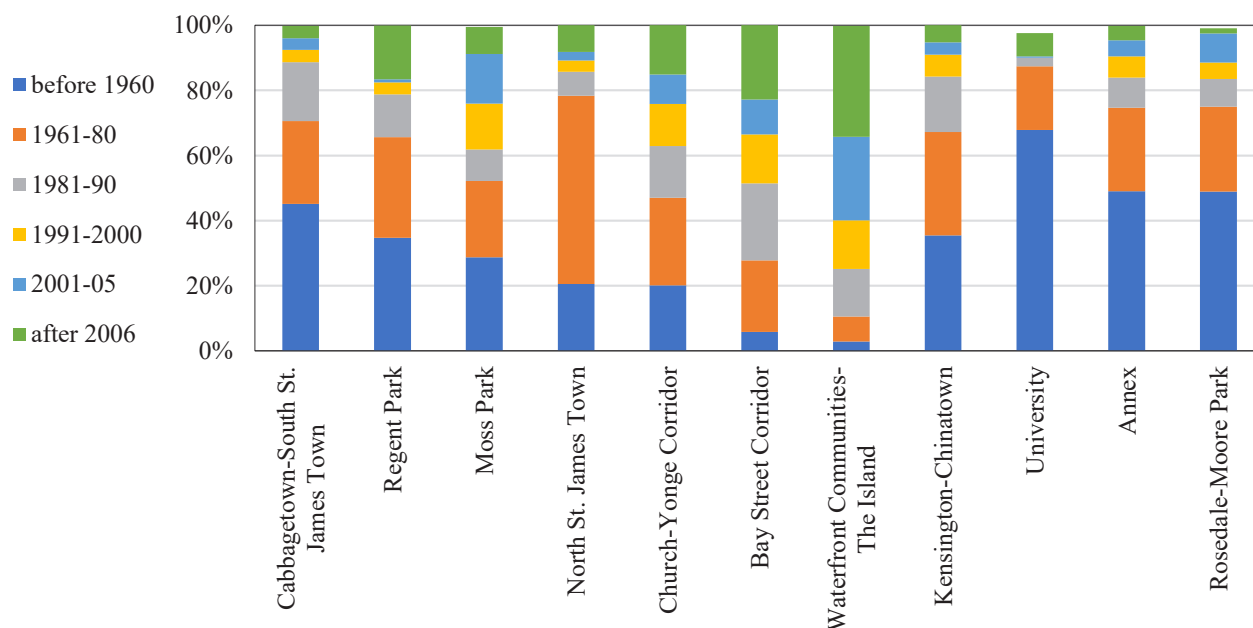


Figure 35: Overview of age of construction of dwellings by neighbourhood. Source: own elaboration of [75].

However, the subdivision in dwelling types provided by the Neighbourhood Profile (more or less than 5 storeys) is different from the one made by the Toronto Platform, which distinguishes residential (less than 7 units) and multi-unit residential buildings (at least 7 units). It was not possible to estimate the energy consumption distinct by subcategories, but it was applied to the whole housing function, without a more detailed categorisation.

A deeper analysis should be performed to understand different consumptions for distinct residential types. The consumption assessment by dwelling category is based on data from the SHEU (2017) (Table 38; Table 39). As explained before, the survey distinguishes values for the whole Canada and for single provinces, among which Ontario was selected, and by main dwelling types and periods of construction. The dwelling category and the age range are provided for each neighbourhood, so that both energy values can be tested for Toronto.

Considering the different subdivision in temporal ranges from the two sources, three equal belts are identified for energy values (with an average) and neighbourhood (sum of dwellings) (Figure 36). Also in this case, a normalisation of data is introduced for assessing them at the same level.

Table 38. Values of energy consumption (measured) for different residential types for Ontario by SHEU. Source: [77].

Ontario: Type of dwellings	Electricity (EE)		Natural gas (NG)		Energy intensity	
	GJ/household	GJ/m <sup>2</sup>	GJ/household	GJ/m <sup>2</sup>	GJ/household	GJ/m <sup>2</sup>
Single detached	34.8	0.14	n. a.	0.39	128.5	0.52
Double/row houses	27.1	0.15	n. a.	0.4	90.4	0.51
Low-rise apartments	30.6	0.32	n. a.	0.63	53.8	0.57
High-rise apartments	19	0.18	n. a.	0.7	33	0.32

Table 39. Values of energy consumption (measured) for different residential ages for Ontario by SHEU. Source: [77].

Ontario: age of construction	Electricity		Natural gas		Energy intensity	
	GJ/household	GJ/m <sup>2</sup>	GJ/household	GJ/m <sup>2</sup>	GJ/household	GJ/m <sup>2</sup>
Before 1946	31.2	0.17	n. a.	0.51	111.9	0.6
1946 - 1960	29.8	0.15	n. a.	0.44	108.3	0.56
1961 -1977	28	0.16	n. a.	0.44	87.1	0.49
1978 - 1983	32.2	0.16	n. a.	0.39	96.4	0.48
1984 - 1995	34.5	0.15	n. a.	0.38	116.7	0.52
1996 - 2000	34.4	0.16	n. a.	0.37	108	0.49
2001 - 2010	31.5	0.12	n. a.	0.32	106.8	0.42
2011 or later	30.6	0.14	n. a.	0.34	95.9	0.45

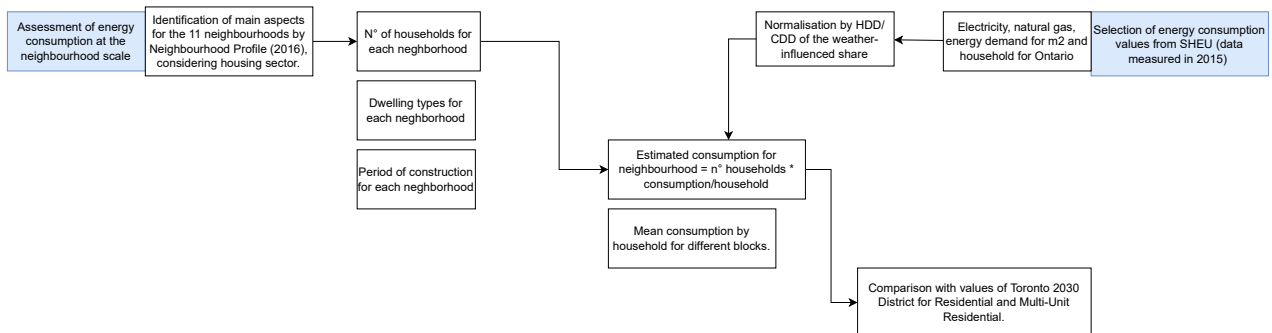


Figure 36. Summary flowchart for assessing consumption at the neighbourhood scale.

Following the procedure in Figure 36, the neighbourhood consumption is calculated as:

$$C_{\text{neighbourhood}} = \sum n_{\text{HH}} * C_{\text{HH}}$$

where:

- $C_{\text{neighbourhood}}$  is the overall consumption of the neighbourhood to be assessed
- $n_{\text{HH}}$  is the overall number of households provided by the Toronto Neighbourhood Profile (2016) [133], divided by dwelling types
- $C_{\text{HH}}$  is the normalised consumption per household provided by the SHEU (2017) [77] for electricity and by NRCan (2020) for natural gas (due to not available data by SHEU), divided by dwelling types.

According to estimated values, the consumption is clearly higher with more inhabitants. The estimated consumption by household types reveals that the most demanding neighbourhood is the Waterfront area, which also counts the highest population (65,913 inhabitants in 2016) with mostly high-rise structures (Figure 37; Figure 38). Church Yonge Corridor appears still characterised by a several condominiums due to its central location, while the Annex by a more mixed housing stock which

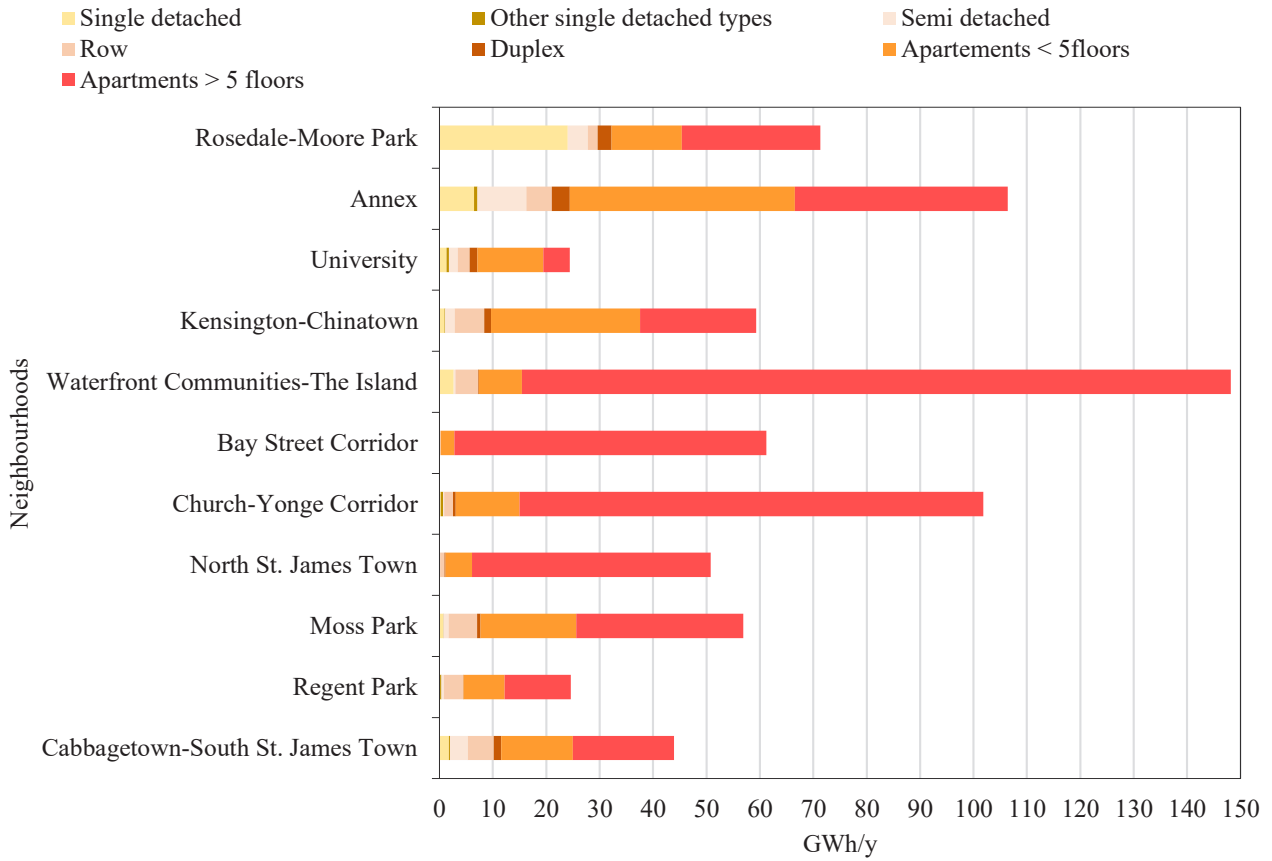


Figure 37. Estimation of total electricity consumption by household types, divided by the 11 neighbourhoods. Source: own elaboration of [133].

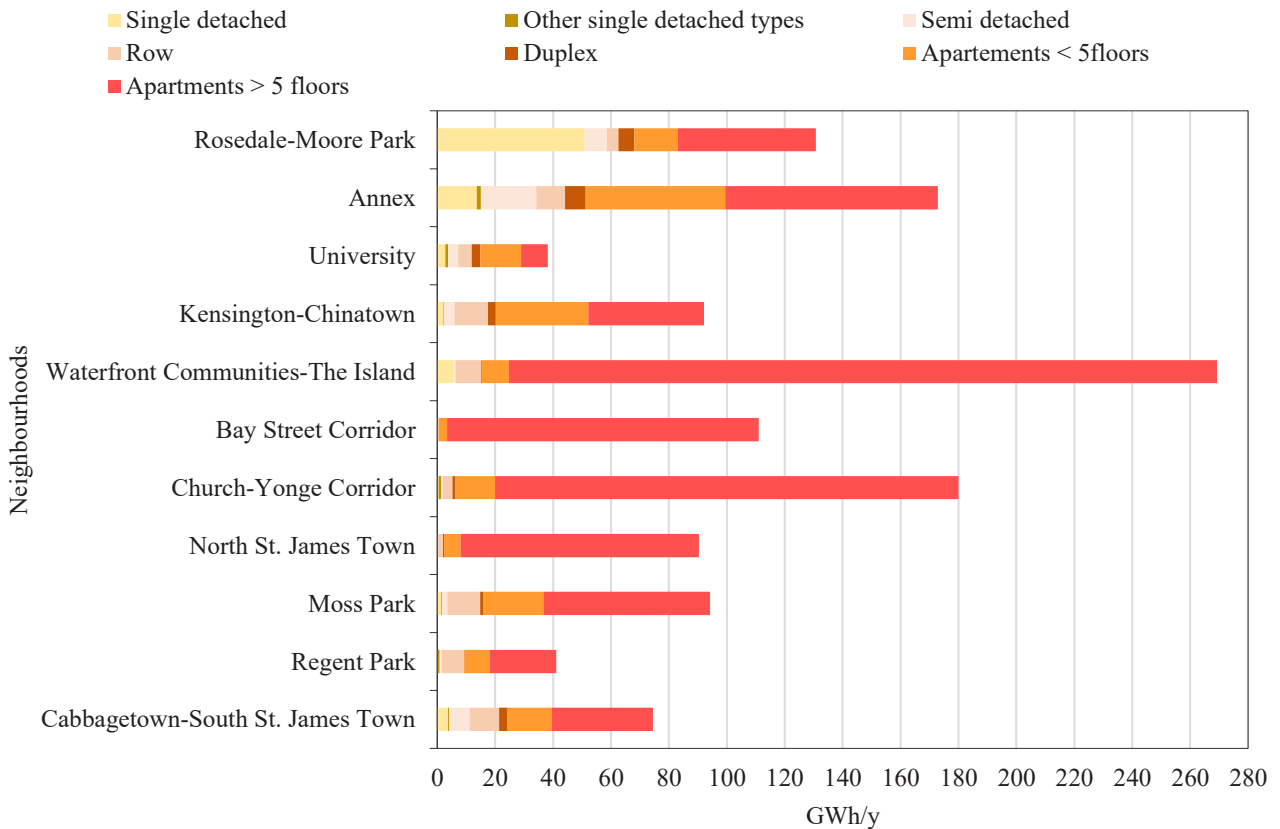


Figure 38. Estimation of total natural gas consumption by household types, divided by the 11 neighbourhoods. Source: own elaboration of [133].

differently contributes to the energy profile of the area.

To have an overview of consumption not influenced by population, an additional analysis is applied:

$$C_{\text{reference per HH}} = \Sigma (C_{\text{neighbourhood}} / n_{\text{HH}})$$

where:

- $C_{\text{reference per HH}}$  is the mean consumption for one household of the neighbourhood;
- $C_{\text{neighbourhood}}$  is the overall consumption of the neighbourhood previously calculated;
- $n_{\text{HH}}$  is the overall number of households provided by the Toronto Geoportal (2016)..

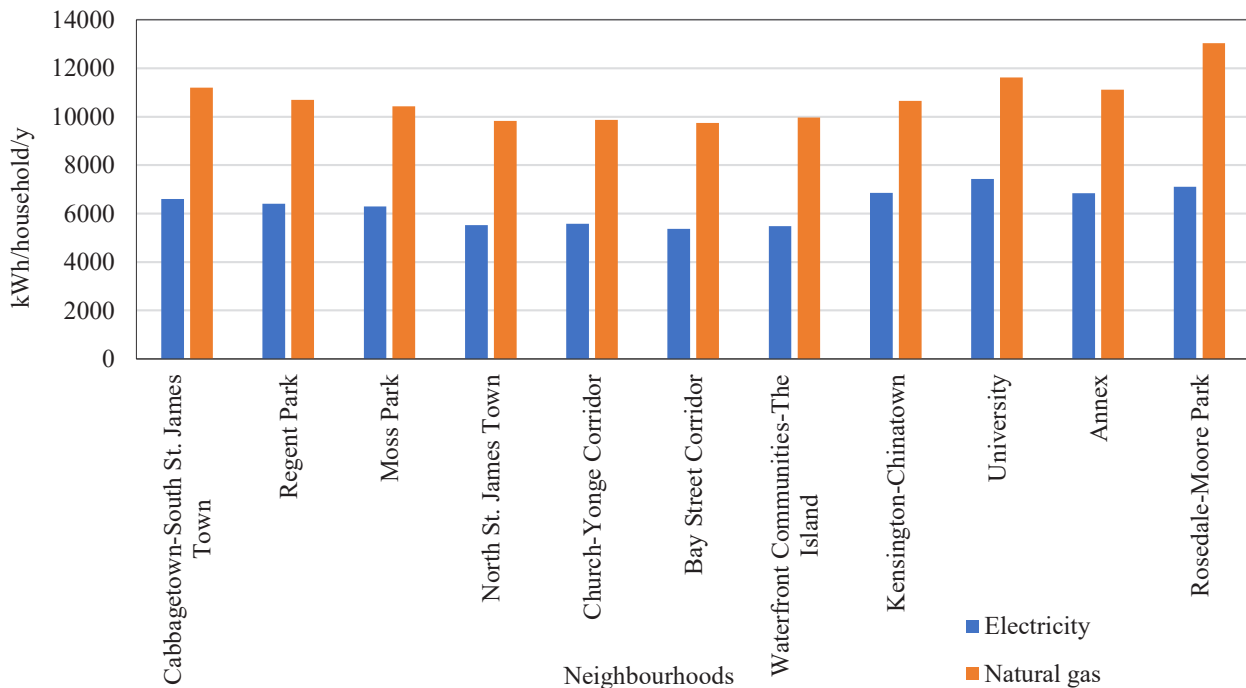


Figure 39. Mean consumption (electricity and natural gas) of household, divided by the 11 neighbourhoods. Source: own elaboration of [133].

The average consumption by neighbourhood (Figure 39) lets emerge the University area as the most demanding for electricity (7,417.69 kWh/y per household), while Rosedale for natural gas (13,039.15 kWh/y per household). This is due to the significant presence of most consuming household types, as single detached houses, and low-rise apartments.

An additional final comparison with the 2030 District consumption cannot be performed because boundaries of the neighbourhoods are different (generally more extended) from the 2030 District limits. Therefore, in the following steps, a more detailed analysis on the 2030 District blocks will be provided.

## 5. APPLICATION OF THE STATISTICAL MODEL

### 5.1 Preliminary steps

Main aspect of the statistical model is the correspondence between the useful heated surface (UHS) and the energy consumption. The UHS have been identified in GIS environment to have specific estimated demand per square meter easily comparable.

The development of the analyses is firstly based on the availability and typology of data: in this case, the dataset for Toronto has been developed with data for three different territorial scales (Table 40):

- building, which are the most specific one, even if limited due to privacy concerns
- blocks and district, available from the Toronto 2030 Platform
- neighbourhoods, downloadable from the Toronto Geoportal.

Table 40. Main features, pros and cons of available data at the different scales for Toronto.

Territorial scale	Source	Year	Pros	Cons
Building	Toronto Geoportal and OSM	2017	<ul style="list-style-type: none"> <li>• Most detailed level</li> <li>• Assessment of geometric features</li> <li>• Sufficiently updated dataset.</li> </ul>	<ul style="list-style-type: none"> <li>• Only building shape and height available, from which calculate other geometric variables</li> <li>• Lack of function and age of construction for single buildings.</li> </ul>
Block	Toronto 2030 Platform	2017	<ul style="list-style-type: none"> <li>• Characterisation by function, age, energy source consumption</li> <li>• Good level of detail</li> <li>• Presence of recurrent block mixes.</li> </ul>	<ul style="list-style-type: none"> <li>• Modelled and not measured energy block consumption</li> <li>• Lack of characterisation for single buildings, at least for age of construction and function.</li> </ul>
Neighbourhood	Toronto Geoportal	2016, 2021	<ul style="list-style-type: none"> <li>• Detailed overview on population, household composition and housing</li> <li>• Frequent updates</li> </ul>	<ul style="list-style-type: none"> <li>• Quite extended and general scale to be applied to single buildings</li> </ul>
2030 District	Toronto 2030 Platform	2017	<ul style="list-style-type: none"> <li>• Measured data by energy suppliers</li> <li>• Distinction by function and energy source.</li> </ul>	<ul style="list-style-type: none"> <li>• General and not detailed consumption values.</li> </ul>

The first step consists of elaborating the main data from the shp. format of building outlines, available from the City of Toronto Open Data Portal. Buildings are outlined for the whole Metropolitan Area but only the ones within the 2030 District have been selected. The file contains information about area, height, and system of survey, from which other building geometric characteristics have been assessed. However, prior to analyses, the shapefile was cleaned from polygons which represents not habitable structures, identified with the following rules (Table 41):

Table 41. Deleted geometries from the building shp.

Type of geometry	Deleted elements	% Deleted on overall buildings (out of 14,279)
Area less than 50 m <sup>2</sup>	2,397	16.66%
Height less than 4 m	369	2.58%
Overlapped polygons	976	6.84%

The whole Toronto 2030 Platform was reproduced on shp. format to make available the block use mix and further validated with the recent updated zoning of the city of Toronto (2021). From the cleaned shapefiles, different geometric variables have been assessed.

### ***Number of floors***

The number of floors is obtained dividing the height of each building by 3 m.

### ***Heated surface***

It is obtained from the base area per the number of floors.

$$\text{Heated surface (m}^2\text{)} = \text{Area} * \text{n}^\circ \text{ of floors}$$

### ***Heated volume***

It is the multiplication between the base area and the average height of one floor (3 m), according to the number of floors considered an average height of 3 meters.

$$\text{Heated gross volume (m}^3\text{)} = \text{Area} * \text{n}^\circ \text{ of floors} * \text{Height per floor}$$

### ***Heated loss surfaces and common surfaces***

The loss surface is the wall area being directly in contact with the external environment or with non-heated rooms. In case of a stand-alone structure, it is equal to:

$$\text{Loss S (m}^2\text{)} = 2 * \text{Area} + (\text{Perimeter} * \text{Height})$$

Considering the downtown dense urban morphology, isolated buildings will be rare, while most of them will be adjoining. In case of attached buildings, the common portions (not exposed to the outside) must be not considered from the loss surface:

$$\text{True Loss S (m}^2\text{)} = \text{Loss S} - \text{Common S}$$

The procedure to obtain common surfaces exploits GIS environment, through the conversion polygon to line, the identification of shared surfaces and the calculation of their area, which have been subtracted from the overall loss surfaces. The assessment of common walls and not is fundamental for the following compactness factor.

### ***Compactness factor***

The surface-to-volume ratio (S/V) is the relation between the loss surface and gross heated volume, which represent the compactness of the structure.

Low values for compact structures (as condominiums) reduce heat exchanges (and energy dispersions) between buildings and outdoor context. Therefore, they are generally preferable even if they also reduce the solar heat gains. On the other hand, higher results are for low and stand-alone buildings, which show a large heated loss surface.

A multiplicative factor has been then applied to the initial S/V ratio in order to avoid interior areas that remain unheated, such as stairwells, elevator shafts and entrance halls, and which form additional unheated spaces to the previous heat loss surfaces: for this reason, the actual compactness factor of each building is slightly different from the calculated S/V (Table 42).

### ***Building Coverage Ratio (BCR)***

The BCR is defined as the percentage of built area compared to a sample area; it can range from 0 (empty lot) to 1 (full lot), calculated at the block scale.

Table 42. SV ratio classes and average multiplicative factors. Source: [169].

Dwelling type	SV ratio calculated ( $m^2/m^3$ )	Average multiplicative factor
Detached building	$S/V > 0.71$	1.31
Semi-detached, row house, duplex	$0.56 < S/V \leq 0.71$	1.25
Low rise apartments	$0.4 < S/V \leq 0.56$	1.21
High rise condominiums	$S/V \leq 0.4$	1.08

### Building Density (BD)

For the block scale, the BD is the ratio between built volume and a sample lot, by which high values suggest high densities and vice versa. This is an interesting variable to consider in downtown Toronto due to the increasing planning policies to favour in-height developments, as skyscrapers, due to the limitation of space and high land financial values (Figure 40).

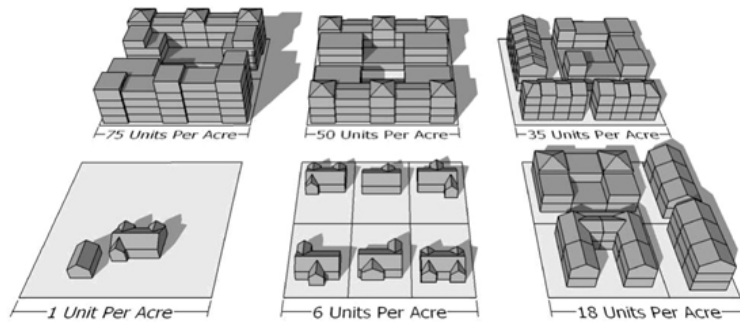


Figure 40. Representative drawings of different BCR and BD for a block configuration.

Table 43. Summary table of the variables calculated from the building shapefile.

Variable	Unit	Formula	Source	Scale of resolution
Ground Floor Area	$m^2$	-	Toronto Geoportal	Building
Building height (h)	m	-	Toronto Geoportal	Building
N° floors	-	Height/3	Toronto Geoportal	Building
Heated surface (UHS)	$m^2$	Area * floors	Calculated	Building
Heated volume (HGV)	$m^3$	GFA*h	Calculated	Building
Heat loss surface (HLS)	$m^2$	$(GFA * 2) + (2p * h) - \text{common S}$	Calculated	Building
S/V ratio	$m^2/m^3$	HLS / HGV	Calculated	Building; mean value for blocks
Residential type	-	according to SV ratio	Calculated; Toronto Geoportal	Building
Building coverage ratio (BCR)	-	$\Sigma \text{ Built Area} / \text{Area block}$	Calculated	Block
Building density (BD)	$m^3/m^2$	$\Sigma \text{ Built Vol} / \text{Area block}$	Calculated	Block

## 5.2 Assessment of energy consumption: from block to building scale

The statistical regression models are based on energy data at the building level. The estimation of energy consumption at the building scale needs to downscale the modelled values by blocks from the Platform [6]. To do so, the characterisation of single blocks is required.

The heterogeneity of functions in the downtown is identified by the blocks archetypes which show similar and recurrent aspects. Archetypical block can be used as a “guide” for the energy demand, especially for mixed areas. The archetypes are distinguished in residential and mixed (Figure 41), with then further subdivision according to the shares of functions provided by the Platform (2017) [6] and the zoning maps for Toronto (2021) [170]. However, the model will be applied only on blocks with a prevalence of residential function. The distinction in four residential archetypes reflects the different classes in national surveys [77] and other studies of the Canadian housing stock [53] [54]: detached single houses, semi-detached houses, low-rise and high-rise apartments.

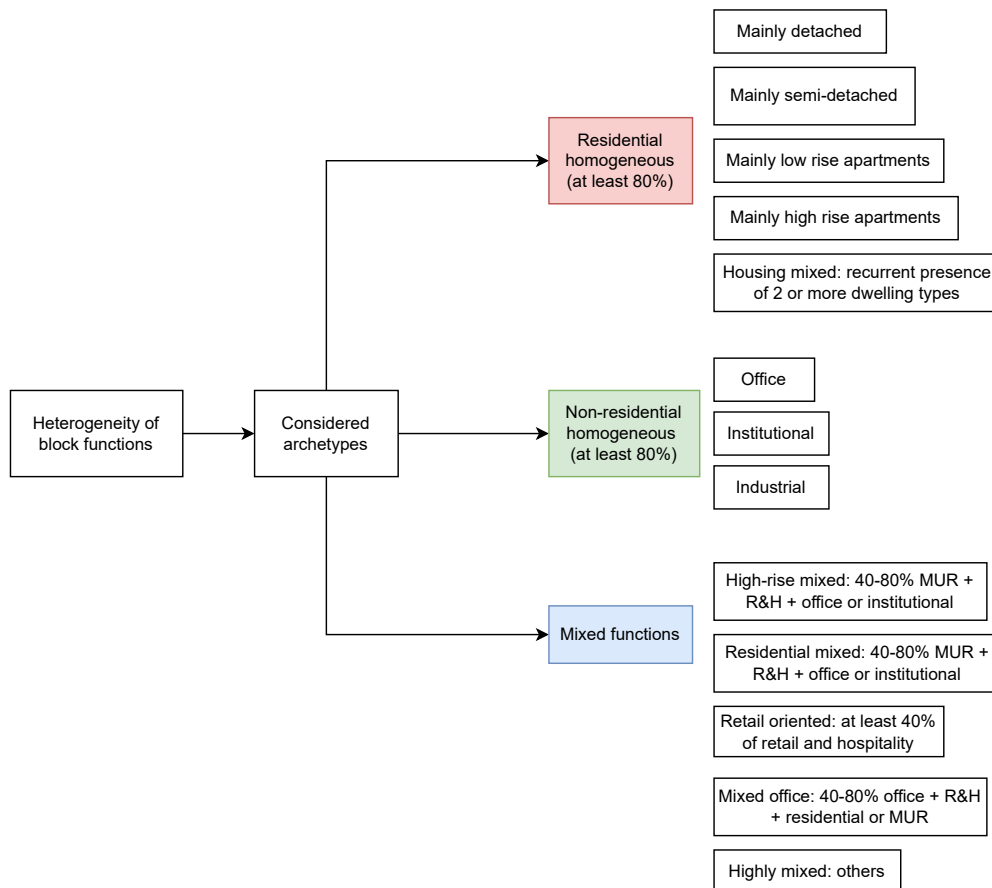


Figure 41: Summary flowchart for distinction in block archetypes.

The distribution of blocks archetype is shown in Figure 42 and their energy-related characterisation in Table 44. As expected, more homogeneous residential areas (mainly with detached and semi-detached housing) are located in border areas, where buildings are less developed in height (see Figure 34). In the centre core, taller structures and financial/commercial activities are concentrated. Mixed blocks are distributed in the TOcore, generally matching residential buildings with other functions: most common are high-rise mixed and mixed office. High-rise structures have also a higher mean consumption per block compared to low-density areas. Most of the building stock was built before

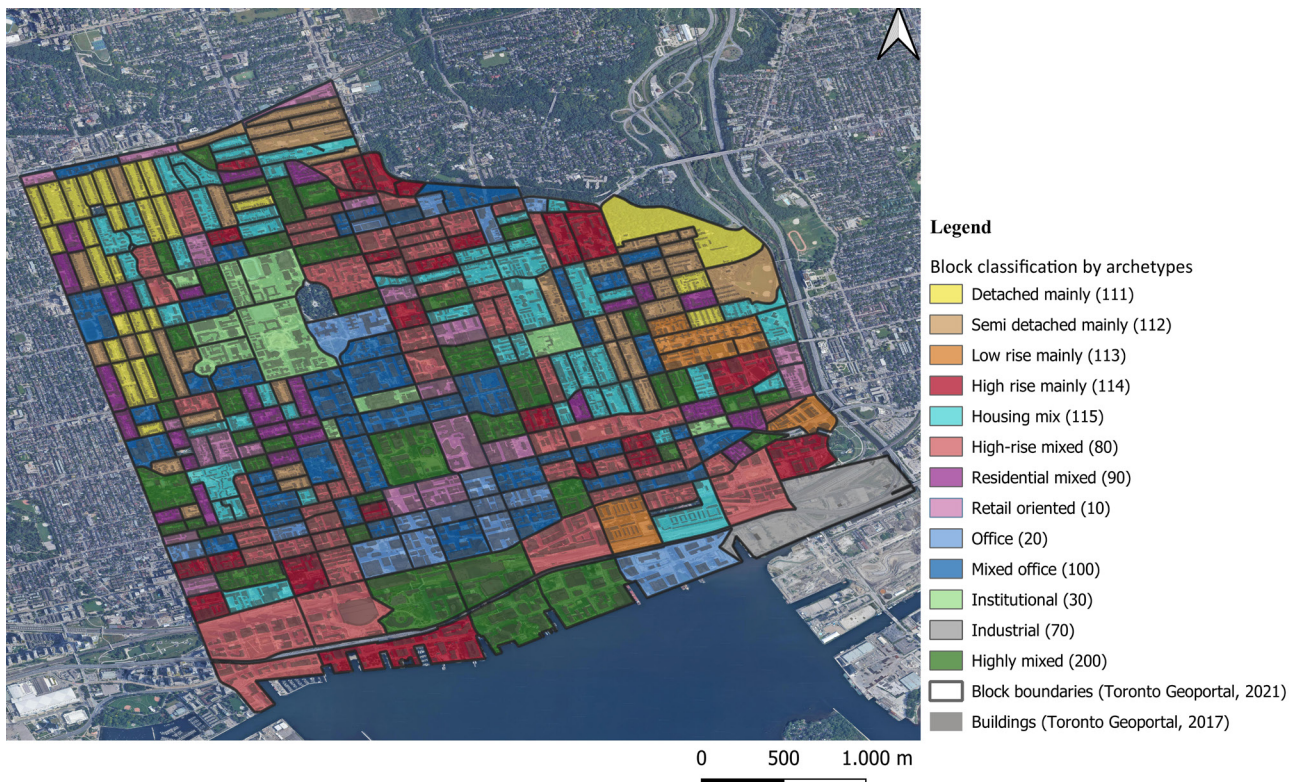


Figure 43. Archetype distinction of blocks within the 2030 District, according to the proposed classification.

Table 44. Summary table for the main characteristics of the considered block archetypes. EUI = energy use intensity, EE = electricity, NG = natural gas.

Archetype	N° of blocks	Main period of construction	Mean EUI (kWh/m <sup>2</sup> /y)	Mean GHG buildings (etCO <sub>2</sub> /y)	Mean EE (MWh/y)	Mean NG (MWh/y)
Retail oriented (10)	20	Pre 1980 (56.5%)	384.5	12,854	39,640	48,930
Office (20)	16	Pre 1980 (48.1%)	279.38	5,631.25	31,300	11,075
Institutional (30)	10	Pre 1980 (77%)	327	4,302	17,900	17,130
Industrial (70)	1	Pre 1980 (100%)	360	20	200	100
High-rise mixed (80)	52	Pre 1980 (42.4%)	265.8	3,441.7	12,971.15	14,571.15
Residential mixed (90)	27	Pre 1980 (92%)	255.5	512.6	3,114.8	2,251.85
Mixed office (100)	44	Pre 1980 (69%)	318.86	4,254.77	19,543.18	14,309.09
Detached mainly (111)	26	Pre 1980 (98%)	277.69	435.77	3,050	1,784.65
Semidetached mainly (112)	37	Pre 1980 (98%)	207.02	466.48	3,116.22	2,005.41
Low rise mainly (113)	5	Pre 1980 (56%)	244	2616	8,560	12,880
High rise mainly (114)	25	Post 2004 (41.4%)	247.6	2,842.8	8,020	13,447.8
Housing mix (115)	54	Pre 1980 (75%)	260.74	1,447.78	4,716.67	6,831.48
Highly mixed (200)	41	Pre 1980 (64.76%)	312.2	4,251.95	15,980.49	16,234.15

1980, with exception of high-rise apartments.

For residential blocks, the initial threshold of 80% GFA occupied by residential function (Figure 41) is further increased to have a more accurate estimation of energy consumption by single dwelling type. Therefore, the disaggregation from block to building data is performed on highly residential blocks: the sum of the shares of residential and multi-unit residential must be equal or higher than the 95% of the overall GFA. The residential function is displayed in the Platform and confirmed by the zoning maps. More mixed blocks could have been influenced by other functions, while the 5% of the overall GFA does not strongly impact on the energy values of the Platform. Rather than 100% GFA, the 95% threshold can be also more representative for all 11 neighbourhoods, excluding only the mainly financial one of Bay Street Corridor (Figure 43; Table 45).



Figure 43: The 75 residential blocks with GFA  $\geq$  95% residential, selected for the following steps.

Table 45 distinguishes the blocks with at least 80% GFA covered by only one residential archetype, block with housing mix and the main age of construction. In the whole district, the housing development was concentrated before 1980 with a prevalent component of low-density housing (detached and semidetached). On the other hand, the number of blocks mainly low-rise and realised 1980-2004 is a limited sample. Housing mix blocks often count a share of high-rise condominiums, which are more sparse than detached and semi-detached dwellings.

Table 45. Summary table for the selected 75 blocks: prevalent archetype and age of construction.

Classification of the 75 blocks	N° of blocks	Period of construction	N° of blocks
Mainly detached	18	Mainly pre-1980	66
Mainly semi-detached	20	Mainly 1980 – 2004	2
Mainly low-rise	2	Mainly post 2004	6
Mainly high-rise	9	Mixed	2
Housing mix	26		

An overall characterisation by housing type is provided in Table 46. The characteristics are retrieved from national and provincial surveys for occupancy, technological and equipment aspects, income, and emissions of each category.

The majority of household and maximum floorspace is occupied by detached houses, followed by apartments. Smaller households generally live in flats by rent, while families with more than two components in single-family buildings of own property. This is also relatable to the lower average income of occupants, which is the highest for detached and the lowest for low-rise apartments at the national level. Low-rise apartments also count the lower share of households with air conditioning compared to more than 60% for the other three archetypes. The main heating equipment registers a discrepancy between single houses and apartment buildings for the national level, respectively furnace and electric resistance, while a uniformity of natural gas use for Ontario.

Table 46. Summary table of main features for the 4 residential archetypes (buildings) from previous studies. Sources: NL = national level (SHEU, 2017) [77], OL = Ontario level (NRCAN, 2018) [43] in which \* is the generic “apartments” category.

	Detached buildings	Semi-detached buildings	Low rise apartments	High rise apartments
Main features	No shared wall; between 2 and 3 floors.	At least one shared wall with another property.	Condominiums within 5 floors and multiple units.	Condominiums with or more than 5 floors and multiple units.
Total floor space (million m <sup>2</sup> ) (ON)	558.7	127.2	159.9 *	5,631.25
Total households (thousands)	3,105.8	846.3	1,585.2*	4,302
Mean n° of members per household (NL)	2.6	2.3	1.6	1.4
Main construction date (NL)	1961-1977 (19.9%)	1961-1977 (22.54%)	1984-1995 (24.81%)	1961-1977 (33.87%)
Main period of construction (ON)	1984-1995 (21.2%)	1984-1995 (22.8%)	1961-1977 (20.4%) *	512.6
Occupation mode (NL)	Own (95.11%)	Own (77.51%)	Rent (56.99%)	Rent (62.97%)
Type of heating unit (NL)	Dwelling unit	Dwelling unit	Dwelling unit	Central unit
Main type of heating equipment (NL)	Furnace	Furnace	Electric baseboards	Electric baseboards
Households with air conditioning (NL)	62%	63%	39%	61%
Main heating system type (ON)	Natural gas with high efficiency (49.6%)	Natural gas with high efficiency (54.5%)	Natural gas with high efficiency (55.9%) *	2,842.8
Main water heater (ON)	Natural gas (74.8%)	Natural gas (74.8%)	Natural gas (74.8%) *	1,447.78
Average household income (NL)	\$150,000 and over	\$60,000 to less than \$80,000	\$20,000 to less than \$40,000	\$40,000 to less than \$60,000
Total GHG emissions by end use (Mt CO <sub>2</sub> e) (ON)	15.3	3.1	3.5*	

For the selected blocks (75 out of 359, equal to the 21%), the useful heated area (UHS) and heated volume are assessed in the GIS environment, based on the shp. provided by the Toronto Geoportal.

The aggregation of volumes and areas by dwelling type is calculated for each block through the “summarise” tool.

Knowing the modelled energy consumption by block for electricity and natural gas, the next step is to disaggregate the demand for each building. As mentioned before, also blocks with 95% residential have been included, considering the low amount of data for high- and low-rise apartments. The limited share (5%) of other functions is mainly covered by offices, institutional buildings, and retail hospitality. The 5% non-residential consumption is assumed from the energy intensity (kWh/m<sup>2</sup>/y) for electricity and natural gas of homogeneous blocks of that function, as fully commercial or office areas. The consumption is then applied to the considered housing-mix block (kWh/m<sup>2</sup>/y \* UHS) and subtracted from the total block consumption given by the Toronto 2030 Platform. The remaining share represents the residential function.

### 5.2.1 Model I: method by subtraction

The first method to disaggregate building consumption is easy to replicate. It consists of finding highly homogeneous blocks and assess the block consumption divided by UHS. The energy intensity for certain uses can be extended to other blocks, where the unknown share is then subtracted from the overall demand. According to the typological classification, homogeneous blocks with only one residential type (at least 95% GFA occupied by one residential archetype) and age (100% GFA realised in one period of construction) are the first considered to find an average annual consumption for electricity and natural gas. The obtained average consumptions are used for the mix housing blocks to assess the remaining share.

- Homogeneous residential blocks

Block mainly composed by detached and semi-detached houses are realised before 1980 and they are the first housing category to be assessed.

According to the previous analysis, 12 fully detached blocks have been identified built before 1980 (Table 47). However, one block (DBUID = 35200792010) presents underestimated values for electricity and natural gas, so that it was taken apart from the calculation. Having the electricity and natural gas consumptions (by the Platform) and the assessed UHS (from GIS modelling), the energy intensity is calculated for these 11 blocks. The average electricity consumption for detached blocks built before 1980 is 83.53 kWh/m<sup>2</sup>/y and natural gas 75.95 kWh/m<sup>2</sup>/y. Then, the average intensity is applied for other blocks with a share of detached houses built no later than 1980.

Table 47. Characterisation of homogenous blocks of detached houses built before 1980: neighbourhood; EUI, mean electricity (EE) and natural gas (NG) consumption provided by the Platform; EE and NG intensity calculated.

DBUID	Neigh.	UHS (m <sup>2</sup> )	EUI (kWh/m <sup>2</sup> /y)	Mean EE (GWh/y)	EE intensity (kWh/m <sup>2</sup> /y)	Mean NG (GWh/y)	NG intensity (kWh/m <sup>2</sup> /y)
35200907001	79	21,816.84	170-190	2.1	96.26	1.15	87.85
35201436001	78	18,675.42	160-180	1.6	85.67	0.8	71.40
35201047001	95	35,491.62	170-190	2.95	83.12	1.6	75.14

35201047002	95	34,032.15	160-180	2.65	77.87	1.3	63.67
35201048002	95	32,591.52	170-190	2.65	81.31	1.7	86.93
35201049002	95	29,428.93	170-190	2.45	83.25	1.35	76.46
35201053001	95	57,141.05	170-190	4.65	81.38	2.95	86.04
35201061001	95	28,529.23	170-190	2.45	85.88	1.35	78.87
35201062001	95	29,896.73	170-190	2.5	83.62	1.25	69.68
35203183004	71	41,727.75	160-180	3.35	80.28	1.7	67.90
35201050001	95	26,820.78	170-190	2.15	80.16	1.15	71.46

For semi-detached houses (Table 48), 9 blocks realised before 1980 are identified to assess the average consumption of electricity and natural gas, respectively 69.17 kWh/m<sup>2</sup>/y and 37.80 kWh/m<sup>2</sup>/y.

Table 48. Characterisation of homogenous blocks of semidetached houses built before 1980: neighbourhood; EUI, mean electricity (EE) and natural gas (NG) consumption provided by the Platform; EE and NG intensity calculated.

DBUID	Neigh.	UHS (m <sup>2</sup> )	EUI (kWh/m <sup>2</sup> /y)	Mean EE (GWh/y)	EE intensity (kWh/m <sup>2</sup> /y)	Mean NG (GWh/y)	NG intensity (kWh/m <sup>2</sup> /y)
35200869001	78	12,198.52	160-180	0.45	36.89	0.2	16.40
35200907002	79	24,832.39	170-190	2.1	84.57	1.05	42.28
35200792010	71	11,585.43	160-180	0.75	64.74	0.35	30.21
35200795001	71	26,160.43	160-180	1.9	72.63	0.95	36.31
35203183010	71	33,233.05	160-180	2	60.18	0.95	28.59
35200792006	71	26,558.35	160-180	2.2	82.84	1.05	39.54
35200792010	71	15,390.93	200-220	1.1	71.47	1.05	68.22
35200796003	71	34,393.82	160-180	2.75	79.96	1.35	39.25
35201048001	95	36,800.06	170-190	2.55	69.29	1.45	39.40

Only one block of fully low-rise was realised before 1980 (Table 49): so that, results are limited to only one reference area, which is not sufficiently representative. A further issue with low-rise apartment is the lack of a specific class in the data from the Comprehensive Energy Use Database [43] (see above Table 46; only “apartments” class), while they are distinguished in the SHEU (2017) [77]. It is important to specify that this block has a 95% GFA realised before 1980, while only 5% after 2004. The final residential archetype are high-rise apartment buildings, which are very common in downtown Toronto, especially due to the in-height development policies. However, most of these structures are not within a single but rather sparse among different areas. Only 3 blocks are selected as fully high-rise and built before 1980, as shown in Table 53.

Table 49. Characterisation of the homogenous block of low-rise apartments built before 1980: neighbourhood; EUI, mean electricity (EE) and natural gas (NG) consumption provided by the Platform; EE and NG intensity calculated.

DBUID	Neigh.	UHS (m <sup>2</sup> )	EUI (kWh/m <sup>2</sup> /y)	Mean EE (GWh/y)	EE intensity (kWh/m <sup>2</sup> /y)	Mean NG (GWh/y)	NG intensity (kWh/m <sup>2</sup> /y)
35204021001	72	87,394.82	280-310	9.5	108.7	23.35	267.18

Table 50. Characterisation of the homogenous blocks of high-rise apartments built before 1980: neighbourhood; EUI, mean electricity (EE) and natural gas (NG) consumption provided by the Platform; EE and NG intensity calculated.

DBUID	Neigh.	UHS (m <sup>2</sup> )	EUI (kWh/m <sup>2</sup> /y)	Mean EE (GWh/y)	EE intensity (kWh/m <sup>2</sup> /y)	Mean NG (GWh/y)	NG intensity (kWh/m <sup>2</sup> /y)
35201038002	95	72,555.27	290-320	2.95	40.66	7.5	103.37
35204567001	74	328,207.54	290-330	18.6	56.67	46	140.16
35204562002	74	479,147	300-330	24.3	50.72	58.3	121.67

- Mixed residential blocks

Starting from the consumption before 1980, other residential blocks with different vintage mix have been analysed, to have a full picture of energy trends by period of construction and dwelling types. It must be underlined that the great majority of detached houses have been realised before the end of XX century: therefore, recent detached structures are limited in the central area of Toronto, while they are more common in the surrounding suburbs.

An example of mixed residential block (with more than two housing types and age mix) is reported in Table 51: from the consumption of detached and semi-detached calculated from homogeneous blocks, the procedure assesses values from the high-rise share.

Table 51. Example of a mixed residential block and procedure to calculate the unknown electricity and natural gas consumption, in this case from high-rise.

DBUID	Neigh.	Pre 1980 (%GFA)	1980-2004 (%GFA)	Post 2004 (%GFA)	UHS (m <sup>2</sup> )	EUI (kWh/m <sup>2</sup> /y)	Mean EE (GWh/y)	Mean NG (GWh/y)
35204228005	95	5	0	95	85,120.14	140-150	1.7	1.55

Type of dwelling	N° of structures	UHS (m <sup>2</sup> )	EE consumption (kWh/y)	EE intensity (kWh/m <sup>2</sup> /y)	NG consumption (kWh/y)	NG intensity (kWh/m <sup>2</sup> /y)
Detached	1	289.11	24,149.70	83.53*	21,958.22	75.95*
Semi-detached	1	1,189.85	82,301.95	69.17*	44,976.34	37.8*
Low rise	-	-	-	-	-	-
High rise	13	83,641.18	1,700,000 – (24,149.70 + 82,301.95) = 1,593,548.35	19.05	1,550,000 – (21,958.22 + 44,976.34) = 1,483,065.44	17.73

\* from previous calculations on homogenous residential blocks.

The same steps are applied for the other mixed residential blocks of the TOcore area. Table 52 distinguishes the share for each period of construction, overall electricity and natural gas consumption as shown in the Toronto 2030 Platform and the UHS (m<sup>2</sup>) by the four housing archetypes as assessed on GIS. Having the average consumption values from homogeneous blocks built before 1980 (kWh/m<sup>2</sup>/y), the remaining unknown share of residential consumption is estimated.

Table 52. Calculation to assess energy consumption from mixed residential block for electricity and natural gas consumption, distinguishing dwelling types and age of construction.

DBUID	Pre 1980 (%GFA)	1980-2004 (%GFA)	Post 2004 (%GFA)	EE (GWh/y/block)	NG (GWh/y/block)	Detached UHS (m <sup>2</sup> )*	Semi-detached UHS (m <sup>2</sup> )*
35204228005	0.05	0	0.95	1.7	1.55	24,149.70	82,301.95
35202818007	0.05	0.45	0.5	1.55	2.5	1,249.61	1,954.84
35201050002	0.85	0.1	0.05	3.8	7.75	1,596.38	-
35201046001	1	0	0	3.65	4	4,939.75	27,266.00
35201045004	1	0	0	2.75	4.2	-	16,929.70
35201039002	0.6	0.4	0	2.65	2.95	1,192.12	27,257.04
35200898001	1	0	0	2	2.5	-	11,866.97
35200830005	0.5	0.5	0	11.4	14	-	19,578.77
35200815001	1	0	0	4.3	6.15	9,424.02	18,550.64
35200813005	0.8	0.2	0	1.9	1.4	8,359.15	9,308.44
35200810002	0.35	0	0.65	5.9	4.35	592.49	12,004.57
35200801002	0.3	0	0.7	8.55	8.55	1,632.18	20,263.99

\* from previous calculations on homogenous residential blocks.

Semi-detached (1980-2004)			
DBUID	UHS (m <sup>2</sup> )	Electricity (kWh/m <sup>2</sup> /y)	Natural gas (kWh/m <sup>2</sup> /y)
35201050002	13,362.36	54.88	39.46

DBUID	Low rise apartments (pre-1980)			Low rise apartments (1980-2004)		
	UHS (m <sup>2</sup> )	Electricity (kWh/m <sup>2</sup> /y)	Natural gas (kWh/m <sup>2</sup> /y)	UHS (m <sup>2</sup> )	Electricity (kWh/m <sup>2</sup> /y)	Natural gas (kWh/m <sup>2</sup> /y)
35200830005	23,448.67	262.75	141.76	-	-	-
35200815001	19,389.43	80.78	159.71	-	-	-
35200813005	-	-	-	3,965.83	128.66	71.13
35200810002	71,160.04	188.29	49.31	-	-	-

DBUID	High rise apartments (pre-1980)			High rise apartments (1980-2004)		
	UHS (m <sup>2</sup> )	Electricity (kWh/m <sup>2</sup> /y)	Natural gas (kWh/m <sup>2</sup> /y)	UHS (m <sup>2</sup> )	Electricity (kWh/m <sup>2</sup> /y)	Natural gas (kWh/m <sup>2</sup> /y)
35202817006	36,037.33	49.53*	121.73*	23,4614.69	21.55	49.82
35201046001	16,016.91	84.37	161.96	-	-	-
35201045004	22,116.59	71.39	160.97	-	-	-
35201039002	-	-	-	21,196.24	31.38*	86.30*
35200898001	12,267.07	96.12	167.23	-	-	-
35200830005	51,603.47	49.53*	121.73*	42,341.31	31.38*	86.30*
35200815001	13,442.42	49.53*	121.73*	-	-	-
35200813005	-	-	-	1,518.36	31.38*	86.30*

DBUID	High rise apartment (post 2004)		
	UHS (m <sup>2</sup> )	Electricity (kWh/m <sup>2</sup> /y)	Natural gas (kWh/m <sup>2</sup> /y)
35204228005	83,641.18	19.05	17.73
35202818007	56,137.87	23.34*	41.53*
35200810002	71,160.04	23.34*	41.53*
35200801002	271,412.78	25.84	28.22

\* from previous calculations on homogenous residential blocks.

The most variable data are assessed for low rise apartment, for which results must be considered with caution also due to the limited sample of blocks. The situation for high rise apartments can cover all the three temporal ranges and consumptions are generally lower for more recent buildings. Only one residential block shows a share of detached houses built between 1980 and 2004.

The same steps to calculate the consumption of each archetype and to disaggregate values at the building scale are applied for blocks with a 5% GFA occupied by other functions, as mentioned before. Average values and comparison with the model by equation will be discussed in paragraph 5.3.

## 5.2.2 Model II: method by equation

The model by equation provides another way to estimate building energy consumption for the selected blocks ( $\geq 95\%$  residential GFA), knowing the useful heated area assessed in the GIS environment, the electricity and natural gas consumption by block from the Toronto 2030 Platform. Before disaggregating consumption with this second method, it is important to underline that most of detached and semi-detached houses (98%) was built before 1980. The main period of construction is also con-

firmed by the national survey [77]. Therefore, the method by equation is based on the relationships among dwelling types provided by the SHEU (2017) [77]. The national survey distinguishes energy consumption by different types of dwellings and ages. These relations are adapted to the consumption of each residential block in the TOcore area by the Equation (1):

$$\text{Block consumption} = UHS_{DTC} * x + UHS_{SMDTC} * (x * a) + UHS_{LR} * (x * b) + UHS_{HR} * (x * c) \quad (1)$$

where:

- $UHS_{DTC}$  is the useful heated surface of detached houses for the block;
- $UHS_{SMDTC}$  is the useful heated surface of semi-detached houses for the block;
- $UHS_{LR}$  is the useful heated surface of low-rise apartments for the block;
- $UHS_{HR}$  is the useful heated surface of high-rise apartments for the block;
- $x$  is the consumption of detached houses before 1980 given by the survey (SHEU, 2017) calibrated to the modelled block consumption;
- $a$  is the multiplicative coefficient given by the different share between the calibrated consumption of detached houses before 1980 and of semi-detached houses for the considered age (SHEU, 2017);
- $b$  is the multiplicative coefficient given by the different share between the calibrated consumption of detached houses before 1980 and of low-rise apartments for the considered age (SHEU, 2017);
- $c$  is the multiplicative coefficient given by the different share between the calibrated consumption of detached houses before 1980 and of high-rise apartments for the considered age (SHEU, 2017).

The multiplicative coefficients are calculated as:  $a = 1 - ((C_{DTC} - C')/C_{DTC})$ , where

- $C_{DTC}$  is the consumption of detached houses before 1980 by the survey (SHEU, 2017)
- $C'$  is the consumption to assess.

The Equation (1) firstly needs to assess the  $x$  value, which represent the calibration of Canadian values for detached houses to the energy consumption of the selected block, applied both for electricity and natural gas. In case some blocks do not count any detached dwelling, semi-detached houses will represent the  $x$  in the Equation (1). The multiplication between the  $x$  value and the considered coefficient will identify the demand per  $m^2$  of the selected dwelling type by energy source. The reference year for each block has been selected according to the higher share of GFA in the vintage mix of the Platform, considering that building level data are not available. Based on the SHEU (2017) [77], the different shares of consumption and related multiplicative coefficients are the following:

Table 53. Summary table of average electricity consumption by temporal ranges and multiplicative factors. Source: own elaboration of SHEU [77].

Electricity consumption for detached houses pre-1980: 59.81 kWh/m <sup>2</sup> /y	Semi-detached		Low Rise		High rise	
	Consumption (kWh/m <sup>2</sup> /y)	Multiplicative factor	Consumption (kWh/m <sup>2</sup> /y)	Multiplicative factor	Consumption (kWh/m <sup>2</sup> /y)	Multiplicative factor
Pre 1980	76.5	1.28	83.84	1.4	51.73	0.86
1980 – 2004	53.86	0.9	86.77	1.45	67.47	1.13
Post 2004	52.41	0.88	71.22	1.19	93.98	1.57

Table 54. Summary table of average natural gas consumption by temporal ranges and multiplicative factors. Source: own elaboration of SHEU [77].

Natural gas consumption for detached houses pre-1980: 126.23 kWh/m <sup>2</sup> /y	Semi-detached		Low Rise		High rise	
	Consumption (kWh/m <sup>2</sup> /y)	Multiplicative factor	Consumption (kWh/m <sup>2</sup> /y)	Multiplicative factor	Consumption (kWh/m <sup>2</sup> /y)	Multiplicative factor
Pre 1980	108.85	0.86	212.48	1.68	208.38	1.65
1980 – 2004	118.55	0.94	192.45	0.94	n. a.	n. a.
Post 2004	102.95	0.82	174.02	1.38	204.53	1.62

Considering the lower data quality for natural gas distinguished by temporal ranges, another hypothesis is tested: only one value for each dwelling type is assessed, without subdividing by age of construction.

Table 55. Summary of average natural gas consumption and multiplicative factor, assuming only one temporal range. Source: own elaboration of SHEU [77].

Natural gas consumption for detached houses pre-1980: 108.33 kWh/m <sup>2</sup> /y	Semi-detached		Low Rise		High rise	
	Consumption (kWh/m <sup>2</sup> /y)	Multiplicative factor	Consumption (kWh/m <sup>2</sup> /y)	Multiplicative factor	Consumption (kWh/m <sup>2</sup> /y)	Multiplicative factor
Pre 1980	111.11	1.03	175	1.62	194.45	1.79

Table 56 summarises the main values for residential consumption calculated with the model by equation. Values provide a characterisation of blocks and of dwelling archetypes for volume, UHS, electricity and natural gas (with the two hypotheses) consumptions. The minimum values reported in the table are outliers and have been excluded from the calculations of the average values.

High-rise apartments show the lower electricity consumption intensity, while low-rise the maximum. For natural gas, values for detached and semi-detached are similar and lower than 50 kWh/m<sup>2</sup>/y, whereas about the double for apartment buildings. High-rise dwellings report the peak consumption for natural gas for both the hypotheses.

Table 56. Summary table of main characteristics of calculated consumption by residential types.

	Considered feature	Mean	Min. (among blocks with a % of it)	Max. (among blocks with a % of it)	Sum
<b>Block values</b>	Pre 1980	85%	5%	100%	-
	1980 - 2004	5.9%	5%	90%	-
	Post 2004	8.7%	5%	95%	-
	Electricity - EE (GWh/y)	3.85	0.30	24.30	288.65
	Natural gas - NG (GWh/y)	5.05	0.00	58.30	378.64
<b>Detached buildings</b>	Volume detached houses (m <sup>3</sup> ) per block	18,561.87	980.66	83,787.18	1,392,140.83
	UHS (m <sup>2</sup> ) per block	5,477.78	289.11	24,701.86	410,833.33
	EE intensity (kWh/ m <sup>2</sup> /y)	56.37	2.63	108.06	-
	NG intensity (kWh/ m <sup>2</sup> /y) – I	48.46	1.79	105.85	-
	NG intensity (kWh/ m <sup>2</sup> /y) – II	43.61	1.66	96.64	-

<b>Semi-detached buildings</b>	Volume semi-detached houses (m <sup>3</sup> ) per block	67,750.47	4,035.90	231,774.75	5,081,285.25
	UHS (m <sup>2</sup> ) per block	19,872.75	1,189.85	68,331.06	1,490,456.29
	EE intensity (kWh/ m <sup>2</sup> /y)	72.16	3.37	143.25	-
	NG intensity (kWh/ m <sup>2</sup> /y) – I	44.22	1.54	193.18	-
	NG intensity (kWh/ m <sup>2</sup> /y) – II	46.51	1.71	211.61	-
<b>Low-rise apartments</b>	Volume low-rise (m <sup>3</sup> ) per block	12,550.44	514.10	96,280.50	941,283.13
	UHS (m <sup>2</sup> ) per block	3,555.73	151.57	28,385.10	266,679.56
	EE intensity (kWh/ m <sup>2</sup> /y)	77.47	8.29	156.68	-
	NG intensity (kWh/ m <sup>2</sup> /y) – I	89.26	3	377.38	-
	NG intensity (kWh/ m <sup>2</sup> /y) – II	77.30	2.69	332.82	-
<b>High-rise apartments</b>	Volume high-rise (m <sup>3</sup> ) per block	172,572.25	1,010.43	1,558,982.45	12,942,918.46
	UHS (m <sup>2</sup> ) per block	50,877.17	297.89	459,614.01	3,815,788.08
	EE intensity (kWh/ m <sup>2</sup> /y)	46.61	2.26	96.24	-
	NG intensity (kWh/ m <sup>2</sup> /y) – I	89.38	2.95	370.64	-
	NG intensity (kWh/ m <sup>2</sup> /y) – II	82.76	2.97	367.75	-

### 5.3 Result assessment and comparison

After building and testing the two different disaggregation techniques, a comparison between results shows strengths and weaknesses. A general consideration must be underlined for the whole assessment: the lack of functions and period of construction at the building scale is a main limit for the accuracy and completeness of the models, whereas a manual identification would not have been purely accurate and supported by accredited sources.

Table 57 and Table 58 show the average assessed consumption respectively of electricity and natural gas, distinguished by residential archetypes and age of construction. The model by equation tends to assess lower consumption, while the method by subtraction appears to overestimate values for low-rise buildings. The method by equation has also the main limit of lacking data for post-1980 buildings, due to the limited presence in the TOcore area. In this case, results are based on age generalisation: the prevalent vintage type is extended to the block, without distinguishing minor ages.

In both cases, the electricity consumption is higher than natural gas for detached and semidetached houses (especially for the latter). The assumption of electric resistance and space cooling from the ASHRAE template (IECC 2015) may have influenced these results. On the other hand, natural gas prevails on electricity for apartment buildings, except for low-rise assessed with the method by subtraction. The consumptions from older to more recent dwellings tend to decrease, even if only average values are considered until now.

Table 57. Summary table of calculated results for electricity consumption by model I (method by subtraction) and model II (method by equation).

Electricity (kWh/m <sup>2</sup> /y)	Detached houses		Semi-detached houses		Low-rise apartments		High-rise apartments	
	I model	II model	I model	II model	I model	II model	I model	II model
Age range								
Pre 1980	83.53	59.61	69.17	76.43	128.08	82.67	63.24	49.89
1980 – 2004	-	-	54.88*	15.51	128.66	24.99	28.1	19.47
Post 2004	-	-	-	-	-	-	22.89	23.84
Average (on the whole sample)	83.53	59.61	68.46	45.97	128.27	53.83	44.23	46.16

\* Assessed on one block only.

Table 58. Summary table of calculated results for natural gas consumption by model I (method by subtraction) and model II (method by equation).

Natural gas (kWh/m <sup>2</sup> /y)	Detached houses		Semi-detached houses		Low-rise apartments		High-rise apartments	
	I model	II model	I model	II model	I model	II model	I model	II model
Age range								
Pre 1980	76.22	49.26	38.70	45.02	145.18	92.66	138.39	92.09
1980 – 2004	75.95	-	39.10*	23.93	71.13	40.28	74.14	47.28
Post 2004	-	-	-	-	-	-	32.25	21.26
Average (on the whole sample)	76.09	49.26	38.90	34.48	120.50	66.47	94.63	89.38

\* Assessed on one block only.

The average results obtained from the two methods are then normalised (according to HDDs and CDDs values of 2017) and compared with data provided by SHEU [77] (measured in 2015) and the Comprehensive Energy Use Database (in 2017) [43]. The comparisons of dwelling types are reported in Table 59 for electricity and Table 60 for natural gas consumptions.

Results are quite satisfying for electricity consumption, even if overestimated for detached and semi-detached houses (Table 59; Figure 44). As explained before, data by NRCan (2020) [43] do not distinguish between low and high-rise but have more similar values with the latter: therefore, they have been considered as representative of high-rise condominiums. Values from the method by subtraction decrease with lower S/V ratio and tend to follow the trend by the NRCan survey, except for low-rise. As mentioned before, low-rise apartments have the most variable consumption and are more challenging to be assessed. The electricity trend is less defined for values from the method by equation, which are closer to the SHEU [77] for apartment buildings.

Table 59. Comparison of electricity consumption by residential types between the two methods and available energy databases.

Electricity (kWh/m <sup>2</sup> /y)	Detached	Semi-detached	Low rise	High rise
Model I, not normalised	83.68	68.07	181.07	44.73
Model I, normalised	87.98	70.37	184.39	45.55

Model II, not normalised	68.11	74.42	87.88	43.35
Model II, normalised	71.61	76.94	89.49	44.15
SHEU, 2015 [77]	39.74	41.89	88.33	49.69
NRCan, 2017 [43]	56.06	51.43	-	47.96

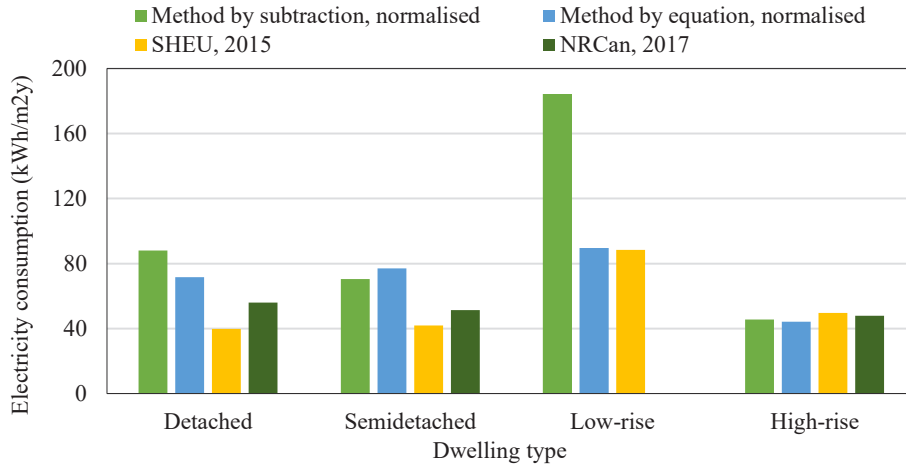


Figure 44: Comparison of electricity consumption by residential types between the two methods and available energy databases.

On the other hand, the natural gas assessment appears more problematic, mainly due to availability and quality of data (Table 60; Figure 45). An overall underestimation of consumption emerges with both methods, except for the similar values for high-rise with the Energy Database [43]. The minimum consumption is assessed for semidetached and maximum for low-rise, which cannot reflect the increasing trend with lower S/V ratio from SHEU [77].

Table 60. Comparison of natural gas consumption by residential types between the two methods and available energy databases.

Natural gas (kWh/m²/y)	Detached	Semi-detached	Low rise	High rise
Model I, not normalised	76.21	38.71	122.04	97.40
Model I, normalised	52.62	43.29	107.96	88.58
Model II, not normalised	76.06	38.71	122.04	97.40
Model II, normalised	52.51	43.29	107.96	88.58
SHEU, 2015 [77]	101.79	105.04	166.78	185.31
NRCan, 2017 [43]	114	104.23	-	96.41

Main pros and cons for both methods to disaggregate energy consumption from block to building scale are summarised in Table 61, considering both the workflows and results.

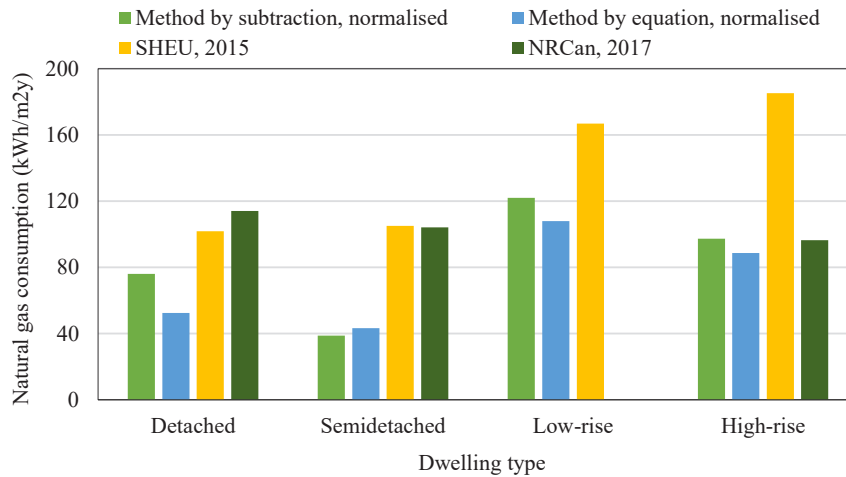


Figure 45. Comparison of natural gas consumption by residential types between the two methods and available energy databases.

Table 61. Summary table of pros and cons of both methods to disaggregate energy consumption data from block to building scale.

Model	Elaboration type	Pros	Cons
Model by subtraction	Mainly distinction by building shape; identification of archetypical consumption; application on blocks.	<ul style="list-style-type: none"> <li>Homogeneous assessment of building demand for similar types</li> <li>Possible application for both residential and non-residential functions</li> <li>Easily adaptable to different contexts and feasible on different areas</li> </ul>	<ul style="list-style-type: none"> <li>Lack of differentiate consumption for the same dwelling type of same age</li> <li>Unfitted for certain blocks</li> <li>Careful attention on the archetypical block to consider</li> <li>To be more consistent, necessary information about single building age</li> </ul>
Model by equation	Equation built on the different consumption shares at wider scale; application on the consumption of the whole block.	<ul style="list-style-type: none"> <li>Adaptation of results to the block consumption</li> <li>Based on reliable data sources</li> <li>Only need of UHS at block scale for different dwelling types, without having reference to single buildings</li> <li>Very quick assessment after defining the equation</li> </ul>	<ul style="list-style-type: none"> <li>Strictly influenced by accuracy of data on which the equation is based on</li> <li>Relationship among building types can be different in different areas</li> <li>Building age equally applied to all block structures as higher share of the block</li> <li>Issues to find reliable data for other functions to build the equation</li> </ul>

Some points must be highlighted from these methods:

1. quality of data for low-rise apartments was not as satisfying as for the other dwelling types, especially for natural gas consumption;
2. more recent data were available (as for 2018 by the Comprehensive Energy Use Database), but without the distinction between low and high-rise apartments. Considering their two different configurations and geometric characteristics, it is preferable to keep them divided;
3. within the sample of 75 blocks, residential ones mainly realised between 1980 and 2004 cover an inconsistent share (only 2 blocks), unbalanced by pre 1980 due to the significant urban development of housing;
4. the model for natural gas assessment less satisfying than electricity for other blocks;
5. calculations are based on modelling at the block scale provided by the Toronto 2030 Platform: therefore, measured data (as from energy providers) would have further validated results.

The assumptions by ASHRAE applied on the building models of the Platform provide a simplification of consumptions for different structures, materials, and age. Except for low rise consumptions, the two methods show similar results while discrepancies with Ontario data are recurrent.

In the method by subtraction, values rely only on Toronto, starting from the consumption block data of the 2030 Platform rather than on external datasets. Housing mix can have a more limited accuracy because values represent only an average from homogenous blocks. On the other hand, the approach by equation follows the relation among dwelling types of a survey at the provincial scale. Between the two approaches, the method by subtraction is more coherent and specific for the case study. It is also easily flexible and adaptable to other contexts if aggregated consumption energy data and building features are available. On the contrary, the approach by equation must be based on reliable and comprehensive energy values distinguished by housing types, which might not be accessible in all contexts.

## 5.4 Regression analyses

The method by subtraction is chosen to disaggregate consumption data from block to building scale. The assessed consumption values allow to build statistical models by energy end uses from electricity and natural gas.

The energy end-uses have been assessed as reported in the methodology paragraph (3.4.1). From the values of natural gas and electricity, energy end-uses are derived for each building. Table 62 shows average results of energy uses for each dwelling type. SC is assumed as part of electricity-use, while the remaining share for App. According to Ontario data [171] for 2017, SC is assessed as 14% of electricity demand for detached houses, 9.4% for semi-detached and 5.1% for apartments. DHW is calculated with the Equation (2) as included in natural gas, while the remaining part is covered by SH. Space heating and appliances vary more than DHW and cooling among the dwelling types. The different materials of construction may also impact on the energy demand and, consequently, on the regression results. For instance, the structure of recent high-rise can have glass/steel with high glazing ratio, while older ones mainly concrete and bricks [172].

Table 62. Assessed energy-end uses for each dwelling type, using natural gas and electricity values obtained from the method by subtraction.

Housing type	$SH_{NG}$ (kWh/m <sup>2</sup> )	$DHW_{NG}$ (kWh/m <sup>2</sup> )	$App_{EE}$ (kWh/m <sup>2</sup> )	$SC_{EE}$ (kWh/m <sup>2</sup> )
Detached	76.2	8.1	71.7	9.3
Semidetached	38.7	7.9	61.7	7.2
Low-rise	122	7.3	116	3.5
High-rise	97.4	7.5	42.4	1.8

On the other hand, it must be underlined that the heterogeneity of consumptions for each residential type and for each vintage range cannot be fully represented by the Platform, by the disaggregation method and by the following statistical models. The assumptions adopted for modelling the Platform used the ASHRAE framework and did not distinguish older or new low-density housing for detached and semi-detached (see Table 29).

Low- and high-rise apartments are the most likely to vary consumption in the three age ranges due to the different values of building components by the ASHRAE models. However, they have the same type of walls, roofs, and HVAC systems.

As next step, regression analyses are performed between independent variables and dependent energy-uses (Table 63). Correlations for space cooling and appliances energy intensities can build MLR models, both having quite high relations with the S/V ratio. DHW intensity shows higher values with residential density (inh/m<sup>2</sup>) because it is directly calculated from it, whereas the remaining natural gas share for space heating has results lower than 0.2. Therefore, DWH and SH intensities are joined to have a whole natural gas consumption model. The sum of natural gas uses has higher values with higher S/V ratio: increasing proportion of loss surfaces can increase consumption related to space, as heating and cooling. Indeed, space cooling per m<sup>2</sup> shows a R<sup>2</sup> = 0.4. The S/V ratio also influences appliances and lighting consumption, which is correlated even more with older residential stocks realised before 1980. The statistical models attempt to distinguish by age only natural gas, whereas SC and App include pre-1980 as a variable in the multiple linear regressions. Indeed, considering the low results obtained by linear correlations, multiple linear regressions (MLR) are necessary to obtain more satisfying energy uses.

Table 63. Pearson's correlations of energy-related variables with energy-use intensities.

	Vol (m <sup>3</sup> )	S/V (m <sup>2</sup> /m <sup>3</sup> )	UHS (m <sup>2</sup> )	n° floors	Inh/ m <sup>2</sup>	% pre-1980	DHWm <sup>2</sup>	SC/m <sup>2</sup>	App/m <sup>2</sup>
SH <sub>NG</sub> /m <sup>2</sup>	0.06	0.04	0.06	0.14	0.04	0.12	0.06	0.18	0.11
DHW <sub>NG</sub> /m <sub>2</sub>	0.003	0.01	0.02	0.01	<b>0.80</b>	0.11	1	0.06	0.05
(SH+DHW) <sub>NG</sub> /m <sup>2</sup>	0.09	<b>0.31</b>	0.07	0.14	0.18	0.07	<b>0.23</b>	0.03	0.03
SC <sub>EE</sub> /m <sup>2</sup>	0.15	<b>0.40</b>	0.15	<b>0.25</b>	0.02	0.15	0.04	1	<b>0.35</b>
App <sub>EE</sub> /m <sub>2</sub>	0.15	<b>0.30</b>	0.14	<b>0.23</b>	0.15	<b>0.41</b>	0.05	<b>0.36</b>	1

### 5.4.1 Electricity: SC and App consumption

SC is assumed as part of electricity-use. According to Ontario data [43] for 2017, SC is assessed as 14% of electricity demand for detached houses, 9.4% for semi-detached and 5.1% for apartments. The low values for a linear regression require MLRs. Appliances and lighting cover the remaining electricity consumption, based on which another MLR is performed too. The obtained values from the regression are then used in the formula for space cooling (Table 64). The MLR model for appliances has a quite good coefficient of determination and low significance p-value respectively equal to R<sup>2</sup> = 0.596 and F = 1.36E-199, while for space cooling R<sup>2</sup> = 0.631 and F = 2.6E-223. The average calculated values of the other archetypes are in line with assessment. As seen before, electricity consumption confirms a decreasing trend with lower S/V ratio, having minimum results for high-rise buildings (Figure 46; Figure 47). For appliances, Figure 46 underlines higher values for low-rise apartments which is the most variable and challenging category to evaluate: this confirms the trend of electricity consumption in Table 59. The decreasing space cooling consumption emerges also in Figure 47 for lower compactness factors: the calculated values are slightly higher than the assessed ones for low- and high-rise apartments, while in line for the other two archetypes.

Table 64. Variables selected to build MLR models for appliances (App) and space cooling (SC) energy-use intensity.

Variables	App EUI		SC energy intensity	
	Coefficients	p-values	Coefficients	p-values
Intercept	26.6283	3.741E-68	-3.1531	2.4E-28
N° of floors	-0.6543	1.212E-20	-	-
S/V ratio	22.7825	7.198E-35	8.6972	1E-101
% Pre-1980	27.8844	1.77E-103	1.7955	4.2E-11
App/m <sup>2</sup>	-	-	0.065	3.6E-92

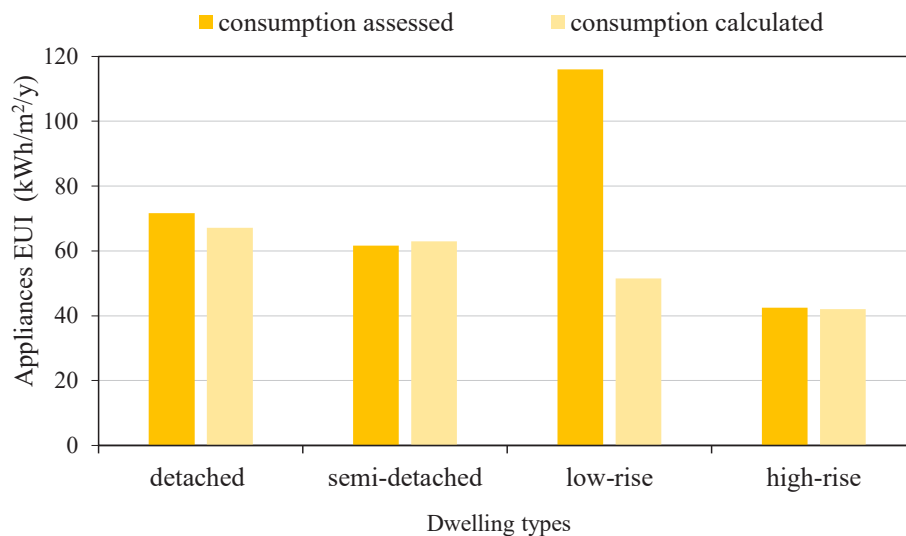


Figure 46. EUI data (dark yellow) and calculated values (light yellow) for appliances and lighting by dwelling types.

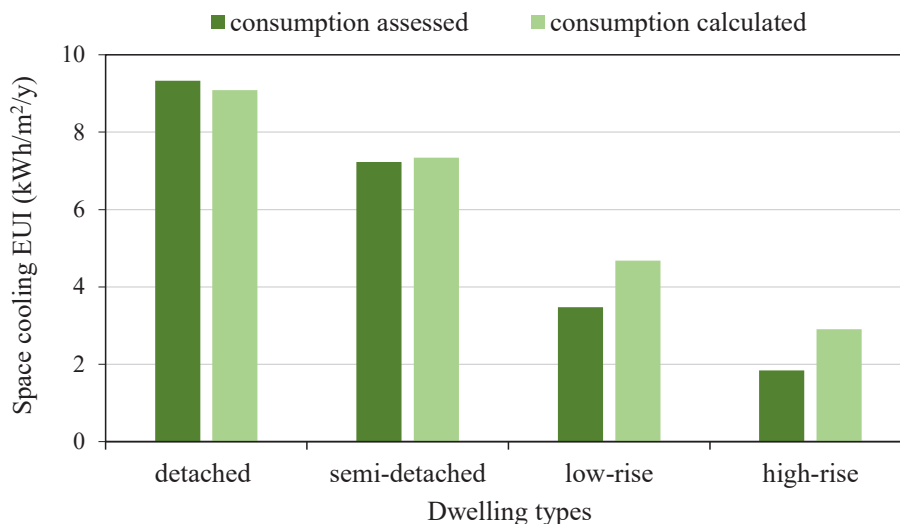


Figure 47. EUI data (dark green) and calculated values (light green) for space cooling by dwelling types.

Additional analyses with material properties and operating systems would have underlined further differences, especially for space cooling. For instance, apartment buildings can have central cooling or larger fenestration area and/or higher glazing thermal transmittance (U-value) which can increase space-related loads due to higher solar gains and heat losses by transmission [102]. Moreover, space cooling loads are likely to rise in following years due to warmer temperature expected.

## 5.4.2 Natural gas: SH and DHW consumption

The analysis of natural gas consumption results more complicated, as already mentioned in Paragraph 5.3. Correlations with independent building variables are lower and disaggregated data by dwelling types have significant variations for multi-family dwellings.

The DHW energy intensity has higher correlation ( $R^2=0.80$ ) (Table 64) with residential density (inh/m<sup>2</sup>) because it is directly assumed from the number of inhabitants by neighbourhood. On the other hand, SH covers the remaining share of natural gas and shows low correlations to obtain an applicable equation. Therefore, DHW and SH are studied as a joined total amount of natural gas consumption. The analysis is then performed by S/V ratio and period of construction, as shown in Figure 48.

Natural gas energy-use intensity (EUI) highlights opposite trends for the two temporal ranges, probably due to the different construction techniques, materials, level of maintenance and HVAC systems characterising the housing types and impacting on their demand. The application of these two equations leads to results shown in Figure 49 and Figure 50. Slightly different S/V ratio distinguish the dwelling categories in the two age ranges.

Low-density dwellings (detached and semidetached) do not vary significantly for different construction ages: respectively 76.22 and 75.95 (4% difference) kWh/m<sup>2</sup>/y and 38.70 and 39.10 (8% difference) kWh/m<sup>2</sup>/y. Only few blocks (3) present detached buildings after 1980 because they are limited in the downtown where high-rise buildings prevail. On the other hand, low-rise and high-rise allow a more representative analyses on blocks built on different periods.

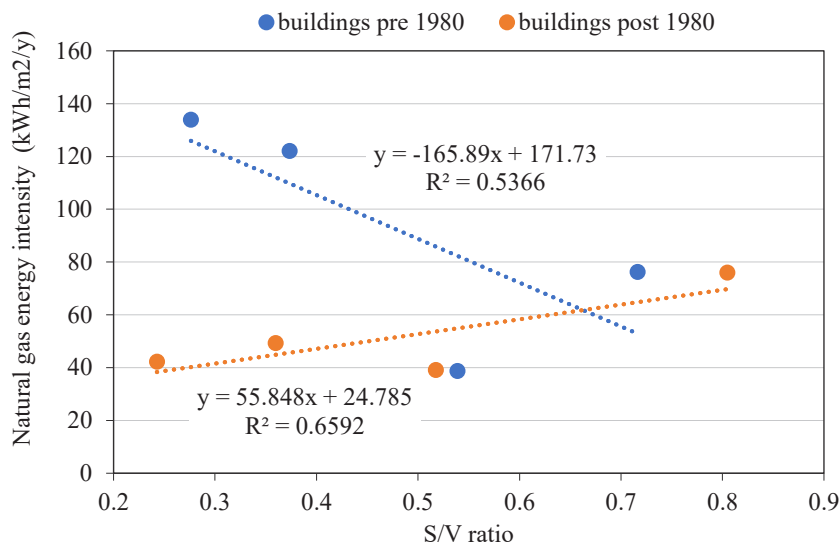


Figure 48. Average natural gas intensities correlations for SH and DHW by period of construction and S/V.

Applying the equations in Figure 48, values are closer to assessed consumption for the post-1980 residential stock, showing higher natural gas demand for detached houses (Figure 50). Pre-1980 results are less satisfying, especially for the two central classes, while they are closer for high-rise apartments (Figure 49). As mentioned before, low-rise has the most variable consumption, while semi-detached houses show the lowest demand in the pre-1980 equation.

The unsatisfying results for natural gas consumption led to a further analysis (even if simplified), divided for low-density dwellings and low- and high-rise apartments. The correlation used for natural gas EUI for detached and semi-detached houses is reported in Figure 51. The scarcity of post-1980 housing stock contributes to have similar values for different construction periods. The linear regres-

sion for detached and semidetached can be applied for dwellings realised before 1980, while cautions is needed for more recent stock. Generally, this type of buildings has brick walls, gable roofs, basements, and natural gas furnaces.

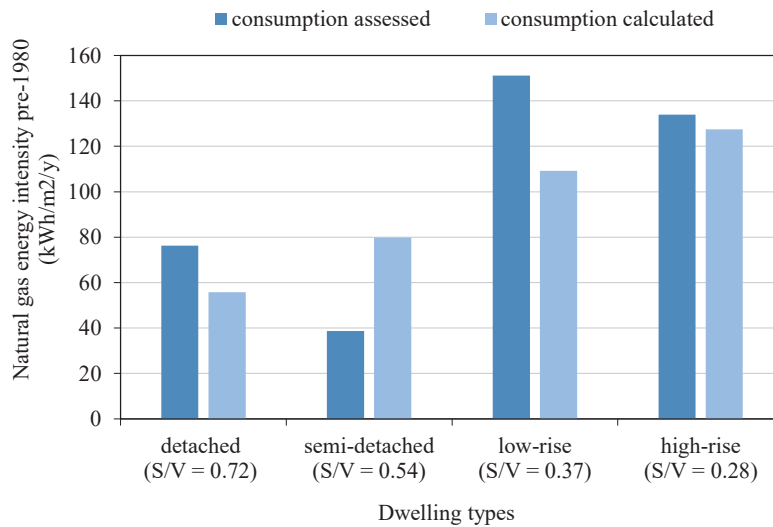


Figure 49. Energy consumption data (dark blue) and calculated from linear regression (light blue) for SH and DHW in the pre-1980 period by S/V-dwelling types.

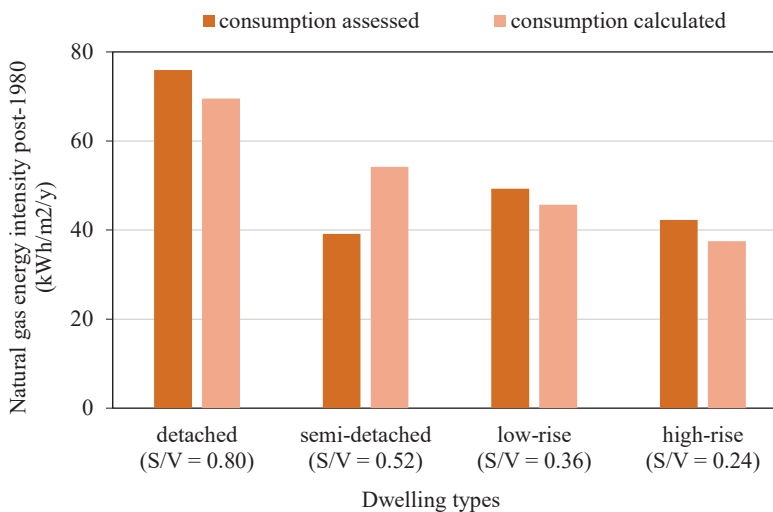


Figure 50. Energy consumption data (dark orange) and calculated from linear regression (light orange) for SH and DHW in the post-1980 periods by S/V-dwelling types.

For low- and high-rise buildings, natural gas EUI shows recurring trends (Figure 52; Table 65):

- higher EUI for older buildings, lower EUI for 1980-2004 and lowest EUI for after-2004 blocks, with expected more insulated envelope and more efficient technological systems;
- low-rise apartments show higher EUIs and  $S/V_{avg}$  ( $0.35 \text{ m}^2/\text{m}^3$ ) compared to high-rise with  $S/V_{avg}=0.25 \text{ m}^2/\text{m}^3$ ); only a limited number of buildings have much higher consumptions. Low rise buildings realised after 2004 are not found.

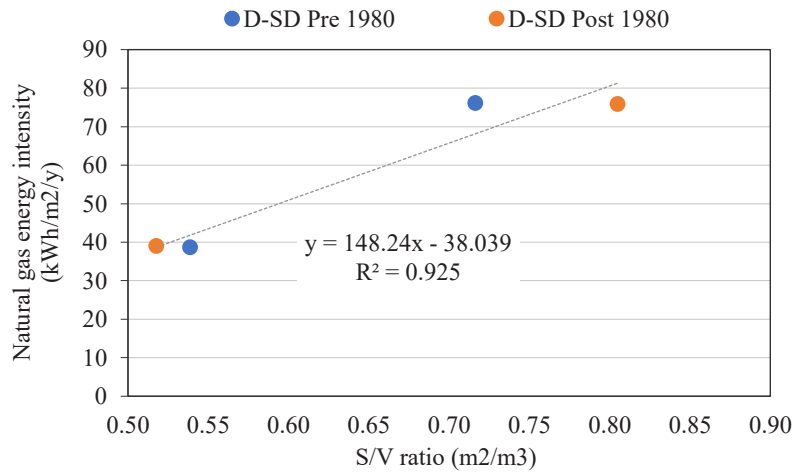


Figure 51. Linear regression model for NG energy-use intensity (SH+DHW) for typology of buildings (D=detached; SD=semidetached) and age. Blue dots refer to NG values for detached and semi-detached realised before 1980, while orange dots after 1980. The regression line considers both values.

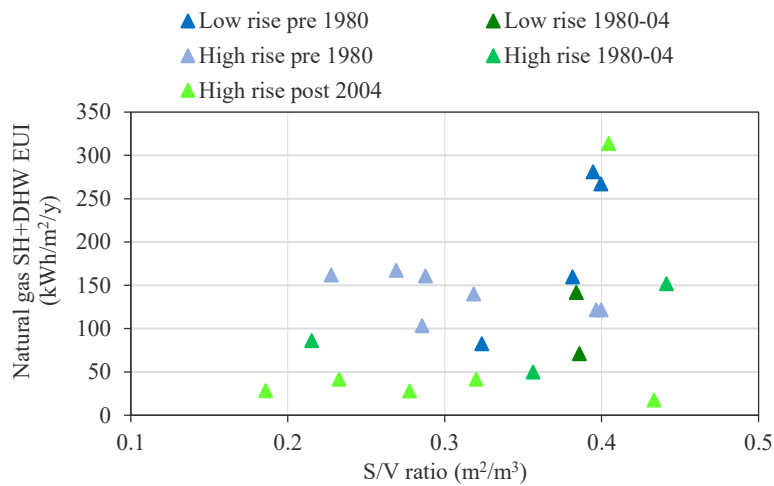


Figure 52. Values of natural gas EUI for low- and high-rise buildings, distinguished by period of construction.

Table 65. Average natural gas energy-use intensity (kWh/m²/y) for low- and high-rise apartments by the three periods of construction.

Period of construction	Low-rise NG intensity (kWh/m²/y)	N° blocks considered	High-rise NG intensity (kWh/m²/y)	N° blocks considered
Pre 1980	184.54	6	134.23	10
1980 - 2004	106.45	2	92.11	5
Post 2004	n. a.	0	78.46	6

As already highlighted by [172], natural gas intensity for low- and high-rise are highly variable, due to the heterogeneity of building and system typologies. This implies lower correlations than expected in the regression analyses. Construction materials (e.g., reinforced concrete-bricks, glass, and steel buildings), technological systems, maintenance level, type of use can characterise the overall consumption. A further factor could be the mix of systems especially in more recent buildings, with both electricity and gas-based technologies.

Therefore, a sufficiently reliable model is not found for high- and low-rise apartments due to the high variability of measured results for same age ranges. For apartment buildings, the average values

reported in Table 65 can be applied distinguishing the three main periods of construction and the different S/V ratios. The demanding character of older high-rise MURBs in Canada and for Toronto emerged already in other studies, especially if structures are constructed between 1945 and 1980 and if gas heated [102] [173]. The diffused poor maintenance contributes to their low performance and high energy losses, whereas tenants and owners are generally reluctant to invest in retrofit measures. To address similar issues, the City of Toronto launched the Tower Renewal Program in 2004 to improve energy savings [173].

Despite representing an initial characterisation, the statistical models are affected by lack of measured data at the building scale, mainly for function and age of construction, as already underlined in Paragraph 5.3. Instead of relying on blocks and buildings categories retrieved from the 2030 Platform, a dataset on single buildings would have supported stronger statistical regressions and more detailed evaluation.

## 5.5 GIS-based extension

The statistical models for energy-end uses can be then applied to the residential buildings stock of the Platform area in a GIS environment. This approach allows to evaluate and calculate all typological and geometric information about dwellings and population, which influence energy consumption.

The analysis can be extended to the whole city of Toronto using the building shapefile [74], the 140 Neighbourhood Profile data for the construction period [75] and the residential zones reported by zoning plan [76]. The most demanding areas can be easily visualised in GIS [76].

An example is provided in Figure 53 for the Humewood-Cedarvale neighbourhood (North from downtown Toronto), mainly low-density residential zone with few educational buildings and with 91% houses built before 1980.

The GIS-based mapping distinguishes energy consumption variations for the different building types. In the example, higher consumption (kWh/m<sup>2</sup>/y) characterise buildings with higher S/V ratio, which represent most of dwellings. On the other hand, the overall annual consumption is concentrated for high rise apartments along the main neighbourhood roads.

The model can be further extended at a city scale, as shown in Figure 54. Bar charts summarise electricity consumption by neighbourhood and by residential archetype. The residential function covers most of the areas surrounding Toronto downtown, alternating more sprawl-based zones with denser centres with high-rise prevalence. A similar energy mapping represents a useful tool to spatialise energy consumption and identify the most demanding areas. A higher level of detail would be more useful for specific actions.



Figure 53. Buildings' S/V classes (left) and App + SC electrical consumption based on linear regressions (right) for the southern part of Humewood-Cedarvale neighbourhood.

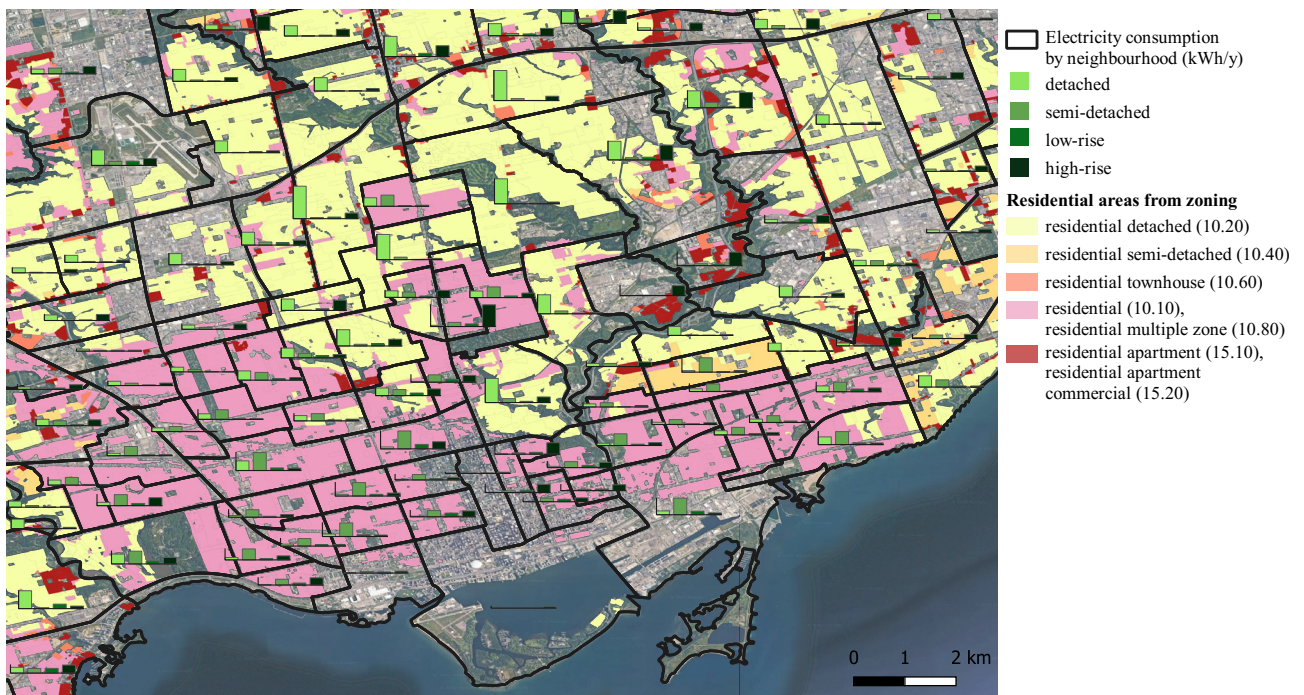


Figure 54. Extension of the electricity consumption model (SC + App) for residential areas of the City of Toronto, distinguishing main dwelling types by zone.

## 5.6 Solar analysis

The top-down statistical assessment of energy consumption has been more satisfying for the electricity component, distinguished in appliances and space cooling. The electrical consumption of dwellings can be partially satisfied by PV installation on rooftops, even in urban environments. An urban-scale solar assessment is performed with a GIS-based method for the TOcore area.

The Toronto climate zone 5A (cool humid) has average temperatures around and below 0°C in winter months and warmer values toward summers, with rising temperature projections by the end of this century [127]. For 2017, the monthly solar irradiation peak is between June and July, while minimum values are in the period when daylight is limited (Table 66). Higher daily solar radiation is in June, when daylight length is longer, while maximum temperatures are registered one month later.

Table 66. Average air temperatures, hours of daylighting and solar radiation on building rooftops in Toronto for 2017.  
Source: [73].

Months	Average air T (°C)	Hours of daylighting (h/d)	Solar irradiation on the rooftop of Toronto buildings (kWh/m <sup>2</sup> /month)
January	-0.4	9.02	42.56
February	0.1	10.17	66.78
March	-0.4	11.44	107.48
April	6.7	13.16	138.93
May	10.7	14.37	155.58
June	18.1	15.2	179.42
July	21	15.03	181.44
August	20.3	13.55	163.82
September	18.6	12.27	144.05
October	14.4	10.54	83.42
November	5.1	9.29	50.67
December	-2.5	8.42	44.85

GIS simulations are carried out monthly to consider different positions of the sun and humidity in the atmosphere. The components of direct and diffuse radiation and the transmissivity of the atmosphere differ along the year and seasons. Maximum diffuse radiation is in winter months when the scattering is generally higher and the presence of clouds more diffused. On the other hand, the Linke turbidity factor shows a peak in summer months due to more humidity and lack of transparent atmosphere (with values equal to 1). Diffuse radiation and transmissivity are grouped according to the average daily hours of light per month. The grouping criterion follows the standard deviation from the average value of hours of light for all months. For the four intervals ( $\mu + SD$ ,  $\mu + 2 SD$ ,  $\mu - SD$  and  $\mu + 2 SD$ ), the average values for diffuse radiation and transmissivity in Table 67 are the input data to launch the ArcGIS simulations. The evaluation of incident solar radiation is performed only for the residential blocks of the TOcore area, but they can be extended to the whole City of Toronto. Residential blocks of the 2030 Platform area count 2,449 residential buildings with an available roof area of 1,355,902.5 m<sup>2</sup>, assuming at least one pitch facing South-East or South-West.

Table 67. Input solar parameters used to launch the Area Solar Radiation plugin in ArcGIS.

Months	Diffuse to global ratio	Linke Turbidity Factor TF	Transmissivity	Diffuse ratio <sub>avg</sub>	Transmissivity <sub>avg</sub>
December	0.52	2.6	0.34	0.52	0.34
January	0.55	2.55	0.31		
November	0.49	2.68	0.36		
February	0.44	2.83	0.43	0.41	0.47
October	0.37	3.07	0.49		
March	0.42	2.93	0.49		
September	0.24	3.16	0.61	0.30	0.60
April	0.36	3.34	0.58		
August	0.31	3.39	0.62		
May	0.36	3.56	0.60	0.33	0.63
July	0.32	3.59	0.63		
June	0.30	3.68	0.65		

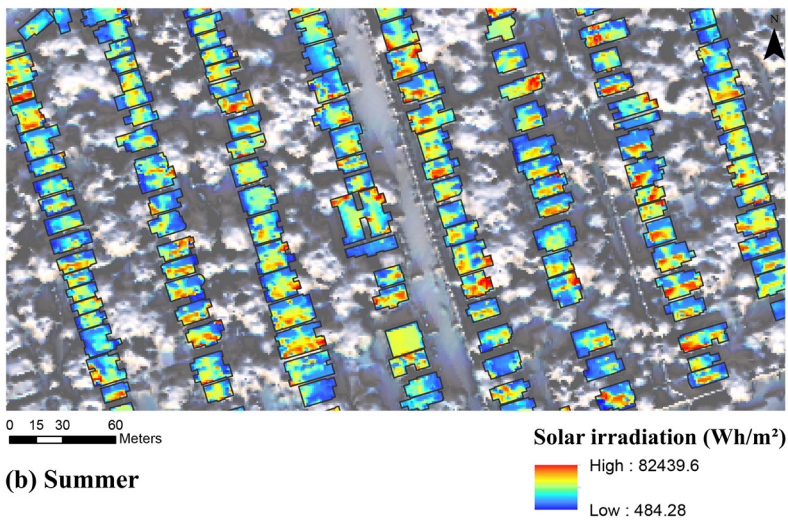
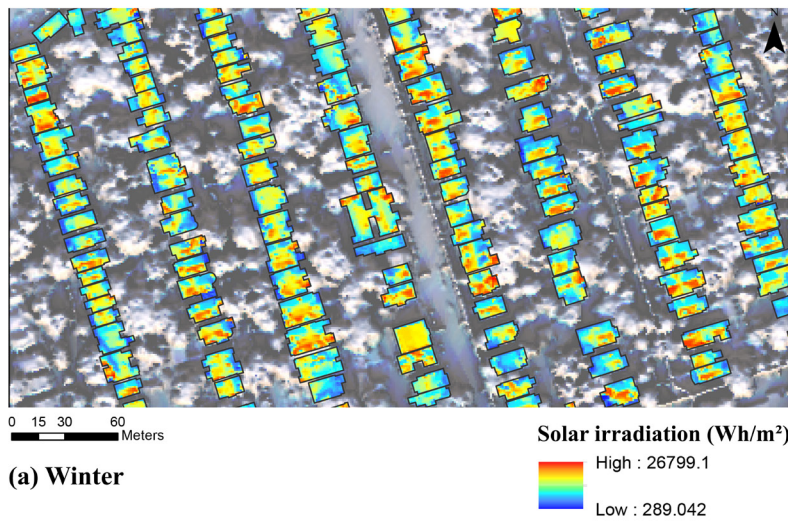


Figure 55. Solar irradiation (Wh/m<sup>2</sup>) on residential rooftops for some residential blocks in downtown Annex area, during December (a) and July (b) in 2017.

Figure 55 shows the ArcGIS output for the Area Solar Radiation tool for December and July. Using a DSM to launch solar simulations, results consider all natural and artificial shading obstructions which can impact on PV performance, as presence of close (and tall) buildings and vegetation. Indeed, especially an urban context generally counts several obstacles to the radiation, among which higher structures and skyscrapers. Pitches to the SE orientation have higher irradiation and should be favoured for photovoltaic installations. Maximum assessed values in summer months are more than three times higher than in winter, during which electric production could be higher.

GIS-based results are compared with the assessment of PVGIS tool [73], taking values from the roof of the Toronto City Hall (100 Queen Street) in Figure 56. In both cases, the peak is between June and July, when also the maximum average temperature is registered. The radiation values have similar trends along the year, but differences emerge mainly in winter months. January, February, November, and December irradiations are from 45.25% to 67.27% higher in PVGIS, while in warmer periods from 21% to 44% lower than calculations in GIS. The most align month is September, with 0.32% difference. The discrepancies between the two methods could be caused by:

- the location selected from PVGIS. The town hall roof is a conventional location to represent the municipality, whereas results from GIS are an average from the whole TOcore area;
- the assumptions considered for the input values in GIS. Input data of diffused radiation and transmissivity are a seasonal average. The simplification may not underline some monthly differences, which instead emerge from PVGIS values.

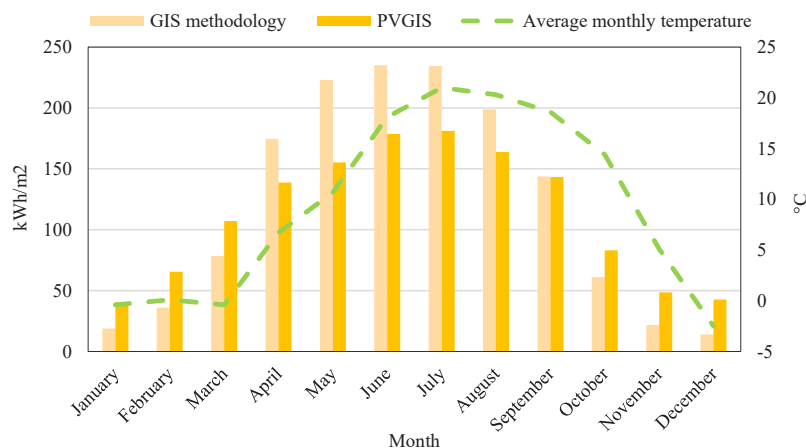


Figure 56. Monthly irradiation for 2017 values from GIS-based methodology and PVGIS with temperature trend.

Table 68. Total and average PV production by technology for the TOcore area, assuming 40% of usable rooftop surface.

Technology	Total production (kWh/y)	Average for dwelling (kWh/y)
InP crystalline cell	140,573,642.7	57,400.4
GaAs multicrystalline	130,561,423.	53,312
CzTS thin film	64,429,586.3	26,308.5

Applying the equation (3) for solar production, three PV technologies with different efficiencies indicated in paragraph 3.5 are selected: InP crystalline cell, GaAs multicrystalline and CzTS thin film. This analysis firstly takes as assumption a 40% feasible area for each residential roof [88] [91], inte-

grating a constant-value method with a GIS elaboration. As shown by Figure 57, the installation of monocrystalline-Si PV modules would cover the highest share of annual electrical consumptions for all dwelling types, while lowest are registered for the less performative thin film. The percentage of covered electrical consumption decreases with lower S/V ratio, as in the case of high-rise apartments due to the higher building electricity in relation to the feasible rooftop area.

The monocrystalline-Si can produce a surplus for detached and semidetached between April and June, while for low-rise in May and June even if with a minimum additional output (Figure 58). Indeed, these categories have a more balanced relation between consumption and feasible rooftop surface for solar installation. On the other hand, in winter months the photovoltaic share is minimum for all typologies with less than 30% coverage in January, February, November and December. The annual satisfied electricity by PV mono-Si is the lowest for high-rise apartments (32.64%). Despite higher PV production between June and July, the share of covered electricity consumption is maximum in May due to the still limited cooling needs.

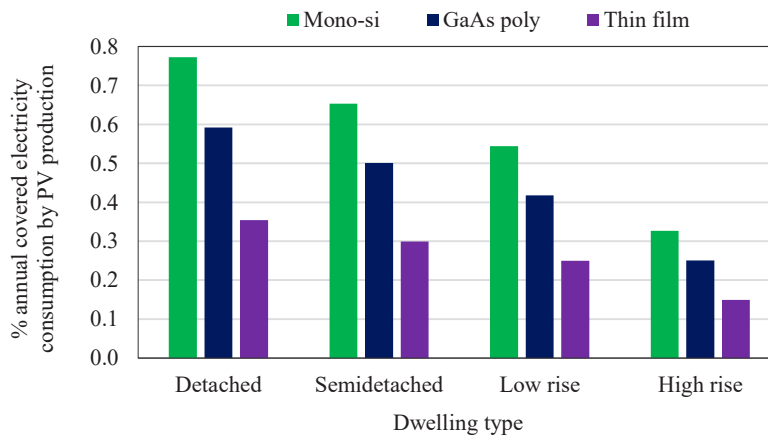


Figure 57. Annual share of electricity covered by PV modules for the residential blocks in TOcore, assuming 40% of usable rooftop surface.

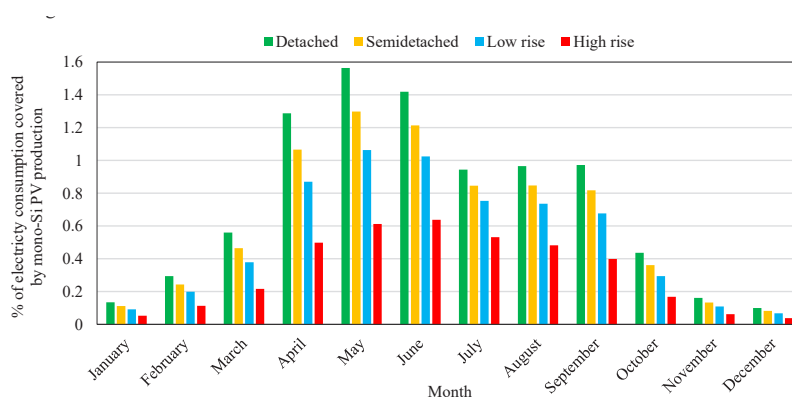


Figure 58. Average share of electrical consumption covered by Mono-Si technology by dwelling types in TOcore, assuming 40% of available rooftop area.

The main contribution for solar production derives from semi-detached dwellings, which have a satisfying relation between solar production and electricity consumption. Lower output is from low rise apartments, which are the less common even if they have a quite significant available rooftop area. Main contribution is registered in summer months, while the winter period is more challenging to cover the residential electricity needs.

Assuming 40% of available roof surface is a simplification which requires a more detailed assessment. Therefore, the GIS-based methodology described in the paragraph 3.5 allows to determine feasible roof portions based on their orientation and slope (Figure 59; Figure 60). The considered rooftops must be South or South-East facing because they receive the maximum radiation, which is confirmed by PVGIS optimisation (azimuth =  $-2^\circ$ ). The slope range is assumed from the SolarTO Map [92] which considers all roofs less than  $45^\circ$ . Similarly, a study on 10 Canadian cities [63] identified that the optimal tilt angle is slightly less than latitude, with an average tilt of  $9.6^\circ$  less than the location latitude, while the average optimal azimuth angle should be  $1.9^\circ$  west of due South.

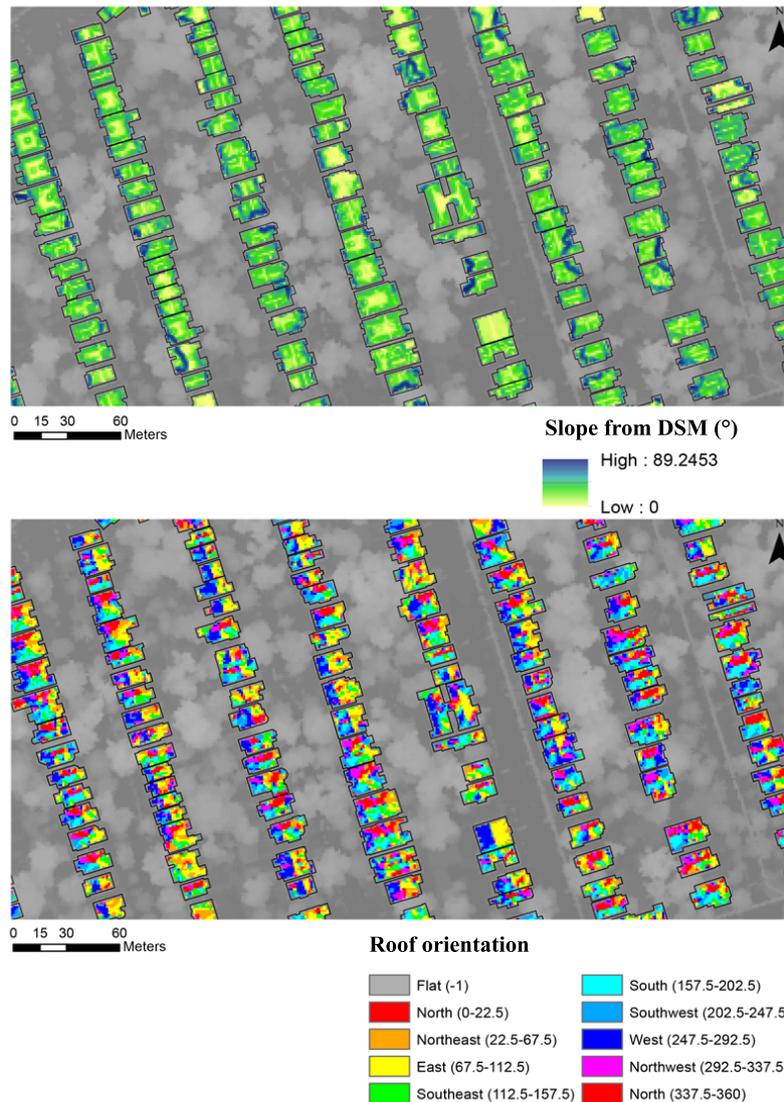


Figure 59. Output in GIS environment for slope (above) and orientation (below) of roofs, based on DSM, for some residential blocks in the Annex area.

The sum of all the feasible areas for residential blocks is equal to  $104,743.4 \text{ m}^2$ . Areas less than  $1 \text{ m}^2$  are deleted and the remaining surface is  $98,015.9 \text{ m}^2$  and  $92,796.7 \text{ m}^2$  only in residential buildings, with an average of  $41.2 \text{ m}^2$  per roof. Therefore, the available roof area is significantly lower than having 40% as reference value and the overall usable surface is equal to the 7% of the total residential roof areas. Solar installation should be therefore optimised due to the limited assessed surfaces. The total production by PV (Table 69) is calculated with the same equation (Equation 3, see paragraph 3.5) for the three technologies.

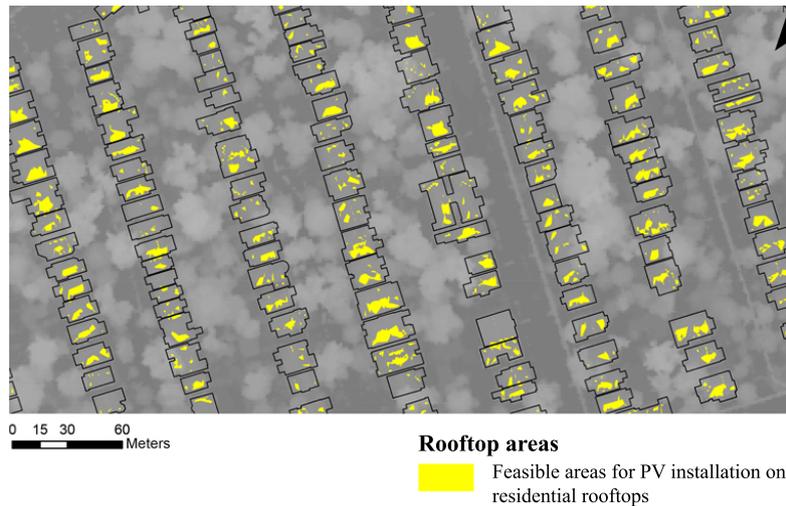


Figure 60. Feasible areas in GIS environment for PV installation, based on DSM, for some residential blocks in the Annex area.

Table 69. Total and average PV production by technology for the TOcore area, with slope and orientation constraints.

Technology	Total production (kWh/y)	Average for dwelling (kWh/y)
InP crystalline cell	23,280,272	10,337.6
GaAs multicrystalline	17,700,703	7,860
CzTS thin film	10,581,942	4,698.91

Figure 61 confirms the reduction of the coverable electricity share for the four different dwelling types and by the considered technologies. Values are consistent for detached and semi-detached dwellings, even if with results less than a half of previous assessed shares. On the other hand, high rise buildings seem to cover a very low percentage of their electricity consumption due to the discrepancy between available roof and overall demand. The share of covered electricity with monocrystalline PV distinguished by building type does not overcome 50% by month in Figure 62, except for May for detached houses (51.83%). Also in this elaboration, more significant contribution is registered for low-density dwellings, while low rise and high rise have respectively maximum values of 27.26%

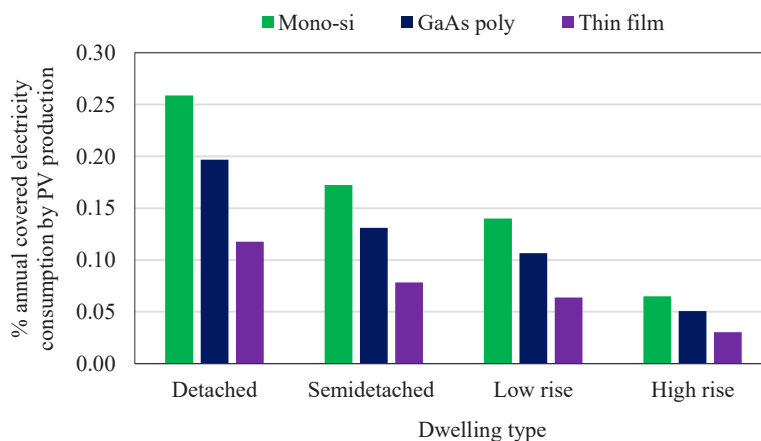


Figure 61. Annual share of electricity covered by PV modules for the residential buildings in TOcore, with slope and orientation constraints.

and 12.33% in May. The 40%-area assumption has clearly higher production than hypothesis with slope and orientation constraints. Overproduction is not assessed for any type of dwelling, neither in summer. Electricity consumption can be met for less than 10% in all cases. Detached and semi-detached housing show still the most interesting values, with respectively 26% and 17.22% overall covered electricity with monocrystalline silicon installed, compared to 77% and 65% of the fixed roof area assumption (Figure 62).

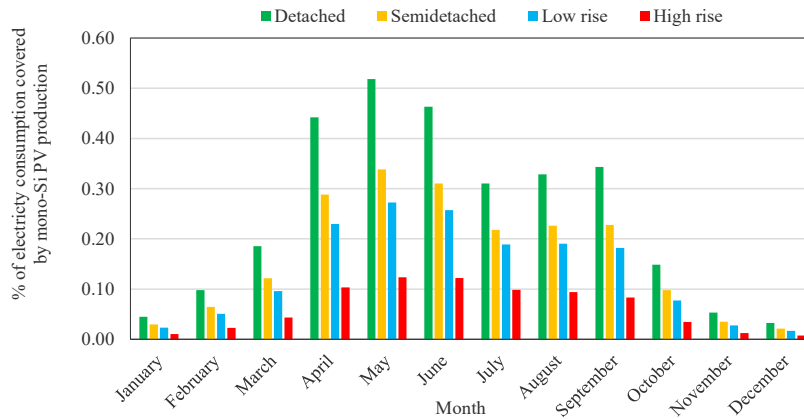


Figure 62. Average share of electrical consumption covered by Mono-Si technology by dwelling types in TOcore, considering slope and orientation constraints.

The model does not consider any storage: the eventual mismatch of solar production and electricity consumption could be partially face with batteries, which release the PV output later and in peak-demand moments. Moreover, the financial feasibility and optimisation could change the preferable sizing, based on the relation between costs, production, and long-term benefits.

Another aspect to consider is the orientation and slope of the PV panels. For this analysis, only the optimal configuration to maximise summer production is considered. However, different combinations can contribute to satisfy distinct load profiles and energy end-uses to address. The typical residential load has higher consumption in the late afternoon and evening, while PV produces more along the day when sunlight is available. As shown in the evaluation of Mutani and Todeschi [67] for Turin, changing and integration distinct exposures could be used to better cover electricity load profiles based on the environment. The study demonstrates how the energy self-sufficiency as well as financial benefits for inhabitants would increase exploiting the available rooftop areas. Therefore, it could be useful to use all the potential roof orientations (generally, two) for photovoltaic panels instead of only the optimal ones. In denser urban environment, maximisation of PV installations could improve energy security and support long-lasting economic benefits for residential occupants.

## 5.7 Results and considerations

The assessment of residential energy consumption with statistical models and solar production in a GIS environment show potentials and limits.

The disaggregated data of electricity and natural gas consumption are retrieved from the block scale to the single dwelling, based on the Toronto 2030 Platform. Results allow to realise a top-down statistical model, based on regressions. The identification of single-building energy-use from block data can lead to inaccuracies, especially for blocks with housing mix. Moreover, assumptions by

ASHRAE applied on building models in the Toronto 2030 Platform had already provided a simplification of consumptions for different structures, materials, and age. Between the two approaches of downscaling data, the method by subtraction is more coherent and specific for the case study because it is based on specific values from the Toronto 2030 Platform. It is also easily flexible and adaptable to other contexts if aggregated energy values and typological features are available. On the other hand, the approach by equation must be based on reliable and comprehensive energy data for housing types and construction period, which might not be always accessible.

Based on the disaggregated values for energy consumption, the MLRs for electricity uses highlight decreasing intensities with lower S/V ratio, or rather for high-rise dwellings. The only discrepancy between assessed and calculated values is for low-rise apartments, with the most variable demand.

Natural gas consumptions have opposite trend for buildings before and after 1980 in relation to S/V ratio. However, detached and semidetached types show close values for the two periods due to the scarcity of more recently built blocks. A second hypothesis is performed for natural gas, distinguishing low-density houses and apartments buildings in relation to the S/V ratio and the period of construction. Values are very similar for low-density housing due to the limited number of post-1980 dwellings. A sufficiently reliable model is not found for high- and low-rise apartments due to the high variability of measured results for the same age ranges. The demanding character of older high-rise MURBs in Canada and for Toronto has been already underlined by other studies, also connected to their low maintenance [102] [173]. According to GIS mapping, high-rise consumption is mainly concentrated in the city centre and in infrastructural nodes (i.e., subway and railway stops), while single-family houses are in more decentralised zones. Despite providing an initial characterisation, the statistical models are affected by lack of measured data at the building scale, mainly for function and age. Instead of relying on age and function categories retrieved from the 2030 Platform, a dataset with results for single-building level would have supported stronger regressions. Privacy limitations and constraints on data accessibility have represented obstacles to data accessibility and spatial resolution, as discussed by [12].

The GIS-based calculation of solar PV output on rooftops estimates the potential share of covered electricity. The simulations based on a LiDAR DSM consider all the built and natural obstacles: indeed, solar production can vary significantly due to self-shading effects by other parts of the building and the presence of surrounding constraints to let the sunlight hits panels [16]. The roof PV production can be effective in summer months when electricity consumption increases for space cooling (growing as temperatures rise) and the solar output is maximised. The projected warmer temperatures [127] are likely to increase air conditioning demand in summer months, with even higher charges on the network and increasing prices in peak hours. The higher electric consumption of taller buildings cannot be fully satisfied by PV. Indeed, the most interesting results characterise detached and semi-detached houses, which are spread both in the downtown but even more in the outskirt. Solar overproduction is registered assuming a 40% available roof area, while the monthly covered electricity is not higher than 55% introducing slope and exposure constraints. A constant value returns more simplified results, but easier and faster to be assessed for a large number of buildings. A GIS-based identification is more specific case by case: however, only South and South-East facing parts have been considered. Analyses can be extended to other orientations too (also not optimal) to increase the solar production for each dwelling.

Policies and incentives for PV diffusion can contribute to more decentralised and distributed ener-

gy systems, increasing self-consumption and self-sufficiency, diminishing the withdrawal from the electrical energy grid [81]. Eventual solar overproduction during summer could lead to incentive programs and activate sharing mechanisms, especially between low- and high-density residential buildings. However, micro-generation in urban contexts also leads to more fluctuating power supply: this increases pressures on the electrical network when solar production lacks or when different mechanisms of purchase and selling (i.e., net metering) are active on one generator [15]. Adding electricity storage with appropriate sizing can contribute to smooth instabilities caused by renewable generation. Batteries release overproduced electricity later in the day, as when demand is higher in the evening, but solar radiation is limited [81]. The PV installation and storage sizes need to be adapted to different scales and eventually towards community-based projects rather than standalone structures.

## 6. BLOCK-SCALE OPTIMISATION

### 6.1 Modelling with URBANopt

The creation of a top-down statistical model was the first step to characterise the energy consumptions of residential blocks for the area considered by the Toronto 2030 Platform. The output shows limitations, as the use of disaggregated energy data from models and the lower accuracy for blocks with housing mix. The simulation will shift to a more detailed engineering model for the dwellings of the selected area. As mentioned before, the model provides for the single building level energy system, thermal characterisation, and assessment of solar production.

The selected tool for the analysis is URBANopt, which represents a compromise between single buildings assessments and district level analyses. The direction towards new community-scale projects is one of the policy-directions adopted by the Toronto 2030 District towards zero-carbon [174]. URBANopt is not a standalone program for end users but a set of open-source modules which supports a variety of multi-building design and functions. Building modelling is based on EnergyPlus and OpenStudio. In this study, the focus is the residential function for the four selected archetypes.

The methodology is summarised in Figure 63, having input data, consumption assessment and solar optimisations with different scenarios to be compared in a cost-optimal analysis.

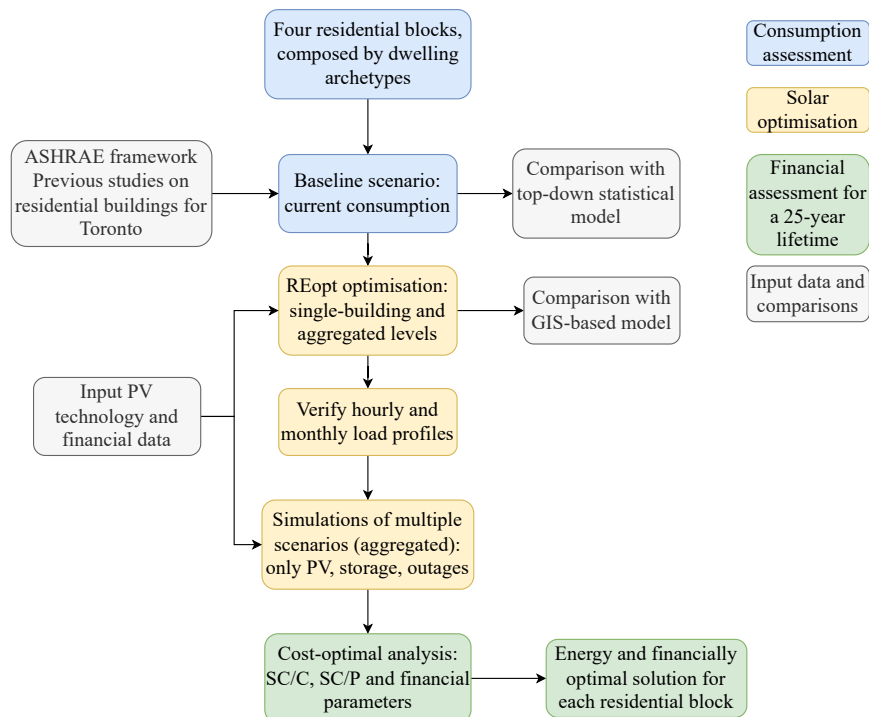


Figure 63. Flowchart methodology for URBANopt simulations at the block scale.

The GitBash terminal is used to launch the commands and elaborations, while Visual Studio Code, GIS software and Excel allow to build feature files, visualise, and elaborate results.

URBANopt models building consumptions for a baseline scenario and optimise possible renewable installations, in this case rooftop PV with eventual storage/generator. Based on weather events in 2017, possible weather-related outages with different durations are simulated to understand the opti-

mal size and backup system to face similar disturbances. Installing local distributed resources increases self-sufficiency and resilience, but also determines costs over a lifecycle period. A cost-optimal analysis with the different assumptions underlines the preferable solution(s) to improve self-consumption and self-sufficiency of the residential blocks, based on the PV potential and storage.

Considering the laptop storage space and time in simulations, the analyses are performed on representative residential blocks of the area rather than overall TOcore. The blocks are composed by the four dwelling archetypes (described in Paragraph 6.3) used in the statistical models.

## 6.2 Residential input data

URBANopt accepts most of building functions (residential, office, commercial, industrial, education, services) in simulations, keeping some baseline assumptions. The available residential workflows supported in URBANopt are:

- single-family detached
- single-family attached
- multifamily, which is supposed to include low-rise and high-rise apartments.

General information to complete the building characterisation (GeoJSON file) are summarised in Table 70. They are retrieved from a set of previous studies about the building stock for low-density housing and apartments dwellings in the central area of Toronto..

Table 70. Main building inputs for characterisation of each dwelling category.

Field	Single detached	Single semi-detached	Multifamily
Roof type	Gable	Gable	Flat roof
Foundation type	Basement conditioned	Basement conditioned	Ambient
Attic type	Vented	Vented	Flat roof
System type	Furnace and evaporative cooler	Furnace and evaporative cooler	Gas furnace and apartment AC
Heating system fuel type	Natural gas	Natural gas	Natural gas
Considered studies	[97] [98] [99]	[97] [98] [99]	ASHRAE templates, [100] [101] [102]

As mentioned before, the two low-density dwelling types (detached and semidetached) are only represented by the Residential International Energy Conservation Code (IECC) template. The IECC template is based on values which established minimum energy efficient requirements, with performance-related provisions and updates. However, most of the stock in Toronto was realised before 1980. The characterisation of enclosures (walls, windows, ceiling, foundation) made by IECC is not realistic for dated buildings: values result too performative and associated to newer technologies.

Modifications are applied to the standard templates, based on previous studies on detached and semi-detached houses of downtown Toronto (Table 70). The three analyses distinguish four temporal ranges, based on housing evolution, regulations, and on-site surveys for the central area of Toronto.

1. Century detached and semi-detached: 1945 or older.

Main characteristics of the building stock:

- Finished attic, full-width porch
- Gable roof
- Cladding in brick
- Wall assembly: double-wythe brick, 20mm air space, 25mm fibreglass, lath, and plaster
- Foundation: quadruple wythe brick
- Double-glazed air-filled window.

Table 71. Insulation values for detached and semi-detached houses built before 1945 and by the IECC 2006. Source: [97] [98] [99].

Component	RSI (m <sup>2</sup> *K/W)	R-value (h*ft <sup>2</sup> *R/Btu)	R-value (h*ft <sup>2</sup> *R/Btu) by IECC 2006, zone 5A
Ceiling	2.74	15.56	38.46
Main walls	1.11	6.30	16.67
Windows	0.39	2.21	2.86
Foundation walls	0.52	2.95	15.39

## 2. Wartime detached and semidetached: built between 1946 and 1969.

Main characteristics of the building stock:

- Finished attic, full-width porch
- Roof: gable front, flat rear
- Cladding in brick
- Wall assembly: light wood framed
- Foundation: quadruple wythe brick
- Double-glazed air-filled window.

Table 72. Insulation values for detached and semi-detached houses built between 1946 and 1969 and by the IECC 2006. Source: [97] [98] [99].

Component	RSI (m <sup>2</sup> *K/W)	R-value (h*ft <sup>2</sup> *R/Btu)	R-value (h*ft <sup>2</sup> *R/Btu) by IECC 2006, zone 5A
Ceiling	3.66	20.78	38.46
Main walls	1.41	8.01	16.67
Windows	0.39	2.21	2.86
Foundation walls	0.74	4.20	15.39

## 3. 70s detached and semidetached: built between 1970 and 2000.

Main characteristics of the building stock:

- Half-width porch
- Gable roof
- Cladding in brick
- Wall assembly: brick, 20mm air space, OSB (Oriented Strand Board), 64mm fibreglass, gypsum
- Foundation: 300mm concrete, 38mm fibreglass, gypsum
- Double-glazed air-filled window.

Table 73. Insulation values for detached and semi-detached houses built between 1970 and 2000 and by the IECC 2006. Source: [97] [98] [99].

Component	RSI (m <sup>2</sup> *K/W)	R-value (h*ft <sup>2</sup> *R/Btu)	R-value (h*ft <sup>2</sup> *R/Btu) by IECC 2006, zone 5A
Ceiling	4.18	23.73	38.46
Main walls	1.71	9.71	16.67
Windows	0.39	2.21	2.86
Foundation walls	1.16	6.59	15.39

#### 4. Modern detached and semidetached: after 2000.

Main characteristics of the building stock:

- Attached garage, walkout basement, narrow porch
- Hip roof with gable accents
- Cladding in brick
- Wall assembly: brick, 20mm air space, OSB (Oriented Strand Board), 50mm fibreglass, gypsum
- Foundation: 300mm concrete, 25mm fibreglass, gypsum
- Double-glazed air-filled window

Table 74. Insulation values for detached and semi-detached houses built after 2000 and by the IECC 2006. Source: [97] [98] [99].

Component	RSI (m <sup>2</sup> *K/W)	R-value (h*ft <sup>2</sup> *R/Btu)	R-value (h*ft <sup>2</sup> *R/Btu) by IECC 2006, zone 5A
Ceiling	5.76	32.71	38.46
Main walls	2.79	15.84	16.67
Windows	1.14	6.47	2.86
Foundation walls	2.01	11.41	15.39

Table 75. Air leakage values for detached and semi-detached houses for the four temporal ranges and by the IECC 2006. Source: [97] [98] [99].

	1945 or older	1946-1969	1970-2000	After 2000	IECC 2006, zone 5A
Air leakage (ACH 50 Pa)	11.24	7.5	5.75	3.42	7

Tables show how values vary between IECC 2006 template and the values by Toronto studies, especially for the older temporal ranges. Dated detached and semidetached dwellings are mostly realised before 1980, having higher consumption compared to more recent constructions. Blocks of detached and semidetached built before 1980 are indeed considered in the URBANopt simulations and templates are adapted to the characterisation.

High-density multifamily dwellings are subdivided in the three temporal ranges following the Toronto 2030 Platform, which reflects already the ASHRAE template. URBANopt recognises only template from IECC regarding the residential function, with more generous values. Therefore, the input files should be manually updated with ASHRAE pre-1980, 1980-2004 and post-2004 models and verify with the studies previously mentioned.

#### 1. Midrise and high-rise apartments built before 1980.

Main features:

- Apartments with central corridor on each floor
- Built-up flat roof with insulation entirely above deck (metal decking)
- Steel frame wall (Steel frame: 0.4 in. stucco, 5/8 in. gypboard, wall Insulation, 5/8 in. gypboard)
- Mass floor
- Interior partitions in 2\*4 steel-frame with gypsum board
- Gas furnace and gas water heater
- Space cooling by split system DX.

Table 76. Insulation values for apartment buildings built before 1980 and by the IECC 2006. Source: ASHRAE template pre-1980.

Component	R-value (h*ft <sup>2</sup> *R/Btu)	R-value (h*ft <sup>2</sup> *R/Btu) by IECC 2006, zone 5A
Ceiling	16.97	38.46
Main walls	6.92	16.67
Windows	1.61	2.86
Foundation walls	6.92	15.39

## 2. Midrise and high-rise apartments built between 1981 and 2004.

Main features:

- Apartments with central corridor on each floor
- Built-up flat roof with insulation entirely above deck (metal decking)
- Steel frame wall (Steel frame: 0.4 in. stucco, 5/8 in. gypboard, wall Insulation, 5/8 in. gypboard)
- Mass floor
- Interior partitions in 2\*4 steel-frame with gypsum board
- Gas furnace and gas water heater
- Space cooling by split system DX.

Table 77. Insulation values for apartment buildings built between 1981 and 2004 and by the IECC 2006. Source: ASHRAE template 1980-2004.

Component	R-value (h*ft <sup>2</sup> *R/Btu)	R-value (h*ft <sup>2</sup> *R/Btu) by IECC 2006, zone 5A
Ceiling	22.53	38.46
Main walls	15.38	16.67
Windows	1.69	2.86
Foundation walls	15.38	15.39

## 3. Midrise and high-rise apartments built after 2004 and assumed with values by IECC 2006.

Main features:

- Apartments with central corridor on each roof
- Built-up flat roof with insulation entirely above deck (metal decking)
- Steel frame
- Foundation: slab-on-grade floors (unheated)
- Gas furnace and electrical water heater with storage tank (50 gal)
- Space cooling by split system DX.

Table 78. Air leakage values for apartment buildings for the four temporal ranges and by the IECC 2006. Source: ASHRAE templates.

	Pre 1980	1980-2004	Post 2004	IECC 2006, zone 5A
Air leakage (ACH 50 Pa)	9.2	9.2	7	7
Window solar heat gain coefficient (SHGC)	0.41	0.39	0.4	0.4

The characterisation of each dwelling type and for each temporal range has been explained. Local studies on the housing stock can identify further differences to have more specific values on Toronto. Therefore, simulations on URBANopt adapt parameters for energy systems and enclosures to have more realistic values compared to recent national frameworks.

### 6.3 Selection of residential blocks

Four residential blocks (with at least 95% GFA covered by residential function) in the 2030 Toronto Platform area are selected to perform simulations and PV optimisations (Figure 64):

- a block composed by detached houses in the Annex area, realised before 1945;
- a block composed by semi-detached dwellings in Cabbagetown, realised before 1945;
- a block composed by low-rise apartments in Regent Park and along Sumach Street, which is council housing and was developed between 1946 and 1960;
- a block composed by high-rise apartments in St. James Town built between 1980 and 2004.

In the block classification provided in Paragraph 5.2, each of these four block has more than 80% GFA occupied by the respective housing type. Each block is representative of one dwelling archetype, which can be then applied to other areas of Toronto. The selected age of construction of each archetype is the prevalent for that housing typology, based on the Toronto 2030 Platform.

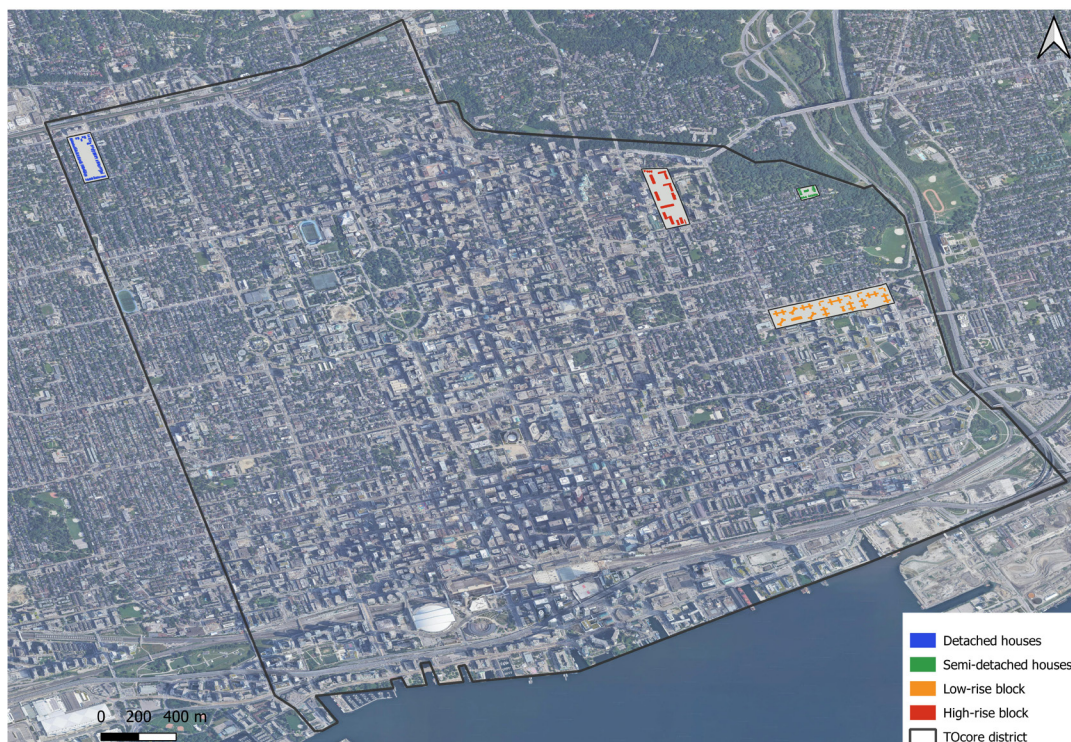


Figure 64. Localisation of the four selected residential blocks in the TOcore area.

Residential blocks are selected from different neighbourhoods, which counts most of that housing typology over the total residential constructions. An overview of each neighbourhood where blocks are located is provided to underline the main socio-economic and housing differences.

- Block with single detached houses in the Annex

The selected detached block is in the Annex neighbourhood, which includes older housing (69% built before 1980). Nearly a half of households (49.5%) is composed by only one person, while larger families are more limited [175]. The area involves both low-density dwelling types in the Western part and apartments with more than five storeys closer to Yonge Street. Indeed, the detached block has been selected from the upper Western area of the neighbourhood.

The proportion of young adults between 20 and 24 years (13.85% in 2011 [133]) is higher than the average, possibly represented by students: indeed, 63.1% population has a bachelor or higher level of degree, compared to 44.1% for the City of Toronto. The share of renters (62% of households) is also higher compared to 47% for the City. Nearly a quarter of those who are employed have part-time jobs and 84% of renters generally spend more than 30% of their income on shelter costs. The workers income (\$40k) is higher than the average for the city (\$34k) [175], which suggests a good financial condition of inhabitants. The presence of young people and workers within the city centre influences the way of commuting to work, with 42% using public transit (average of 37%) and 22% by walk, compared to only 9% for the City and equal to drivers [175].

- Semi-detached block in Cabbagetown

The semi-detached block is located in Cabbagetown, in the North-East area of downtown Toronto. This neighbourhood has a high share of middle-aged residents (over 45 years). In 2011, it counts also the highest average household income, level of home ownership and the lowest immigration percentage in the Core. In 2016, the median family income reached 103k compared to 83k in the City, with 23% of population earning more than 80k/year as individual income. Nuclei are mostly couples, with 72.3% families composed of two members. Indeed, the semi-detached block selected was realised before 1945 in the low-density part of the neighbourhood. The 42% houses were built before 1960 and 27% between 1961-1980, with majority of households (56%) as renters. For the work force (66% of population), public transit (33%) and walk (30%) are the main ways of commuting to their workplace.

- Low rise block in Regent Park

A representative cluster of low-rise apartments is along Sumach Street, in the Norther border of Regent Park. The neighbourhood is the result of a multi-year redevelopment of public and private housing and social infrastructure, with a significant presence of families compared to one-person households [133]. The neighbourhood has the largest household size in the TOcore, with a high presence of children in all age ranges. The median family income (\$53k) is lower than the City level (\$83k) and 52% inhabitants have an individual income between \$10,000 and \$49,999 [175]. Indeed, the second lowest average household income (\$59k) is registered here and the highest social assistance rate in the Core. It is also the most multilingual neighbourhood, with over 54% of residents speaking a language other than English at home but an overall lower level of education. The 88% of private dwellings are apartments buildings and the period of construction is divided between older structures built before 1980 (41%) and 35% of newer buildings realised between 2011 and 2016. The selected low rise block is in line with both the prevalent age of construction and type of dwellings for Regent Park.

- High rise block in St. James Town

St. James Town is the most populated neighbourhood in the TOcore area. 47.4% of households is

composed by lone parent households and 50.5% of seniors living alone, which is higher than the average for the TOcore and compared to other neighbourhoods. The share of renter households is almost double compared to the average (90.1% versus 47.2%), leading to a marginal presence of owner ones. The prevalent dwelling type is high-rise apartments with more than 5 storeys (92.6%), mostly not condominium (86%), while low-density housing or with less than 5 floors cover only the 7% [175]. Indeed, the group of high-rise buildings is selected from this neighbourhood.

The median household and family incomes are respectively \$41,000 and \$53,000. It has the highest number of people living below the low-income threshold (36.5%), interesting all the age groups. The lower income influences also the way of commuting, which is 57% by public transit rather than owning a vehicle. The unemployment rate (10.4%) is the second highest in the Core and almost a quarter of those who are employed have only part-time work. The area is also multicultural and with diverse ethnicities, most recently from the Philippines, Nepal, and India [133].

## 6.4 Evaluation of the baseline scenario

The evaluation of a baseline scenario sets the minimum and starting design performance from which renewable installations are optimised [176]. Table 79 reports input values for the four selected residential blocks, including block features, population, and typological characterisation.

Table 79. Characterisation of the four selected residential blocks.

	Detached	Semidetached	Low-rise	High-rise
Block area (m <sup>2</sup> )	46,782.8	8,972.7	95,057	59,766.8
N° buildings	73	14	16	11
Average footprint area per building (m <sup>2</sup> )	147.3	215.8	3,700	1,059.1
Average n° floors above ground	2	2	3	12
Average floor area per building (m <sup>2</sup> )	618.31	935.33	12,150.89	16,299.46
Estimated n° inhabitants	248	65	498	1,738
Roof type	Gable	Gable	Flat	Flat
Foundation type	Basement conditioned	Basement conditioned	Ambient	Ambient
Attic type	Vented	Vented	Flat roof	Flat roof
System type	Furnace and evaporative cooler	Furnace and evaporative cooler	Gas furnace and apartment AC	Gas furnace and apartment AC
Heating system fuel type	Natural gas	Natural gas	Natural gas	Natural gas
Building type, based on IECC 2006	Single-family detached	Single-family attached	Multi-family	Multi-family
Ceiling (RSI)	2.74	2.74	2.99	3.97
Main walls (RSI)	1.11	1.11	1.22	2.71
Windows (RSI)	0.39	0.39	0.28	0.30
Foundation walls (RSI)	0.52	0.52	0.54	0.54

Air leakage (ACH 50 Pa)	11.24	11.24	9.2	9.2
Starting ASHRAE template	IECC 2006	IECC 2006	DOE pre-1980	DOE 1980-04

### 6.4.1 Detached block

The selected detached block is composed by 73 residential buildings in the Annex area. The URBANopt simulation identifies as main consumption component for the cluster natural gas (77.85%). Electricity (remaining 22.15%) is under 100,000 kWh/month for the whole year, but it overcomes natural gas in the period from May to August due to warmer temperatures and lack of heating needs (Figure 65). The electricity consumption is higher in winter months, especially for the use of interior equipment and lights, according to the schedules proposed by ASHRAE. The peak of cooling demand is in July, with 562.7 kWh assessed for the block. As expected, natural gas is mostly used to satisfy the heating needs of dwelling in winter times, with more than 85% on the overall amount (Figure 65). On the other hand, water and interior equipment have a more stable trend, with slightly lower values between June and September.

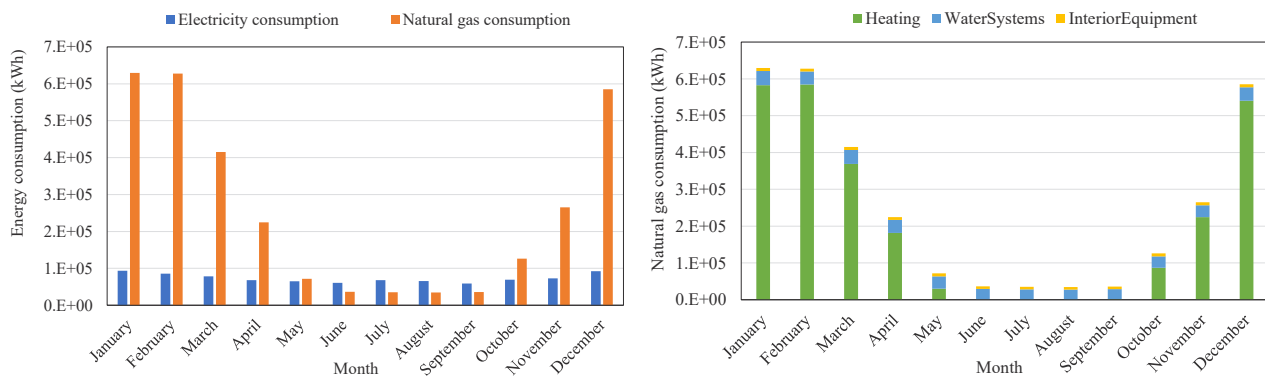


Figure 65. Consumption trend distinguished by natural gas and electricity (left) and energy use components of natural gas consumption (right) for the detached block.

Single buildings have an average energy intensity of electricity equal to 26.19 kWh/m<sup>2</sup>/y and 92.58 kWh/m<sup>2</sup>/y for natural gas. The comparison with values by the statistical model underlines a main difference: the share of electricity is significantly lower for URBANopt simulation (Table 80). The discrepancy could be linked to two main factors:

- the scarcer level of detail in the top-down analysis.

The statical model is based on disaggregated data from the block scale and the assumption made in modelling the data for the Platform itself. Values calculated from the equation result from assumptions which could not fully represent the housing characteristics;

- the different characterisation of house components and consumptions.

The engineering model has been adapted to local features of the housing stock (from previous studies), while the Toronto Platform data used in the statical approach are performed from 2015 IECC. The IECC 2015 considers electric resistance for the HVAC system, which probably increased the values of electricity consumption during the year.

The average EUI from the software is slightly higher than the average for the block in the Platform. Despite a maximum EUI equal to 342.64 kWh/m<sup>2</sup>/y, the median is 183.75 kWh/m<sup>2</sup>/y, meaning that

most values are lower or equal to the average. Despite differences in electricity and natural gas components, the overall energy intensity (kWh/m<sup>2</sup>/y) is similar in both models, with average error equal to 12% for the 73 detached dwellings.

Table 80. Overall values of energy consumption from URBANopt simulation, the realised statical model and the Toronto 2030 Platform.

	Mean	Minimum	Maximum	Median
Electricity (kWh/m <sup>2</sup> /y) with URBANopt	26.19	22.72	44.18	25.69
Natural gas (kWh/m <sup>2</sup> /y) with URBANopt	92.58	69.31	157.45	92.18
Total energy consumption (kWh/m <sup>2</sup> /y)	136.20	92.82	203.29	132.23
Electricity (kWh/m <sup>2</sup> /y) by statistical model	76.82	68.48	89.71	75.97
Natural gas (kWh/m <sup>2</sup> /y) by statistical model	59.38	24.34	113.58	56.58
Total energy consumption (kWh/m <sup>2</sup> /y)	118.77	92.03	201.63	117.82
EUI (kWh/m <sup>2</sup> /y) with URBANopt	183.75	154.05	342.64	180.67
EUI (kWh/m <sup>2</sup> /y) by Toronto 2030 Platform	180	170	190	-

## 6.4.2 Semidetached block

The considered semidetached block is composed by 14 buildings in Cabbagetown. The use of the same characterisation of detached dwellings implies similar consumption values (Figure 66), composed by 25.43% electricity and 74.57% natural gas. The trends for both electricity and natural gas reflects the ones of detached houses, with peaks in the winter season. Electricity consumption keeps more stable values along the year, covered by both lights and various equipment. Semi-detached dwellings have an average energy intensity 125.03 kWh/m<sup>2</sup>/y, with a predominant component in natural gas. The comparison with values calculated from the statistical model underlines a discrepancy in the proportion of natural gas and electricity (Table 81), while the overall consumption has an average error of 13.29%. A close 15% is also the difference between the EUI calculated in URBANopt and the intensity displayed in the platform. As in the case of detached houses, reasons derive mainly to the types of assumptions considered in modelling and to the simplification level of calculations.

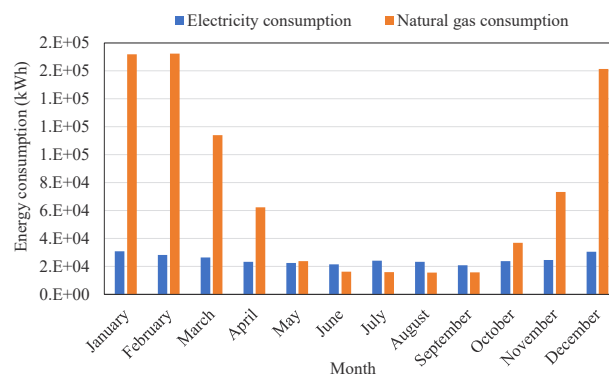


Figure 66. Consumption trend distinguished by natural gas and electricity for the semi-detached block.

Table 81. Overall values of energy consumption from URBANopt simulation, the realised statical model and the Toronto 2030 Platform.

	Mean	Minimum	Maximum	Median
Electricity (kWh/m <sup>2</sup> /y) with URBANopt	31.75	25.06	41.04	32.00

Natural gas (kWh/m <sup>2</sup> /y) with URBANopt	93.28	69.29	122.70	96.13
Total energy consumption (kWh/m <sup>2</sup> /y)	125.03	94.36	163.74	128.43
Electricity (kWh/m <sup>2</sup> /y) by statistical model	73.77	69.43	77.20	74.41
Natural gas (kWh/m <sup>2</sup> /y) by statistical model	46.35	25.51	60.46	48.81
Total energy consumption (kWh/m <sup>2</sup> /y)	120.12	94.94	137.66	123.08
EUI (kWh/m <sup>2</sup> /y) with URBANopt	201.67	154.48	262.99	205.55
EUI (kWh/m <sup>2</sup> /y) by Toronto 2030 Platform	170	160	180	-

### 6.4.3 Low rise apartment block

The low-rise apartment block is composed by 16 buildings, with an average of 3 floors. Different assumptions for low rise apartments characterise a similar trend for natural gas, but higher peaks for electricity consumption between June and August (Figure 67). Space cooling needs are relevant compared to the ones for detached and semi-detached in summer months.

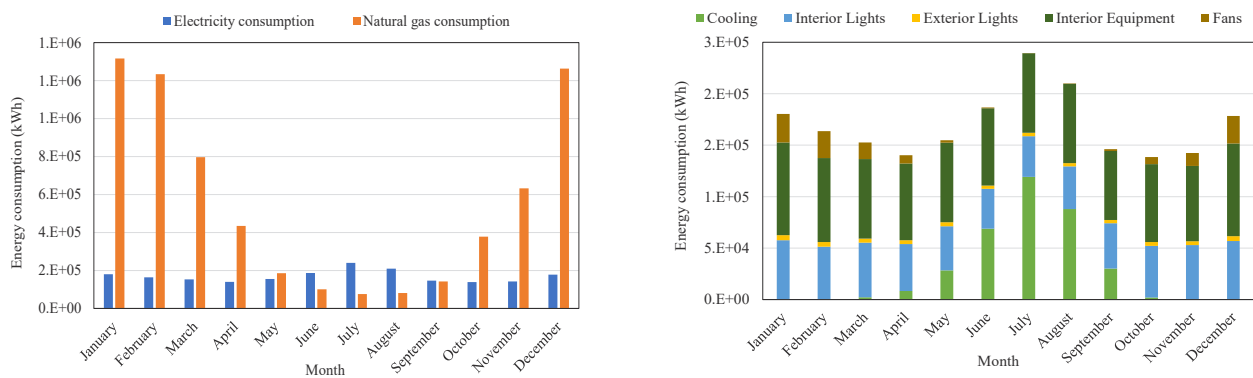


Figure 67. Consumption trend distinguished by natural gas and electricity (left) and energy use components of electricity consumption (right) for the low-rise apartment block.

Table 82. Overall values of energy consumption from URBANopt simulation, the realised statical model and the Toronto 2030 Platform.

	Mean	Minimum	Maximum	Median
Electricity (kWh/m <sup>2</sup> /y) with URBANopt	36.12	30.31	51.55	34.98
Natural gas (kWh/m <sup>2</sup> /y) with URBANopt	123.10	86.92	194.92	114.95
Total energy consumption (kWh/m <sup>2</sup> /y)	159.23	117.22	246.48	148.49
Electricity (kWh/m <sup>2</sup> /y) by statistical model	66.85	59.19	76.69	67.10
Natural gas (kWh/m <sup>2</sup> /y) by statistical model, with equation	103.05	59.70	133.74	104.42
Total energy consumption (kWh/m <sup>2</sup> /y)	169.90	136.39	192.93	171.52
Natural gas (kWh/m <sup>2</sup> /y) by statistical model, assuming 184.54 kWh/m <sup>2</sup> /y	184.54			
Total energy consumption (kWh/m <sup>2</sup> /y)	251.39	243.73	261.23	251.64
EUI (kWh/m <sup>2</sup> /y) with URBANopt	247.84	190.2	374.57	231.74
EUI (kWh/m <sup>2</sup> /y) by Toronto 2030 Platform	295	280	310	-

Maximum demand for cooling is in July (119,220.71 kWh/y for the block) (Figure 67), while the trend for space heating is similar. A gas furnace heating system is assumed as for detached but room air conditioning represents the main difference.

The comparison with calculated values from the statistical model highlights differences. The overall consumption and single components are all lower in the URBANopt simulations for electricity, but higher for natural gas consumption by equation. The overall consumptions are therefore similar between the engineering simulations and the top-down model. The average EUI of the Toronto Platform is about 16% higher than the simulated in the software: this could be due to the different assumptions introduced in modelling and the different calibration of results adopted in the Platform. Another influencing factor could be the considered occupancy, downscaled from neighbourhood values: assumptions could overestimate or underestimate the actual number of users in each dwelling.

#### 6.4.4 High rise apartment block

The high-rise block in St. James Town is composed by 11 high-rise buildings and an average of 12 floors. It represents the most populated among the analysed areas, with 1,787 estimated inhabitants. The applied input values for enclosure and energy systems are the same of low-rise apartments. The structure dimensions and population contribute to be the most energy consuming block, with monthly peaks of more than 2 GWh for natural gas in January, February, and December (Figure 68). As for other types, heating reveals a prevalence in natural gas consumption during winter, which covers more than 85% in January, February, and December. Towards summer period, it leaves space to water and interior equipment while heating is a minor share. Electricity overcomes natural gas between May and September when demand for space cooling is higher (Figure 68). The most variable electricity component is cooling, with an increasing trend toward July, similarly to the one for low-rises.

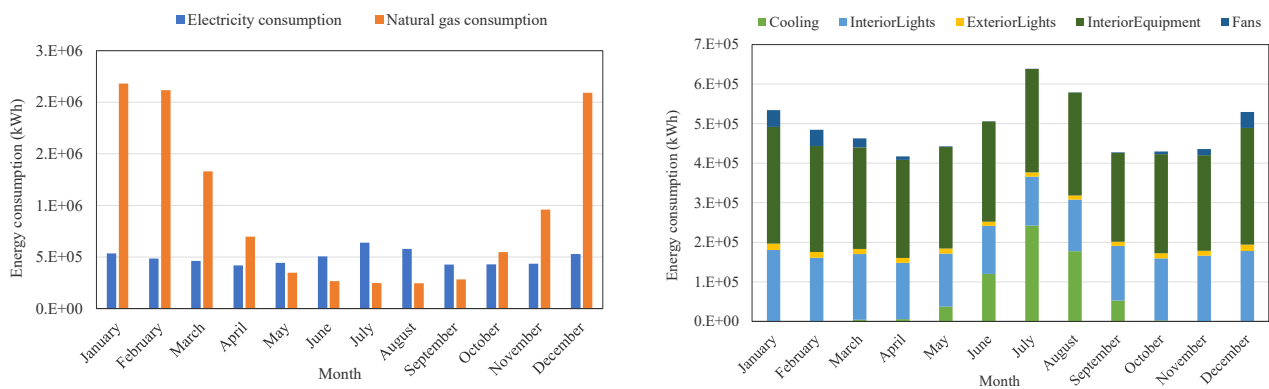


Figure 68. Consumption trend distinguished by natural gas and electricity (left) and energy use components of electricity consumption (right) for the high-rise apartment block.

The comparison with the statistical model underlines discrepancies with simulations in URBANopt, which are generally lower (Table 83). Lower estimations can be mainly related to the integration of ASHRAE framework for DOE pre-1980 with other studies made on Toronto. Electricity and the overall consumption are on average 36% lower than the calculated consumption from the statistical model. The electricity intensity is lower than consumption values for detached and semidetached, but the overall consumption per single building will be significantly higher due to dimensions and number of occupants. Based on the statistical model, the natural gas value is assumed with an average of 134.23 kWh/m<sup>2</sup>/y for a mean S/V ratio of 0.34 m<sup>2</sup>/m<sup>3</sup>. Natural gas EUI is slightly lower than for low-rise, confirming that lower building compactness factors contribute to decrease space heating consumption.

Table 83. Overall values of energy consumption from URBANopt simulation, the realised statical model and the Toronto 2030 Platform.

	Mean	Minimum	Maximum	Median
Electricity (kWh/m <sup>2</sup> /y) with URBANopt	36.34	26.29	50.28	36.66
Natural gas (kWh/m <sup>2</sup> /y) with URBANopt	87.44	43.29	176.46	76.24
Total energy consumption (kWh/m <sup>2</sup> /y)	123.78	71.05	218.82	113.16
Electricity (kWh/m <sup>2</sup> /y) by statistical model	57.43	41.61	80.33	54.74
Natural gas (kWh/m <sup>2</sup> /y) by statistical model, assuming 134.23 kWh/m <sup>2</sup> /y	134.23			
Total energy consumption (kWh/m <sup>2</sup> /y)	191.66	175.84	214.56	188.97
EUI (kWh/m <sup>2</sup> /y) with URBANopt	209.87	131.78	327.74	199.57
EUI (kWh/m <sup>2</sup> /y) by Toronto 2030 Platform	310	290	330	-

### 6.4.5 Comparison

The comparison of values for the four residential blocks let emerge differences in the assessed consumptions. The recent IECC and DOE (pre 1980 and 1980-2004) frameworks in the Platform present greater variations between single-family and multifamily buildings for the four considered blocks. EUI in the URBANopt simulations are closer among dwelling types due to the input data for enclosures and energy systems, even if higher values are registered for low-rise. The furnace-based systems led to higher consumption of natural gas in the URBANopt modelling, mainly during winter months. Electricity registers peak in the summer period, especially for low-rise and high-rise due to the presence of space cooling for each apartment.

A recurrent aspect is that electricity has lower consumption in the engineering model compared to results from the statistical approach for all the four archetypes. On the other hand, natural gas has higher values for detached, semi-detached and low-rise with URBANopt, but lower consumption for the high-rise apartments.

The overall energy use intensities (EUI, kWh/m<sup>2</sup>) calculated with URBANopt show an increasing trend from detached toward low-rise, which reach 247.8 kWh/m<sup>2</sup> (Figure 69). The EUI for high-rise is 16% lower (209 kWh/m<sup>2</sup>) than low-rise buildings. Selecting the same four residential blocks from the Platform, the average EUI is greatly higher for high-rise and low-rise, respectively 310 and 295 kWh/m<sup>2</sup>. Differences are related to the applied ASHRAE templates, especially for the simplification and calibration adopted in the online tool, and the occupancy rates introduced in the engineering model.

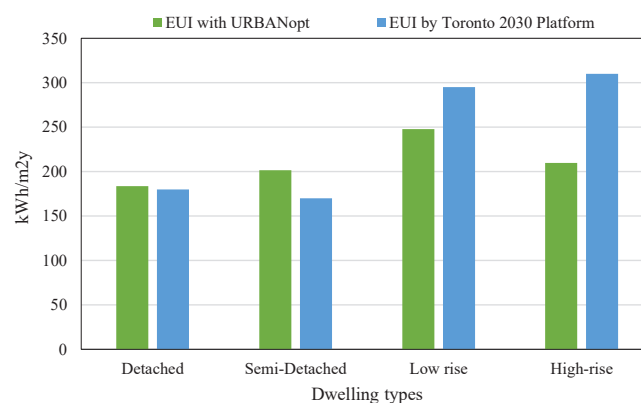


Figure 69. Comparison of EUI (kWh/m<sup>2</sup>/y) assessed with URBANopt and the Toronto 2030 Platform.

The shares of electricity and natural gas on the total consumption by URBANopt are coherent with estimations by the Net-Zero Existing Building Strategy [157] (see Figure 21), except for low-rise apartments. The strategy evaluates 64% consumption covered by natural gas and 36% by electricity for MURBs and 77%-23% for single family homes. Detached and semi-detached have 77.85%-22.15% and 74.57%-25.43% respectively, while high-rise 65.78%-34-22% with URBANopt simulations. Low-rise apartments are characterised by 73.44% natural gas and 26.55% electricity, which is closer to the semi-detached typology. The structure of low-rise buildings can be more like row houses or multiple attached houses. However, main differences are in the enclosure types, the energy systems and internal subdivision in residential units.

## 6.5 Solar optimisation: single building vs. aggregated evaluation

Based on the evaluations of the baseline consumption, the assessment of rooftop solar resources is performed for each residential block. The solar production is modelled with Radiance, an accurate software to assess solar potential which considers specular and diffuse reflections from urban obstacles [177]. REopt builds a decision-making model to select the cost-optimal DER design and hourly annual supply of solar photovoltaic, storage, and diesel generation [95]. Buildings (single or group) integrated with this model allows to assess cost-optimal DER solutions. This work considers only PV installations and eventual backup systems to connect. A summary of values for efficiency and installation costs is reported in Table 84 for each PV technology. Table 85 shows data for each REopt optimisation, distinguishing technical and financial aspects.

Table 84. Main values for each PV technology assumed in the REopt optimisations.

Variable	Monocrystalline	Polycrystalline	Thin film
PV module type	Premium (1)	Standard (2)	Thin film (3)
Efficiency ( $\eta$ )	0.24	0.18	0.11
Installation PV costs (US\$/kW)	2,500	2,410	2,440

Table 85. PV installation and financial variables considered in the REopt optimisations.

Variable	Unit	Value	Source (s)
Location	-	Roof	URBANopt
PV array type	-	Rooftop, fixed	URBANopt
Annual PV operation and maintenance costs	US\$/kW/y	20 US\$/kW/y	Jordan et al. (2016)
State rebates based on installed capacity	US\$/kW	1,000 US\$/kW	Government of Canada (2022)
Maximum state rebate	US\$/kW	5,000 US\$/kW	Government of Canada (2022)
Annual rate of degradation in PV energy production	%	0.05	SolarTO (2022); Jordan et al. (2016)
Azimuth angle (optimal)	°	178	PVGIS (2022)
PV system tilt (optimal)	°	35°	PVGIS (2022)

PV system performance losses	%	14%	Gagnon et al. (2016)
PV DC-AC ratio	-	1.2	Kouhestani et al. (2019); Gagnon et al. (2016)
PV inverter efficiency	%	96%	Gagnon et al. (2016)
PV ground cover ratio (max)	%	40% for gable roofs, 70% for flat roofs.	Kouhestani et al. (2019); Gagnon et al. (2016)

In the following sections, the comparison for the three technologies is run with scenario and feature optimisations for each of the four residential blocks. The potential PV installations for monocrystalline, polycrystalline, and thin film are initially considered without storage and without net metering. This helps to understand which is the preferable solution and if considered as stand-alone structures (feature optimisation) or aggregation (scenario optimisation). Each optimisation is financially optimal for the selected technology. The combination of different possible cases is evaluated later in the cost-optimal analysis in Paragraph 6.6.

### 6.5.1 Detached block

The baseline scenario is the starting point to perform solar evaluations. Detached houses have generally a more limited available roof surface but the overall electricity consumption is lower than high-rise structures. The total roof area is 11,965.6 m<sup>2</sup> and the maximum assumed 40% fraction is 4,786.24 m<sup>2</sup>, which is not reached by any simulation. Photovoltaic costs can be divided among few inhabitants (generally, one household) per dwelling, leading to possible constraints in the investment. The three solar technologies without storage would reach about 23% self-sufficiency annually, with peaks close to 35% in June. The required area for thin film (Table 88) is 48% more than the surface for monocrystalline due to the lower efficiency per unit. The financially optimal sizing highlights higher annual electricity production for polycrystalline (Table 87), while monocrystalline has the highest output per m<sup>2</sup> (Table 86). The performance for multicrystalline also allows the best reduction in energy bills, about 28% compared to the business-as-usual condition.

Table 86. Results for financially optimal installation of monocrystalline for the selected detached block. Scenario (left) and feature (right) level optimisations are shown.

Monocrystalline	Scenario optimisation	Feature optimisation
PV area installed (m <sup>2</sup> )	911	911.04
PV size (kW)	173.09	173.1
Average annual PV electricity production (kWh/y)	220,057	220,068
Average annual PV electricity production (kWh/m <sup>2</sup> y)	241.56	241.56
Self-sufficiency (%)	23.08	23.04
Max % covered in June	34.09	33.98
LCC – life cycle costs (\$)	1,215,192	1,588,183
Optimal net present value (\$)	136,256	135,487

Energy bills, year 1 (\$)	77,717.1	107,124.76
Business as usual energy bills (\$)	106,555.95	135,904.28

Table 87. Results for financially optimal installation of polycrystalline for the selected detached block. Scenario (left) and feature (right) level optimisations are shown.

Polycrystalline	Scenario optimisation	Feature optimisation
PV area installed (m <sup>2</sup> )	1,218.98	1,221.18
PV size (kW)	182.85	183.18
Average annual PV electricity production (kWh/y)	229,815	230,229
Average annual PV electricity production (kWh/m <sup>2</sup> y)	188.53	
Self-sufficiency (%)	23.86	23.84
Max % covered in June	34.87	34.79
LCC – life cycle costs (\$)	1,203,606	1,576,629
Optimal net present value (\$)	147,842	147,041
Energy bills, year 1 (\$)	76,769.47	106,147.8
Business as usual energy bills (\$)	106,555.95	135,904.3

Table 88. Results for financially optimal installation of thin film for the selected detached block. Scenario (left) and feature (right) level optimisations are shown.

Thin film	Scenario optimisation	Feature optimisation
PV area installed (m <sup>2</sup> )	1,753.01	1,755.29
PV size (kW)	175.3	175.53
Average annual PV electricity production (kWh/y)	224,671	224,965
Average annual PV electricity production (kWh/m <sup>2</sup> y)	128.16	
Self-sufficiency (%)	23.16	23.13
Max % covered in June	34.44	34.37
LCC – life cycle costs (\$)	1,208,648	1,581,642
Optimal net present value (\$)	142,800	142,028
Energy bills, year 1 (\$)	77,599.96	106,985.9
Business as usual energy bills (\$)	106,555.95	135,904.3

For all the three technologies, the aggregated optimisation (scenario) is more effective than the single-building evaluation (feature). This is not mainly related to energy-aspects which are slightly more performative, but rather to financial results. Lifecycle costs are 23% lower for scenario optimisation and energy bills reduced around 27% compared to the feature evaluation. The energy bills are around 27% lower compared to the business-as-usual (BAU) scenario, while 21% with feature optimisation. Polycrystalline PV shows the most satisfying production-costs relation: LCC are lower than the other options and annual electricity production is higher than monocrystalline and thin film. The self-suffi-

ciency is slightly better (23.86%), with a peak of 34.87% in June (Table 87).

Considering polycrystalline, two other orientations have been tested with the optimal one by PVGIS (South  $-2^\circ$ ): South-West with the azimuth of  $+60^\circ$  and South-East with the azimuth of  $-60^\circ$ , which can be installed on gable roofs. Figure 70 shows the PV production of the three orientations in the 12 typical days. The typical days are the hourly average production or consumption calculated for each month.

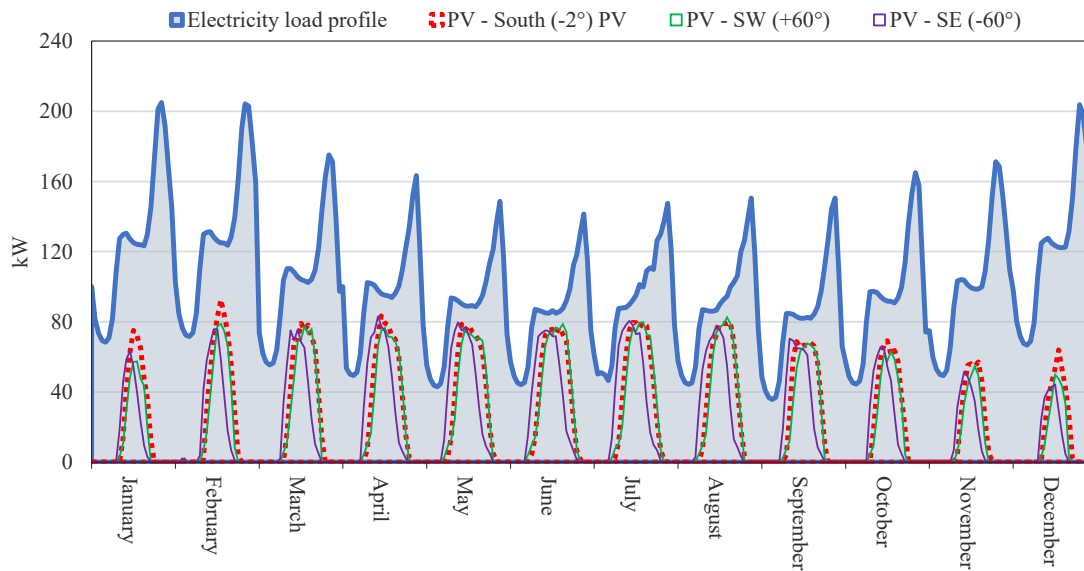


Figure 70. Hourly profiles of the load and PV production (with 3 orientations) for 12 typical days representative of each month for 2017, simulated on the detached block.

The South-East option (SE,  $-60^\circ$ ) shows a higher output in the early morning, between 4 a.m. and 8 a.m., compared to the other orientations, but it decreases rapidly after midday. SE installation can catch the sunlight from the first hours of the day along all the year. South and SW orientations have similar hourly profiles. South allows to have peak production in winter around 1 p.m., whereas SW production is slightly later. No one of the tested orientations can satisfy the peak load in the late afternoon. The more effective for winter months appears the South exposure. The sum of the production by the 12 typical days shows highest output for the South ( $-2^\circ$ ) option equal to 6,895.12 kW for the whole block. South-installed panels will be the simulated orientation for the following steps.

### 6.5.2 Semidetached block

From the baseline scenario, the simulations are launched to assess the three different PV technologies on rooftops for semi-detached houses. The rooftop area of the block is equal to 3,378.55 m<sup>2</sup>: applying the 40% usable surface for gable roofs, the maximum installable area is 1,351.42 m<sup>2</sup>, with an average of 96.53 m<sup>2</sup> for each building.

The comparison of the three technologies have limited differences for the PV production in aggregated (scenario) and single-building (feature) optimisations. Rather than the energy output, the aggregated evaluation shows a financial opportunity, as for the detached block. The main economic indicators perform better than the feature-level case. Indeed, LCCs are around 14% less in the scenario optimisation and the payable energy bills 16.6-16.8% less for all three technologies. The PV electricity

production with an aggregated evaluation allows to reduce annual bills of 27%, which can be a great benefit for occupants and families. The locally generated electricity decreases purchased energy costs for a 25-year lifetime, even if a 0.5% degradation per year is considered in the inputs. However, both for detached and semidetached, the NPV which represents revenues over the 25-year lifetime vary only 0.4-0.5% compared to the single-building evaluations.

Table 89. Results for financially optimal installation of monocrystalline for the selected semi-detached block. Scenario (left) and feature (right) level optimisations are shown.

Monocrystalline	Scenario optimisation	Feature optimisation
PV area installed (m <sup>2</sup> )	310.7	310.74
PV size (kW)	59.03	59.04
Average annual PV electricity production (kWh/y)	74,969	74,967
Average annual PV electricity production (kWh/m <sup>2</sup> y)	241.29	241.25
Self-sufficiency (%)	23.17	23.15
Max % covered in June	32.43	32.39
LCC – life cycle costs (\$)	416,732	484,136
Optimal net present value (\$)	47,712	47,515
Energy bills, year 1 (\$)	26,686.03	31,999.53
Business as usual energy bills (\$)	36,619.42	41,918.43

Table 90. Results for financially optimal installation of polycrystalline for the selected semi-detached block. Scenario (left) and feature (right) level optimisations are shown.

Polycrystalline	Scenario optimisation	Feature optimisation
PV area installed (m <sup>2</sup> )	413.57	413.31
PV size (kW)	62.04	62
Average annual PV electricity production (kWh/y)	77,964	77,898
Average annual PV electricity production (kWh/m <sup>2</sup> y)	188.51	188.47
Self-sufficiency (%)	23.88	23.84
Max % covered in June	33.12	33.06
LCC – life cycle costs (\$)	412,746	480,160
Optimal net present value (\$)	51,698	51,491
Energy bills, year 1 (\$)	26,392.16	31,711.48
Business as usual energy bills (\$)	36,211.8	41,918.43

Table 91. Results for financially optimal installation of thin film for the selected semi-detached block. Scenario (left) and feature (right) level optimisations are shown.

Thin film	Scenario optimisation	Feature optimisation
PV area installed (m <sup>2</sup> )	598.62	596.33
PV size (kW)	58.86	59.63

Average annual PV electricity production (kWh/y)	76,555	76,252
Average annual PV electricity production (kWh/m <sup>2</sup> /y)	127.89	127.87
Self-sufficiency (%)	23.26	23.18
Max % covered in June	32.72	32.61
LCC – life cycle costs (\$)	414,591	481,988
Optimal net present value (\$)	49,853	49,663
Energy bills, year 1 (\$)	26,645.63	31,982.63
Business as usual energy bills (\$)	36,619.42	41,918.43

The difference between monocrystalline, polycrystalline, and thin film emerges from the annual production per unit (m<sup>2</sup>). The polycrystalline output (188.51 kWh/m<sup>2</sup>/y) is 21.87% less than mono-Si and 47% less (127.88 kWh/m<sup>2</sup>/y). As expected, the peak production in all months is registered for mono-silicon technology, which can be performative also at lower temperatures (Figure 71). The difference in the monthly output goes from 20% in winter up to 23.7% in summer for multicrystalline and from 48.76% in winter to 47.18% in summer for thin film. Thin film reduces less its production than polycrystalline in winter months.

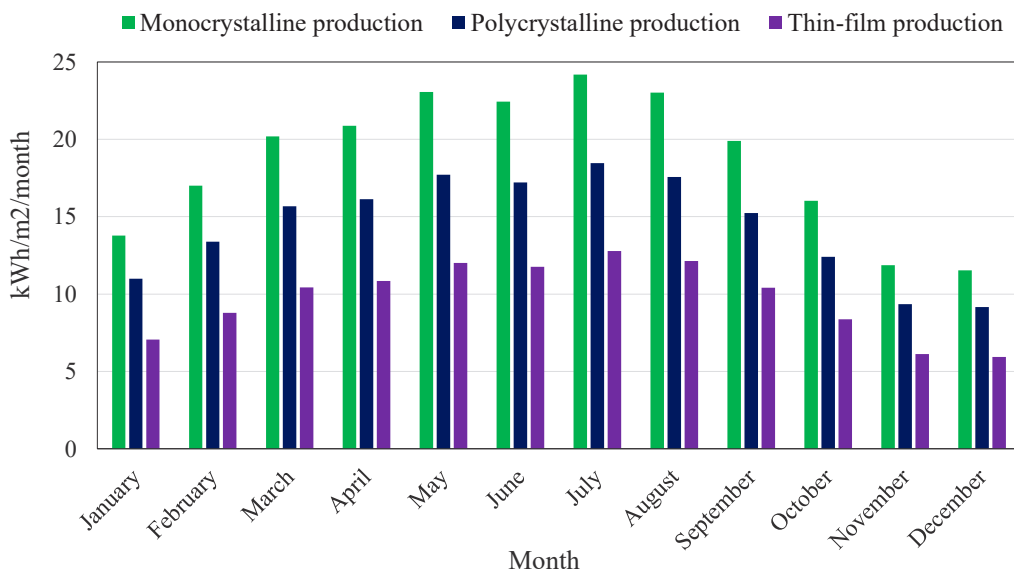


Figure 71. Comparison of monthly electricity production by m<sup>2</sup> of monocrystalline, polycrystalline, and thin film from scenario optimisations for the semi-detached block.

Polycrystalline shows the best relation between energy production, costs and revenues based on the financial optimisation of REopt. Polycrystalline can reach the highest annual electricity production and self-sufficiency in a financially optimal scenario, while having lower LCC, NPV and energy bills.

### 6.5.3 Low rise apartment block

Apartment buildings can have a larger available roof surface, even if it consists mainly of flat areas rather than with an appropriate slope. The maximum input threshold is 70% of the total roof surface,

which is equal to 11,188.36 m<sup>2</sup> and not completely covered in neither simulation. The optimal PV configuration would be with a scenario optimisation for the three technologies. In all three cases, the level of self-sufficiency (SC/C) reaches about 18%, with slightly higher values for grouped-based assessment. Therefore, low-rise may have further possibilities to increase PV installations and obtain lower LCCs and higher SC/C. Financial aspects are more performative with aggregated evaluations rather than at the single-building level, despite minor benefits. Differently from low-density blocks, LCCs are only 2.5% less than optimisation by single low-rise building and energy bills 3% lower.

Table 92. Results for financially optimal installation of monocrystalline for the selected low-rise apartment block. Scenario (left) and feature (right) level optimisations are shown.

Monocrystalline	Scenario optimisation	Feature optimisation
PV area installed (m <sup>2</sup> )	1,553.09	1,541.6
PV size (kW)	295.09	292.91
Average annual PV electricity production (kWh/y)	374,753	371,346
Average annual PV electricity production (kWh/m <sup>2</sup> y)	241.30	240.88
Self-sufficiency (%)	18.23	18.07
Max % covered in June	25.47	25.27
LCC – life cycle costs (\$)	3,159,790	3,239,067.0
Optimal net present value (\$)	58,906	57,174.0
Energy bills, year 1 (\$)	200,605.06	207,214.71
Business as usual energy bills (\$)	253,780.51	259,894.73

Table 93. Results for financially optimal installation of polycrystalline for the selected low-rise apartment block. Scenario (left) and feature (right) level optimisations are shown.

Polycrystalline	Scenario optimisation	Feature optimisation
PV area installed (m <sup>2</sup> )	2,057.86	2,047.98
PV size (kW)	308.68	307.2
Average annual PV electricity production (kWh/y)	387,935	385,436
Average annual PV electricity production (kWh/m <sup>2</sup> y)	188.51	188.20
Self-sufficiency (%)	18.81	18.69
Max % covered in June	26.16	26.03
LCC – life cycle costs (\$)	3,146,069	3,225,394.0
Optimal net present value (\$)	72,627	70,847.0
Energy bills, year 1 (\$)	198,952.52	205,442.72
Business as usual energy bills (\$)	253,780.51	259,894.73

The aggregated evaluation allows also to reduce energy bills about 21% for the entire block compared to the current situation. Polycrystalline have slightly better overall values compared to monocrystalline: this could be related to the higher number of occupants and the wider available roof space.

Table 94. Results for financially optimal installation of thin film for the selected low-rise apartment block. Scenario (left) and feature (right) level optimisations are shown.

Thin film	Scenario optimisation	Feature optimisation
PV area installed (m <sup>2</sup> )	3,080.48	3,039.26
PV size (kW)	308.05	303.93
Average annual PV electricity production (kWh/y)	393,947	387,965
Average annual PV electricity production (kWh/m <sup>2</sup> y)	127.88	127.65
Self-sufficiency (%)	19.04	18.78
Max % covered in June	26.79	26.45
LCC – life cycle costs (\$)	3,141,402	3,220,925.0
Optimal net present value (\$)	77,294	75,316.0
Energy bills, year 1 (\$)	198,131.2	205,064.69
Business as usual energy bills (\$)	253,780.5	259,894.73

Figure 72 shows the monthly production by the three PV technologies. Thin film shows a peak production in warmer months, between May and September. Polycrystalline have a more constant trend, with higher output in winter months compared to the other two technologies, which could be an advantage for cold climates. Indeed, thin film reaches 26.79% of covered electricity consumption in May, while multicrystalline 17.26% in February. The lower production by monocrystalline is probably due to the more limited area optimised by the software, even if it is very close to thin-film and polycrystalline production, especially in winter months.

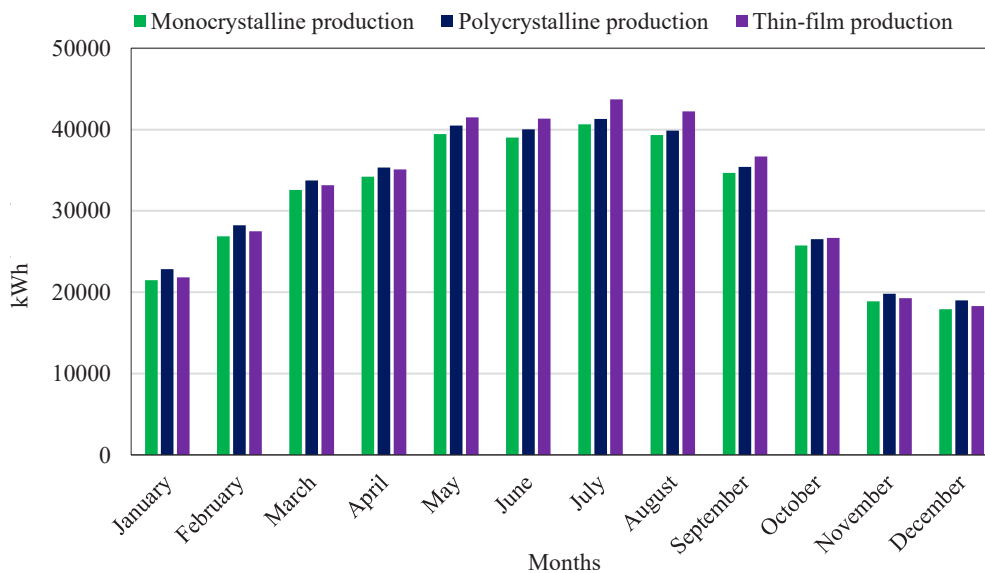


Figure 72. Monthly electricity production by three PV technologies for the low-rise apartment block, with scenario-level optimisation.

A comparison of the electricity daily load profile for the low-rise block can underline some differences between polycrystalline and thin film technologies. Two representative days of summer and winter season are chosen: 21<sup>st</sup> June and 21<sup>st</sup> December.

Thin film can satisfy almost all the electricity demand in June at 11 a.m. (208.71 kW), but it cannot satisfy the peak load in late evening. Despite the longer daylight, the output is reduced in late afternoon. Polycrystalline shows a slightly lower production for June having a similar path of thin film. For December, polycrystalline contributes to satisfy the demand in the late morning (12 a.m. to 2 p.m.) only for less than ¼ of the hourly consumption (Figure 73): unfavourable daylight and weather conditions do not help to meet a higher share.

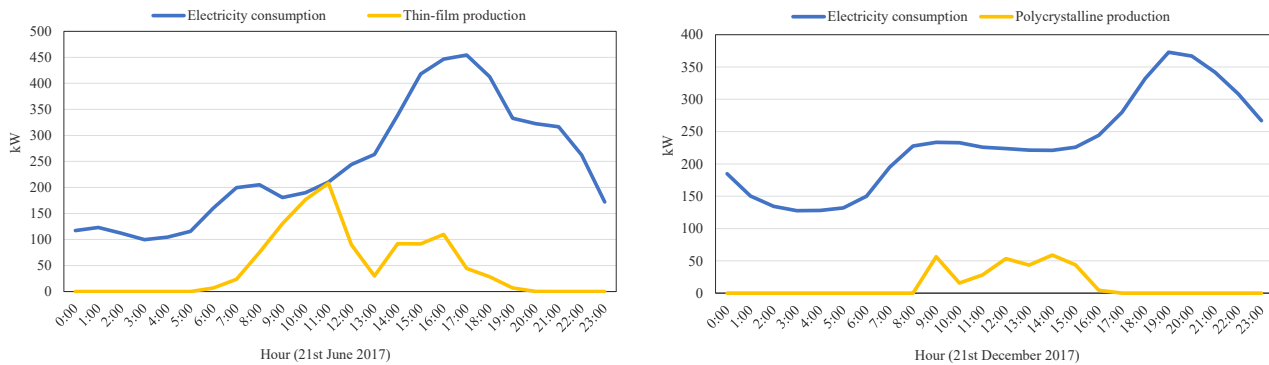


Figure 73. Load profile of thin film production and electricity consumption on June 21, 2017 (left) and polycrystalline production and electricity consumption on December 21, 2017 (right).

The installation of storage would be necessary to support the peak load in afternoon-evening. Batteries can help to shift the pressures to the main grid in peak hours thanks to the release of energy produced in the morning. Benefits could be for both the users and the power network. On the other hand, a scenario with net-metering allows to install more PV power without wasting locally produced energy because overproduction can be sold to the grid.

### 6.5.4 High rise apartment block

For the block of high-rise buildings, the maximum installable surface is 7,307.36 m<sup>2</sup>, with an average of 664.31 m<sup>2</sup> for each high-rise building. The solar output should address the electricity demand during summer months, when the consumption increases due to space cooling for each apartment. The scenario optimisations prevail for the energy side of each technology because panel size and area are higher than the single-building evaluation. The level of self-sufficiency is lower (around 18%) than previous blocks due to the higher consumption per building and eventual minor shading among buildings. The optimal net present value (NPV), the life cycle costs (LCC), and reduction of energy bills are also more convenient for the aggregated evaluations. The aggregated scenario allows about 21% reduction of energy bills, whereas the single-feature level is 17 % less compared to the BAU condition. LCC have only 0.8% lower than single-building optimisation and 13-15% NPV more, with higher revenues for polycrystalline.

Table 95. Results for financially optimal installation of monocrystalline for the selected high-rise apartment block. Scenario (left) and feature (right) level optimisations are shown.

Monocrystalline	Scenario optimisation	Feature optimisation
PV area installed (m <sup>2</sup> )	4,435.48	3,637.44
PV size (kW)	842.74	691.11

Average annual PV electricity production (kWh/y)	1,068,377	877,058
Average annual PV electricity production (kWh/m <sup>2</sup> y)	240.87	241.12
Self-sufficiency (%)	18.05	14.86
Max % covered in June	25.67	21.07
LCC – life cycle costs (\$)	8,951,903	9,023,100
Optimal net present value (\$)	165,183	145,683
Energy bills, year 1 (\$)	567,220.06	597,770.68
Business as usual energy bills (\$)	718,843.39	722,919.55

Table 96. Results for financially optimal installation of polycrystalline for the selected high-rise apartment block. Scenario (left) and feature (right) level optimisations are shown.

Polycrystalline	Scenario optimisation	Feature optimisation
PV area installed (m <sup>2</sup> )	5,618.28	4,689.09
PV size (kW)	842.74	703.36
Average annual PV electricity production (kWh/y)	1,056,704	883,110
Average annual PV electricity production (kWh/m <sup>2</sup> y)	188.08	188.33
Self-sufficiency (%)	17.88	14.94
Max % covered in June	25.26	21.08
LCC – life cycle costs (\$)	8,914,847	8,993,100
Optimal net present value (\$)	202,239	175,683
Energy bills, year 1 (\$)	568,842.85	597,183.72
Business as usual energy bills (\$)	718,843.39	722,919.55

Table 97. Results for financially optimal installation of thin film for the selected high-rise apartment block. Scenario (left) and feature (right) level optimisations are shown.

Thin film	Scenario optimisation	Feature optimisation
PV area installed (m <sup>2</sup> )	8,427.41	6,993.1
PV size (kW)	842.74	699.31
Average annual PV electricity production (kWh/y)	1,076,467	893,872
Average annual PV electricity production (kWh/m <sup>2</sup> y)	127.73	127.82
Self-sufficiency (%)	18.16	15.11
Max % covered in June	25.98	21.58
LCC – life cycle costs (\$)	8,899,449	8,978,764
Optimal net present value (\$)	217,637	190,019.0
Energy bills, year 1 (\$)	566,113.91	595,441.03
Business as usual energy bills (\$)	718,843.39	722,919.55

Monocrystalline optimisation has a total higher production compared to polycrystalline and with only the 38.07% and 31.22% of roof area installed for scenario and feature evaluation respectively. However, thin film is the PV technology which can cover slightly higher electricity consumption at lower costs. The lower efficiency by thin film implies a 34% more of installed area on rooftops than monocrystalline and a 2% more of installed panel surface than the 70% threshold. The slightly higher solar output for thin film can be registered between May and September, when the technology can perform better in the central hours of the day (Figure 74), while the lowest is for polycrystalline.

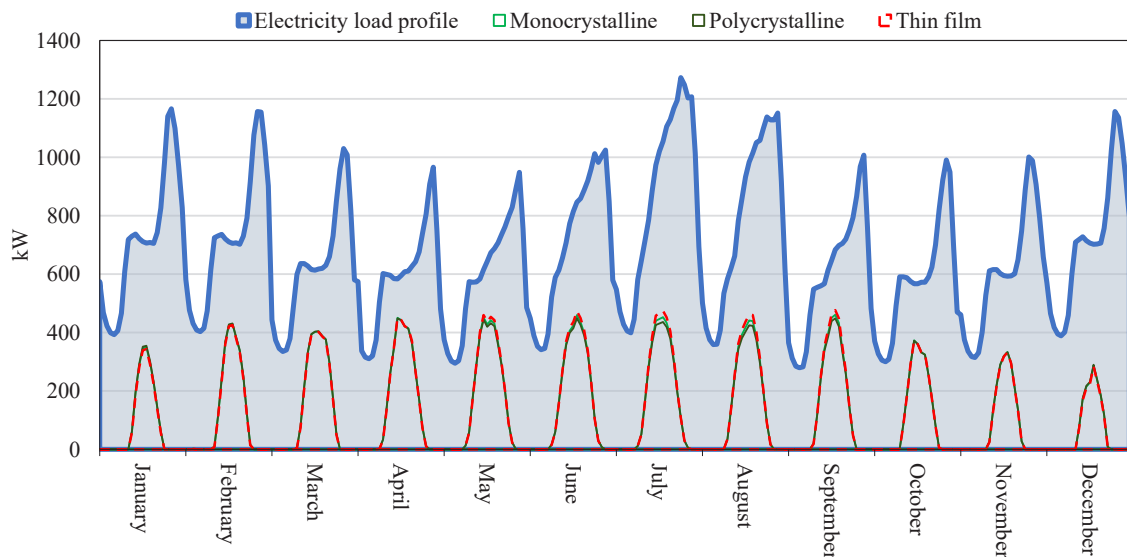


Figure 74. Hourly profiles of the load and PV production by the three orientations for 12 typical days representative of each month for 2017, simulated on the high-rise apartment block.

Figure 75 shows the maximum thin production for a representative day in July, which is the month with peak space cooling consumption. The difference is between 3 and 21 kW for the whole block from 9 a.m. to 5 p.m. For high-rise, the peak production in summer is particularly useful due to the assumption of space cooling demand for single apartments, which impact on the daily load. Monocrystalline registers a higher solar output in the late afternoon from 4 to 6 p.m.

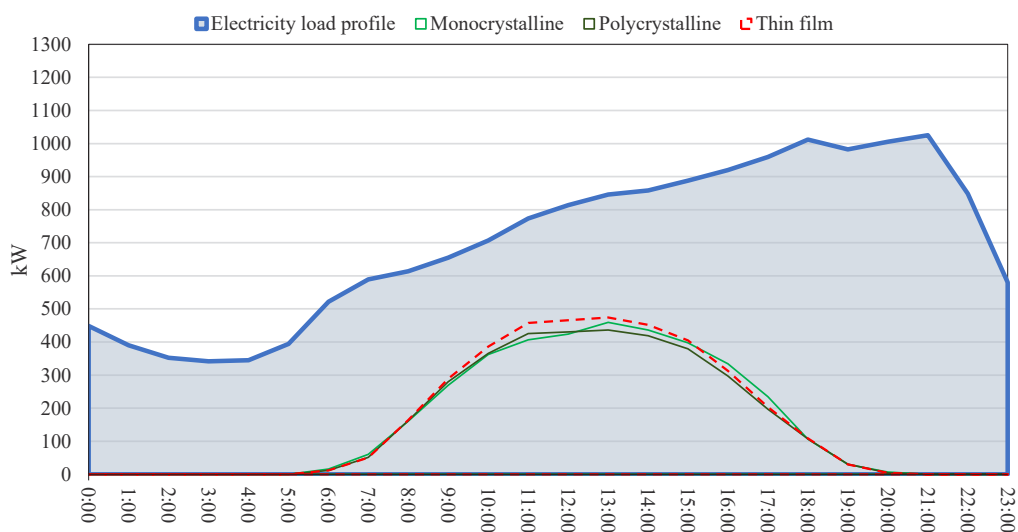


Figure 75. Hourly load profile for electricity consumption and the three PV technologies for a representative average day in July 2017, considering scenario optimisation for the high-rise apartment block.

### 6.5.5 Comparison

The electricity consumption has been the starting point to optimise PV installations. Financially optimal situations are with aggregated scenarios, towards a perspective of urban energy community rather than by single prosumer. Both energy performance and economic aspect are favourable compared to single-building evaluations. Installations for a group of buildings allow interchange of energy production, which impacts on bills reduction and higher covered electricity demand. Low-density blocks (detached and semi-detached) showed lower LCCs with community optimisations, from -14% to -23%. On the other hand, revenues with NPV are about 13% higher for high-rise block compared to analyses by single building. In all four residential blocks, energy bills would be reduced more than 20% than the current condition thank to the PV contribution.

Polycrystalline silicon shows performative results for the four blocks, in a financially optimal condition without net-metering. For detached and semi-detached blocks, it has highest production and lowest LCC in a 25-year lifetime. For low-rise and high-rise, polycrystalline production is close to the optimised thin film output, but with 33% less of installed area.

Considering polycrystalline silicon, the mean annual solar production by URBANopt is 177.53 kWh/m<sup>2</sup>/y. URBANopt production is calculated as an average among the monthly electricity output for the four residential blocks in Figure 76. The URBANopt average PV output is slightly lower than results from PVGIS (182.10 kWh/m<sup>2</sup>/y) and from the GIS-based methodology (190.75 kWh/m<sup>2</sup>/y). URBANopt has the smoother and more gradual curve: it assesses the highest production in months with scarcer radiations, while lower than the other two sources during summer. The GIS-based methodology shows the greatest variation between winter and summer, with 1.80 kWh/m<sup>2</sup> in December and 24.46 kWh/m<sup>2</sup> in July, and highest production between April and September. Differences can be related to the assumptions applied by the distinct approaches. The GIS elaboration relies on the DSM of Toronto with high accuracy, but average seasonal values are applied for diffuse ratio and transmissivity in the input data. Radiation values from PVGIS are considered for the Town Hall as a representative and conventional point. This reference point may not embody average values for the whole city.

URBANopt relies on Radiance to assess solar production, which considers local obstructions in a

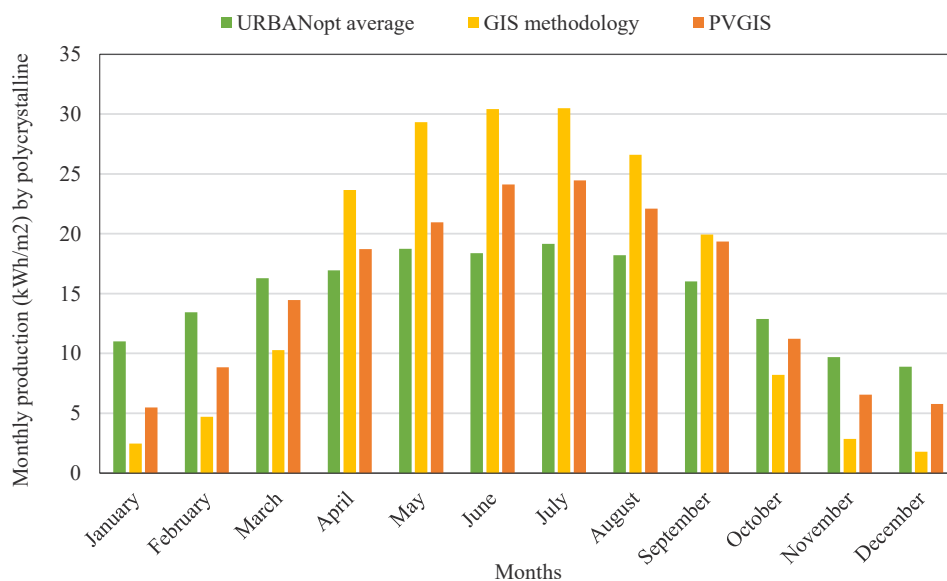


Figure 76. Comparison between monthly electricity production by polycrystalline calculated with URBANopt, PVGIS and GIS methodology for 2017.

high-detail model.

The usable rooftop area for PV installation varies for the two different approaches and by dwelling types. Figure 77 compares the assessed share of used areas for each dwelling types from URBANopt optimisations without net-metering and GIS evaluations selecting the four residential blocks. The GIS-base methodology calculates a usable surface for each rooftop, based on input constraints of slope, orientation, minimum radiation, and eventual obstacles. URBANopt optimises the PV size and area according to the energy performance of each technology, costs, and available roof surfaces: therefore, wider surfaces are required for thin film, while more limited area for polycrystalline to reach similar electricity production. The GIS-based methodology (ref. paragraph 5.6) registers values (10.03%) closer to the scenario optimisation for the detached block, mainly for polycrystalline (10.19%). GIS results identify a higher area for semidetached and low-rise buildings because it does not perform a financially optimal analysis. For high-rise, GIS-based values are 48% lower than the scenario optimisation for monocrystalline. The criteria adopted in GIS reduced the extension of suitable surface, especially considering only South and South-East exposures. One advantage is that the DSM help to identify natural and anthropic obstructions which can reduce the solar output. On the other hand, URBANopt using REopt optimises the PV surface based on technical and financial criteria to minimise LCC and it also exploits the other orientations if necessary.

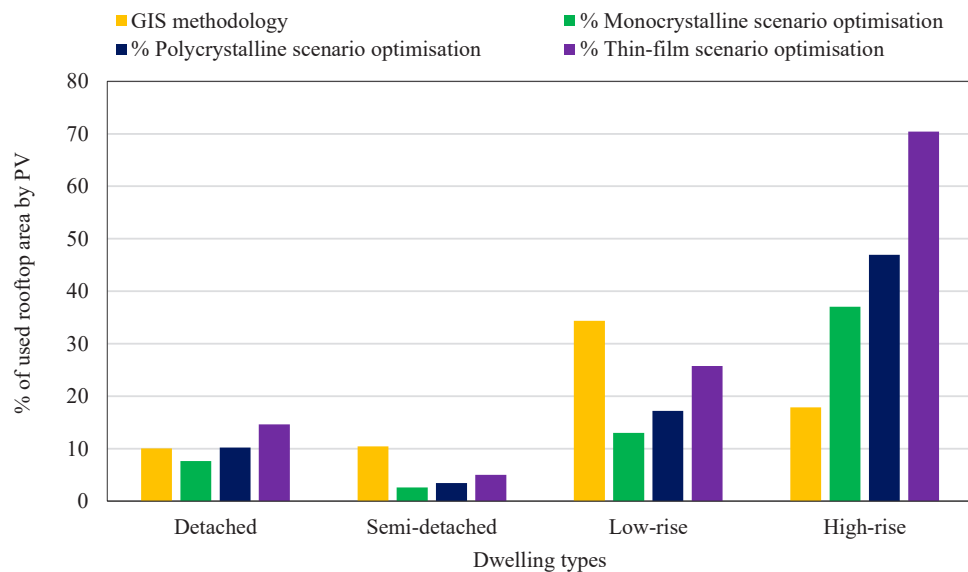


Figure 77. Comparison between suitable installable PV areas by URBANopt optimisations and GIS methodology.

For all the four blocks, the scenario optimisations perform better values and relations between self-sufficiency and LCCs for the 25-year range. The annual self-sufficiency values for financial optimisations range from 23% to 18% without storage nor net-metering option. Other aggregated scenarios are likely to increase this range, except for the most challenging high-rise block.

The advantages of grouped evaluations confirm the potential of community-scale projects rather than stand-alone interventions. Indeed, solar PV can be installed with different sizes and shares on the roofs of the considered buildings. Different energy profiles allow to exchange energy among structures, especially in case of overproduction.

## 6.6 Cost-optimal analysis towards resilience

The optimisation of PV rooftop installation without net metering returns a financially optimal condition to satisfy part of the electricity consumption along the year. The covered share and PV sizing for each technology vary based on the solar output, dwelling typology, available roof area and related financial parameters. The next step is to identify the cost-optimal solution for each residential block to increase local produced solar energy and improve the independence of dwellings from the main grid. The main aim of the cost-optimal analysis is to increase self-sufficiency of electricity along the year at the lower global costs.

### 6.6.1 Considered aspects and options

The cost-optimal analysis allows to identify the optimal PV-battery sizing and configuration, based on inputs, total costs and energy-related parameters. The energy parameters considered to reduce dependence from the main energy grid are:

- self-consumption (SC/P), which is the ratio between the consumed energy produced locally and the total energy produced locally;
- self-sufficiency (SC/C), which is the ratio between the energy locally produced and the total electricity consumption.

Paragraph 6.4.5 shows that for the four residential blocks an aggregated evaluation is the most suitable for energy production and especially for financial results. Therefore, evaluations in the cost-optimal analysis are considered for scenario-level optimisations for the four residential groups.

The cost-optimal analysis is performed on a 25-year period, which is the considered lifetime for PV panels. Total global costs (US\$) of installed technologies are included in the analysis:

- investment costs of PV panels, batteries and eventual generators;
- operation and maintenance costs after taxation for the installed technologies;
- replacement costs for batteries while PV are assumed to operate for 25 years;
- total energy costs, that include expenses of energy from the grid and eventual revenues;
- statal incentives from the Canada Greener Homes for the eligible residential types;
- microgrid upgrade costs.

The monocrystalline technology is the most performative due to higher efficiency while polycrystalline could reach good production levels at lower costs per kW. Previous evaluations (see paragraph 6.5) show the potential of polycrystalline for financially optimal condition and in community-based scale. Different possible options are evaluated for each block:

- only polycrystalline PV installation with and without net metering;
- polycrystalline PV installation and battery with and without net metering;
- polycrystalline PV installation, battery and generator with and without net metering optimised for a 24-hours outage in winter;
- polycrystalline PV installation, battery, and generator with and without net metering optimised for a 24-hours outage in summer.

The 24-hours outage is chosen because other tests have shown that variation of size are limited compared to longer blackouts.

## 6.6.2 Hourly profiles: single dwellings and aggregated blocks

A comparison between the hourly energy profile for each residential type is made. The hourly and annual energy profiles allow to identify when electricity consumption can be satisfied, from which self-consumption and self-sufficiency can be assessed.

The considered scenarios are sized for polycrystalline panels with net metering, but without storage: the eventual over-production sold to the grid can emerge for monthly typical days. Polycrystalline showed good performance for the four residential blocks, while net metering can highlight the share of overproduction sold to the grid sizing the PV panels with this requirement. Each block is composed by the same dwelling types and hourly loads among them are similar. One residential building is selected as representative from each block, with the daily average load by month.

Hourly profiles for detached and semidetached dwellings have similarities. Compared to apartments, they have lower electricity consumption during summer due to the assumed lack of unit air conditioning. The PV production is lower for detached houses (Figure 78) due to the more limited rooftop surface, whereas semidetached reaches almost 7 kWh (Figure 79). Advantage of polycrystalline is the high output also in winter months, even if concentrated only in few central hours of daylight. The overproduction is significant in both cases and mainly in warmer months: in the net metering scenario, the surplus can be sold back to the grid, having financial returns for the residents. Overproduction happens in the central hours of the day, mostly between 10 a.m. and 4 p.m. and ranges from 9% to more than 65% hourly for the detached house. Hourly overproduction for semidetached ranges between 6% in November to 76% in June. However, for both single family housing types, the PV output can instantly cover mainly the morning and early afternoon demand but not the peak load in the evening from 5 to 9 p.m.

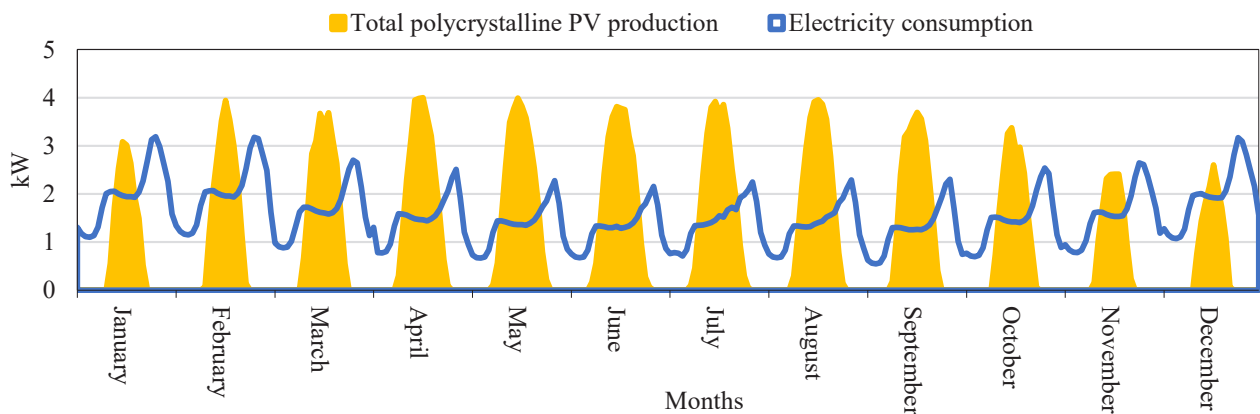


Figure 78. Hourly profiles of the load and total polycrystalline PV production for 12 typical days representative of each month for 2017, simulated for building 1484 of the detached block.

Figure 80 highlights differences for a representative low-rise building. The PV output in summer months partially satisfies instantly the electricity peak demand for space cooling, especially in July. This important advantage could increase self-sufficiency compared to detached and semi-detached blocks. Solar contribution can reduce pressures on the main load and provide energy locally produced for the users. The available roof surface is more extended, so that the total PV production for each building is higher. Hourly overproduction reaches a peak of 76% in April, when demand is more limited than in summer when overcomes 15 kWh.

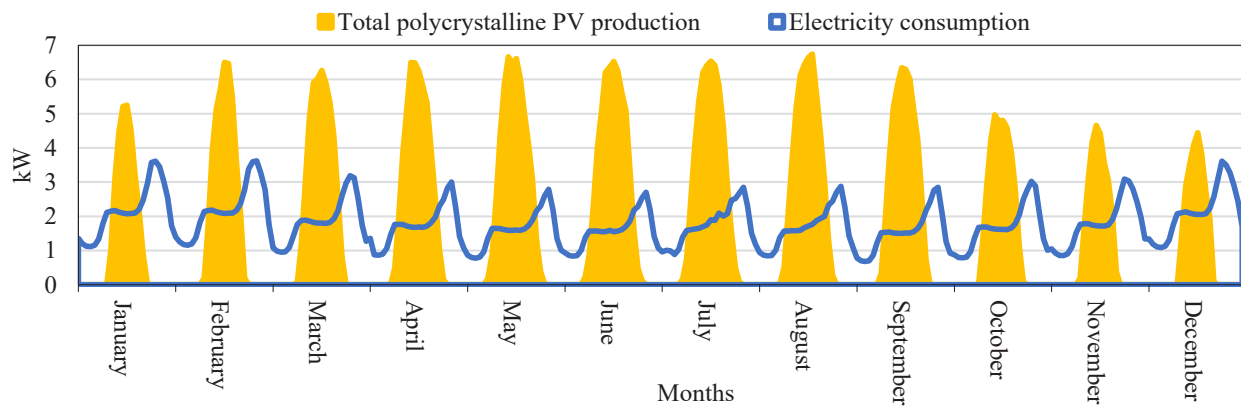


Figure 79. Hourly profiles of the load and total polycrystalline PV production for 12 typical days representative of each month for 2017, simulated for building 2001 of the semi-detached block.

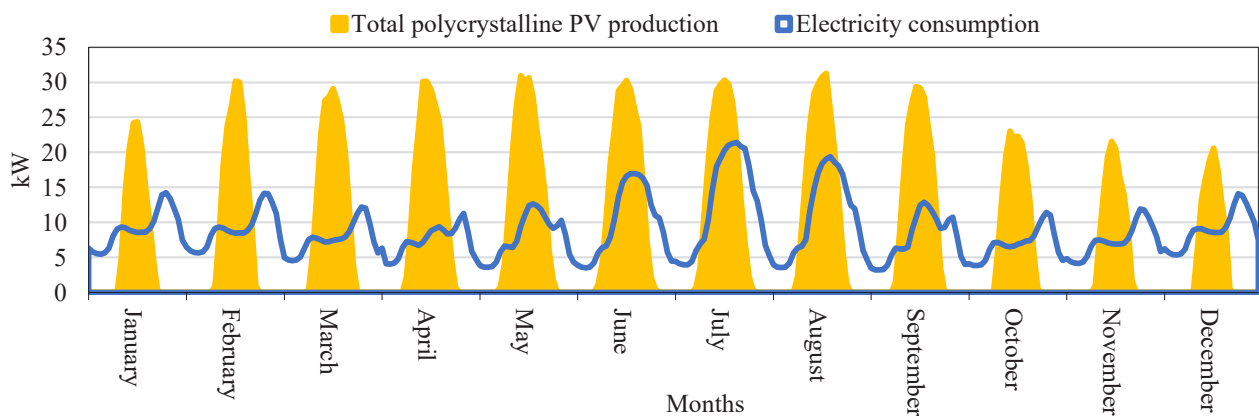


Figure 80. Hourly profiles of the load and total polycrystalline PV production for 12 typical days representative of each month for 2017, simulated for building 2462 of the low-rise apartment block.

Among the four archetypes, high-rise is the only residential category which does not show over-production along the year (Figure 81). Indeed, the solar output is not sufficient to satisfy the whole electricity demand in the 12 representative days: the number of occupants and the loads are always above 30 kWh. Despite PV cannot satisfy the space cooling demand between June and August, it can cover between 30% and 60% hourly consumption during the morning and early afternoon. Still, peak load in the evening cannot be satisfied and purchase of electricity from the main grid is required.

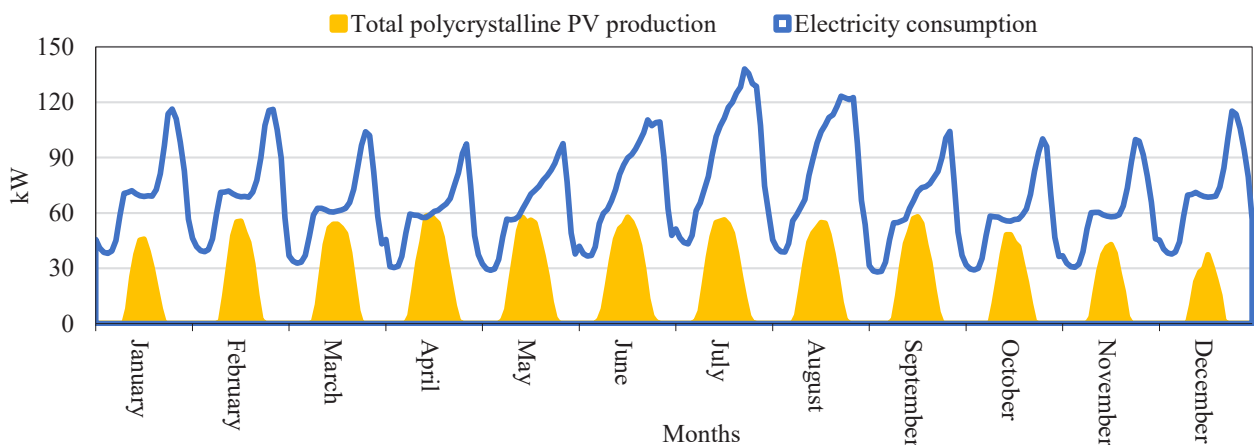


Figure 81. Hourly profiles of the load and total polycrystalline PV production for 12 typical days representative of each month for 2017, simulated for building 1711 of the apartment high-rise block.

The aggregated scenarios represent the monthly trend for all the dwellings of each block. Self-consumption and self-sufficiency vary along the year and for each residential aggregation.

Block of detached and semi-detached dwellings show similar monthly trends in Figure 82 and Figure 83. Self-consumption is higher in winter while it tends to decrease during summer, whereas self-sufficiency is the opposite. Overproduction occurs between April and September for the detached block and between March and September when electricity is sold to the grid. This is also related to the lower consumption compared to winter months. For the detached block (Figure 82), self-consumption is higher than 50% and PV production lower than 60 MWh in winter but self-sufficiency below 30%. The peak self-sufficiency for detached is in June, with 50.29%.

For the semidetached block (Figure 83), self-consumption is above 40% in winter and self-sufficiency

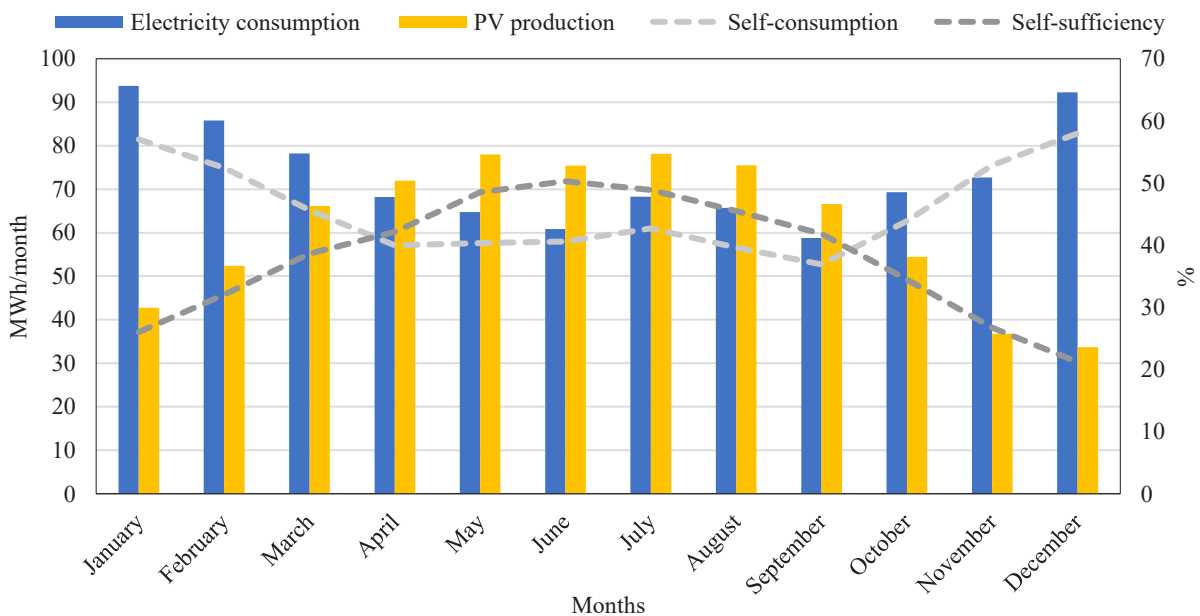


Figure 82. Electricity consumption, PV production, self-consumption, and self-sufficiency monthly profile for the detached block.

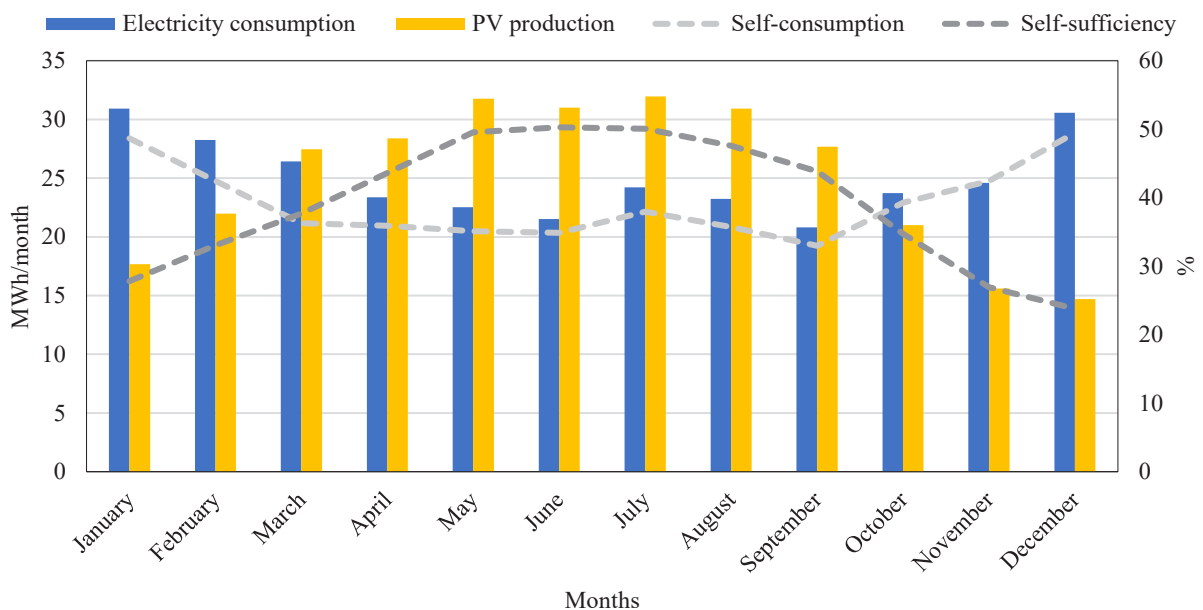


Figure 83. Electricity consumption, PV production, self-consumption, and self-sufficiency monthly profile for the semi-detached block.

below 30%. The self-sufficiency is more stable for semi-detached during summer, with self-sufficiency between 49.56% and 47.58% from May to August.

Monthly trends change for multi-family denser dwellings due to the different relation between available rooftop area and the total electricity consumption of the block. With taller structures, greatest chances of shadings among buildings can also occur, especially among high-rises.

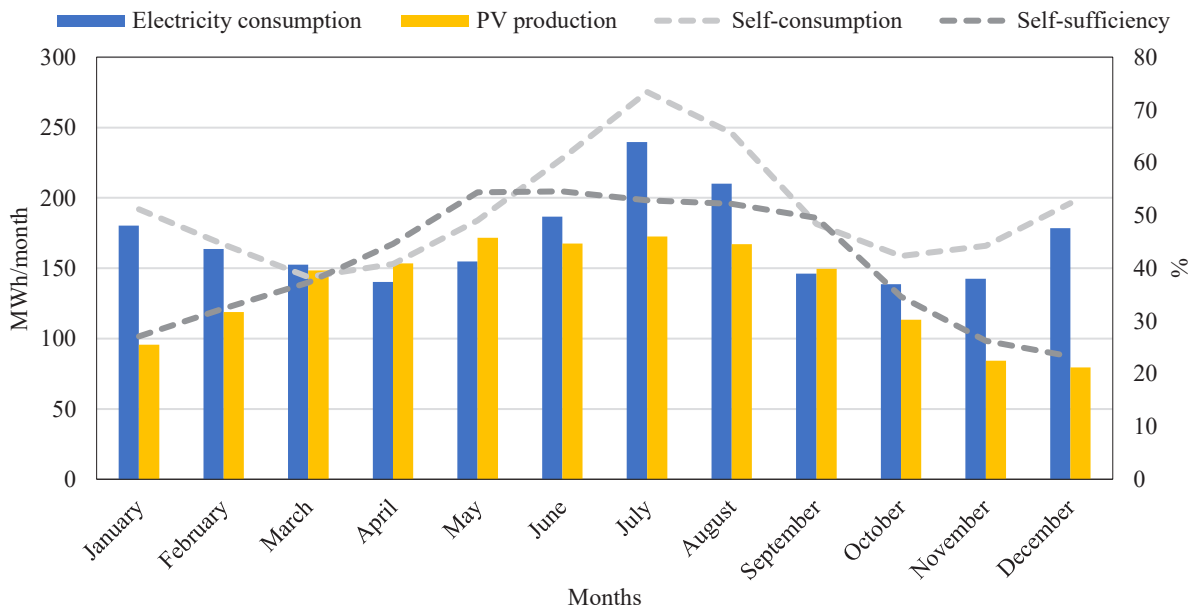


Figure 84. Electricity consumption, PV production, self-consumption, and self-sufficiency monthly profile for the low-rise apartment block.

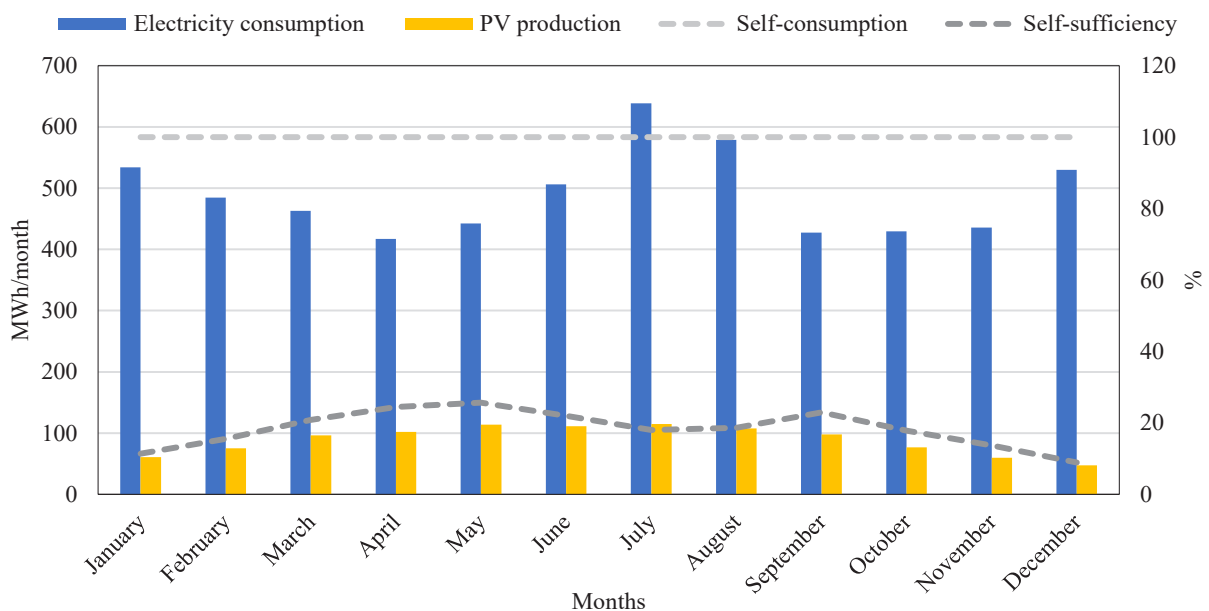


Figure 85. Electricity consumption, PV production, self-consumption, and self-sufficiency monthly profile for the high-rise apartment block.

Figure 84 shows a peak of self-consumption in July for the block of low-rise apartments, which is different from detached and semi-detached cases. In July, the block reaches 73.40% self-consumption, having 239.65 MWh electricity consumption and 172.58 MWh PV production. A lower share of electricity is sold to the grid due to the higher instantly consumed proportion for space cooling, which

can meet the hourly load profile (see Figure 80). On the other hand, self-sufficiency is lower than 30% in winter, while it overcomes 50% between May and August when its trend is stable. The flatten curve in summer is due to the higher solar production compensated by the increasing demand.

The monthly characterisation for high-rise block shows the impacts of a significant electricity consumption (always above 400 MWh) compared to the rooftop solar production (Figure 85). Locally produced electricity is totally instantly consumed in all months, without any share sent to the grid: self-consumption is always equal to 100%. This is in line with the hourly load profile in Figure 81. However, self-sufficiency ranges from a minimum in December (8.91%) to a maximum in May (25.66%), which can only partially cover space cooling needs. During summer, self-sufficiency tends to be lower due to the increasing cooling consumption: in July, consumption reaches 638.60 MWh, PV production 114.85 MWh, but self-sufficiency is equal to 17.99% only. Self-sufficiency for high-rise is expected to be not extremely higher than these thresholds in other scenarios.

### 6.6.3 Scenarios for weather-related grid outages

One of the options considered in the cost-optimal analysis is how PV with battery and eventual generator can face weather-related outages. During electric blackouts, the REopt software simulates the renewable system running off-grid for a given period. For each block, potential PV and storage systems can satisfy consumption during grid outages, with different temporal durations and surviving probabilities. A historical database of weather-related power outages for the City of Toronto is still unavailable. Therefore, the identification of blackouts is assumed from the local historical weather database provided by the Government of Canada for 2017 [116]. Outages are considered to occur when extreme conditions are registered for maximum and minimum temperatures for 2017 (Table 98). Intervals are selected if there is the maximum number of peaks for that weather phenomena in a 24-hours frame. Simulations are launched for each residential block, considering the two weather events.

Table 98. Selected temporal intervals for 2017, with weather peak events and assumed to cause a grid outage.

Events	24h outage	Start hour	End hour
Heatwave	7/30	5039	5063
Colder temperatures	12/31	8735	8759

Heatwaves and high temperatures are the first phenomenon to be analysed. The 24-hours interval is in July, when higher maximum and average temperatures are registered for Toronto (ref. paragraph 4.2.2). The highest temperature is registered on July 30<sup>th</sup>, between 3 and 4 p.m., with hourly value of 30.2°C (Figure 86). Based on projections and studies (ref. paragraph 4.1 and 4.2.2), more frequent and longer heatwaves are likely to recur in the area, with even more extreme values. For instance, June and July 2022 reached temperatures around 35°C in more than one day and heat warnings were multiple along the summer [116]. High temperatures and pressures on the grid rise chance of blackouts. On the other hand, favourable conditions during summer can produce higher solar output, but warmer temperatures lead to increasing cooling needs for indoor comfort. The assumptions consider the event of July 30<sup>th</sup> as the more extreme for 2017, limited to one day and with peak in the early afternoon.

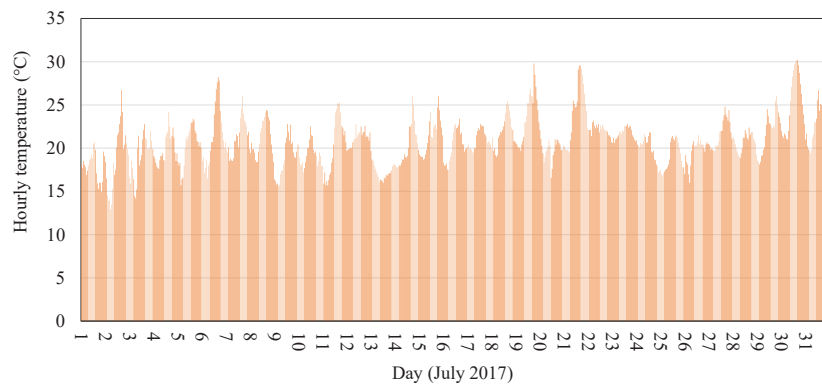


Figure 86. Hourly temperature trend in July 2017. Source: [116].

Extreme low temperatures characterise colder months, with long-lasting period below zero. Matching wind and temperature can freeze the power lines and impact on the delivery on electricity to households. On the other hand, winter period makes even more challenging the on-site production of solar energy, due to the shorter daylight and lower radiation received by panels.

The coldest period for 2017 is registered on last three days of December, having 31<sup>st</sup> as minimum value (Table 99 and Figure 87). The temperature is always below zero, with also a breeze around 16 km/h. Minimum values are during the night, with rising temperature trends in the day. Possibilities of power lines to freeze can greatly increase in longer cold period, impacting on the energy delivery.

Table 99. Main aspects of the selected coldest days. Source: [116].

Event	Min temperature (°C)	Min wind chill (°C)	End hour
12/31	- 19.3 (12/31)	- 28 (12/31)	5063

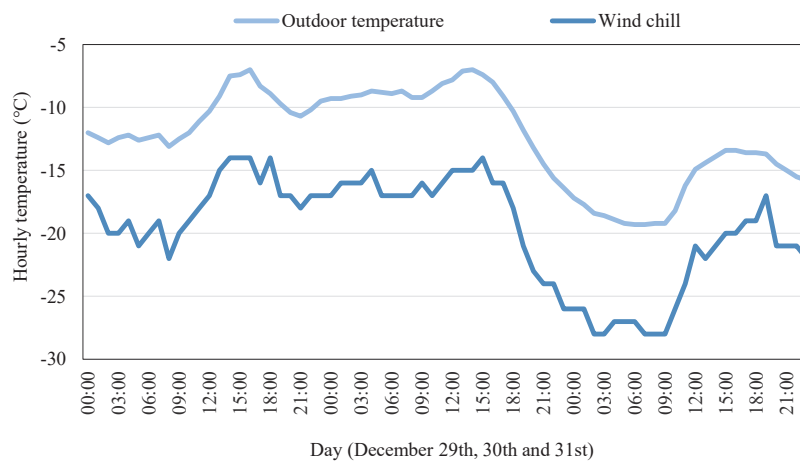


Figure 87. Temperature trends between 29th and 31st December 2017. Source: [116].

30<sup>th</sup> July and 31<sup>st</sup> December are assumed as the two days in 2017 when blackout occurred. These should be considered as reference days to estimate the size of the distributed generation in case of outage. Estimations change considering different intervals and year on which perform the off-grid analyses.

## 6.7 Cost-optimal results and comparison

The results from different scenarios are compared for the four residential blocks. In all four cases, simulations without net-metering tend to maximise self-consumption with values above 95% of total produced energy because the surplus of produced electricity is not sold to the grid. On the other hand, scenarios admitting net metering increase self-sufficiency but have a lower self-consumption: consistent part of the produced electricity are sold to the grid due to the advantageous tariffs.

### 6.7.1 Low-density residential blocks

Detached and semidetached blocks show similar trends of self-sufficiency and global costs. Options with net-metering tend to over-produced electricity to gain a financial credit at the end of each month. For net-metering scenarios, self-consumption is lower than 45% of annual production but the higher power of the system increases self-sufficiency (SC/C) above 36%. The highest SC/C is obtained sizing the system for a 24-hours outage in winter: in this case, solar production is reduced, and the backup system tends to increase in the optimisation. However, net-metering scenarios with PV and battery and with a 24-hours outage in winter or summer have similar SC/C, above 37%. A 24-hours blackout does not significantly impact neither on global costs nor self-sufficiency, even if a main role is covered by the generator. For both blocks, scenarios with batteries are clustered in similar positions of the graphs (Figure 88 and Figure 89), based on the presence or not of net-metering. Optimal options are with net-metering due to the competitive tariffs to sell the energy to the grid.

Figure 88 shows the relation between global costs and self-sufficiency for the whole block of detached dwellings. The cost-optimal solution is polycrystalline panels with net-metering: it reaches a 36.92% self-sufficiency with global costs of 925,480 US\$. In case of monocrystalline, values would be very close with same installed power of 582.28 kW, with 36.75% self-sufficiency and 948,668 US\$.

Trends are distinguished for solutions with and without batteries in Figure 88. Hypothesis with polycrystalline and storage are aligned along the line trend and clustered. Batteries can be helpful in retaining part of the electricity produced, even if they do not significantly increase the SC/C but rather SC/P. The minor impact of storage is due to the advantageous net-metering tariffs to sell the PV over-production to the grid, which equal of purchasing electricity. Slightly higher costs (1,072,455 US\$) are in case of monocrystalline and battery with net-metering: SC/C is equal to 36.83% and SC/P to 43.72%. Performing a scenario with a default 50% self-sufficiency, global costs rapidly increase and confirm its financial unfeasibility. Except for the 50% self-sufficiency, all scenarios have lower global costs than business-as-usual, equal to 1,351,448 US\$ for the whole detached block.

The situation for semi-detached aggregation is like the detached one, even if the trends with and without batteries are closer. Costs are more similar to options with storage, which reach 38.84% self-sufficiency in the scenario with winter outage. Polycrystalline with net-metering is still identified as the cost-optimal solution, with SC/C equal to 38.15%. Aiming at 50% self-sufficiency will entail global costs for the block higher than the current situation (464,444 US\$), being not financially feasible.

For the two blocks of detached and semi-detached dwellings, 100% self-consumption from locally

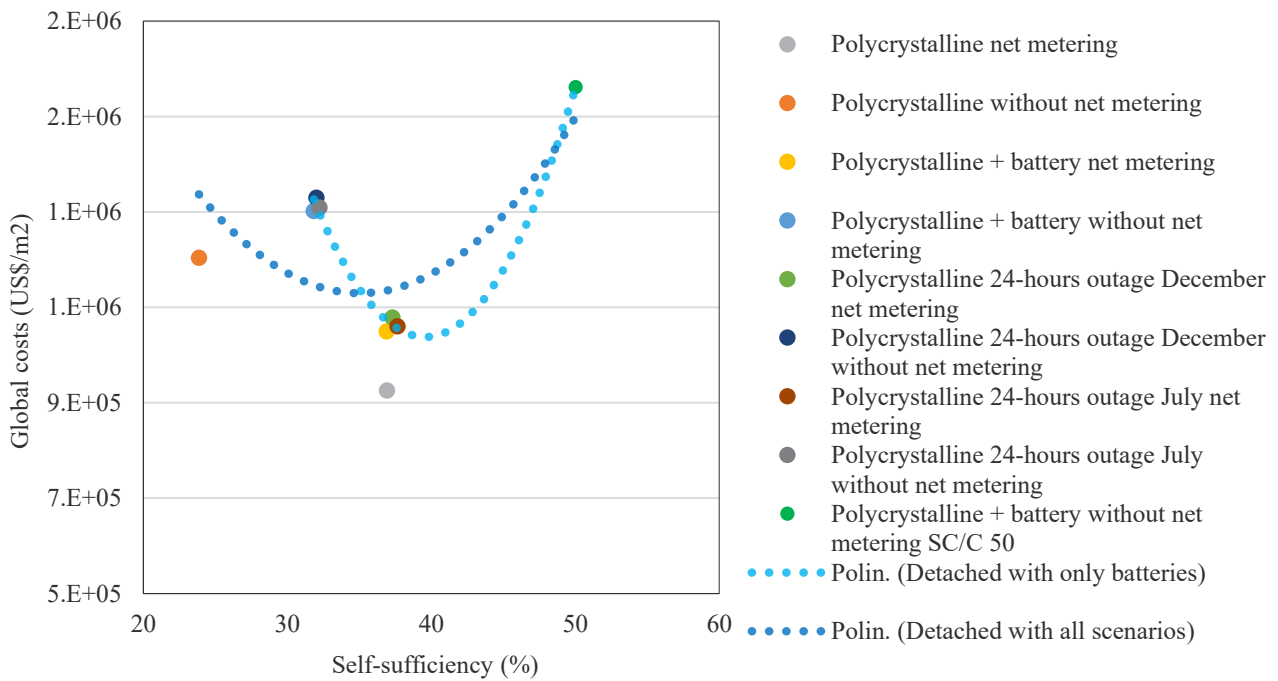


Figure 88. Global costs (US\$/block) for detached block: relation between global costs and self-sufficiency with different polycrystalline scenarios.

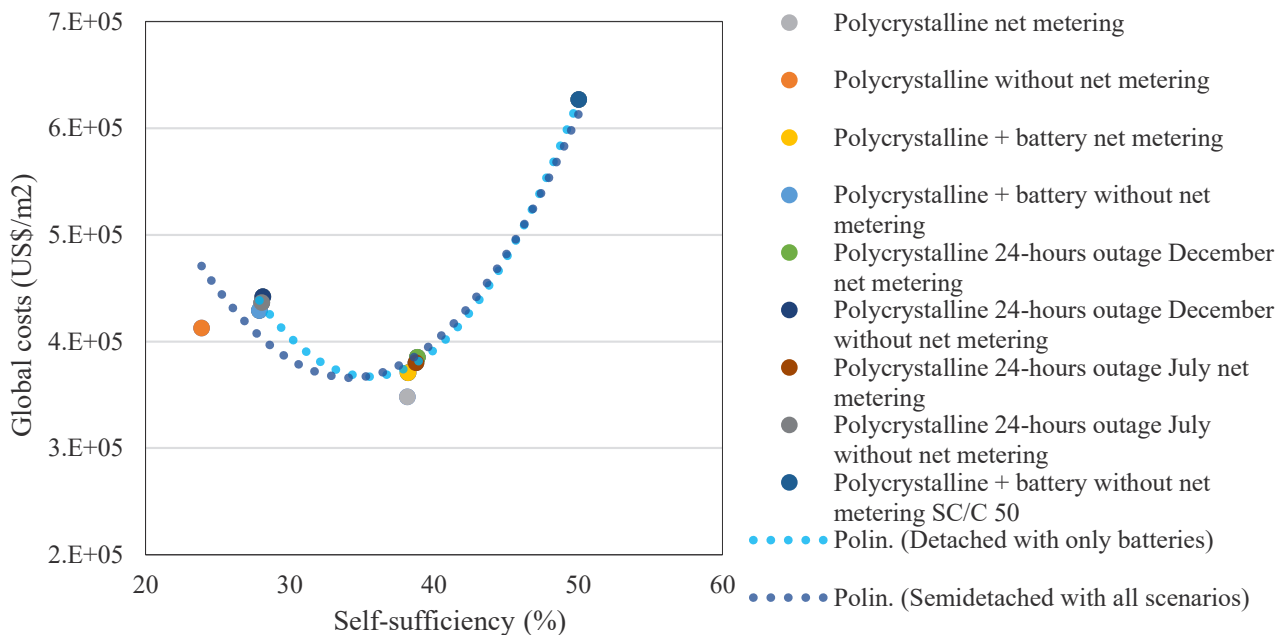


Figure 89. Global costs (US\$/m<sup>2</sup>) for semi-detached block: relation between global costs and self-sufficiency with different polycrystalline scenarios.

produced PV energy is reached with only panel installation without net-metering. Indeed, PV production is instantly self-consumed by the users in the residential block, but self-sufficiency over the total consumption is not higher than 24%. A 100% self-consumption for polycrystalline reaches only 23.08% and 23.17% SC/C for detached and semi-detached respectively.

Adding net metering implies that larger PV size and a share of not-instantly used energy will be sent to the main grid. Sizing for net-metering allows to increase self-sufficiency, while without net-metering maximises self-consumption (Figure 90). Considering storage, SC/P ranges between 96% and 98% for both blocks.

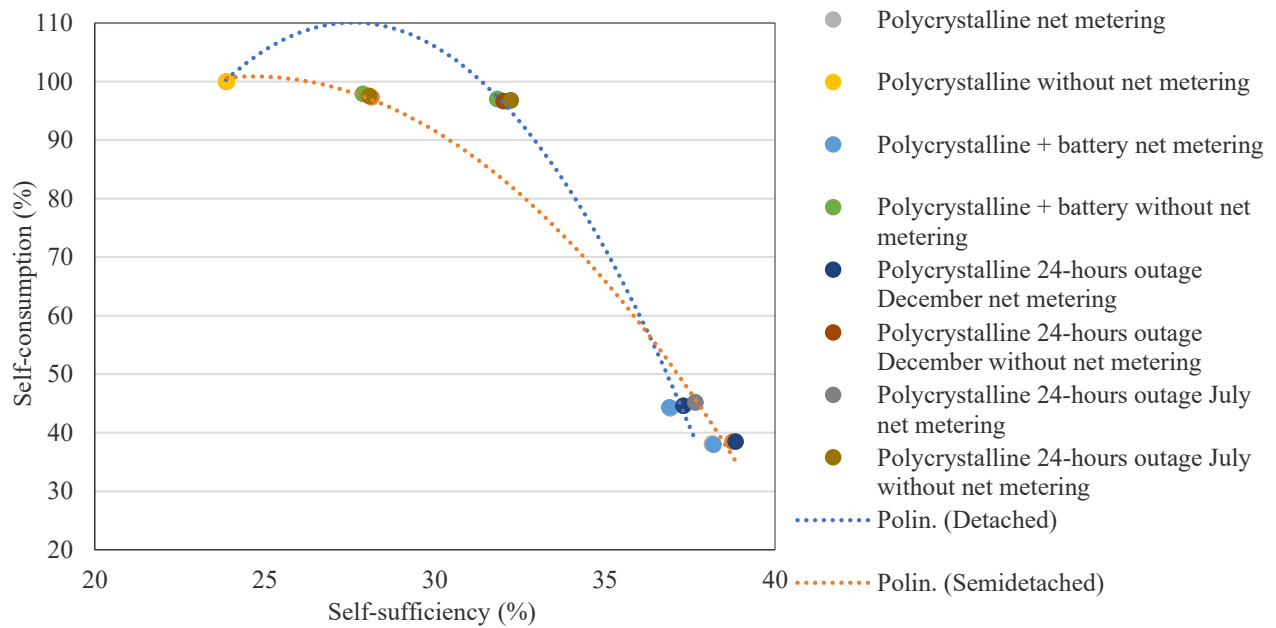


Figure 90. Relation between self-sufficiency and self-consumption (\*) for detached and semi-detached blocks, with monocrystalline scenarios.

\* self-consumption cannot be higher than 100%. The y axis has 110 as maximum value only to show the trend of the curve by the two blocks.

Polycrystalline PV with storage in a net-metering condition has minimum self-consumption, about 44.31% for detached and 37.97% for semi-detached (Figure 90). The threshold is slightly higher than the estimated 30% by the Solar Ready Guidelines, even if it only considers household lighting and appliances electricity use [82]. The Guidelines consider a tilt angle equal to the latitude (equal to 45° for Toronto), while this study a 35° angle. The share reaches a peak in June, when production is higher, and electricity consumption is lower than July.

Maximum SC/C around 38% decreases also LCCs compared to only monocrystalline or polycrystalline without net-metering: LCCs result below 1.07 M \$US for detached and 390k \$US for semidetached block. The optimal configuration depends on the direction towards a maximum self-consumption of locally produced energy or self-sufficiency to be more independent from the energy network. Values for same scenarios are slightly different for monocrystalline. Self-sufficiency is 0.5% to 3.27% lower, while global costs are 0.18% to 2.54% higher for detached dwellings. Semidetached present from 0.29% to 1.89% higher costs for monocrystalline options. Overall differences are limited but can still impact on large investments.

The installed PV area on rooftops increases more rapidly in detached houses to reach higher self-sufficiency, where the overall roof area available is 4,786.24 m<sup>2</sup>. Semidetached dwellings have more extended contiguous surface to install solar PV, whereas roofs in stand-alone houses are smaller. The installed area for these two blocks is 21% and 25% more extended for polycrystalline, considering the lower efficiency and the higher area required compared to monocrystalline. Therefore, one of the main aspects to consider is the actual available surface on rooftops. The eventual installation of other technologies, as solar thermal collectors, could occupy the remaining space which can be higher if installing monocrystalline. On the other hand, PV power (kW), eventual storage, and generator for each dwelling increases more rapidly for semidetached houses, with a peak of 19.59 kW/dwelling in case of winter blackout. The higher assessed power for semidetached influences global costs. Prices are

between 11% and 27% higher for semi-detached houses that range between 34.56 US\$/m<sup>2</sup> to 62.26 US\$/m<sup>2</sup> for global costs per area.

Options with and without net metering impact differently on the energy expenses and savings with PV, based on Figure 91 and Figure 92. Energy costs are lower, and electricity covered by PV is higher with net-metering optimisations, while the opposite emerges without selling the produced energy to the grid. On the other hand, initial capital investments increase admitting net-metering because of the larger size of the system installed. The comparison between business-as-usual and post-investment LCCs is reported by the net present value (NPV), which if positive represents revenues. All options reduce total energy expenses of at least 22% compared to the BAU scenario. Higher revenues during the 25-year lifetime are estimated for the cost-optimal option, or rather polycrystalline panels with net-metering. NPV progressively decreases without net-metering and turns into losses (-210,134 US\$ for detached and -162,641 US\$ for semi-detached) assessing a 50% self-sufficiency. Therefore, this last option is not financially feasible for these two blocks because it entails economic losses at the end of the 25 years.



Figure 91. Total energy expenses, total energy savings with PV, net present value and initial capital costs after incentives using polycrystalline for the detached block. Poly = polycrystalline, NM = net metering, BES = battery energy storage.

Benefits of options with net metering emerge also with the comparison between NPV and simple payback time in Figure 93. For these cases, the payback time is below 11 years for all cases, while total revenues are the highest along the 25 years. The competitive prices of selling overproduced energy shorten the time to recover the investment costs, which are further reduced with national incentives. The minimum payback time is reached by the scenario without net-metering (7.78 years for detached and 7.69 for semi-detached), even if lower revenues for the NPV occur too. On the other hand, imposing 50% self-sufficiency can quickly increase the temporal range to repay the capital costs and turn the NPV into a cost.

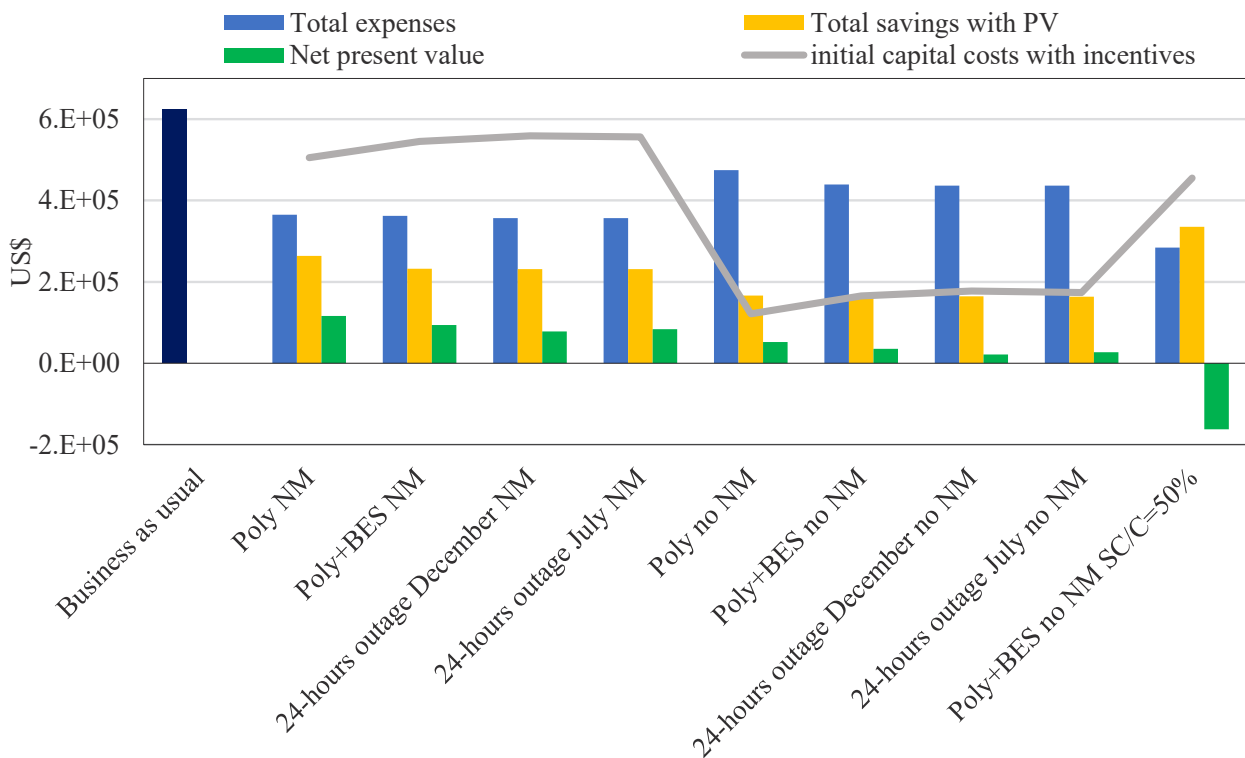


Figure 92. Total energy expenses, total energy savings with PV, net present value and initial capital costs after incentives using polycrystalline for the semi-detached block. Poly = polycrystalline, NM = net metering, BES = battery energy storage.

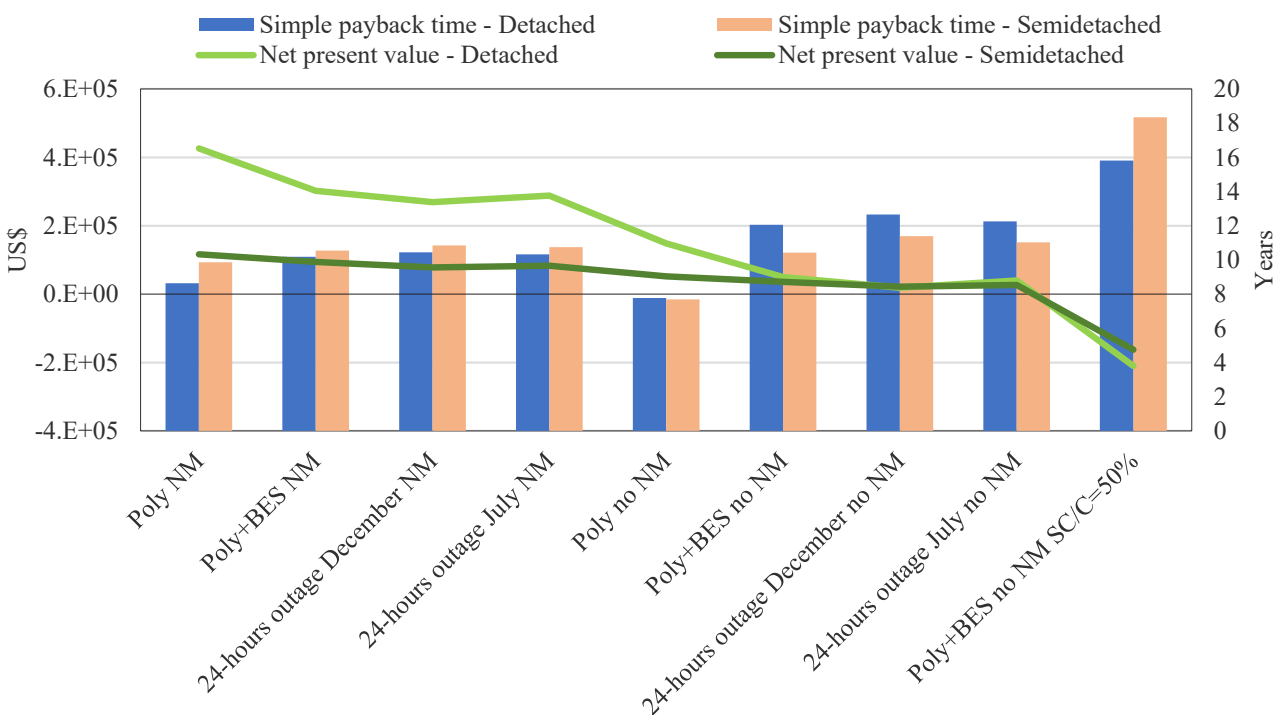


Figure 93. Net present values and simple payback time for detached and semi-detached blocks in the 25-years lifetime for the detached and semi-detached blocks. Poly = polycrystalline, NM = net metering, BES = battery energy storage.

Finally, the comparison with 2017 and 2022 tariffs let emerge in Table 100 a growth about 12% of expenses as well as savings from PV production. The rising electricity tariffs (see Table 10) will increase the respective value of energy savings from PV production. The same TOU prices to sell the

solar overproduction will impact on the LCCs or SPT. At the same time, expenses for the purchased electricity will rise too: higher bills may push more users to install local renewable technologies, even if it implies a long-term process.

Table 100. Comparison between expenses and savings with 2017 and 2022 electricity tariffs. The detached and semidetached blocks are compared for the cost-optimal scenario (polycrystalline with net-metering).

Block type	Expenses: 2017 tariff (US\$)	Expenses: 2022 tariff (US\$)	Total savings: 2017 tariff (US\$)	Total savings: 2022 tariff (US\$)	Variation (%)
Detached	1,106,520.96	1,255,293.14	742,503.68	828,515.47	+12%
Semidetached	365,015.41	414,357.24	263,859.61	294,420.64	+12%

For polycrystalline (and similarly, for monocrystalline), the combination of technologies and conditions can be grouped in two macro-results for detached and semi-detached blocks:

- self-consumption lower than 45%, self-sufficiency higher than 35% and maximum LCCs of 1.06M US\$ for the detached block and below 390k US\$ for the semi-detached block, which include net-metering scenarios;
- self-consumption higher than 95%, self-sufficiency lower than 30% and costs higher than 1.2M US\$ for the detached block and higher than 412k US\$ for the semi-detached block which include solutions without net-metering.

## 6.7.2 Apartment building blocks

Results change for denser housing typologies, where the available roof area for each building is more extended but the number of occupants and electricity consumption is higher.

The low-rise block has a total roof area equal to 15,983 m<sup>2</sup> and, applying the 70% limit, it reduces to 11,188.36 m<sup>2</sup> for 16 buildings. The available space is higher as well as the electricity consumption, especially during summer, due to space cooling. Figure 94 shows the relation between self-sufficiency and global costs for the whole block. A discrepancy emerges between scenarios with and without net-metering, both clustered in two areas of the graph. Global costs of the former are between 48.60 and 50.74 US\$/m<sup>2</sup>, while without net metering are higher than 53 US\$/ m<sup>2</sup>. SC/C without net metering ranges between 18.81% and 21.05%, while the opposite between 41.44% and 41.75%. As for the other two residential blocks, options with net metering show a cost-optimal position: higher self-sufficiency allows lower global costs, mainly due to revenues from electricity sold back to the grid and the lower expenses of total energy used. However, costs rapidly increase if overcoming the 40% SC/C threshold: investments result higher than the BAU LCCs (3,218,696 US\$), they are not balanced by savings from PV and NPV is negative (Figure 95).

Similarly to detached and semi-detached houses, installations without net-metering reach higher self-consumption, more than 96%. Self-consumption drops around 50% when considering net-metering because the system is allowed to sell back to the grid the energy non instantly used.

It is interesting to underline that the level of self-sufficiency reached by low-rise block can be around 3% higher than for low-density blocks. The electricity production by PV can partially satisfy the peak load in the afternoon (see Figure 84), which rapidly rises in summer due to space cooling demand. Covering a portion of peak demand in the evening helps both to increase self-sufficiency and

self-consumption for low-rise. The more extended roof surface also contributes to satisfy about 41% share of electricity demand, which is even more concentrated in summertime due to the assumption of air conditioning for each unit.

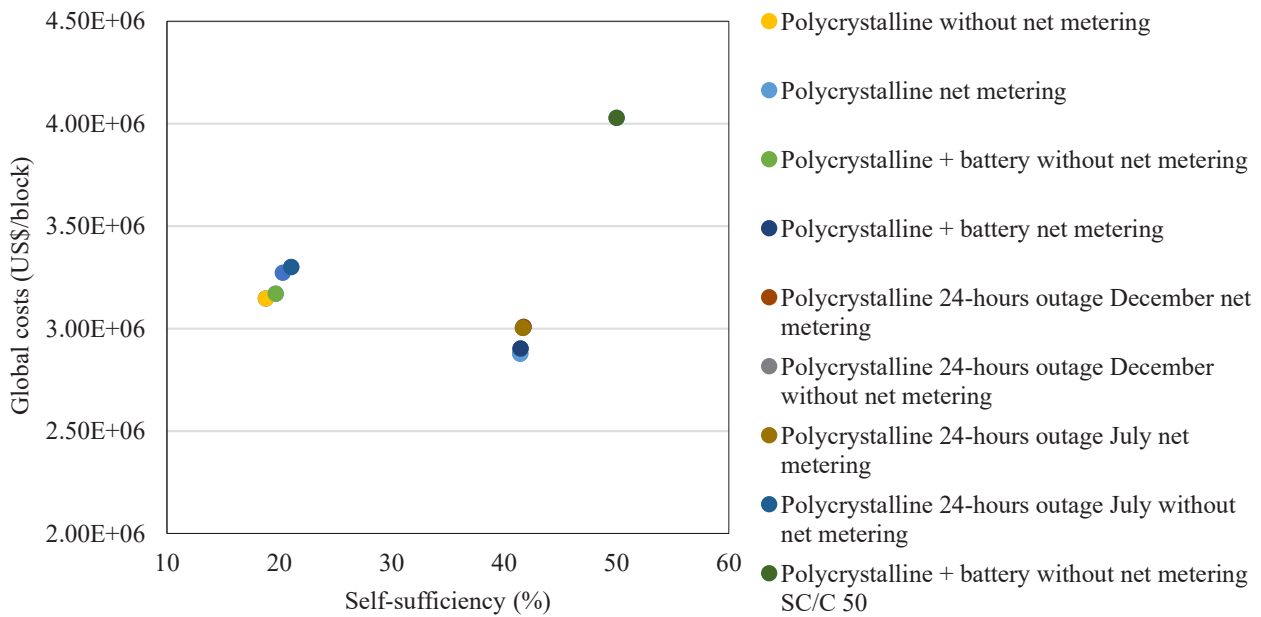


Figure 94. Global costs (US\$/block) for low-rise apartment block: relation between global costs and self-sufficiency with different polycrystalline scenarios.

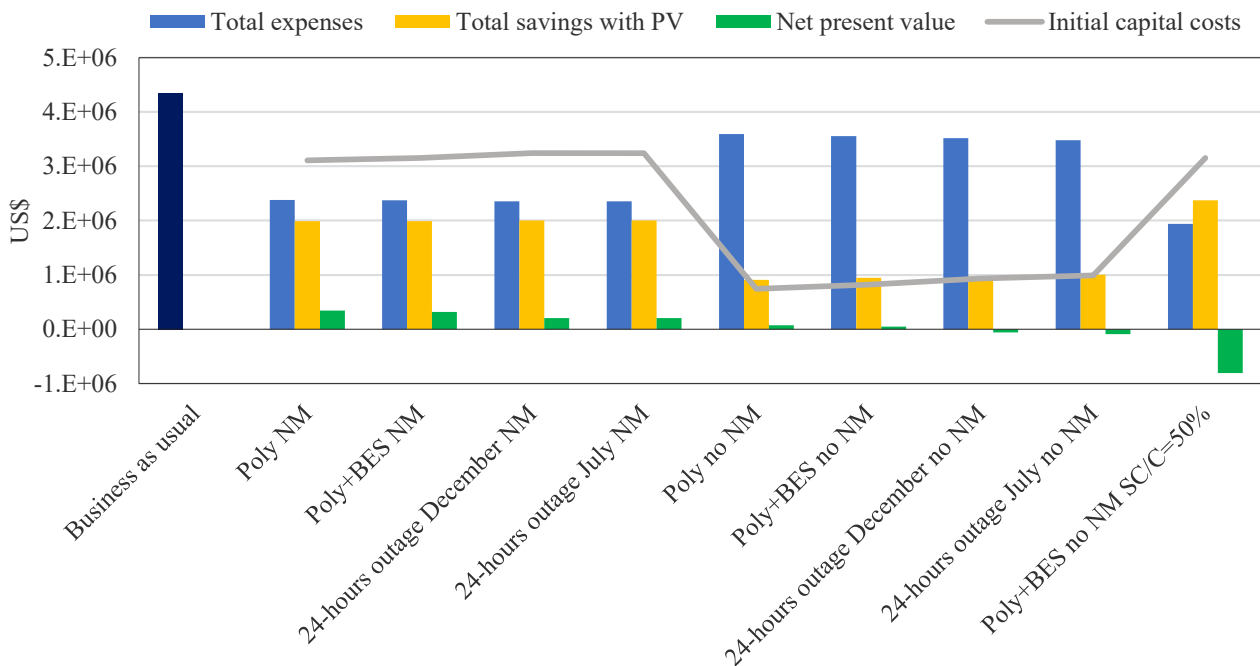


Figure 95. Total energy expenses, total energy savings with PV, net present value and initial capital costs after incentives using polycrystalline for the low-rise apartment block. Mono = monocrystalline, NM = net metering, BES = battery energy storage.

The outage scenarios without net-metering appear not convenient: indeed, the NPV is negative, which represent a loss in the assumed 25-years lifetime (Figure 95). This is also in line with Figure 94, where both points are in the left part, or rather higher global costs and lower self-sufficiency.

Initial capital costs are above US\$3 million for the block in case of optimisation with net-metering. The higher power of the system contributes to increase PV savings and decrease energy expenses along the lifetime. The situation is unfavourable for scenarios without net-metering because energy costs remain above US\$3 million, while savings from PV below US\$1 million for the whole block. The initial investment costs are more limited and follows the trend of financial savings from PV. Similarly to detached and semi-detached, the 2022 tariffs for electricity increase expenses, values of savings and revenues from net-metering for each scenario about 13%.

High-rise apartments are the most challenging residential type. The available roof surface is about 7,307.36 m<sup>2</sup> and can host a significant PV power. On the other hand, each building is composed by at least 5 floors up to 25 and has a total electricity consumption higher than the other dwelling categories. Both the monocrystalline and polycrystalline technologies are evaluated in this case because more kW can be installed on the rooftop area compared to thin film: 1 kW occupies about 5.7, 6.7 and 10 m<sup>2</sup> respectively. Higher total costs for each building and whole block are eventually shared among several occupants.

For all the performed scenarios, self-sufficiency is around 18% and self-consumption is always higher than 98%. Global costs are between 49.7 US\$/m<sup>2</sup> and 52.37 US\$/m<sup>2</sup> for different hypotheses with SC/C = 18%. Results are therefore very similar and cannot cover more than 20% electricity consumption, as reported in Table 101. The lower shares of satisfied consumption are in line with the hourly and monthly profiles for high rise (see paragraph 6.6.2), where the amount of PV electricity produced is significantly lower than the total consumption.

The output by solar PV is mainly consumed instantaneously due to the high demand compared to production. Therefore, scenarios with and without net metering perform very similar values because the energy produced from the local system is immediately consumed and not sold back to the grid. The high consumption and the immediate used of locally produced energy do not require the installation of storage with high capacity. The scenario with lower global costs (8,900,285 US\$) and higher NPV (216,801 US\$) is the installation of polycrystalline panels with net-metering, which has a self-sufficiency of 18.05%.

Table 101. Main results of PV optimisations for the high-rise apartment block. Mono = monocrystalline, Poly = polycrystalline, BES = battery energy.

Scenario	SC/P (%)	SC/C (%)	PV (m <sup>2</sup> )	Storage (kW)	Generator (kW)	Global costs (US\$/block)
Mono no net metering	100.00	18.05	4,435.48	-	-	8,951,903
Mono net metering	99.49	18.05	4,435.48	-	-	8,942,081
Poly no net metering	100	17.88	5,618.28	-	-	8,914,847
Poly net metering	99.49	18.05	5,618.28	-	-	8,900,285
Mono + BES no net metering	99.86	18.05	4,435.48	7.84	-	8,968,469
Mono + BES net metering	99.86	18.05	4,435.48	7.84	-	8,968,469
Poly + BES no net metering	99.86	17.87	5,618.28	7.84	-	8,931,593
Poly + BES net metering	99.86	17.87	5,618.28	7.84	-	8,931,593

Mono 24-hours outage December no net metering	99.16	18.20	4,435.48	15.33	560.03	9,302,018
Mono 24-hours outage December net mete- ring	99.16	18.20	4,435.48	15.33	560.03	9,302,018
Mono 24-hours outage July no net metering	98.06	18.12	4,435.48	83.21	527.54	9,415,995
Mono 24-hours outage July net metering	98.06	18.12	4,435.48	83.21	527.54	9,415,995
Poly 24-hours outage December net mete- ring	99.16	18.02	5,618.28	15.67	559.68	9,265,302
Poly 24-hours outage July net metering	97.96	17.92	5,618.28	89.66	521.09	9,389,626
Mono, no net mete- ring, SC/C = 0.25	100	25	7,219.06	-	-	18,115,957
Mono, no net mete- ring, SC/C = 0.30	100	30	8,672.25	-	-	18,062,736
Poly, no net metering, SC/C = 0.25	100	25	9,229.64	-	-	18,039,260
Poly, no net metering, SC/C = 0.30	100	30	11,089.08	-	-	17,974,379

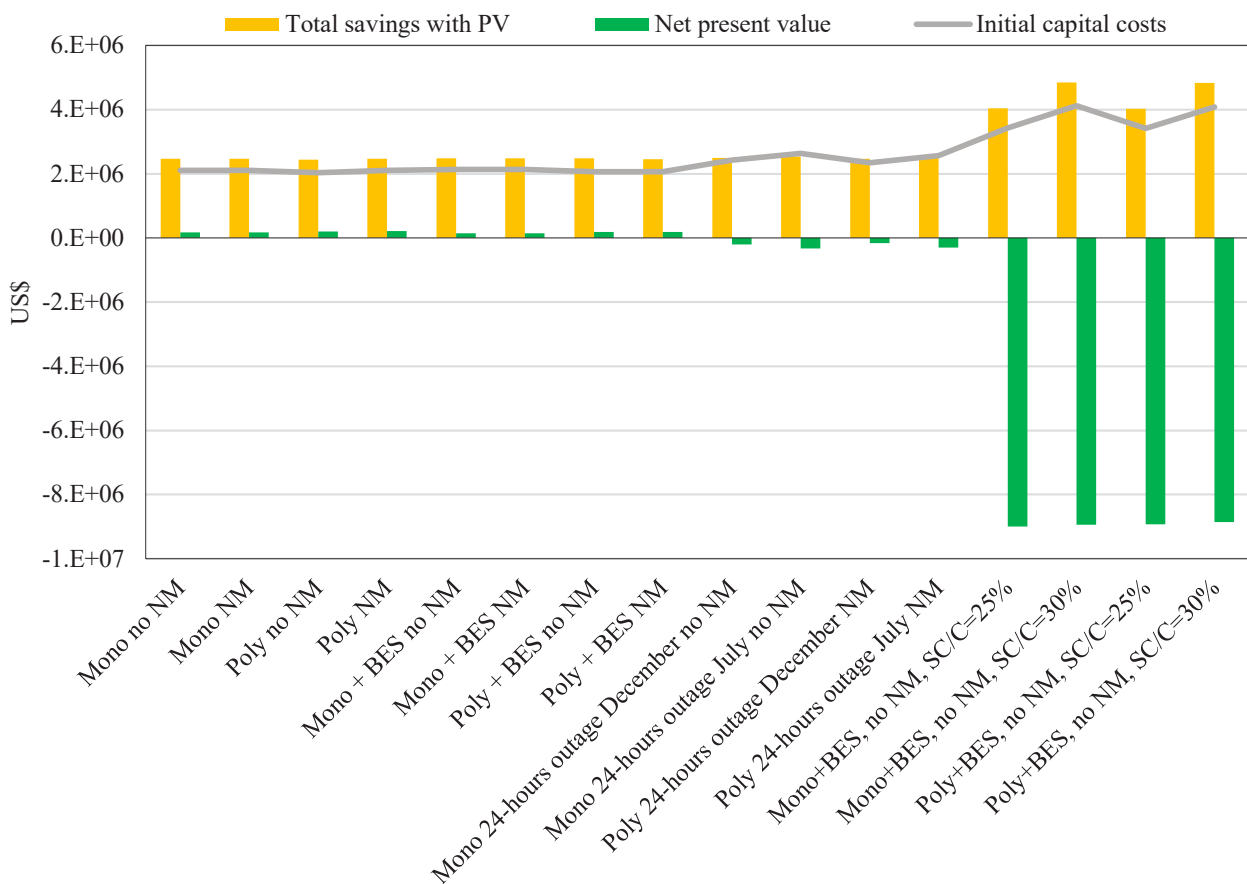


Figure 96. Total energy savings with PV, net present values and initial capital costs using monocrystalline and polycrystalline for the high-rise apartment block. Mono = monocrystalline, Poly = polycrystalline, NM = net metering, BES = battery energy.

On the other hand, batteries and generators are useful in simulations with 24-hours outage and can slightly increase self-consumption. In these cases, optimisations tend to increase the backup system rather than the installed panel area and PV size. The power rises from 77.32 kW/building and 50 US\$/m<sup>2</sup> in simulation without outages to more than 130 kW/building and 52 US\$/m<sup>2</sup> to face blackouts. Costs are translated to more than US\$ 9.3 million for the whole apartment block. A proper incentive is not available by the City of Toronto or by the country, but only a possible credit by the Hi-RIS programme in the energy bills [111].

The high-rise block is also tested setting a priori the minimum share of electricity consumption to satisfy by PV. The share of installed roof area reaches the 83% of total roof surface but self-sufficiency cannot overcome 30% due to the substantial consumption and the high space cooling demand during the summer. This implies a significant increase in the global costs, as shown in Table 101. The 30% SC/C is reached without storage nor net metering because the solar electricity is instantly consumed by the building. Higher self-sufficiencies have been also tested: however, values higher than 30% cannot be satisfied (even with net-metering) for the high-rise block.

Figure 96 shows how PV savings in 25 years are similar for the scenarios without a pre-fixed level of self-sufficiency, whereas with maximum SC/C the solar contribution increases too. The net present value is a cost in the four outage scenarios, due to the slightly higher investments but the lower impact on overall savings. The same happens for SC/C=25% and 30% because initial capital costs increase rapidly, but the impact on total expenses is not sufficient to balance it: these scenarios are inconvenient from an economic perspective. NPV represents a revenue only for scenarios with only PV and/or batteries, even if it is never higher than US\$ 220k for the whole high-rise block.

While low-rise can achieve high levels of self-sufficiency with polycrystalline, the high-rise block results the most challenging. The ratio between total electricity consumption and roof surface is not sufficient to overcome 18% SC/C with financially feasible configurations. This limit should be considered in Toronto, due to the diffused presence of high-rise apartment especially in downtown.

## 6.8 Result and considerations

The assessment of residential energy consumption and solar optimisation shows potentials and limits for the engineering model. As for the first part of the methodology, only the residential function is considered and subdivided in the main four dwelling archetypes. Analyses are performed on four selected residential blocks of downtown Toronto, one for each archetype.

Building simulations estimate electricity and natural gas consumption, with hourly definition. Analyses on URBANopt are based on the residential ASHRAE frameworks and local studies for the envelope characterisation and the energy system parameters. Consumptions for each residential archetypes show differences from the regression model, mainly for high-rise apartment buildings (Figure 97). The statistical model worked on 75 residential blocks with disaggregated energy data, while modelling on URBANopt works on the single-building characterisation to assess their demand. Low-rise showed a total consumption in line with the statistical model, while high-rise values are 35% lower than the total consumption (kWh/m<sup>2</sup>y) by the two regression models. Occupancy rates for high-rises may be underestimated by assumptions due to lack of more specific data. Detached and semi-detached houses have similar total consumptions compared to values from the statistical analysis, but

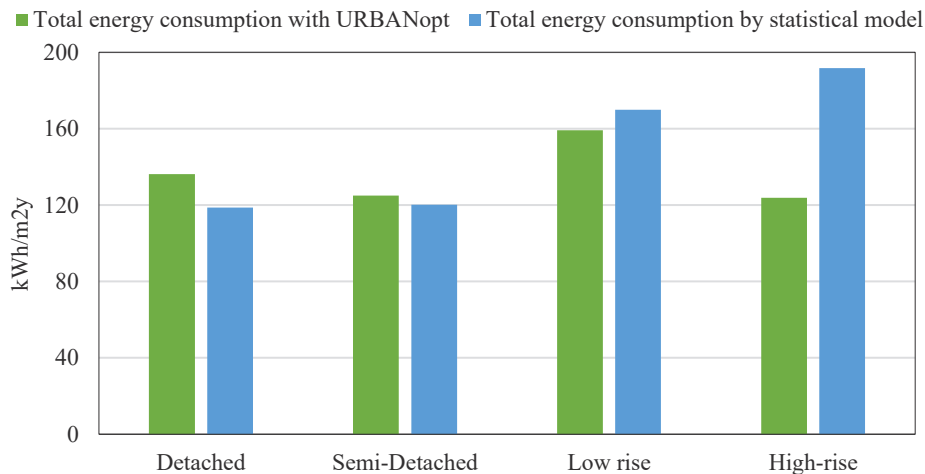


Figure 97. Comparison between total energy consumption ( $kWh/m^2/y$ ) assessed by URBANopt and the statistical model.

with different proportions of electricity and natural gas consumption. This difference is mainly related to the recent ASHRAE template applied in modelling the Toronto Platform, which assumed electric resistance for single family dwellings.

The baseline scenario is the starting point to optimise rooftop solar PV. For a preliminary evaluation, financially optimal options without net-metering are performed for monocrystalline, polycrystalline, and thin film. Polycrystalline provides a balance between investment costs, savings, and energy performance. The aggregated evaluations by blocks (scenario level) show benefits for energy production and mostly for the financial side: lower LCCs characterise mainly low-density blocks, while they are less evident for low-rises and high-rises. Optimising at the block scale would also reduce energy bills, while increase PV production and electricity self-sufficiency. For groups of buildings, this is related to the fact that centralised installations are more performative and economical than distributed standalone ones, as shown by [178] due to the smaller size required and reduction of overall costs. However, configurations need to equilibrate the amount of buildings, the share of prosumers and only consumers and the overload limits of the available infrastructures.

Different scenarios are then performed, including net metering, storage, and possible blackouts on the grid. Each option considers aggregated evaluations for the four residential groups and optimised by REopt. Results are compared in a cost-optimal analysis to the related financial parameters, as global costs, revenues and NPV, with energy-related performances, which are self-sufficiency and self-consumption. Cost-optimal scenarios for blocks of detached, semidetached, and low rises are polycrystalline panels with net-metering: self-sufficiency is respectively equal to 36.92%, 38.15% and 41.44%. Low-rise block reaches slightly higher values because PV production can meet a part of the peak load in the afternoon, mainly for summer months (see paragraph 6.6.2). Hourly overproduced electricity by rooftop PV is purchased with the same TOU tariffs of consumed one. Therefore, sizing for net-metering is more convenient than adding storage: in a financial perspective, it can be said that net-metering acts similarly to batteries in this case. Community scenario can also benefit from the community net metering schema, recently introduced by the Ontario Energy Board [104]. However, net-metering or feed-in-tariffs must be careful considered case by case and with occurring variations. The greatest challenge to increase self-sufficiency is for high-rise block, where electricity consumption overcomes 500 MWh in summer months. The high-rise block achieves a maximum self-suffi-

ciency of 18.05% for monocrystalline and polycrystalline with net-metering, with global costs below 9M \$US. Higher shares can reach up to 30% with monocrystalline and 83% of occupied roof area (more than the 70% input threshold), but with disadvantageous LCCs (above 17M \$US) and negative NPVs. Negative NPVs are also assessed for outage events where self-sufficiency only slightly improves.

Finally, a comparison between solar results with GIS assessment and URBANopt financial optimisations is reported in Figure 98 for the four residential blocks. The identified optimised surfaces in URBANopt are always more extended than the feasible ones with GIS-methodology. The GIS assessment considers only favourable exposures and slope for PV production. On the other hand, the block-scale evaluations optimise PV panels to reduce LCCs during the 25 years and balance local production with building consumption. Consequently, levels of self-sufficiency are higher for the second approach, with main discrepancies for the semidetached (38.15% vs. 24.12%) and high-rise blocks (18.05% vs. 6.50%).

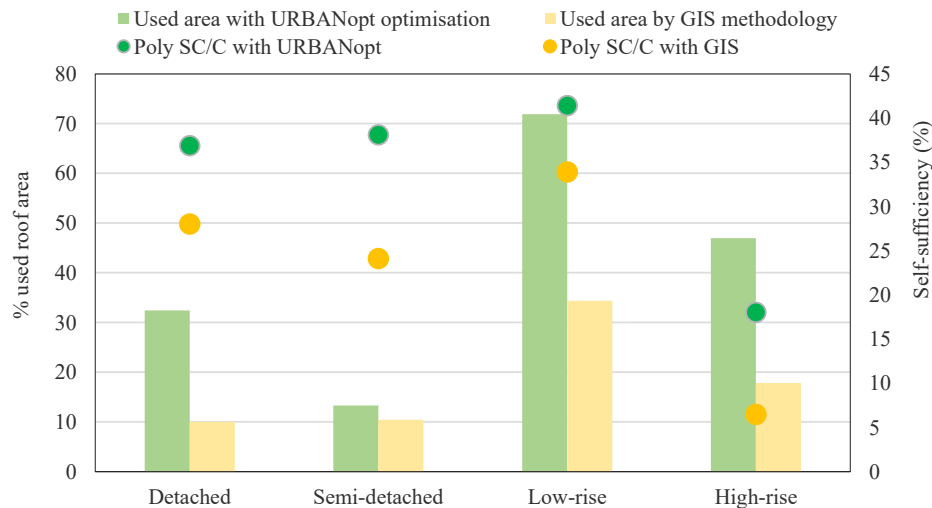


Figure 98. Comparison between used roof area (columns) by GIS methodology and URBANopt optimisation for the four residential blocks. Based on electricity consumption assessed with the engineering model, level of self-sufficiency (dots) reached by each method. Poly = polycrystalline.

Results of potential PV production are determined by the selected criteria and assumed scale: consideration of only favourable orientations or financially optimal solutions. In this study, the investment costs for the GIS-based sizing would be lower due to the more limited PV area. On the other hand, higher NPVs and limited LCCs are identified by the block-scale optimisations, with SC/C always above 18%. Evaluations at the aggregated level rather than on single buildings can create benefits for energy performance and for the financial side of interventions, with an increasing appeal for investments. Future studies can also consider the integration of different daily and hourly load profiles of functions, as residential, commercial, recreational spaces. The mismatch between production and consumption of distinct building functions should be exploited, especially if an eventual PV overproduction not instantly consumed can be used by other structures. Similar integration needs careful energy assessments and planning. Community-scale studies and projects should be supported to reduce consumption and diffuse solar development, as mentioned by the Toronto Net Zero Strategy [157]. New sections of the Toronto 2030 Platform should display consumption by single building, whereas both building and aggregated levels could be added for PV implementation.

## 7. CONCLUSIONS

Urban building energy modelling can be a starting point to study the distribution of energy consumption, make evaluations for energy transition and guide pathways of decarbonisation. Building energy models and evaluations of renewables represent supporting tools for energy planning, which is interdependent to spatial planning. However, the complexity of cities and heterogeneity of energy profiles require analyses with different approaches and scales. Assuming downtown Toronto as case study, the assessment of residential building consumption and PV solar potential on rooftops was based on two levels: a statistical top-down model and GIS-based solar assessment for the urban area, followed by an engineering model with PV optimisation by residential blocks.

The top-down approach integrated GIS in different steps, starting from the disaggregation of block energy data to single buildings. Between two downscaling methods, the option by subtraction was chosen to estimate energy end-uses from electricity and natural gas. The statistical model used MLRs to derive the electricity consumption from independent variables, with decreasing intensities for lower S/V ratio. The natural gas assessment was more complex and did not lead to stable regressions for apartment buildings. Starting from electricity consumption, solar potential with GIS-based evaluations underlined higher covered share for detached and semi-detached houses, with a 25% maximum self-sufficiency considering slope and exposure constraints. Values were lower for apartment buildings, due to the less balanced relation between total electricity consumption and available rooftop area. High-rise energy-demanding dwellings are common in Toronto and impact on the total energy needs of the area.

The engineering model confirmed the energy-demand character of high-rise buildings. Simulations adapted the building characterisation to the context of Toronto, starting from the ASHRAE templates. The balance between electricity and natural gas consumptions were different from calculations with the statistical model, while total consumptions were more similar. Differences were mainly related to simplified assumptions applied in the Toronto 2030 Platform and the parameters introduced in URBANopt. The financial PV optimisations for each block highlighted the advantages of modelling at district scale rather than by single buildings to reduce LCCs. Aggregated evaluations reached slightly better energy performances and had financial benefits mainly for low-density dwellings. Indeed, a 23% and 13% reduction of LCCs was assessed for detached and semidetached in block evaluations, whereas only 2.4% difference for low-rise and 0.9% high-rise because they already represent agglomerations. The financial side can be a main driver to implement new actions with community-scale approaches and to persuade customers towards renewables. Consumers and individual prosumers are generally interested in maximising individual profits, while community configurations should be planned to increase self-sufficiency. The economic efficiency has a key role in PV projects because its feasibility guarantees the implementation in different steps and pushes investors to fund similar projects [178]. The relationships between economic and energy aspects were performed with cost-optimal analyses, which showed polycrystalline with net-metering as optimal solution. Self-sufficiency varied for each archetype, based on installable areas on rooftops, total electric consumption, and ability of PV to meet the peak load. The peak load in summer can be partially satisfied by PV production for the low-rise block, reaching 41% self-sufficiency. The competitive tariffs to sell back electricity to the grid favoured net-metering configurations rather than storage. Batteries were not useful for

high-rise buildings, where PV production is almost totally consumed instantly by the high demand. Having only 18% self-sufficiency, high-rise apartments were the most challenging to satisfy electricity consumption, even with aggregated simulations.

The multi-scalar methodology allows to have a general picture of the urban environment for the residential stock, with variable levels of detail, and understand its potentials. The GIS-based approach localises consumption for an urban environment, to assess more effective PV system at the city level and its preliminary coverage of electricity. Then, possible aggregations for consumption and solar generation can be studied for district and block scale. Improving the active interactions among buildings can maximise the use of renewable production while providing financial benefits. The challenge will be to define the optimal balance of scales to install community-based PV and to work on the most demanding areas, integrating different load profiles. The aim of the projects should guide its planning. Redefining the Toronto 2030 Platform with building energy data (rather than block scale) would provide more detailed assessments for policymakers and users. Availability and spatial resolution of data should match the requirements for more accurate energy maps, reducing simplifications. An additional solar assessment integrated to the 2030 Platform would make citizens and policymakers more aware on potential new installations: a starting point could be the available SolarTO Map tool [92]. The PV energy mapping can be structured for both single buildings and aggregations, as blocks or districts. The potential of community-scale projects should emerge for energy performance and long-term financial benefits to users, starting from electricity.

The 2030 District considers decarbonised pathways also for heating, which is a major component of energy consumption in Canada. The 2030 District [174] identified electrification as the most mature option to cover heating needs towards net-zero by 2050: lowest costs for heat fuel switching were assessed for single-family houses. Despite being the most inexpensive option, the expansion of electrical resistance will increase electricity pressures, while installation of heat pumps is currently competitive for single-family dwellings. Starting from low-density housing, matching heat pumps with roof PV installation could support electrification in coming years while the diffusion of renewable local generation can reduce dependency from local loads. Further assessments should study the integration and pressures of solar installations on the energy grid. This challenge would be even greater for dated energy infrastructures, as in the case of Toronto.

According to the NUA [8] and the PCFCGCC [148], infrastructures and communities should be more resilient to face future climate hazards and extreme weather events. At the same time, perspectives of renewable resources in cities should aim at collective users' aggregations, from a centralised to a polycentric system. The perspective of local generation by organised urban energy communities could rise self-sufficiency and improve integrated approaches between energy, financial and environmental sectors towards more sustainable cities.

# REFERENCES

- [1] UN environment programme, «Goal 7: Affordable and clean energy,» [Online]. Available: <https://www.unep.org/explore-topics/sustainable-development-goals/why-do-sustainable-development-goals-matter/goal-7>.
- [2] C. Delmastro, G. Mutani, S. Corgnati, «A supporting method for selecting cost-optimal energy retrofit policies for residential buildings at the urban scale». *Energy Policy*, vol. 99, n. 9, pp. 42-56, 2016. <https://doi.org/10.1016/j.enpol.2016.09.051>
- [3] L. Swan, V. Ugursal, «Modelling of end-use energy consumption in the residential sector: A review of modelling techniques». *Renewable and Sustainable Energy Reviews*, vol. 13, n. 8, pp. 1819-1835, 2009. <https://doi.org/10.1016/j.rser.2008.09.033>
- [4] F. Kouhestani, J. Byrne, D. Johnson, L. Spencer, P. Hazendonk, B. Brown, «Evaluating solar energy technical and economic potential on rooftops in an urban setting: the city of Lethbridge, Canada». *International Journal of Energy and Environmental Engineering*, vol. 10, n. 11, pp. 13-32, 2019. <https://doi.org/10.1007/s40095-018-0289-1>
- [5] J. Hofierka, J. Kanuk, «Assessment of photovoltaic potential in urban areas using open-source solar radiation tools». *Renewable Energy*, vol. 34, n. 10, pp. 2206-2214, 2009. <https://doi.org/10.1016/j.renene.2009.02.021>
- [6] 2030 District, «Toronto 2030 Platform» 2020. [Online]. Available: <https://www.toronto2030platform.ca/>. [Consultato il giorno 10th June 2022].
- [7] Alliance for Sustainable Energy, LLC, «URBANopt» 2019. [Online]. Available: <https://docs.urbanopt.net/>. [Accessed on 24<sup>th</sup> August 2022].
- [8] United Nations, «The New Urban Agenda» in Habitat III Conference, Quito, Ecuador, 2016.
- [9] F. Fuso Nerini, J. Tomei, L. Seng To, I. Bisaga, P. Parikh, M. Black, A. Borrion, C. Spataru, V. Castàn Broto, G. Anandarajah, B. Milligan, Y. Mulugetta, «Mapping synergies and trade-offs between energy and the Sustainable Development Goals». *Nature Energy*, vol. 3, n. 1, pp. 10-15, 2018. <https://doi.org/10.1038/s41560-017-0036-5>
- [10] UN Global Compact, «SDG Compass - SDG 7: Ensure access to affordable, reliable, sustainable and modern energy for all» 2015. [Online]. Available: <https://sdgcompass.org/sdgs/sdg-7/>. [Accessed on 20<sup>th</sup> November 2022].
- [11] IRENA, «Energy transition outlook» 2022. [Online]. Available: <https://www.irena.org/Energy-Transition/Outlook>. [Accessed on 23<sup>rd</sup> November 2022].
- [12] M. Fremouw, A. Bagaini, P. De Pascali, «Energy Potential Mapping: Open Data in support of Urban transition planning». *Energies*, vol. 13, n. 5, pp. 1264-1279, 2020. <https://doi.org/10.3390/en13051264>
- [13] J. Gaspari, M. De Giglio, E. Antonini, V. Vodola, «A GIS-based methodology for speedy energy efficiency mapping: a case study in Bologna». *Energies*, vol. 13, n. 9, 2230, 2020. <https://doi.org/10.3390/en13092230>
- [14] A. Steingrube, K. Bao, S. Wieland, A. Lalama, P. Kabiro, V. Coors, B. Schröter, «A method for optimizing and spatially distributing heating systems by coupling an urban energy simulation platform and a energy system model». *Resources*, vol. 10, n. 5, 2021. <https://doi.org/10.3390/resources10050052>
- [15] A. Alhamwi, W. Medjroubi, T. Vogt, C. Agert, «Development of a GIS-based platform for the allocation and optimisation of distributed storage in urban energy systems». *Applied Energy*, vol. 251, n. 10, 2019. <https://doi.org/10.1016/j.apenergy.2019.113360>
- [16] G. Lobaccaro, M. Lisowska, E. Saretta, P. Bonomo, F. Frontini, «A methodological analysis approach to assess solar energy potential at the neighbourhood scale». *Energies*, vol. 12, n. 18, 3554, 2019. <https://doi.org/10.3390/en12183554>
- [17] M. Ferrando, F. Causone, T. Hong, Y. Chen, «Urban building energy modelling (UBEM) tools: A state-of-the-art review of bottom-up physic-based approaches». *Sustainable Cities and Society*, vol. 62, n. 32, 2020. <https://doi.org/10.1016/j.scs.2020.102408>
- [18] D. Macumber, K. Gruchalla, N. Brunhart-Lupo, M. Gleason, J. Abbot-Whitley, J. Robertson, B. Polly, K. Fleming, M. Schott, «City scale modelling with OpenStudio» in ASHRAE and IBPSA SimBuild, Salt Lake City, Utah, 2016.

- [19] F. Mougouei, M. Mortazavi, «Effective approaches to energy planning and classification of energy systems models». *International Journal of Energy Economics and Policy*, vol. 7, n. 2, pp. 127-131, 2017. <https://dergi-park.org.tr/en/pub/ijeep/issue/31921/351188?publisher=http-www-cag-edu-tr-ilhan-ozturk>
- [20] J. Hourcade, R. Richels, J. Robinson, «Estimating the cost of mitigating greenhouse gases» in *Climate Change 1995: Economic and Social Dimensions of Climate Change*. Contribution of Working Group III to the Second Assessment Report of the IPCC, Cambridge, University Press, 1996, pp. 263-296.
- [21] N. van Beck, «Classification of energy models» Tilburg University & Eindhoven University of Technology, 1999.
- [22] J. Sargunam, S. Iniyar, «A review of energy models». *Renewable and Sustainable Energy Reviews*, vol. 10, n. 4, pp. 281-311, 2006. <https://doi.org/10.1016/j.rser.2004.09.004>
- [23] M. Grubb, J. Edmonds, P. ten Brink, M. Morrison, «The Costs of Limiting Fossil-Fuel CO<sub>2</sub> Emissions: A Survey and Analysis». *Annual Review of Energy and the Environment*, vol. 18, pp. 397-478, 1993. <https://doi.org/10.1146/annurev.eg.18.110193.002145>
- [24] S. Torabi, C. Delmastro, S. Corgnati, P. Lombardi, «Urban energy planning procedure for sustainable development in the built environment: A review of available spatial approaches». *Journal of Cleaner Production*, vol. 165, n. 1, pp. 811-827, 2017. <https://doi.org/10.1016/j.jclepro.2017.07.142>
- [25] L. Swan, «Residential Sector Energy and GHG Emissions Model for the Assessment of New Technologies» Doctor of Philosophy - Dalhousie University, Halifax, 2010.
- [26] M. Kavacic, A. Mavrogianni, D. Mumovic, A. Summerfield, M. Djurovic-Petrovic, «A review of bottom-up building stock models for energy consumption in the residential sector». *Building and Environment*, vol. 45, n. 7, pp. 1683-1697, 2010. <https://doi.org/10.1016/j.buildenv.2010.01.021>
- [27] G. Mutani, V. Todeschi, «GIS-based urban energy modelling and energy efficiency scenarios using the energy performance certificate database». *Energy Efficiency*, vol. 14, n. 47, pp. 1-28, 2021. <https://doi.org/10.1007/s12053-021-09962-z>
- [28] T. Hong, Y. Chen, X. Luo, N. Luo, S. Hoon Lee, «Ten Questions on Urban Building Energy Modelling». *Urban Integrated System*, vol. 168, n. 5, 2020. <https://doi.org/10.1016/j.buildenv.2019.106508>
- [29] V. Todeschi, R. Boghetti, J. Kampf, G. Mutani, «Evaluation of urban-scale building energy-use models and tools - Application for the city of Fribourg, Switzerland». *Sustainability*, vol. 13, n. 4, pp. 1595-1617, 2021. <https://doi.org/10.3390/su13041595>
- [30] S. Torabi, G. Mutani, P. Lombardi, «GIS-based energy consumption model at the urban scale for the building stock» in 9th IEECB&SC'16, Frankfurt, Germany, 2016.
- [31] M. Prina, G. Manzoloni, D. Moser, B. Nastasi, W. Sparber, «Classification and challenges of bottom-up energy system models – A review». *Renewable and Sustainable Energy Reviews*, vol. 129, n. 9, pp. 1-16, 2020. <https://doi.org/10.1016/j.rser.2020.109917>
- [32] G. Mutani, V. Todeschi, «Space heating models at urban scale for buildings in the city of Turin (Italy)». *Energy Procedia*, vol. 122, n. 9, pp. 841-846, 2017. <https://doi.org/10.1016/j.egypro.2017.07.445>
- [33] M. Aydinalp-Koksal, V. Ugursal, «Comparison of neural network, conditional demand analysis, and engineering approaches for modelling end-use energy consumption in the residential sector». *Applied Energy*, vol. 85, pp. 271-296, 2008. <https://doi.org/10.1016/j.apenergy.2006.09.012>
- [34] G. Mutani, G. Vicentini, «Analisi del fabbisogno di energia termica degli edifici con software geografico libero. Il caso studio di Torino». *La termotecnica*, vol. 6, n. 7-8, pp. 63-67, 2013. <http://www.verticale.net/analisi-del-fabbisogno-di-energia-termica>; <https://www.verticale.net/ricerca.php?q=mutani>
- [35] C. Reinhart, C. Cerezo Davila, «Urban building energy modelling - A review of a nascent field». *Building and Environment*, vol. 97, n. 12, pp. 196-202, 2016. <https://doi.org/10.1016/j.buildenv.2015.12.001>
- [36] G. Mutani, V. Todeschi, S. Beltramino, «Energy consumption models at urban scale to measure energy resilience». *Sustainability - Bridging the Gap: The Measure of Urban Resilience*, vol. 12, n. 14, pp. 1-31, 2020. <https://doi.org/10.3390/su12145678>
- [37] G. Mutani, V. Todeschi, «Building Energy Modeling at Neighborhood Scale». *Energy Efficiency*, vol. 13, p. 1353–1386, 2020. <https://doi.org/10.1007/s12053-020-09882-4>

- [38] V. Cheng, K. Steemers, «Modelling domestic energy consumption at district scale: A tool to support national and local energy policies». *Environmental Modelling & Software*, vol. 26, n. 10, pp. 1186-1198, 2011. <https://doi.org/10.1016/j.envsoft.2011.04.005>
- [39] R. Kadian, R. Dahiya, H.P. Garg, «Energy-related emissions and mitigation opportunities from the household sector in Delhi». *Energy Policy*, vol. 35, n. 12, pp. 6195-6211, 2007. <https://doi.org/10.1016/j.enpol.2007.07.014>
- [40] G. Mutani, R. Fontana, A. Barreto, «Statistical GIS-based analysis of energy consumption for residential buildings in Turin (IT)». in 2nd IEEE CANDO Conference, Budapest, Hungary, 2019.
- [41] A. Sola, C. Corchero, J. Salom, M. Sanmarti, «Simulation tools to build urban-scale energy models: a review». *Energies*, vol. 11, n. 12, 3269, 2018. <https://doi.org/10.1109/CANDO-EPE47959.2019.9111035>
- [42] C. Yin Siu, Z. Liao, «Is building energy simulation based on TMY representative: A comparative simulation study on doe reference buildings in Toronto with typical year and historical year type weather files». *Energy and Buildings*, vol. 211, n. 1, 109760, 2020. <https://doi.org/10.1016/j.enbuild.2020.109760>
- [43] Energy Efficiency at NRCan, «Comprehensive Energy Use Database 2020» [Online]. Available: <https://oee.nrcan.gc.ca/corporate/statistics/neud/dpa/home.cfm>. [Accessed on 28<sup>th</sup> May 2022].
- [44] ClimateData.ca, «Climate data for resilient Canada» 2nd June 2022. [Online]. Available: <https://climatedata.ca/>.
- [45] R. Erhardt, «Mid-twenty-first-century projected trends in North American heating and cooling degree days». *Environmetrics*, vol. 26, n. 11, pp. 133-144, 2014. <https://doi.org/10.1002/env.2318>
- [46] U. Berardi, P. Jafarpur, «Assessing the impact of climate change on building heating and cooling energy demand in Canada». *Renewable and Sustainable Energy Reviews*, vol. 121, n. 4, 109681, 2020. <https://doi.org/10.1016/j.rser.2019.109681>
- [47] P. Bezerra, F. de Silva, T. Cruz, M. Mistry, E. Vazquez-Arroyo, L. Magalar, E. De Cian, A. Lucena, R. Schaeffer, «Impacts of a warmer world on space cooling demand in Brazilian households». *Energy and Buildings*, vol. 234, n. 3, 110696, 2021. <https://doi.org/10.1016/j.enbuild.2020.110696>
- [48] G. Mutani, C. Delmastro, M. Gargiulo, S. Corgnati, «Characterization of building thermal energy consumption at the urban scale». *Energy Procedia*, vol. 101, n. 11, pp. 384-391, 2016. <https://doi.org/10.1016/j.egypro.2016.11.049>
- [49] M. Carozza, G. Mutani, S. Coccolo, J. H. Kaempf, «Introducing a hybrid energy-use model at the urban scale: The case study of Turin (Italy)». in 3rd IBPSA-Italy Conference, Bozen, Italy, 2017.
- [50] L. Martin, L. March, «Urban Space and Structures». *Urban History*, vol. 1, n. 5, 1974.
- [51] S. Tsoka, A. Tsikaloudaki, T. Theodosiou, «Analyzing the ENVI-met microclimate model's performance and assessing cool materials and urban vegetation applications—A review». *Sustainable Cities and Society*, vol. 43, n. 11, pp. 55-76, 2018. <https://doi.org/10.1016/j.scs.2018.08.009>
- [52] B. Polly, C. Kutscher, D. Macumber, M. Schott, S. Pless, B. Livingood, O. Van Geet, «From zero energy buildings to zero energy districts». in 2016 ACEEE Summer Study on Energy Efficiency in Buildings, Pacific Grove, California, 2016.
- [53] H. Farahbakhsh, V. Ugursal, A. Fung, «A residential end-use energy consumption model for Canada». *International Journal of Energy Research*, vol. 22, n. 13, pp. 1133-1143, 1998. [https://doi.org/10.1002/\(SICI\)1099-114X\(19981025\)22:13<1133::AID-ER434>3.0.CO;2-E](https://doi.org/10.1002/(SICI)1099-114X(19981025)22:13<1133::AID-ER434>3.0.CO;2-E)
- [54] L. Swan, V. Ugursal, I. Beasuoleil-Morrison, «Implementation of a Canadian residential energy end-use model for assessing new technology impacts». in Building Simulation - 11th International IBPSA Conference, Glasgow, Scotland, 2009.
- [55] IRENA, «Renewable power generation costs in 2021» Abu Dhabi, 2022.
- [56] D. Kammen, D. Sunter, «City-integrated renewable energy for urban sustainability». *Science*, vol. 352, n. 6288, pp. 922-928, 2016. <https://doi.org/10.1126/science.aad9302>
- [57] IRENA, «Renewable power generation costs in 2018» Abu Dhabi, 2019.
- [58] S. Odeh, T. Nguyen, «Assessment method to identify the potential of rooftop PV systems in the residential districts». *Energies*, vol. 14, n. 7, pp. 4240-4251, 2021. <https://doi.org/10.3390/en14144240>

- [59] V. Muteri, M. Cellura, D. Curto, V. Franzitta, S. Longo, M. Mistretta, M. Parisi, «Review on life cycle assessment of solar photovoltaic panels». *Energies*, vol. 13, n. 1, 252, 2020. <https://doi.org/10.3390/en13010252>
- [60] Québec Solar, «What is the difference between monocrystalline and polycrystalline solar panels?» Québec Solar Panels, [Online]. Available: <https://quebecsolar.ca/what-is-the-difference-between-monocrystalline-and-polycrystalline-solar-panels/>. [Accessed on 9<sup>th</sup> November 2022].
- [61] V. Benda, L. Cerna, «PV cells and modules – State of the art, limits and trends». *Heliyon*, vol. 6, n. 12, 2020. <https://doi.org/10.1016/j.heliyon.2020.e05666>
- [62] D. Jordan, S. Kurtz, K. VanSant, J. Newmiller, «Compendium of photovoltaic degradation rates». *Progress in photovoltaics: research and applications*, vol. 24, n. 2, pp. 978-989, 2016. <https://doi.org/10.1002/pip.2744>
- [63] B. Kemery, I. Beausoleil-Morrison, I. Rowlands, «Optimal PV orientation and geographic dispersion: a study of 10 Canadian cities and 16 Ontario locations». in Proceedings of eSim 2012: The Canadian Conference on Building Simulation, Halifax, Nova Scotia, Canada, 2012.
- [64] Office of Energy Efficiency and Renewable Energy, «Using distributed energy resources. A how-to guide for federal facility managers» 2002.
- [65] K. Takahashi, S. Baker, L. Kurdgelashvili, «Policy options to support distributed resources». Newark, Delaware, USA, 2005.
- [66] L. Kurdgelashvili, J. Li, C. Shih, B. Attia, «Estimating Technical Potential for Rooftop Photovoltaics in California, Arizona and New Jersey». *Renewable Energy*, vol. 95, n. 9, pp. 286-302, 2016. <https://doi.org/10.1016/j.renene.2016.03.105>
- [67] G. Mutani, V. Todeschi, «Optimization of costs and self-sufficiency for roof integrated photovoltaic technologies on residential buildings». *Energies*, vol. 14, n. 7, 4018, 2021. <https://doi.org/10.3390/en14134018>
- [68] N. Manoj Kumar, A. Ghosh, S. Chopra, «Power resilience enhancement of a residential electricity user using photovoltaics and a battery energy storage system under uncertainty conditions». *Energies*, vol. 13, n. 8, 4193, 2020. <https://doi.org/10.3390/en13164193>
- [69] S. Castellanos, D. Sunter, D. Kammen, «Rooftop solar photovoltaic potential in cities: how scalable are assessment approaches?». *Environmental research letters*, vol. 12, n. 12, 125005, 2017. <https://doi.org/10.1088/1748-9326/aa7857>
- [70] L. Wiginton, H. Nguyen, J. Pearce, «Quantifying rooftop solar photovoltaic potential for regional renewable energy policy». *Computers, Environment and Urban Systems*, vol. 34, n. 4, pp. 345-357, 2010. <https://doi.org/10.1016/j.compenvurbsys.2010.01.001>
- [71] J. Melius, R. Margolis, S. Ong, «Estimating rooftop suitability for PV: a review of methods, patents and validation techniques». Golden, Colorado, USA, 2013.
- [72] P. Gagnon, R. Margolis, J. Melius, C. Philips, R. Elmore, «Rooftop solar photovoltaic technical potential in the United States: a detailed assessment». Golden, Colorado, 2016.
- [73] Eu Science Hub, «PVGIS Photovoltaic Geographical Information System» [Online]. Available: [https://joint-research-centre.ec.europa.eu/pvgis-photovoltaic-geographical-information-system\\_en](https://joint-research-centre.ec.europa.eu/pvgis-photovoltaic-geographical-information-system_en). [Accessed on 5<sup>th</sup> June 2022].
- [74] City Planning, «3D Massing 2021 - Toronto Open Data» [Online]. Available: <https://open.toronto.ca/dataset/3d-massing/>. [Accessed on 28<sup>th</sup> May 2022].
- [75] Social Development, Finance & Administration, «Neighbourhood Profiles - Toronto Open Data» [Online]. Available: <https://open.toronto.ca/dataset/neighbourhood-profiles/>. [Accessed on 28<sup>th</sup> May 2022].
- [76] City of Toronto, «Planning & Development, Zoning By-law 569-2013. Last update March 9, 2022» 2013. [Online].
- [77] NRCan, «2017 Survey of Household Energy Use» [Online]. Available: <https://www150.statcan.gc.ca/n1/daily-quotidien/171201/dq171201f-cansim-eng.htm>. [Accessed on 28<sup>th</sup> May 2022].
- [78] M. Touchie, C. Binkley, K. Pressnail, «Correlating energy consumption with multi-unit residential building characteristics in the City of Toronto». *Energy and Buildings*, vol. 66, n. 11, pp. 648-656, 2013. <https://doi.org/10.1016/j.enbuild.2013.07.068>

- [79] G. Mutani, M. Fontanive, M. Arboit, «Energy-use modelling for residential buildings in the metropolitan area of Gran Mendoza (AR)». *Italian Journal of Engineering Science*, vol. 61, n. 2, pp. 74-82, 2018. <https://doi.org/10.18280/ti-ijes.620204>
- [80] Government of Canada, «Energy Efficient Product Information - Water Heaters». 10th June 2022. [Online]. Available: <https://www.nrcan.gc.ca/energy-efficiency/products/product-information/water-heaters/13735>.
- [81] G. Mutani, Y. Usta, «Design and Modeling Renewable Energy Communities». *International Journal of Sustainable Development and Planning*, vol. 17, n. 4, pp. 1041-1051, 2022. <https://doi.org/10.18280/ijstdp.170401>
- [82] Natural Resources Canada and CanmetENERGY, «Solar Ready guidelines for solar domestic hot water and photovoltaic systems» 2013.
- [83] Ontario Ministry of Natural Resources and Forestry, «Ontario Digital Surface Model (Lidar-Derived) 2020» [Online]. Available: <https://geohub.lio.gov.on.ca/maps/mnrf::ontario-digital-surface-model-lidar-derived/explore?location=45.711563%2C-81.109300%2C4.13>. [Accessed on 10<sup>th</sup> June 2022].
- [84] Meteotest, «Meteonorm Software 8.0.4» [Online]. Available: <https://meteonorm.com/en/>.
- [85] A. Green, E. Dunlop, J. Hohl-Ebinger, M. Yoshita, N. Kopidakis, H. Hao, «Solar cell efficiency tables (version 59)». *Progress in photovoltaics Res Application*, vol. 30, n. 10, pp. 3-12. <https://doi.org/10.1002/pip.3506>
- [86] G. Mutani, V. Todeschi, «Roof-integrated green technologies, energy saving and outdoor thermal comfort: insights from a case study in urban environment». *International Journal of Sustainable Development and Planning*, vol. 16, n. 1, pp. 13-23, 2021. <https://doi.org/10.18280/ijstdp.160102>
- [87] D. McKenney, S. Pelland, Y. Poissant, R. Morris, M. Hutchinson, P. Papadopol, K. Lawrence, K. Campbell, «Spatial insolation models for photovoltaic energy in Canada». *Solar energy*, vol. 82, n. 11, pp. 1049-1061, 2008. <https://doi.org/10.1016/j.solener.2008.04.008>
- [88] S. Pelland, Y. Poissant, «An evaluation of the potential of building integrated photovoltaics in Canada». in 31st Annual Conference of the Solar Energy Society of Canada (SESCI), Montréal, Canada, 2006.
- [89] H. Nguyen, J. Pearce, «Automated quantification of solar photovoltaic potential in cities». *International Review for Spatial Planning and Sustainable Development*, vol. 1, n. 1, pp. 57-70, 2013. [https://doi.org/10.14246/irspds.1.1\\_49](https://doi.org/10.14246/irspds.1.1_49)
- [90] J. Hofierka, J. Kanuk, «Assessment of photovoltaic potential in urban areas using open-source solar radiation tools». *Renewable Energy*, vol. 34, n. 10, pp. 2206-2214, 2009. <https://doi.org/10.1016/j.renene.2009.02.021>
- [91] H. Wirth, *Recent Facts about Photovoltaics in Germany*. Fraunhofer ISE, Freiburg, Germany, 2020.
- [92] City of Toronto, «SolarTO Map» [Online]. Available: <https://www.toronto.ca/services-payments/water-environment/environmental-grants-incentives/solar-to/solar-to-map/#location=&lat=43.717520&lng=-79.380341>. [Accessed on 20<sup>th</sup> July 2022].
- [93] U. Berardi, S. Jones, «The efficiency and GHG emissions of air source heat pumps under future climate scenarios across Canada». *Energy & Buildings*, vol. 262, n. 5, pp. 1-14, 2022. <https://doi.org/10.1016/j.enbuild.2022.112000>
- [94] R. El Kontar, B. Polly, T. Charan, K. Fleming, N. Moore, N. Long, D. Goldwasser, «URBANopt: an open-source software development kit for community and urban district energy modelling». in Building Performance Modeling Conference and SimBuild co-organized by ASHRAE and IBPSA-USA, 2020.
- [95] D. Cutler, D. Olis, E. Elqvist, X. Li, N. Laws, N. DiOrio, A. Walker, K. Anderson, «REopt: a platform for energy system integration and optimisation». Golden, Colorado, 2017.
- [96] geojson.io. [Online]. Available: <http://geojson.io/#map=2/20.0/-0.2>.
- [97] D. Jermyn, «Deep energy retrofits: Toronto's urban single family housing stock». Toronto, Ontario, 2008.
- [98] K. Blaszk, «Towards sustainability: prioritizing retrofit options for Toronto's single family homes». Toronto, Ontario, 2010.
- [99] S. Niger, «High performance retrofit opportunities of Toronto's 1970s residential detached and semi-detached houses». Toronto, Ontario, 2016.
- [100] C. Binkley, M. Touchie, K. Pressnail, «Energy consumption trends of multi-unit residential buildings in the City of Toronto». Toronto, Ontario, 2012. <https://hdl.handle.net/1807/33339>

- [101] Y. Huang, «Energy benchmarking and energy saving assessment in high-rise multi-unit residential buildings». Toronto, Ontario, 2012.
- [102] S. Alsaadani, M. Roque, K. Trinh, A. Fung, V. Straka, «An overview of research projects investigating energy consumption in Multi-Unit residential buildings in Toronto». in *The Sixth Asian Conference on Sustainability, Energy and the Environment*, Kobe, Japan, 2016.
- [103] Ontario Energy Board Act, Ontario Regulation 541/05. Net metering, Last amendement: 386/22 a cura di, 1998.
- [104] Ontario Energy Board, Ontario Regulation 679/21 - Community net metering projects, under Ontario Energy Board Act, 1998, S.O. 1998, c. 15, Sched. B.
- [105] J. Vellone, G. Minichini, H. Case, «Net metering regulation in Ontario: Information to start your community net metering project». Canada's law firm, November 2021. [Online]. Available: <https://www.blg.com/en/insights/2021/11/net-metering-regulation-in-ontario-information-to-start-your-community-net-metering-project#:~:text=Net%20metering%20allows%20households%20and,they%20return%20to%20the%20grid.> [Accessed on 20<sup>th</sup> October 2022].
- [106] Hydro One, «Technical interconnection requirements for distributed generation» 2010.
- [107] Ontario Energy Board, «Managing costs with Time-of-Use rates» [Online]. Available: <https://www.oeb.ca/consumer-information-and-protection/electricity-rates/managing-costs-time-use-rates>.
- [108] National Renewable Energy Laboratory, «International utility rate database». OpenEI, 2017. [Online]. Available: [https://apps.openei.org/IURDB/?country=CAN&sectors%5B%5D=Residential&service\\_type=&is\\_default=&search=](https://apps.openei.org/IURDB/?country=CAN&sectors%5B%5D=Residential&service_type=&is_default=&search=).
- [109] K. Anderson, D. Olis, L. Parkhill, N. Laws, X. Li, S. Mishra, T. Kwasnik, A. Jeffery, E. Elqvist, K. Krah, D. Cutler, A. Zolan, N. Muerdter, R. Eger, A. Walker, C. Hampel, G. Tomberlin, A. Farthing, «The REopt web tool user manual» 2021.
- [110] Government of Canada, «Eligible retrofits and grant amounts» 2022. [Online]. Available: <https://www.nrcan.gc.ca/energy-efficiency/homes/canada-greener-homes-grant/start-your-energy-efficient-retrofits/plan-document-and-complete-your-home-retrofits/eligible-grants-for-my-home-retrofit/23504>.
- [111] City of Toronto, «High-Rise Retrofit Improvement Support Program (Hi-RIS)» [Online]. Available: <https://www.toronto.ca/community-people/community-partners/apartment-building-operators/hi-ris/>. [Accessed on 25<sup>th</sup> October 2022].
- [112] R. Fu, D. Fieldman, R. Margolis, «U.S. Solar photovoltaic system cost benchmark: Q1 2018». Golden, Colorado, 2018.
- [113] R. Fu, T. Remo, R. Margolis, «2018 U.S. Utility-scale photovoltaics-plus-energy storage system costs benchmark». Golden, Colorado.
- [114] IRENA, «Electricity storage and renewables: costs and markets to 2030» 2017.
- [115] G. Mutani, S. Santantonio, S. Beltramino, «Indicators and representation tools to measure the technical-economic feasibility of a renewable energy community. The case study of Villar Pellice (Italy)». *International Journal of Sustainable Development and Planning*, vol. 16, n. 1, pp. 1-11, 2021. <https://doi.org/10.18280/ijstdp.160101>
- [116] Government of Canada, «Past weather and climate - Historical data» 2022. [Online]. Available: [https://climate.weather.gc.ca/historical\\_data/search\\_historic\\_data\\_e.html](https://climate.weather.gc.ca/historical_data/search_historic_data_e.html).
- [117] A. Kenward, U. Raja, «Blackout: extreme weather, climate change and power outages» 2014.
- [118] Climate Central, «Surging power outages and climate change» 2022.
- [119] V. Todeschi, P. Marocco, G. Mutani, A. Lanzini, M. Santarelli, «Towards energy self-consumption and self-sufficiency in urban energy communities». *International Journal of Heat and Technology*, vol. 39, n. 1, pp. 1-11, 2021. <https://doi.org/10.18280/ijht.390101>
- [120] Istituto della Enciclopedia Italiana, «Canada» Treccani, [Online]. Available: <https://www.treccani.it/enciclopedia/canada>.
- [121] WordAtlas, «Capital cities of Canada's provinces/territories» 2021. [Online]. Available: <https://www.worldatlas.com/geography/capital-cities-of-canada-s-provinces-territories.html>.

- [122] «EnergyHub - Canada's Clean Energy Reference Source» 2022. [Online]. Available: <https://www.energyhub.org/>.
- [123] Environment and Climate Change Canada, «Temperature Change in Canada: Canadian environmental sustainability indicators» 2021. [Online]. Available: [www.canada.ca/en/environment-climate-change/services/environmental-indicators/temperature-change.html](http://www.canada.ca/en/environment-climate-change/services/environmental-indicators/temperature-change.html). [Accessed on 4<sup>th</sup> April 2022].
- [124] Government of Canada, «Changes in temperature» [Online]. Available: <https://www.canada.ca/en/environment-climate-change/services/climate-change/canadian-centre-climate-services/basics/trends-projections/changes-temperature.html>. [Accessed on 3<sup>rd</sup> April 2022].
- [125] E. Bush, J. Loder, T. James, L. Mortsch, S. Cohen, «An overview of Canada's changing climate». in *A changing climate: sector perspectives on impacts and adaptation*, F. Warren e D. Lemmen, A cura di, Ottawa, ON: Government of Canada, 2014, pp. 23-64.
- [126] Government of Canada, «Representative concentration pathways» [Online]. Available: <https://climate-scenarios.canada.ca/?page=scen-rcp>. [Accessed on 4<sup>th</sup> April 2022].
- [127] Prairie Climate Centre, «Climate Atlas of Canada, version 2 (July 10, 2019)» 2019. [Online]. Available: <https://climateatlas.ca/>. [Accessed on 22<sup>nd</sup> July 2022].
- [128] T. Howarth, «Toronto» 2022. [Online]. Available: <https://www.britannica.com/place/Toronto#ref16157>. [Accessed on 17<sup>th</sup> August 2022].
- [129] City of Toronto, «2021 Census: Population and Dwelling Counts» 2022.
- [130] City of Toronto, «Toronto & the Toronto Region» [Online]. Available: <https://www.toronto.ca/city-government/accountability-operations-customer-service/get-involved-how-government-works/toronto-the-toronto-region/>. [Accessed on 29<sup>th</sup> August 2022].
- [131] Canadian Urban Institute, «TOcore community services & facilities study. Phase one: taking stock» 2016.
- [132] Toronto City Planning, «Housing occupancy trends 1996-2016» 2019.
- [133] Canadian Urban Institute, «TOcore neighbourhood population profiles» Toronto, 2016.
- [134] Government of Canada, «Canadian climate normals 1981-2010 station data» [Online]. Available: [https://climate.weather.gc.ca/climate\\_normals/results\\_1981\\_2010\\_e.html?searchType=stnProx&txtRadius=25&optProxType=city&selCity=43%7C39%7C79%7C23%7CToronto&selPark=&txtCentralLatDeg=&txtCentralLatMin=0&txtCentralLatSec=0&txtCentralLongDeg=&txtCentralLongM](https://climate.weather.gc.ca/climate_normals/results_1981_2010_e.html?searchType=stnProx&txtRadius=25&optProxType=city&selCity=43%7C39%7C79%7C23%7CToronto&selPark=&txtCentralLatDeg=&txtCentralLatMin=0&txtCentralLatSec=0&txtCentralLongDeg=&txtCentralLongM). [Accessed on 10<sup>th</sup> August 2022].
- [135] P. Jafarpur, U. Berardi, «Effects of climate changes on building energy demand and thermal comfort in Canadian office buildings adopting different temperature setpoints». *Journal of Building Engineering*, vol. 42, n. 10, 102725, 2021. <https://doi.org/10.1016/j.jobe.2021.102725>
- [136] Toronto and Region Conservation Authority, «Climate change» [Online]. Available: <https://trca.ca/conservation/climate-change/>. [Accessed on 22<sup>nd</sup> August 2022].
- [137] International Energy Agency (IEA), «Canada 2022 - Executive summary» [Online]. Available: <https://www.iea.org/reports/canada-2022/executive-summary>.
- [138] World Energy Council, «Country profile - Canada» 2021.
- [139] Canada Energy Regulator, «Canada's Energy Future 2021» 2021. [Online]. Available: <https://www.cer-rec.gc.ca/en/data-analysis/canada-energy-future/>. [Accessed on 15<sup>th</sup> August 2022].
- [140] Environment and Climate Change Canada, «National inventory report 1990-2020: greenhouse gas sources and sinks in Canada» 2022. [Online]. Available: <https://www.canada.ca/en/environment-climate-change/services/climate-change/greenhouse-gas-emissions/sources-sinks-executive-summary-2022.html>.
- [141] Working Group on Specific Mitigation Opportunities, «Working Group on Specific Mitigation Opportunities Final Report» 2016. [Online]. Available: <https://www.canada.ca/en/environment-climate-change/services/archive/climate-change/clean-growth-working-group-reports.html>.
- [142] Natural Resource Canada, «Energy fact book 2021-2022» 2021. [Online]. Available: <https://www.nrcan.gc.ca/science-and-data/data-and-analysis/energy-data-and-analysis/energy-facts/20061>.
- [143] Canada Energy Regulator, «Provincial and Territorial Energy Profiles – Canada» 2021. [Online]. Available: <https://www.cer-rec.gc.ca/en/data-analysis/energy-markets/provincial-territorial-energy-profiles/provincial-territorial-energy-profiles-canada.html>.

- [144] Y. Poissant, P. Bateman, «Photovoltaic technology status and prospects. Canadian annual report» Ottawa, 2017. <https://publications.gc.ca/site/eng/9.507890/publication.html>
- [145] Natural Resources Canada, «CanmetENERGY Research Brief: integrating electricity storage into smart grid» 2020.
- [146] Natural Resources Canada (NRCan), «Energy Efficiency Trends in Canada 1990-2017» [Online]. Available: <https://oee.nrcan.gc.ca/publications/statistics/trends/2017/index.cfm>. [Accessed on 17<sup>th</sup> August 2022].
- [147] Canada Energy Regulator, «Canada's energy transition: historical and future changes to energy systems – update – an energy market assessment» 2022. [Online]. Available: <https://www.cer-rec.gc.ca/en/data-analysis/energy-markets/canadas-energy-transition/canadas-energy-transition-historical-future-changes-energy-systems-update-energy-market-assessment-trends-canada.html>.
- [148] Government of Canada, «Pan-Canadian framework on clean growth and climate change. Canada's plan to address climate change and grow the economy» 2016. [Online]. Available: <https://www.canada.ca/en/services/environment/weather/climatechange/pan-canadian-framework.html>.
- [149] Government of Canada, «Carbon pollution pricing systems across Canada» [Online]. Available: <https://www.canada.ca/en/environment-climate-change/services/climate-change/pricing-pollution-how-it-will-work.html>. [Accessed on 16<sup>th</sup> August 2022].
- [150] Government of Canada, «Investing in Canada Plan – Building a Better Canada,» [Online]. Available: <https://www.infrastructure.gc.ca/plan/about-invest-a-propos-eng.html?wbdisable=true>. [Accessed on 16<sup>th</sup> August 2022].
- [151] Government of United States e Government of Canada, «Joint United States-Canada electric grid security and resilience strategy» 2016.
- [152] Environment and Climate Change Canada, «2030 emissions reduction plan : Canada's next steps to clean air and a strong economy,» [Online]. Available: <https://www.canada.ca/en/services/environment/weather/climatechange/climate-plan/climate-plan-overview/emissions-reduction-2030/plan.html>. [Accessed on 15<sup>th</sup> July 2022].
- [153] B. Haley, «16 ways Canada's enhanced climate plan advances energy efficiency» 2020. [Online]. Available: <https://www.energycanada.org/blog-16-ways-climate-plan-advances-energy-efficiency/>. [Accessed on 12<sup>th</sup> April 2022].
- [154] Government of Canada, «UN conference on climate action: COP26 in Glasgow» [Online]. Available: <https://www.canada.ca/en/services/environment/weather/climatechange/canada-international-action/un-climate-change-conference/cop26-summit.html>. [Accessed on 5<sup>th</sup> May 2022].
- [155] City of Toronto, «TransformTO» [Online]. Available: <https://www.toronto.ca/services-payments/water-environment/environmentally-friendly-city-initiatives/transformto/#:~:text=for%20more%20information.,TransformTO%20Net%20Zero%20Strategy,most%20ambitious%20in%20North%20America>. [Accessed on 17<sup>th</sup> August 2022].
- [156] Live Green Toronto, «TransformTO - Net zero strategy. A climate action pathway to 2030 and beyond,» 2021.
- [157] City of Toronto, «Net zero existing buildings strategy,» 2021.
- [158] City of Toronto, «Better Buildings Partnership,» 2022. [Online]. Available: <https://www.toronto.ca/services-payments/water-environment/net-zero-homes-buildings/better-buildings-partnership/>.
- [159] Natural Resources Canada (NRCan), «Survey of Energy Consumption of Multi-Unit Residential Buildings (SECMURBs) 2018» [Online]. Available: <https://oee.nrcan.gc.ca/corporate/statistics/neud/dpa/menus/murb/2018/tables.cfm>. [Accessed on 20<sup>th</sup> April 2022].
- [160] Natural Resources Canada (NRCan), «Survey of Commercial and Institutional Energy Use (SCIEU) - Buildings 2014» 2014. [Online]. Available: <https://oee.nrcan.gc.ca/corporate/statistics/neud/dpa/menus/scieu/2014/tables.cfm#wb-sec>. [Accessed on 25<sup>th</sup> April 2022].
- [161] Ontario, «Energy use and greenhouse gas emissions for the Broader Public Sector» [Online]. Available: <https://data.ontario.ca/dataset/energy-use-and-greenhouse-gas-emissions-for-the-broader-public-sector>. [Accessed on 2<sup>nd</sup> May 2022].
- [162] Ontario, «Ontario Energy Quarterly: electricity, oil and gas reports» [Online]. Available: <https://www.ontario.ca/page/ontario-energy-quarterly-electricity-oil-and-gas-reports>. [Accessed on 10<sup>th</sup> May 2022].

- [163] City of Toronto, «Annual energy consumption & greenhouse gas emissions report» 2018. [Online]. Available: <https://www.toronto.ca/services-payments/water-environment/environmentally-friendly-city-initiatives/transformto/torontos-greenhouse-gas-inventory/#:~:text=Key%20findings%3A,per%20cent%20reduction%20in%20emissions..> [Accessed on 24<sup>th</sup> April 2022].
- [164] City of Toronto, «2019 – 2024 Energy Conservation and Demand Management Plan» Toronto, 2019.
- [165] Government of Canada, «Evolution of housing in Canada, 1957 to 2014» [Online]. Available: <https://www150.statcan.gc.ca/n1/pub/11-630-x/11-630-x2015007-eng.htm>. [Accessed on 20<sup>th</sup> July 2022].
- [166] Toronto Weather Stats, «Toronto Weather Stats» [Online]. Available: <https://toronto.weatherstats.ca/>. [Accessed on 17<sup>th</sup> August 2022].
- [167] BizEE Software, «Degree days calculated accurately for locations worldwide» [Online]. Available: <https://degreedays.net/>.
- [168] 2030 Districts Network, «About the Toronto 2030 District» [Online]. Available: <https://www.2030districts.org/toronto/about>. [Accessed on 1<sup>st</sup> May 2022].
- [169] G. Mutani, «Supporting material in the course of Energy Challenges and Environmental Sustainability,» 2020.
- [170] City of Toronto, Planning & Development, «Zoning By-law 569-2013. Last update March 9th, 2022» [Online]. Available: <https://www.toronto.ca/city-government/planning-development/zoning-by-law-preliminary-zoning-reviews/zoning-by-law-569-2013-2/>. [Accessed on 28<sup>th</sup> May 2022].
- [171] Energy Efficiency at NRCan, «Comprehensive Energy Use Database» 2020. [Online]. Available: <https://oee.nrcan.gc.ca/corporate/statistics/neud/dpa/home.cfm>.
- [172] M. F. Touchie, C. Binkley, K. D. Pressnail, «Correlating energy consumption with multi-unit building characteristics in the city of Toronto». *Energy and Buildings*, vol. 66, n. 11, pp. 648-656, 2013. <https://doi.org/10.1016/j.enbuild.2013.07.068>
- [173] United Way Toronto, «Vertical Poverty» 2011. [Online]. Available: <http://www.unitedwaytoronto.com/verticalpoverty/>.
- [174] Toronto 2030 District, «Building Energy Supply Decarbonization – Pathways Project Progress Update» 2021. [Online]. Available: <https://www.2030districts.org/toronto/about>.
- [175] City of Toronto, «Neighbourhood profile data» [Online]. Available: <https://www.toronto.ca/city-government/data-research-maps/neighbourhoods-communities/neighbourhood-profiles/find-your-neighbourhood/#location=&lat=43.774069&lng=-79.421282>. [Accessed on 2<sup>nd</sup> October 2022].
- [176] T. Charan, C. Mackey, A. Irani, B. Polly, S. Ray, K. Fleming, R. El Kontar, N. Moore, T. Elgindy, D. Cutler, M.S. Roudsari, D. Goldwasser, «Integration of open-source URBANopt and Dragonfly energy modeling capabilities into practitioner workflows for district-scale planning and design». *Energies*, vol. 14, n. 18, 5931, 2021. <https://doi.org/10.3390/en14185931>
- [177] S. Xu, Z. Huang, J. Wang, T. Mendis, J. Huang, «Evaluation of photovoltaic potential by urban block typology: A case study of Wuhan, China». *Renewable Energy Focus*, vol. 29, n. 6, pp. 141-147, 2019. <https://doi.org/10.1016/j.ref.2019.03.002>
- [178] R. Aghamolaei, M. Haris Shamsi, J. O'Donnell, «Feasibility analysis of community-based PV systems for residential districts: A comparison of on-site centralized and distributed PV installations». *Renewable Energy*, vol. 157, n. 9, pp. 793-808, 2020. <https://doi.org/10.1016/j.renene.2020.05.024>
- [179] G. Simonet, «The energy intensity of the Canadian residential sector becomes more efficient». *Climate Change - 2018 Annual Report*, vol. 51, n. 28, 2018.
- [180] Environment and Climate Change Canada, «Pan-canadian framework on clean growth and climate change - third annual synthesis report on the status of implementation» 2020. [Online]. Available: <https://www.canada.ca/en/services/environment/weather/climatechange/pan-canadian-framework.html>.
- [181] Canadian Commission on Building and Fire Codes, National Research Council of Canada, «National Energy Code of Canada for Buildings 2017» Ottawa, 2017.
- [182] S. Berkland, «A Comparison of American, Canadian, and European Home Energy Performance in Heating Dominated – Moist Climates Based on Building Codes» Amherst, US., 2014.

- [183] National Research Council of Canada, «Measures for Energy Conservation in New Buildings: 1978» 1978. [Online].
- [184] Government of Canada, «Energy Efficiency Act, S.c. 1992, c. 36» 1992. [Online]. Available: <https://laws-lois.justice.gc.ca/eng/acts/e-6.4/index.html>.
- [185] C. Woodrow, *Global Sustainable Communities Handbook. Green design technologies and economics*. Waltham, MA, USA: Elsevier Science, 2013.
- [186] Efficiency Canada, «The 2020 Model Building Codes» [Online]. Available: <https://www.energycanada.org/building-codes-2020/>. [Accessed on 16<sup>th</sup> August 2022].
- [187] Statistics Canada, «Canadian Housing Survey (CHS)» [Online]. Available: <https://www.statcan.gc.ca/en/survey/household/5269>. [Accessed on 16<sup>th</sup> August 2022].
- [188] A. McAfee, «Housing and Housing Policy». The Canadian Encyclopedia, 2015. [Online]. Available: <https://www.thecanadianencyclopedia.ca/en/article/housing-and-housing-policy>. [Accessed on 15<sup>th</sup> August 2022].
- [189] Government of Canada, «Housing statistics» 2022. [Online]. Available: <https://www.statcan.gc.ca/en/subjects-start/housing>. [Accessed on 15<sup>th</sup> August 2022].
- [190] C. James, K. Winder, «CMHC EQUilibrium™ Sustainable housing demonstration initiative» Ottawa, 2013. <https://publications.gc.ca/site/eng/9.857925/publication.html>

# APPENDIX

## I. Building code evolution

Canada is supporting the update of building codes for a more efficient stock because energy efficiency is a shared responsibility between federal and provincial territories [137]. Energy for heating and cooling buildings accounted indeed for the 12% of national GHG emissions in 2014 [179]. Therefore, the approach to the built environment targets [180]:

- high efficiency for new buildings;
- retrofit on existing buildings, as well as fuel switching. Indeed, it is expected that more than 75% of building stock in 2030 will be composed by already realised today structures;
- energy efficiency for appliances and equipment;
- support of building codes (adopted by provinces and territories) and energy efficient housing in Indigenous communities.

Provincial and territorial governments introduce regulations for building design and construction within their jurisdictions. Over the last 30 years, energy efficiency programs and measures have been adopted at all administrative levels to reduce GHG emissions from the built environment and achieve complementary policies [141]. The evolution has significantly impacted both historical and forecasted emissions [141]. The federal government implements regulations for appliances and equipment and national standards, codes, and benchmarking systems for provinces, territories, and municipalities. These tools are used for local regulations, and to deliver incentives to meet their climate change policies. Local governments adopt the National Energy Code for Buildings (NECB) [181] without change or with modifications to align with the local needs.

The first code for dwellings was introduced during the Great Depression (1920s), when most of building construction was stopped due to the economic crisis. However, in the following recovery and demographic growth, in several main cities the building code was enforced to avoid fire danger and save energy. A National Code for Dwelling Construction in 1950 for the construction of residential homes established minimum requirements and gradually diminished the moisture problems thanks to insulation [182].

Both efficiency sector and energy systems have evolved in Canada, even if energy demand keeps growing. Recent houses consume approximately 34% less energy per m<sup>2</sup> compared to a home realised between the 1960s and 1980s and are about 18% more efficient than one built between 1985 and 1990. Contributions derive from new space heating requirements, insulation levels, more airtight construction [182]. In 1978, the first edition of “Measures for Energy Conservation in New Buildings” was published, even if a following one in 1983 was more articulated with a new section dedicated for housing. The document firstly introduced requirements for buildings with low and high energy demand regarding enclosures, heating, cooling, ventilation, and service water heating [183].

Canadian energy efficiency regulations date back to the Nineties, with the implementation in 1995 of the Energy Efficiency Act (1992) [184]. It enforced minimum performance and labelling for consuming products, including imported appliances into Canada, in order to decrease energy consumption. Regarding building consumption, the Model National Energy Code for Houses released in 1997 was updated in 2012 in relation to the 2010 National Energy Code for Buildings. The 1997 Code applied

a prescriptive approach on building envelope, service water heating, lighting, and electrical power, following the model of Ontario Code, even if its application was voluntary.

The National Energy Code for Buildings (NECB) 2017 re-defined the technical requirements for energy efficiency design and construction for new buildings. It embodies a main step forward the “Net Zero Energy Ready” buildings by 2030 presented by the Pan-Canadian Framework [180]: it introduces requirements for losses and thermal transmittance of roofs, fenestration, and doors as well as more stringent ones for lighting and energy recovery systems [181]. Assessment of these changes identifies a potential energy efficiency improvement between 10.3 and 14.4 % over the 2011 code version [181]. In line with it, an investment of \$40million was devoted from 2016 to revise infrastructure codes and integrate climate-resiliency into building designing.

Along with regulations, different labelling systems promote more sustainable designs and limit the energy consumption of appliances [177]. The main one is EnerGuide, which labels both consumption of household appliances and a complete household audit to provide an efficiency rating under request of the owner. The evaluation scale goes from 0 (with major leakage, no insulation and high consumption) to 100 (maximum energy savings according to the available products). However, it is not compulsory despite the visual aid and the possible sustainable choices proposed by the energy advisor [183]. A more informative and voluntary tool is the R-200 standard, which is specific to reduce the energy footprint of households. According to evaluations, a house compliant to building codes will show an 60-70 EnerGuide rating, while the application of R-200 framework will score around 80 and consume yearly 30% less energy [183].

The NECB has been further updated in 2020 to improve the level of energy efficiency and make buildings consistent with the Canada net-zero policy [184]. Main modifications are reduction of thermal transmittance values for opaque assemblies and fenestration to enhance the performance of the building envelope; alignment of performance requirements for heating, ventilating and air-conditioning (HVAC) and water heating with relevant standards and regulations; introduction of a new compliance path with 4 energy performance tiers to improve energy efficiency in buildings.

Thanks to new efficiency requirements, energy modelling estimated a 9Mt GHG reduction coming from stricter building codes by 2030. Research has also assessed that \$1 of energy efficiency programs spent by utilities and provincial governments lead to \$4 to \$8 of GDP [141]. Indeed, energy efficiency improvements have led to a significant decline in average energy use per household (from 144 GJ/hh/y in 1990 to 104 GJ/hh/y in 2017) and per unit of floor space (from 1.18 GJ/m<sup>2</sup>/y in 1990 to 0.72 GJ/m<sup>2</sup>/y in 2017) [146].

## II. Housing evolution in Canada

Despite steps forward to reduce energy intensity (decrease by 6% between 2011 and 2015), the housing sector has registered an increase in total energy consumption between 1990 and 2015. The consumption rise is related to the +29% growth of the Canadian population (+8 million) and +43% increase of household number (+4.2 million). Changing choices in living space led to a 17% increase in the average living space (in m<sup>2</sup>) between 1990 and 2013 [187], confirmed also until 2017 [146] (Figure 99).

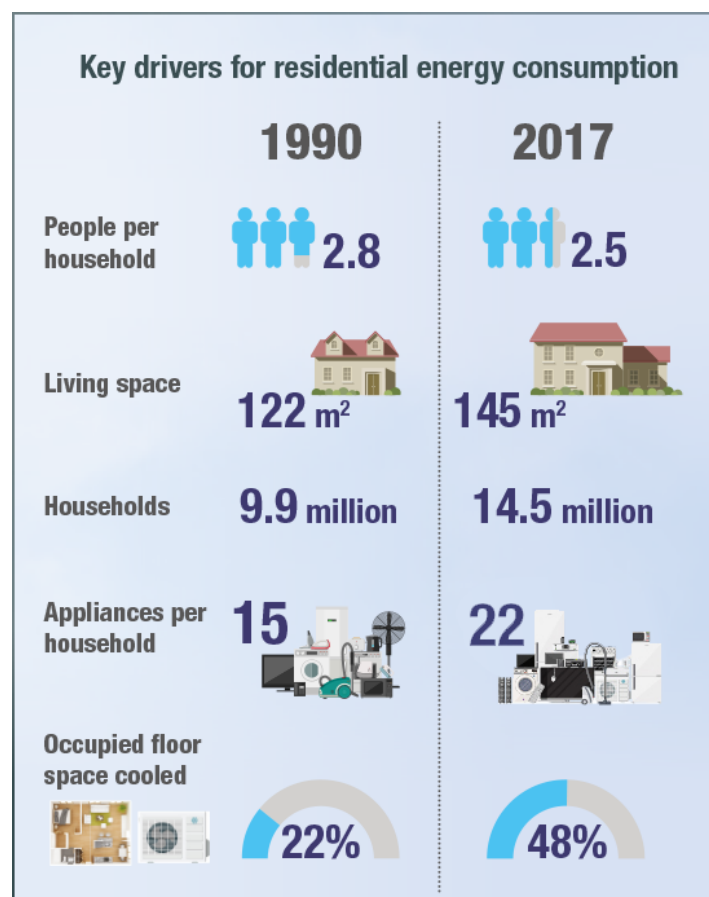


Figure 99. Key drivers for changes in residential energy consumption between 1990 and 2017. Source: [146].

More than half of homes are single-family detached houses and 69% in privately owned dwellings in 2018 [187]. The remaining share is covered by 17% of row houses, duplexes, semi-detached or movable, 18% low-rise and 10% high-rise apartments [188]. The housing evolution in Canada reflects the adoption of different models, which differ along time. The residential expansion has been mainly after the WWII and outward (in suburbs), while currently urban growth develops upward through multi-family dwellings (apartments and condominiums). The emergence of this housing type reflects lifestyle choice, demographic and economic changes, declining household size and characterisation as well as higher prices of single-family homes [165].

In the 1950s, single-family homes prevailed in the residential stock and between 1957 and 1959, they covered 60% of new construction (Figure 100). The introduction of Canada Mortgage and Housing Corporation's mortgage loan model in 1954 guaranteed a more feasible access to single-family homes, which increased demand for new suburban neighbourhoods. However, from 1962 to 1973,

most of building permits started to be issued for multi-family dwellings, which were more affordable than single dwellings. This demand change reflected the post-war demographic and population boom especially of immigrants. Construction of new multi-family units was faster than single-family one from 1974 to 1982, especially during the mid-1970s recession. After peaks and shrinkages, from 1974 to 1982, single and multi-family solutions accounted for an equal share of new dwellings [165]. Considering the slower population growth between the 1980s and 2006, the residential building sector was affected with a progressive decline, mainly for multi-unit dwellings. Mortgage lending rates started to decrease in mid 1980s, so that more people can afford single dwellings.

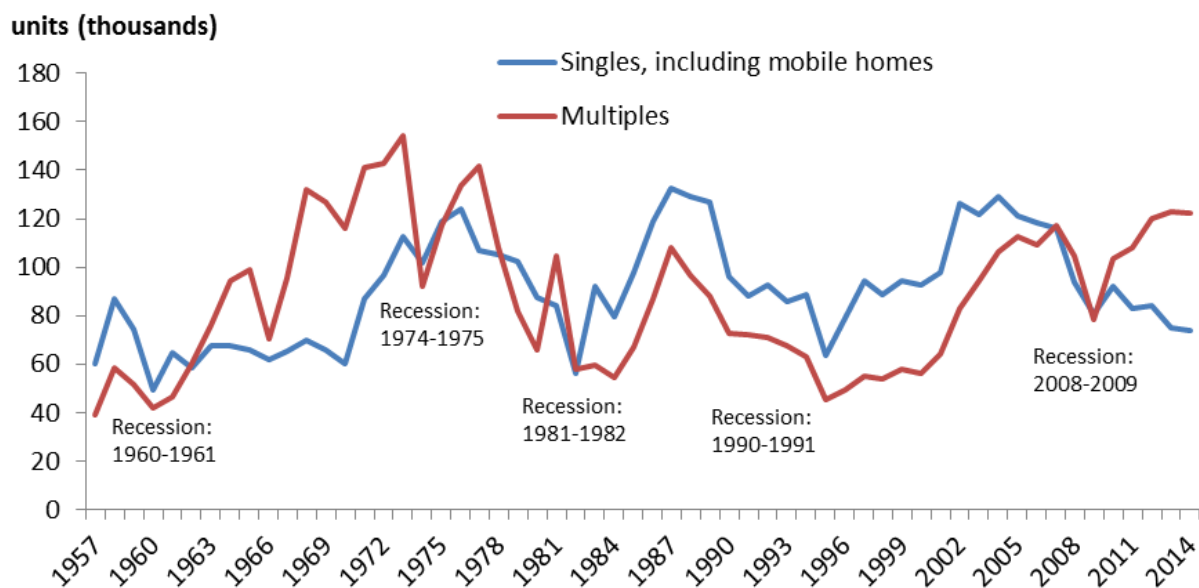


Figure 100: Building permits for single-family and multi-family dwelling units in Canada, from 1957 to 2014. Source: [189].

At the national level, apartment-condominiums have progressively become the dominant type from the early 2000s: they covered 88% of condominium construction intentions in 2014, compared to 62% in 2000. This dwelling type is especially concentrated in Canada's census metropolitan areas (CMAs): land available is generally limited for new residential construction, while apartment-condominiums may more easily fulfil the immigration demand for housing in the metropolitan zones. In 2014, the highest construction intentions for apartments compared to other dwelling types in three largest CMAs, or rather Toronto, Vancouver and Montreal. In Toronto, they accounted for 54% of residential construction, compared with 27% for single-family homes, in Montréal, for 75% compared with 16% for single-family homes and in Vancouver, it was 67% for apartment units and 16% for single-family homes. In all three CMAs, new single-family dwellings started declining from the beginning of the 2000s (-46%), falling from 27,627 dwellings in 2000 to 14,840 in 2014. Since the 2008–09 recession, construction rates for multi-family recovered faster than single-family dwellings. The number of planned multi-family dwellings (103,469) surpassed single-family ones (91,908) in 2010 and reached the maximum in 2013, with the highest number of units (122,908) since 1977 [165]. The prevalence of energy sources for housing varies by region, especially for space heating and domestic hot water [25]. Heating is a main component for Canadian houses due to weather conditions especially during winter. As a result, GHG emissions in the residential sector are correlated with annual weather conditions. The increase in energy consumption and emissions has been registered

in the colder winter of 2013, whereas the drop in GHG emissions (excluding electricity) in 2016 for housing can be linked with the national mean temperature 2.1°C warmer than the reference average (1961 to 1990) [179]. For heating, Atlantic Canada relies on a mix of oil, electricity, and wood, Quebec primarily uses electricity, while Ontario, the West regions and British Columbia mainly have natural gas [25].

Federal initiatives focused on reducing demands for energy and GHG emission in the housing sector mainly from the 2000s, as the Equilibrium Sustainable Housing Demonstration Initiative [190]. Governments encouraged more compact urban development by different directions: further housing in existing neighbourhoods; redevelopment of "brownfield" (old industrial) and "grey field" (low-density commercial) sites; realisation of residential areas close to downtown to make more efficient and sustainable use of land and services [188].

### III. Energy consumption by the Comprehensive Energy Use Database [43]

In the Comprehensive Energy Use Database for Ontario, data have the following subdivision by energy-end uses and consumption per m<sup>2</sup>, household and inhabitants.

Energy use by end use	PJ/y	kWh/m <sup>2</sup> /y	kWh/household/y	kWh/inhabitant/y	Heating/cooling index 2017
Space Heating	346.8	117.20	17,828.21	7,162.57	0.92
DHW	97.0	32.78	4,987.06	2,003.58	-
Appliances	65.8	22.25	3,385.39	1,360.10	-
Lighting	17.9	6.03	917.91	368.77	-
Space Cooling	18.8	8.27	967.06	388.52	1.36

According to the available data, electricity consumption is mainly composed by:

- lighting;
- space cooling, which is divided in central, or room system and it generally interests only a portion of the whole building (76.85%);

Space cooling system type	PJ/y	Share (%)
Room	1.1	5.6
Central	17.8	94.4

- appliances, which are mostly covered by electricity and involve different types, as refrigerators, freezers, dishwashers, ranges.

Appliances	PJ/y	Share (%)
Electricity	62.2	94.4
Natural gas	3.7	5.6

Natural gas is mainly used for:

- space heating, which is of primary importance for Canada, and it is mainly satisfied with natural gas systems (70.4%). At the same time, dual systems are also used, even if in a more limited share of cases (10.9%).

Space heating system type	PJ/y	Share (%)
Heating Oil – Normal Efficiency	0.0	0.0
Heating Oil – Medium Efficiency	7.7	2.2
Heating Oil – High Efficiency	0.0	0.0

Natural Gas – Normal Efficiency	0.2	0.1
Natural Gas – Medium Efficiency	68.5	19.7
Natural Gas – High Efficiency	175.5	50.6
Electric	29.9	8.6
Heat Pump	10.8	3.1
Other1	10.5	3.0
Wood	6.1	1.7
Dual Systems		
Wood/Electric	27.4	7.9
Wood/Heating Oil	7.2	2.1
Natural Gas/Electric	2.4	0.7
Heating Oil/Electric	0.6	0.2

- water heating, which is largely satisfied by natural gas;

Water heating energy source	PJ/y	Share (%)
Electricity	9.7	10.0
Natural gas	83.0	85.5
Heating oil	1.0	1.1
Other	1.0	1.0
Wood	2.2	2.3

- cooking, which is not specified in the database: therefore, the remaining quota of natural gas is assumed to be covered by this usage.